

DEVELOPING NEW STRATEGIES FOR TREATMENT OF *PSEUDOMONAS AERUGINOSA* INFECTION

Minh Tam Tran Thi

B.Sc., M.Sc.



School of Environment and Science
Centre for Cell Factories and Biopolymers
Griffith Institute for Drug Discovery
Griffith University

Submitted in fulfillment of the requirements of the degree of
Doctor of Philosophy

April 2022

General abstract

Pseudomonas aeruginosa (*P. aeruginosa*) is a pathogenic bacterium causing devastating acute and chronic infections among populations with compromised immune systems. Its highly notorious persistence in clinical settings is attributed to the ability to form antibiotic-resistant biofilms. Biofilm is an architecture built mostly by autogenic extracellular polymeric substances that functions as a scaffold to encase the bacteria together on surfaces, protect them from environmental stresses, evade host immune system, and thereby facilitate long-term persistence. Current antibiotics cannot penetrate the biofilm matrix as they were initially designed to modulate mainly the growth of planktonic bacteria. Therefore, there is a dire need to search for novel agents that can interfere with biofilm development and/or eradicate established biofilms.

In this study, a biofilm dispersal assay in 384-well format was developed and optimized to identify anti-*P. aeruginosa* biofilm molecules from three compound collections. The first library, previously shown to inhibit planktonic *P. aeruginosa*, was screened against pre-existing biofilms of wild-type *P. aeruginosa* PAO1 and its isogenic mutant - mucoid variant PDO300, which were established in artificial sputum medium mimicking lung physiology of cystic fibrosis (CF) patients. Active fractions were subjected to bioassay-guided purification to confirm the activity and identify active compounds within the active fractions. The second library consists of NatureBank compounds which were evaluated against PAO1. The third library, David Open Access library, comprises known natural products and their analogues which have therapeutic effects on various diseases such as bacterial infections, viral infections, cancer, malaria, and neurodegenerative disorders. The library was assessed against established PAO1 biofilms. In addition, a set of three natural products, ianthelliformisamines A-C, previously identified as antibiotic adjuvants toward planktonic PAO1, was examined for the first time against PAO1 and its isogenic mutants including PAO1 Δ *pslA*, PAO1 Δ *pelF*, PDO300 and PDO300 Δ *alg8*, to determine their impacts on biofilms as well as biofilm matrix components (alginate, Psl and Pel). A cytotoxicity study against the HEK-293 cell line was carried out along with an investigation of the mechanism of action.

Fifteen confirmed hits from the David Open Access library were identified as promising *P. aeruginosa* biofilm dispersers without adverse effects on the planktonic growth. These potential candidates will be subjected to further investigation.

Ianthelliformisamines A-C inhibited biofilm formation of *P. aeruginosa* and interfered with different biofilm matrix components. Ianthelliformisamines A and B potentiated ciprofloxacin activity, corroborated by 3 - 4-fold reduction in MIC of antibiotic ciprofloxacin. Ianthelliformisamine C alone targeted the viability of suspended cells and biofilms of the studied strains at various levels. Interestingly, this molecule solely impeded both free-living and biofilm populations of mucoid variant PDO300 which was engineered to imitate clinical isolates from CF patient lungs. It was reported that PDO300 derived mucoid biofilms were greatly refractory to antibiotic tobramycin up to 1000 times compared to nonmucoid biofilms. These molecules were not toxic to the HEK-293 cell line. Although further research is required to elucidate the mechanisms of action of these compounds, the current data suggested that ianthelliformisamine C may be a potential efflux pump inhibitor. Overall, ianthelliformisamines A-C could be useful starting points for future anti- *P. aeruginosa* biofilm therapeutics.

Statement of Originality

This work has not previously been submitted for a degree or diploma in any university.

To the best of my knowledge and belief, the thesis contains no material previously published or written by another person except where due reference is made in the thesis itself.

Minh Tam Tran Thi

PhD candidate

Date: 8th April 2022

Acknowledgment

Here I am, almost at the end of the Ph.D. journey, which sometimes seems to be forever. This journey would be unachievable without the inspiration, continuous support, and guidance of many amazing people. My heartfelt thanks to all for being there for me through sad days, happy moments, and crazy times.

First and foremost, I would like to express sincere gratitude to my supervisor, Professor Bernd Rehm, who gave me guidance, encouragement, and support throughout my Ph.D. research. Thank you for reminding me of Thomas Edison's famous quote, "I have not failed. I've just found 10,000 ways that won't work" every time things get tough – it gives me the strength to keep going. I am also thankful to my co-supervisors, Professor Katherine Andrews and Associate Professor Rohan Davis, for their time, constant assistance, and valuable feedback.

I sincerely appreciate the generous assistance of Nature Bank and Associate Professor Rohan Davis. My deepest thanks to Dr. Russell Adison and Ms. Sasha for their time, patience, and guidance to help me understand the process of extraction, isolation, and fractionation of natural products.

I would like to thank Griffith University for Griffith University International Postgraduate Research Scholarship and Griffith University Postgraduate Research Scholarship. Without the funding, this work would have been unfeasible.

It is a pleasure to thank members of GRIDD, Bernd's group, and Frank's group. I wish to articulate my gratitude to Dr. Wankuson Chanasit for her time, enthusiasm, guidance, and thoughtful advice. I have acquired new knowledge and skills from her. I would like to thank Jean and Sam for their valuable help, great camaraderie, and care throughout my Ph.D. Special thanks to all my colleagues: Frank, Anjali, Deeptee, Sytze, Ben, Big Ben, David, Shuxiong, Stefanie, Saranya, Donna, Micol, and Lygie for their support.

Lastly, I am eternally grateful to my mother for her love, prayers, care, unending encouragement, and sacrifices. She always believes in my potential and motivates me to pursue my dream – I could not have completed this journey without her. Many thanks to my friends, Johana, Devathri and Megha, for their help and support throughout my Ph.D. journey. Finally, I would like to thank my loving, caring, patient, and supportive husband, Matthew Taylor. It is a great comfort to know you are standing by my side with your unwavering support when times get tough. I am truly grateful!

An acknowledgement of published and unpublished papers included in the thesis

This thesis contains 6 chapters including **chapter 1** (General introduction), **chapter 2** (General materials and methods), **chapters 3, 4 and 5** (three projects) and **chapter 6** (General discussion).

Chapters 1 and 5 are co-authored published and unpublished papers, respectively. My contribution to each co-authored paper is outlined at the front of the relevant chapter. The bibliographic details for each paper are as follows:

Chapter 1

THI, M.T.; WIBOWO, D.; REHM, B.H.A. *Pseudomonas aeruginosa* Biofilms. *International Journal of Molecular Sciences* **2020**, *21*, doi:10.3390/ijms21228671. A published peer reviewed review article as first author publication.

Chapter 5

TRAN, M.T.T., DAVIS, R.A. & REHM, B. H. A. Bromotyrosine-derived metabolites from a marine sponge inhibit *Pseudomonas aeruginosa* biofilms. Prepared for publication.

Signed: **Minh Tam Tran Thi**

PhD Candidate

Date: 10th April,2022

Countersigned: **Bernd Rehm**

Principal Supervisor

Date: 10th April,2022

Table of content

General abstract	i
Statement of Originality	iii
Acknowledgment.....	iv
An acknowledgement of published and unpublished papers included in the thesis	vi
Table of content	vii
List of figures and tables	xi
Abbreviations	xiv
Abbreviations	xv
CHAPTER 1: General introduction	1
1.1 Introduction	2
1.2 Pseudomonas aeruginosa biofilm	3
1.2.1 Biofilm composition	3
1.2.2 Biofilm development	6
1.2.3 Multispecies biofilm	8
1.3 Quorum sensing in biofilm development	9
1.4 Diagnostics	12
1.4.1 Conventional microbiological culture	13
1.4.2 Molecular biology methods	13
1.4.3 Mass spectrometry	14
1.4.4 Nanoparticle biosensor	14
1.5 Therapeutic strategies	15
1.5.1 Nanoparticles	21
1.5.2 Targeting EPS component and structure	21
1.5.3 Immunotherapies	22
1.5.5 Inhibition of quorum sensing.....	22
1.5.6 Targeting iron metabolism.....	23
1.5.7 Photodynamic therapy	24
1.5.8. Photothermal therapy	25
1.6. Natural products	27

1.6.1.	Plant-derived antibiofilm molecules	27
1.6.2.	Antibiofilm substances from microorganisms	28
1.6.3.	Antibiofilm molecules extracted from marine natural products	30
1.7.	Aims and objectives	32
1.8.	References	34
CHAPTER 2: General materials and methods		63
2.1	Experimental design	63
2.2	Materials and methods.....	65
2.2.1	Bacterial strains.....	65
2.2.2	Medium.....	66
2.2.3	Growth curve	67
2.2.4	xCELLigence - Real-Time Cell Analyzer (RTCA) SP	67
2.2.5	Crystal violet assay	69
2.2.5.1	Biofilm growth curve	69
2.2.6	Resazurin metabolic assay	70
2.2.7	LIVE/DEAD staining	71
2.2.8	Nile Red staining	72
2.2.9	Data analysis	72
2.2.10	Biofilm assay	73
2.3	References	76
CHAPTER 3: Screening of natural product libraries		79
3.1.	Introduction	79
3.2.	Materials and Methods	79
3.2.1	Natural product library.....	79
3.2.2	Library of pure compounds.....	79
3.2.3	Fraction refractation.....	80
3.2.4	Biofilm assay	80
3.2.5	Statistical analysis.....	80
3.3.	Results and discussion.....	80
3.3.1	Assay development.....	80
3.3.1.1	Physiology state of <i>P. aeruginosa</i>	80

3.3.1.2	DMSO tolerability.....	82
3.3.1.3	Biofilm growth curve and antibiotic tests	84
3.3.1.3.1	Biofilm growth and the cell index.....	84
3.3.1.3.2	Antibiotic treatments on established biofilms.....	86
3.3.2	Screening of natural product library	91
3.3.3	Biofilm assay using resazurin as a viability indicator	95
3.4	Conclusion.....	106
3.5	References	109
CHAPTER 4: Screening of Davis Open Access library.....		111
4.1	Introduction	111
4.2	Materials and Methods	111
4.2.1	Compound library	111
4.2.2	Biofilm dispersal assay	112
4.2.3	Data analysis	112
4.3	Results and discussion.....	113
4.4	Conclusion.....	120
4.5	References	121
CHAPTER 5: Bromotyrosine-derived metabolites from a marine sponge inhibit <i>Pseudomonas aeruginosa</i> biofilms.....		125
5.1	Abstract.....	126
5.2	Introduction	126
5.3	Materials and methods.....	128
5.3.2	Determination of minimum inhibitory concentration (MIC).....	129
5.3.3	Checkerboard assay	130
5.3.4	Biofilm inhibition assay.....	130
5.3.5	Ethidium bromide efflux assay	132
5.3.6	NPN uptake assay	132
5.3.7	Cellular bioluminescent assay	133
5.3.8	Cytotoxicity assay.....	133
5.3.9	Fluorescence microscopy.....	134
5.4	Results	137

5.4.1	Minimum inhibitory concentrations	137
5.4.2	Ianthelliformisamines A–C synergistically interact with ciprofloxacin..	137
5.4.3	Influence of Ianthelliformisamines on the outer membrane integrity	145
5.4.4	Efflux assay.....	147
5.4.5	Do Ianthelliformisamines share the mode of action with ciprofloxacin?.	148
5.4.6	Effect of test compounds on HEK293 cells.....	148
5.4.7	Fluorescence microscopy imaging	149
5.4.8	<i>In vitro</i> metabolism of ianthelliformisamines A–C (1–3)	155
5.4.8.1	Positive controls	155
5.4.8.2	Ianthelliformisamine A (1).....	155
5.4.8.3	Ianthelliformisamine B (2)	156
5.4.8.4	Ianthelliformisamine C (3)	158
5.5	Discussion.....	159
5.6	Conclusion.....	163
5.7	References	165
5.8	Acknowledgements	173
5.9	Supplementary Information.....	174
	CHAPTER 6: General discussion and conclusion	187
6.1	Future directions.....	190
6.2	References	192

List of figures and tables

Chapter 1

Figure 1. 1 Cycle of <i>P. aeruginosa</i> biofilm development.	7
Figure 1.2 Hierarchical quorum-sensing (QS) network in <i>Pseudomonas aeruginosa</i>	11
Table 1.1 Summary of therapeutic strategies against <i>P. aeruginosa</i> infections	17
Table 1.2 Plant-derived natural products as modulators of <i>P. aeruginosa</i> biofilms.....	28
Table 1.3 Microorganisms derived antibiofilm molecules against <i>P. aeruginosa</i> biofilms	29
Table 1.4 Marine natural products modulating <i>P. aeruginosa</i> biofilms	31

Chapter 2

Figure 2.1 The development and optimization of biofilm dispersal assay	64
Figure 2.2 Generation of the impedance signals	68
Figure 2.3 The plate template of fractions used in biofilm dispersal assay	74
Figure 2.4 Overview of screening approach used in this study.	75
Table 2.1 List of <i>P. aeruginosa</i> strains used in this study	65
Table 2.2 Components of Artificial Sputum Medium	66
Table 2.3 Antibiotic used in this study	70

Chapter 3

Figure 3.1 Growth curves of PAO1, PDO300 and PDO300 Δ alg8	81
Figure 3.2 Metabolic activity of planktonic and biofilm cells.....	83
Figure 3. 3 Changes in cell index (CI) during 72 h of biofilm formation	85
Figure 3. 4 Effect of antibiotics on pre-formed biofilms of wild-type PAO1	86

Figure 3. 5 The susceptibility of established biofilms to antimicrobial agents	88
Figure 3.6 Impacts of DMSO and antibiotics on the viability of biofilm cells	90
Figure 3.7 Representative images of <i>P. aeruginosa</i> biofilms stained with Nile red.	91
Figure 3.8. Confocal laser scanning microscopic images of bacterial strains	93
Figure 3.9 An alternative approach for biofilm assay	94
Figure 3.10 A scatter plot displays the percentage of growth inhibition and biofilm dispersal	96
Figure 3.11 Effects of screened fractions on growth and established biofilms.	97
Figure 3.12 Activity of selected fractions on growth and biofilm formation.....	98
Figure 3.13 Antibiofilm efficiency of extracts and refractionated fractions	100
Figure 3.14 Impacts of 14 initial fractions and refractionated fractions on the bacterial viability.....	101
Figure 3.15 Viability of PAO1 and PDO300 biofilms upon exposure to 14 initial and refractionated fractions.	102
Figure 3.16 Biofilm dispersing effects of extracts and refractionated fractions.....	104
Figure 3.17 Viability of PAO1 preformed biofilms treated with selected fractions	105
Figure 3.18 Effects of 54 NatureBank compounds on dispersing preformed biofilms of PAO1.	108
 Table 3.1 Origins of selected fractions for small-scale refractionation	99

Chapter 4

Figure 4. 1 Effect of 505 pure compounds on inhibiting growth and dispersing preformed biofilms of wild-type <i>P. aeruginosa</i> PAO1.....	114
Figure 4.2 Growth inhibition and biofilm dispersal activity of 27 compounds in confirmatory screen	116
Figure 4.3 Activity of 15 confirmed compounds.....	117
Figure 4.4 Chemical structures of 15 confirmed hit compounds	119

Chapter 5

Figure 5.1 Biofilm assays to identify compounds that prevent biofilm formation.....	139
Figure 5.2 Ianthelliformisamine A–C (1–3) combined with ciprofloxacin.....	142
Figure 5.3	146
Figure 5.4 Representative fluorescence images of PAO1 biofilms	150
Figure 5.5 Representative fluorescence images of PDO300 biofilms	151
Figure 5.6 Representative fluorescence images of PDO300 Δ <i>alg8</i> biofilms	152
Figure 5.7 Representative fluorescence images of PAO1 Δ <i>pslA</i> biofilms	153
Figure 5.8 Representative fluorescence images of PAO1 Δ <i>pelA</i> biofilms	154
 Table 5. 1 Additional parameters were calculated using listed equations	 136
 Supplementary Figure 5.1 Metabolic stability parameters for 1	 179
Supplementary Figure 5.2 Metabolic stability of 2	180
Supplementary Figure 5.3 Metabolic stability of 3	181
 Supplementary Table 5.1 Structures, formulas and molecular weight of ianthelliformisamines A–C (1–3)	 175
Supplementary Table 5.2 The degradation of 1 in mouse liver microsomes	176
Supplementary Table 5.3 Metabolic stability parameters for 1	176
Supplementary Table 5. 4 The results for degradation of 2	177
Supplementary Table 5.5 Metabolic stability parameters for 2	177
Supplementary Table 5.6 The results for degradation of 3	178

Abbreviations

ASM	Artificial sputum medium
<i>B. cenocepacia</i>	<i>Burkholderia cenocepacia</i>
CF	Cystic fibrosis
CI	Cell Index
CV	Coefficient of variation
CIP	Ciprofloxacin
CV	Crystal violet
c-di-GMP	bis-(3'-5')-cyclic dimeric guanosine monophosphate
°C	Degree Celsius
CCCP	Carbonyl cyanide m-chlorophenyl hydrazone
DCM	Dichloromethane
DMSO	Dimethyl sulfoxide
eDNA	Extracellular deoxyribonucleic acid
EPS	Extracellular polymeric substances
FBS	Fetal bovine serum
FDA	US Food and Drug Administration
GEN	Gentamicin
HIV	Human immunodeficiency virus
H ₂ O ₂	Hydrogen peroxide
HQNO	2-heptyl-4-hydroxyquinoline- <i>N</i> -oxide
HTS	High throughput screening
IPTG	Isopropyl β- d-1-thiogalactopyranoside
LB	Luria-Bertani
MAD	Median absolute deviation
MDR	Multi-drug resistance
MEM	Meropenem
MeOH	Methanol
NIH	National Institute of Health

Abbreviations

NPN	1- <i>N</i> -phenylnaphthylamine
OD600	Optical density at 600 nm
<i>P. aeruginosa</i>	<i>Pseudomonas aeruginosa</i>
PGM	Porcine gastric mucin
PHAs	Polyhydroxyalkanoic acids
PI	Propidium iodide
QS	Quorum sensing
RNA	Ribonucleic acid
RSZ	Resazurin
RTCA	Real time cell analyser
<i>S. aureus</i>	<i>Staphylococcus aureus</i>
SAR	Structure-activity relationship
<i>S. parasanguinis</i>	<i>Streptococcus parasanguinis</i>
TET	Tetracycline
TOB	Tobramycin
WHO	World Health Organization
%	Percentage
µg	Microgram
µge	Microgram equivalent
µm	Micrometer
µM	Micromolar
µL	Microliter
ml	Milliliter

CHAPTER 1: General introduction

Statement of Contribution to Co-authored Published Paper

This chapter is a combination of published peer reviewed review article (**Sections 1.1 - 1.5**) and unpublished review (**Section 1.6**). The bibliographical details are:

THI, M.T.; WIBOWO, D.; REHM, B.H.A. *Pseudomonas aeruginosa* Biofilms. *International Journal of Molecular Sciences* **2020**, *21*, doi:10.3390/ijms21228671. A published peer reviewed review article as first author publication.

Appropriate acknowledgements of those who contributed to the research but did not qualify as authors are included in each paper.

My contribution to the published paper involved:

- Conception and design
- Manuscript preparation

Signed: **Minh Tam Tran Thi**
PhD Candidate

Date: 10th April, 2022

Countersigned: **Bernd Rehm**
Principal Supervisor

Date: 10th April, 2022

1.1 Introduction

Pseudomonas aeruginosa is an ubiquitous Gram-negative bacterium that causes nosocomial infections, as well as fatal infections in immunocompromised individuals, such as patients with cancer, post-surgery, severe burns or infected by human immunodeficiency virus (HIV) [1-3]. In 2017, *P. aeruginosa* was recognized as one of the most life-threatening bacteria and listed as priority pathogen for Research and Development of new antibiotics by the World Health Organization [4]. Common antimicrobial agents like antibiotics frequently exhibit limited efficacy due to adaptability and high intrinsic antibiotic resistance of *P. aeruginosa*, thus increasing mortality [5]. Additionally, treatment of these infections is also hindered by the *P. aeruginosa* ability to form biofilms which protect them from surrounding environmental stresses, impedes phagocytosis and thereby confers capacity for colonization and long-term persistence [6]. Such ability is promoted by effective cell-to-cell communications within the microbial communities of *P. aeruginosa* known as quorum sensing (QS). As a result, highly structured biofilms can be formed which is often identified in patients with chronic infections, such as chronic lung infection, chronic wound infection and chronic rhinosinusitis [7]. It has been estimated that biofilms have a substantial bearing on over 90% of chronic wound infections, resulting in poor wound healing. In the United States alone, approximately 6.5 million patients are affected by chronic wound infections, which results in a high health-care burden and devastating economic consequences estimated at over US\$25 billion annually [8]. It is important therefore to diagnose *P. aeruginosa* infections at an early stage before biofilm development which could enhance the susceptibility of *P. aeruginosa* towards antimicrobial treatments. However, the increasing incidence of acute and persisting infections worldwide also highlights the need to develop therapeutic strategies as an alternative to traditional antibiotics, expectedly to disarm and eradicate this Gram-negative bacterium.

This review highlights the *P. aeruginosa* biofilms starting from its composition, structure and development processes to the extraordinary capabilities of *P. aeruginosa* to invade host immune system and escape antibiotic treatments via biofilm-mediated resistance which is regulated mainly by quorum sensing. In the context of challenges facing *P. aeruginosa* devastating infections, recent diagnostics and therapeutic strategies will be discussed.

1.2 *Pseudomonas aeruginosa* biofilm

In nature, most bacteria can attach to different surfaces and form biofilms [9]. Biofilm is a complex aggregate of bacteria encased in a self-generated matrix of extracellular polymeric substances (EPS) and is one of the key strategies for the survival of species during unexpected changes of living conditions such as temperature fluctuation and nutrient availability [10]. Bacteria within a biofilm can escape host immune responses and resist antimicrobial treatments up to 1,000 times more than their planktonic counterparts [11]. *P. aeruginosa* is a well-known biofilm former, which makes it an excellent model to study biofilm formation [12,13]. A resilient biofilm is a critical weapon for *P. aeruginosa* to compete, survive and dominate in the cystic fibrosis lung polymicrobial environment [14]. *P. aeruginosa* also effectively colonizes a variety of surfaces including medical materials (urinary catheters, implants, contact lenses, etc.) [12], and food industry equipment (mixing tanks, vats and tubing) [15]. Therefore, a greater understanding of the composition and structure of the biofilm, and the molecular mechanisms underlying the antimicrobial tolerance of bacteria growing within a biofilm, are vital for the design of effective strategies to manage, prevent and more importantly to eradicate biofilm-associated infections.

1.2.1 Biofilm composition

The biofilm is a complex aggregate of bacteria encased in a self-generated matrix of extracellular polymeric substances (EPS) and is one of the key strategies for the survival of species against unexpected changes of living conditions such as temperature and nutrient availability [10,16,17].

It has been shown that *P. aeruginosa* biofilm matrix primarily encompasses polysaccharides, extracellular DNA (eDNA), proteins and lipids [12,18]. The matrix, which is responsible for more than 90% of biofilm biomass, acts as a scaffold for adhesion to biotic and abiotic surfaces and shelter for encased bacteria in harsh environmental conditions (antibiotics and host immune responses). It also provides a repertoire of public goods including essential nutrients, enzymes and cytosolic proteins for the biofilm community. The matrix also facilitates cell-to-cell communication [18-20].

The three exopolysaccharides, i.e., Psl, Pel and alginate, are tremendously involved in surface attachment, formation and the stability of biofilm architecture [12,21]. The roles of individual exopolysaccharides are discussed below.

Psl is a neutral pentasaccharide typically comprising D-glucose, D-mannose and L-rhamnose moieties [22,23]. This exopolysaccharide is necessary for adhesion of sessile cells (cells attached to a surface) to surfaces and cell-to-cell interactions during biofilm initiation of both nonmucoid and mucoid strains [12,24,25]. Psl has the following characteristics: (i) Psl is beneficial for biofilm communities, but not for unattached populations; (ii) better growth of non-Psl producing cells was observed in mixed biofilm with Psl producing cells [21,26]; (iii) during biofilm growth, Psl positive populations dominate Psl negative populations; and (iv) Psl nonproducers are unable to exploit Psl producers [26]. In a mature biofilm, Psl is located in peripheries of the mushroom-like structure where it helps maintain structural stability [22]. Increased Psl expression is linked to induction of cell aggregates in a liquid culture which is a phenotype observed in CF patients' sputum [27,28]. Psl functions as a signaling molecule to promote the production of c-di-GMP (bis-(3'-5')-cyclic dimeric guanosine monophosphate) whose level, if elevated, results in thicker and more robust biofilms [28]. Additionally, Psl shields biofilm bacteria from antimicrobials [21] and neutrophil phagocytosis [29], making it an effective defense to achieve persistent infection.

Pel is a cationic polysaccharide polymer of partially deacetylated *N*-acetyl-D-glucosamine and *N*-acetyl-D-galactosamine. Like Psl, Pel is an essential matrix component of biofilm in nonmucoid strains and is involved in the initiation of surface attachment, as well as maintenance of biofilm integrity [30,31]. Pel is responsible for the pellicle biofilm which is formed at the air-liquid interface of a static broth culture [32]. The synthesis of Psl and Pel are strain-specific and can be switched in response to surrounding conditions [33]. Pel promotes the tolerance to aminoglycoside antibiotics for biofilm-embedded bacteria [34]. Furthermore, Pel containing biofilms has been demonstrated to be refractory to the antibiotic colistin and less susceptible to killing mediated by neutrophils derived from human HL-60 cell lines [35]. Unlike Psl, Pel is not public goods and not available for Pel negative cells in both biofilm and unattached populations [26].

Alginate is predominately produced in the biofilm of mucoid *Pseudomonas* strains due to a mutation in *mucA22* allele. The mucoid phenotypes are found mostly in CF isolates, signifying the conversion from acute to chronic infection [36,37]. Alginate is a negatively charged acetylated polymer consisting of mannuronic acid and guluronic acid residues [38]. A wide range of important functions of alginate including biofilm maturation, protection from phagocytosis and opsonization, and decreased diffusion of antibiotics through the biofilm has been well-documented [18,39-41]. The ratios between mannuronic acid and guluronic acid influence the viscoelastic properties of biofilms which lead to impairment of cough clearance in the lung of CF patients infected with *P. aeruginosa* [42-44].

Cell lysis releases DNA into the environment, and this extracellular DNA (eDNA) is one of the crucial constituents of biofilms. Cell lysis can be caused by environmental stress such as the antimicrobial treatment via the endolytic activity of endolysin Lys which is encoded in the R- and F-pyocin gene cluster. This can occur in both early development of biofilms and the planktonic phase where rod-shaped bacteria rapidly turn into round cells resulting from structural damage of the cell wall and followed by lysis. The released eDNA, cytosolic proteins and particularly RNA are subsequently encapsulated into membrane vesicles (MVs) which are formed via membrane fragments originating from the lysed cells [45]. eDNA can also be localized on the surface and the stalk of the mushroom-like microcolonies [46,47]. eDNA is involved in various processes: (i) as a nutrient source for bacteria in the biofilm; (ii) supporting cellular organization and alignment via twitching motility; (iii) as a cation chelator that interacts with divalent cations (Mg^{2+} and Ca^{2+}) on the outer membrane and subsequently activates the type VI secretion system which disseminates virulence factors within the host; (iv) the deposition of eDNA caused biofilm environment and infection sites to become acidic, limiting the penetration of antimicrobial agents; and (v) the presence of eDNA in *P. aeruginosa* biofilms can influence the inflammatory process activated by neutrophil [48-51].

It is noteworthy to mention the intracellular biopolymer, polyhydroxyalkanoate (PHA), that does not directly play a structural role in the biofilm matrix but is produced in cells within the biofilm. PHA, a carbon and energy storage polymer, has been implicated in stress tolerance as well as attachment to abiotic surfaces such as glass [52]. Within microaerophilic/anaerobic zones of the biofilm, PHA might serve as an electron sink to maintain energy-generating metabolic processes [6,16].

1.2.2 Biofilm development

P. aeruginosa has been demonstrated to grow slowly as unattached cell aggregates under hypoxic and anoxic conditions, which are comparable to what has been observed in CF airways and chronic wounds [53]. Slow growth rates in the limited presence of oxygen are ascribed to antibiotic recalcitrance. Generally, biofilms of *P. aeruginosa* can be developed on abiotic surfaces, such as medical implants or industrial equipment. The biofilm development is divided into five distinct stages (**Figure 1.1**). *Stage I*: Bacterial cells adhere to a surface via support of cell appendages such as flagella and type IV pili [54,55]. The restricted flagellar movement has been implicated in mediating twitching motility and biosynthesis of exopolysaccharides required for surface association [56]. This adherence is reversible. A proteomic study with wild-type PAO1 concluded that the bacterial responses and biofilm formation are material specific. It is evident through records of the presence of specific bacterial proteins and their altered quantities when *P. aeruginosa* sense and react in response to a given surface [57]. *Stage II*: Bacterial cells undergo the switch from reversible to irreversible attachment. *Stage III*: Progressive propagation of attached bacteria into a more structured architecture, termed microcolonies. *Stage IV*: These microcolonies develop further into extensive three-dimensional mushroom-like structures, a hallmark of biofilm maturation. *Stage V*: In the center of the microcolony, matrix cavity is disrupted through cell autolysis for the liberation of dispersed cells [22] followed by the transition from sessile to planktonic growth mode for seeding of uncolonized spaces (*Stage VI*), which allows the biofilm cycle to repeat [58]. It was recently demonstrated that endonuclease EndA is required for dispersion of existing biofilm via eDNA degradation [59]. The structure of the formed biofilms is influenced by the swarming motility with flat biofilms resulting from highly motile bacteria, while mushroom-shaped biofilms are generated by cells with low motility, and that the motility rate was nutrient specific [60].

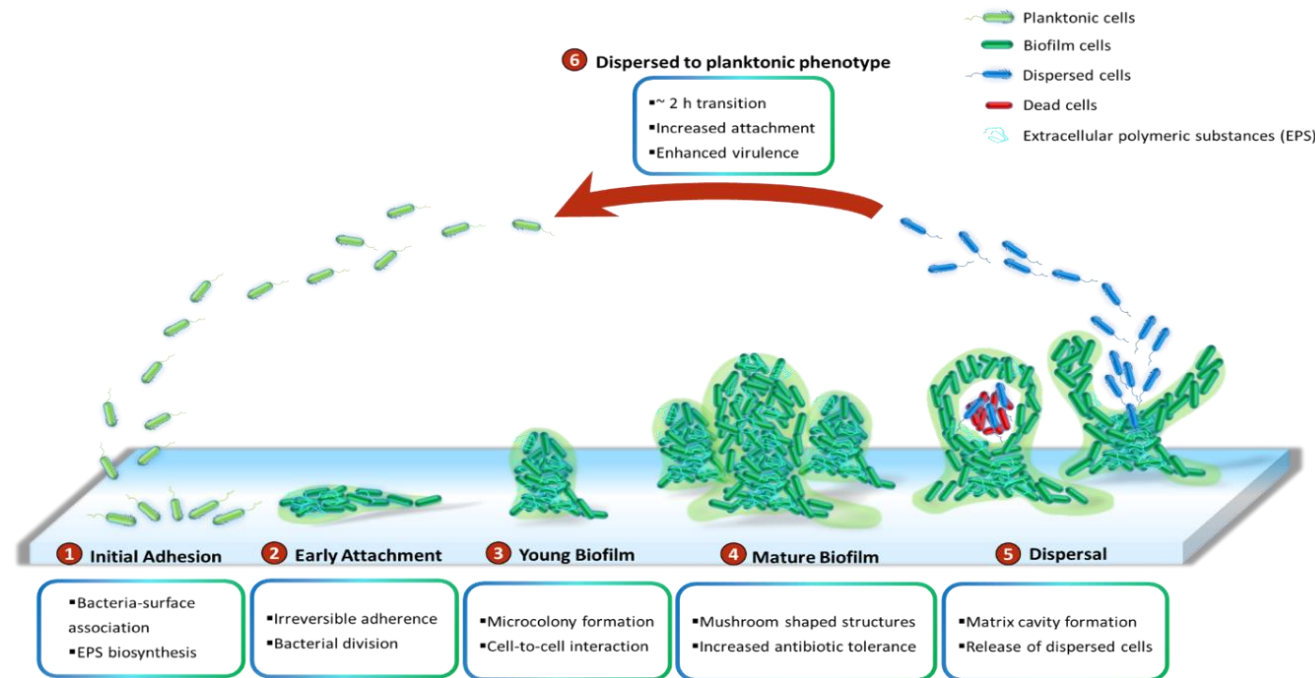


Figure 1. 1 Cycle of *P. aeruginosa* biofilm development. The development cycle is divided into six stages. Initially, the bacteria associate with the surface and produce extracellular polymeric substances (EPS) including proteins, polysaccharides, lipids and eDNA. Next, cell division and the transition of reversible attachment into irreversible take place. The following steps are the formation of microcolonies and the further development of these microcolonies into mushroom-shaped structures. Cell-to-cell interaction and production of virulence factors play essential roles in maturation and robustness of biofilms. Matrix cavity is then formed in the center of microcolony via cell autolysis to disrupt the matrix for the liberation of the dispersed population. Finally, the released cells undergo an approximately 2 h transition into planktonic phenotypes which subsequently occupy uncolonized spaces.

While it is well-perceived that biofilm cells are physiologically different from their planktonic counterparts and more recalcitrant to antimicrobial treatments [10], little is known about intermediate events between attached forms and the free-swimming lifestyle which generates highly virulent detached cells. It is suggested that the transition from detachment to planktonic growth involves a distinct stage of biofilm development (*Stage VI*) (**Figure 1.1**). These cells, in contrast to both planktonic and sessile cells, possess distinct physiology and represent the conversion from chronic to acute infections. They turn into a planktonic phenotype after remaining in a 2-hour lag phase with decreased levels of pyoverdine and intracellular c-di-GMP [61,62]. Upregulation of virulence encoding genes and downregulation of iron uptake genes were observed in the dispersed population [10,63-65]. Both *in vitro* and *in vivo* experiments revealed that liberated cells are highly cytotoxic to macrophages, more sensitive to iron depletion and substantially virulent to nematode hosts relative to planktonic bacteria [63]. Notably, dispersed bacteria originating from biofilms treated with glycoside hydrolase rapidly disseminated and induced fatal septicemia in a mouse chronic wound infection model [66].

1.2.3 Multispecies biofilm

Generally, infections are not caused by monospecies alone but rather colonization of a complex polymicrobial community [67,68]. *P. aeruginosa* is often recognized as a co-colonizer along with other microbes such as *Staphylococcus aureus* (*S. aureus*), *Burkholderia cenocepacia* (*B. cenocepacia*) and *Streptococcus parasanguinis* (*S. parasanguinis*). For example, colonization of the biofilm-forming bacteria *P. aeruginosa* and *S. aureus* coinfects the lungs of CF patients and in diabetic and chronic wounds [69,70]. During co-infection, *P. aeruginosa* could sequester iron and nutrients through lysis of Gram-positive bacteria, including *S. aureus*, *Streptococcus pneumoniae* and *Bacillus anthracis* [67], as well as other Gram-negative bacteria *Burkholderia cepacia* [71].

In dual-species colonization containing *P. aeruginosa* and *S. aureus*, the presence of *S. aureus* derived peptidoglycan, *N*-acetylglucosamine (GlcNAc), induced *P. aeruginosa* to produce pyocyanin which functions as antimicrobials and toxins that could reduce the viability of *S. aureus* within the biofilm [68]. The transition from nonmucoid *P. aeruginosa*, which generate antimicrobial siderophores, rhamnolipids and 2-heptyl-4-hydroxyquinoline-*N*-oxide (HQNO), to mucoid phenotypes, which overproduce alginate,

resulted in the decline of these exoproducts, leading to the cohabitant of *P. aeruginosa* and *S. aureus* [72]. *S. aureus* could also secrete extracellular adhesin known as staphylococcal protein A (SpA) which bound to Psl and type IV pilli on the *P. aeruginosa* cell surface, resulted in the inhibition of both biofilm formation of *P. aeruginosa* and phagocytotic activity of neutrophil towards *P. aeruginosa* [73]. *P. aeruginosa* has been demonstrated to outcompete *S. aureus* in the dual-species community by producing diguanylate cyclase, SiaD, which is activated by Psl, during the early stage of biofilm formation [74].

Similarly, synergistic interactions between *P. aeruginosa* and *B. cenocepacia* have been observed [75]. In planktonic co-cultures, *P. aeruginosa* predominated due to the production of secondary metabolites which inhibited the growth of *B. cenocepacia*. Moreover, co-existence in *B. cenocepacia* biofilm promoted biofilm biomass of *P. aeruginosa*. Co-infection of the two species was found to advance lung damage in a mouse model [75].

Although *P. aeruginosa* remains dominant in mixed-species biofilms by producing antimicrobial compounds which modulate the growth of other microorganisms, its pathogenesis was shown to be inhibited by oral streptococci strains during co-infection, resulting in improved CF lung conditions [76]. The oral commensal streptococci outcompeted *P. aeruginosa* by the production of hydrogen peroxide in the presence of nitrite [77]. Furthermore, it was shown that oral commensal *S. parasanguinis* could effectively exploit the exopolysaccharide alginate produced by *P. aeruginosa* CF isolate FRD1 strain to promote its biofilm *in vitro* through the mediation of the streptococcal surface adhesin BapA1. However, either adhesin BapA1 or Fap1 was adequate to reduce the colonization of alginate producing *P. aeruginosa* in *Drosophila melanogaster* [78].

1.3 Quorum sensing in biofilm development

The development of *P. aeruginosa* biofilms requires population-wide coordination of individual cells within bacterial communities [79]. *P. aeruginosa* uses multiple interconnected signal transduction pathways known as quorum sensing (QS), enabling the bacteria to communicate between the individual cells and ultimately orchestrate collective behavior which is essential for the adaptation and survival of whole communities. *P. aeruginosa* enters into the QS mode in response to changes in cell density and environmental cues or stresses [80]. QS involves the production, secretion and

accumulation of signaling molecules called autoinducers (AI) whose specificity and concentration are sensed by transcriptional regulators [81], resulting in the expressions of specific sets of genes on a population-wide scale. In addition to biofilm development, QS has been linked to the regulation of other physiological processes, including virulence-factor production, stress tolerance, metabolic adjustment and host-microbe interactions [6]. Thus, understanding and controlling these chemical communication systems could lead to new targets for alternative or complementary treatments to conventional antimicrobials and antibiotics.

There are four distinct pathways in the QS circuits of *P. aeruginosa*, namely Las, Rhl, PQS and IQS that intracellularly produces their cognate AI molecules, i.e., *N*-3-oxo-dodecanoyl-L-homoserine lactone (3O-C₁₂-HSL), *N*-butyryl-L-homoserine lactone (C₄-HSL), 2-heptyl-3-hydroxy-4-quinolone (PQS) and 2-(2-hydroxyphenyl)-thiazole-4-carbaldehyde (IQS), respectively (**Figure 1.2**). These QS circuits are organized in a hierarchy with the Las system at the top of the cascade [82]. Both Las and Rhl systems are triggered by an increased cell density at the preliminary exponential growth phase, whereas PQS and IQS systems are activated at late exponential growth phase [83] especially under iron limitation [84] and phosphate starvation conditions [85], respectively. The synthesized AIs undergo membrane trafficking directed to outside then inside of the cells, presumably mediated by free diffusion, efflux pumps or outer membrane vesicles [86]. The trafficked 3O-C₁₂-HSL is then bound to the regulator protein LasR, and the formed complex activates *lasI* synthase gene, leading to the autoinduction feed-forward loop [87]. The LasR–3O-C₁₂-HSL also induces the expression of *rhlR* and *rhlI* genes as well as the *pqsR* and *pqsABCDH* genes which encode the Rhl [82] and the PQS [88] systems, respectively. Similar to the Las system, the RhlR–C₄-HSL complex induces *rhlI* gene expression that activates the second autoinduction feed-forward loop [89]. In the PQS system, the PqsR–PQS complex activates *pqsABCDH* genes as well as feeds back to induce *rhlRI* gene expression [90]. The expression of both *pqsR* and *pqsABCDH* genes can be inhibited by RhlR, which has been suggested as a way to control the correct ratio between 3-oxo-C₁₂-HSL and C₄-HSL, hence controlling the activation of PQS pathway [91]. The identification of IQS system was relatively new as compared to the other QS systems. In the IQS system, the identity of the transcriptional regulator is still unknown although its binding to the IQS has been found to activate the *pqsR* gene [92,93]. In addition, the IQS molecule was proposed to be enzymatically produced from the proteins encoded by *ambBCDE* genes [92]. However, the

recent identification of the IQS molecule (an aeruginaldehyde) revealed that it is a byproduct of the siderophore pyochelin biosynthesis [94,95]. On the other hand, *ambBCDE* genes encode for proteins involved in the biosynthesis of the anti-metabolite L-2-amino-4-methoxy-trans-3-butenic acid (AMB) [96].

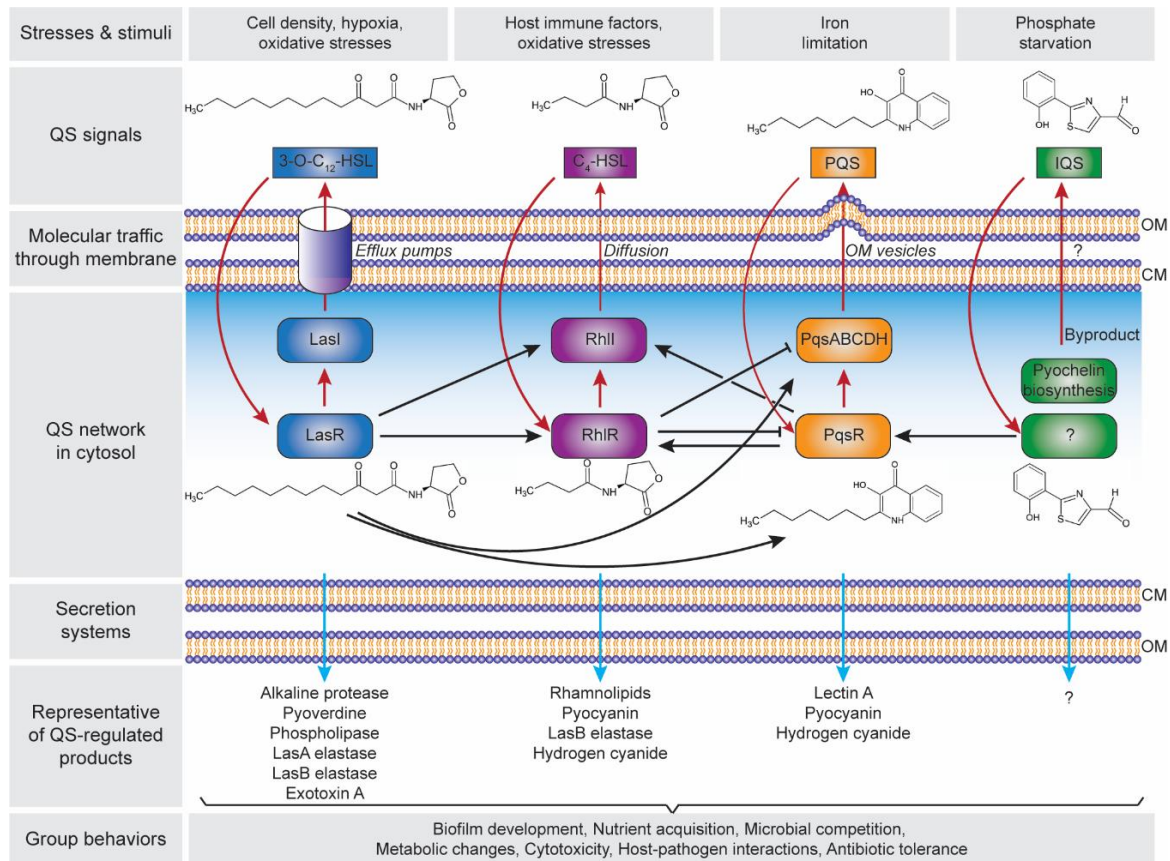


Figure 1. 2 Hierarchical quorum-sensing (QS) network in *Pseudomonas aeruginosa*. The four QS pathways are activated in response to the cell density and environmental stimuli, with four autoinducer synthases including LasI, RhlI, PqsABCDH and AmbBCDE that produce N-3-oxo-dodecanoyl-L-homoserine lactone (3O-C₁₂-HSL), N-butyryl-L-homoserine lactone (C₄-HSL), 2-heptyl-3-hydroxy-4-quinolone (PQS) and 2-(2-hydroxyphenyl)-thiazole-4-carbaldehyde (IQS), respectively. Note: the autoinduction is depicted in red arrows; the receptor for IQS is still unknown. The QS products are secreted through the cell membrane, that control the group behaviors and essential for the adaptation, survival and pathogenicity of *P. aeruginosa*. Abbreviation: CM, cytoplasmic membrane; OM, outer membrane.

The Las, Rhl and PQS systems in the QS network of *P. aeruginosa* play important roles in the production of the functional elements that have an impact on biofilm development (**Figure 1.2**). These include rhamnolipid [97,98], pyoverdine [99], pyocyanin [100,101], Pel polysaccharides [102], and lectins [103,104]. Rhamnolipid is a rhamnose-containing glycolipidic compound (i.e., biosurfactant) that functions to preserve the pores and channels between microcolonies, enabling the passage of liquid and nutrients within mature biofilms. Pyoverdine can sequester iron in the environment and deliver it to the cell which is an essential component for biofilm development. In an environment where iron is limited, twitching motility is more favored than sessile growth and thus inhibiting biofilm formation [105]. Pyocyanin is a secondary metabolite with a cytotoxicity effect, thereby inducing cell lysis and releasing the cells' DNA to extracellular space (i.e., eDNA – one of the biofilm components). Pyocyanin can bind to the eDNA and causes an increase in solution viscosity, thus also increasing the physicochemical interactions between biofilm matrices and the surrounding environment as well as promoting cellular aggregation. Pel polysaccharides can also interact with eDNA through cationic-anionic interactions within the biofilm matrix, strengthening the biofilm structure. Lectins are soluble proteins located in the outer membrane which consist of two forms, i.e., LecA (that binds to galactose and its derivatives) and LecB (that binds to fucose, mannose and mannose-containing oligosaccharides). Such adhesive properties of lectins facilitate the retention of both cells and exopolysaccharides in a growing biofilm, contributing to the biofilm structure, as well as adhesion to biological surfaces such as epithelium and mucosa. Collectively, such molecular and cellular interactions in combination with other polymeric substances lead to the establishment of a robust and mature biofilm.

1.4 Diagnostics

Rapid and accurate diagnostics for *P. aeruginosa* infections, especially at the early stages, are particularly important to ensure effective treatments and to prevent the conversion to devastating chronic infections. Although the conventional microbiological culture of patient sputum is a routine procedure in most of the laboratories, there are currently many innovative technologies that have been developed to improve speed, accuracy and specificity of detection methods, and thereby advancing management and surveillance of diseases. Here, the development of diagnostic tests and their advantages and disadvantages will be discussed.

1.4.1 Conventional microbiological culture

Misidentification of *P. aeruginosa* infections is not uncommon and is an increasing concern in the clinical environment as the bacteria exhibit diverse morphologies such as small colony variants, rough small colony variants, wrinkle variants, etc. As the diseases progress to chronic infections with biofilm formation, the isolated bacteria display distinct phenotype – cell aggregates which form “sticky” colonies [106]. Importantly, biofilm bacteria from long-term chronic infections in CF lung exhibit slow growth or uncultivability, which make biofilm infections difficult to be identified by conventional microbial culture of clinical specimens and biochemical reactions [107,108]. The use of automated identification systems including BD Phoenix [107], the bioMérieux Vitek 2 [109] and MicroScan WalkAway [110] for bacterial detection and antimicrobial susceptibility testing (AST) have been broadly used in several clinical settings. Various readouts such as turbidimetric, kinetic, colorimetric and fluorescent signals resulting from microbial growth, a variety of enzymatic based reactions and broth microdilution tests are measured to detect the bacterial presence and antimicrobial susceptibility [111-113]. Nonetheless, it has been reported that these expensive systems lack specificity and accuracy, and required highly skilled personnel, regular software upgrade and frequent reference database update [109,114].

1.4.2 Molecular biology methods

Polymerase chain reaction (PCR) is one of the most common methods utilized for the identification of *P. aeruginosa*. It has been designed to target several specific genes such as the 16S rRNA, *oprI*, *oprL*, *algD*, *gyrB*, *toxA*, *ecfX*, *ETA*, and *fliC*. Further examination of the specificity of *P. aeruginosa* genes showed that *ecfX*, *oprL* and *gyrB* have high sensitivity and specificity [115,116]. Multiplex PCR targeting more than one gene of interest in a single reaction may be an option to effectively address false positive and false negative results obtained using conventional PCR. This method, albeit faces the main disadvantage of designing primers with high specificity in the abundant presence of gene targets [117]. Real-time fluorescence-based quantitative PCR (RT qPCR) has been established to identify pathogens accurately and specifically. Numerous studies have developed RT qPCR assay to detect *P. aeruginosa* in CF patients with shorter turnaround time [116,118,119]. Another approach is polymerase spiral reaction (PSR) which has

allowed rapid identification of *P. aeruginosa* in the sputum of intensive care unit (ICU) patients within 60 minutes under isothermal conditions with 10-fold higher sensitivity compared to conventional PCR [120].

1.4.3 Mass spectrometry

Matrixed-assisted laser desorption/ionisation time-of-flight mass spectrometry (MALDI-TOF MS) has gained popularity for speedy and reliable detection of *P. aeruginosa* in microbiology practice with high throughput capabilities at low costs [121]. It generates ribosomal protein-based peptide mass fingerprint (PMF) profiles of investigated microorganisms which are compared to reference PMF database to identify and characterize bacteria in clinical samples [122,123]. Microbial identification by MALDI-TOF MS was not affected by culture conditions such as culture media and culture duration [124,125]. Recent applications of this technique include characterization of species and identification of resistance or virulence biomarkers of multidrug-resistant pathogens [126,127]. Additionally, MALDI-TOF MS profiling has been demonstrated to be capable of differentiating different biofilm stages and capturing phenotypic changes during biofilm development. This technique may be a valuable tool for clinical biofilm infection detection, particularly in early stages, and thus improvement of patient outcomes [128].

1.4.4 Nanoparticle biosensor

Quorum sensing of *P. aeruginosa* produces specific molecules, including pyocyanin and LasA protease, that have been subjected to analyses for detection of *P. aeruginosa*. Traditional methods to identify pyocyanin are based on ultraviolet-visible (UV-Vis) spectrophotometry that detects absorbance peaks at both 382 and 521 nm, and liquid chromatography-mass spectrometry (LC-MS) that measure molecular mass at 211 g/mol [129]. On the other hand, LasA protease can be identified using sodium dodecyl sulfate-polyacrylamide gel electrophoresis [130]. However, those methods are time-consuming as they require the target molecules/proteins to be purified from bacterial cultures. Recently, nanoparticles have been developed to allow rapid identification of pyocyanin [131] and LasA protease [132] with high sensitivity even in the presence of other species within cell cultures. Gold nanoparticles (Au NPs) deposited onto indium tin oxide electrodes was able to enhance the detection of pyocyanin at a concentration as low as 40 μ M as compared to

the minimum 80 μM of pyocyanin detected using unmodified electrodes [131]. Encapsulating the Au NPs with a thin layer of polyaniline hydrochloride (PANI) forming PANI/Au core-shell NPs increased the sensitivity of the PANI/Au NPs-modified electrodes towards pyocyanin down to 36 μM , which could accelerate the diagnostic process, achieving effective treatments and prevention of chronic infections [131]. Magnetic NPs have also been developed as biosensors toward LasA protease by functionalizing the NPs with (glycine)₃ peptides and then linking them onto a gold-coated paper substrate [132]. LasA protease in the cell cultures could cleave the peptides from NPs, and the cleaved NPs could attract to external magnetic forces revealing the golden color of the sensor surface which could then be detected colorimetrically [132]. Such simple biochip allowed rapid identification of *P. aeruginosa* in clinical samples such as sputum, ear and wound in less than one minute with a detection limit of 10^2 cfu/mL [132], which could expectedly become a useful point-of-care diagnostic device.

1.5 Therapeutic strategies

Therapeutic management of *P. aeruginosa* infections poses unique challenges for the clinical use of conventional antimicrobials. This bacterium displays multiple drug tolerance mechanisms which can be categorized into intrinsic, acquired and adaptive mechanisms. Biofilm formation as an adaptive mechanism is considered as the key virulence factor enhancing the survival of exposure to antibiotics and initiating chronic infections [133]. As the development and dispersal of biofilm are regulated by a multifactorial process entailing quorum sensing systems, exopolysaccharides and c-di-GMP [58], biofilm remediation strategies are required to target different constituents of biofilm matrix and biofilm-residing cells [134]. Moreover, it is critical to consider the interaction between the host immune system and the infectious agents when treating biofilm-related infections [135,136]. Importantly, clinical chronic infections are frequently diagnosed with co-infections of multi-species, which profoundly worsen the patient outcomes as compared to mono-infections. This has greatly challenged biofilm therapeutic strategies aiming at disrupting biofilm community of mono-species [137,138]. Efforts have been developed to tackle these challenges by targeting biofilm components, inducing biofilm dispersal, inhibiting quorum sensing and targeting iron metabolism using various antimicrobial agents, including antimicrobial peptides, biofilm-degrading enzymes, quorum sensing inhibitor, and iron

chelator. We provided a summary of current therapeutic strategies targeting *P. aeruginosa* biofilms including advantages and limitation of individual approaches (**Table 1.1**).

Table 1. 1 Summary of therapeutic strategies against *P. aeruginosa* infections

Therapeutic approach	Activity	Advantages	Limitation	References
Antimicrobial peptides	<ul style="list-style-type: none"> • Antibacterial • Antibiofilm • Immunological modulator 	<ul style="list-style-type: none"> • Low cytotoxicity • Combined treatment possibility • Low resistance 	<ul style="list-style-type: none"> • Sensitive to salt, serum and pH • Susceptible to host proteolysis • Expensive production 	[139-144]
Antibiotics	<ul style="list-style-type: none"> • Antibacterial 	<ul style="list-style-type: none"> • Inhaled antibiotic class • Broad-spectrum • Safety • Improvement of lung function in CF patients 	<ul style="list-style-type: none"> • Resistance development 	[145]
Lectin inhibitor	<ul style="list-style-type: none"> • Antibiofilm 	<ul style="list-style-type: none"> • High stability • Low resistance 	<ul style="list-style-type: none"> • No <i>in vivo</i> data • Toxicity • Narrow spectrum 	[146-148]
Bacteriophages	<ul style="list-style-type: none"> • Antibacterial 	<ul style="list-style-type: none"> • Delivery at the infection site • High specificity • Fewer side effects • Easy administration 	<ul style="list-style-type: none"> • Poor stability • Undesired cytotoxicity • Resistance development • Insufficient pharmacokinetics and pharmacodynamics data 	[149-153]
Natural products	<ul style="list-style-type: none"> • Antibacterial 	<ul style="list-style-type: none"> • Broad-spectrum 	<ul style="list-style-type: none"> • Cytotoxicity 	[154]

Therapeutic approach	Activity	Advantages	Limitation	References
	<ul style="list-style-type: none"> • Antibiofilm • Quorum sensing modulator 	<ul style="list-style-type: none"> • Multiple mechanisms of action 	<ul style="list-style-type: none"> • Resistance development • Limited penetration into biofilm • Limited killing effects on slow-growing bacteria • Availability and accessibility • Complex extraction and isolation 	
Nanoparticles	<ul style="list-style-type: none"> • Antibacterial • Antibiofilm 	<ul style="list-style-type: none"> • Broad-spectrum • Combination with antibiotics/therapeutic agents • Small size, thus direct delivery to targets 	<ul style="list-style-type: none"> • Cytotoxicity • Host metabolism of nanoparticles 	[155,156]
Nanocarriers (Liposomes, solid lipid and polymeric)	<ul style="list-style-type: none"> • Drug delivery 	<ul style="list-style-type: none"> • Protection of therapeutic agents from inactivation and degradation by bacterial and host system • Enhancement of efficacy • Penetrability into the biofilm matrix 	<ul style="list-style-type: none"> • Cytotoxicity • Host metabolism of nanoparticles 	[157-159]
EPS inhibitors	<ul style="list-style-type: none"> • Anti-EPS 	<ul style="list-style-type: none"> • Biofilm matrix degradation 	<ul style="list-style-type: none"> • Incomplete biofilm 	[35,160,161]

Therapeutic approach	Activity	Advantages	Limitation	References
		<ul style="list-style-type: none"> • Limited/no effect on bacterial viability • Low risk of resistance development • Augmentation of antibiotic efficacy to clear the infection 	<ul style="list-style-type: none"> • matrix disruption • Cytotoxicity 	
Biofilm dispersers	<ul style="list-style-type: none"> • Dispersal induction 	<ul style="list-style-type: none"> • Augmentation of antibiotic efficacy to clear the infection • Promotion of self-disassembly • Low risk of resistance development 	<ul style="list-style-type: none"> • Release of harmful dispersed cells for re-colonization and lethal septic event • Cytotoxicity 	[66,162]
QS inhibitors	<ul style="list-style-type: none"> • Biofilm prevention • Biofilm inhibition 	<ul style="list-style-type: none"> • Reduction of virulence factors • No effect on bacterial viability 	<ul style="list-style-type: none"> • Narrow spectrum • Unwanted effect on bacteria 	[163-165]
Iron chelator	<ul style="list-style-type: none"> • Interference with iron metabolism 	<ul style="list-style-type: none"> • Bactericidal activity • Biofilm prevention • Low risk of resistance development 	<ul style="list-style-type: none"> • Cytotoxicity • Co-administration with antibiotics 	[166,167]
Photodynamic therapy	<ul style="list-style-type: none"> • Antibacterial 	<ul style="list-style-type: none"> • No resistance development 	<ul style="list-style-type: none"> • Potential side effects (e.g 	[168-172]

Therapeutic approach	Activity	Advantages	Limitation	References
	<ul style="list-style-type: none">• Antibiofilm	<ul style="list-style-type: none">• Improved selectivity• No photocytotoxicity	burns, redness swelling of treated skin)	
Photothermal therapy	<ul style="list-style-type: none">• Antibacterial• Antibiofilm	<ul style="list-style-type: none">• No resistance development• Improved selectivity• Negligible cytotoxicity	<ul style="list-style-type: none">• Photothermal ablation of host tissues	[173-176]

1.5.1 Nanoparticles

Nanoparticles (NPs) have been used to assist in the delivery of such antimicrobial agents to the sites of infection such as penetration of antibiotics into biofilms. There are other promising delivery systems including liposomes, solid lipid NPs and polymeric NPs whose *in vivo* efficiency, potential cytotoxicity and interactions between host immunity and NPs, still await further investigation [177-179]. In addition to its carrier functionality, NPs have been used as an antimicrobial agent. For example, silver NPs were shown to have antimicrobial action with minimal cytotoxicity against clinical *P. aeruginosa* strains from nosocomial infections which are resistant to certain antibiotics [155]. Furthermore, polyphosphoester NPs co-loaded with silver acetate and minocycline substantially increased the susceptibility of *P. aeruginosa* [156]. Conjugation of azlocillin antibiotic onto silver NPs resulted in significantly promoted antibacterial efficacy compared to either NPs alone, or azlocillin alone, or co-administration of NPs and azlocillin [180].

1.5.2 Targeting EPS component and structure

Therapeutic approaches targeting components of biofilm matrices are an option to tackle *P. aeruginosa* infections. There are several types of enzymes employed to degrade biofilm matrix: alginate lyases [181], glucanohydrolases (e.g. dextranase and mutanase) [182], glycoside hydrolase (e.g. PelAh and PslGH) [35], and deoxyribonucleases (e.g. DNase I and DNase1L2) [183,184]. Furthermore, therapies involving a combination between biofilm matrix-degrading enzymes and antibiotics can facilitate biofilm dispersal, improve drug penetration, and therefore maximizing efficacy against established biofilms [160,185].

Alginate inhibitor, such as thiol-benzo-triazolo-quinazolinone, has been demonstrated to interfere with the binding of Alg44 to c-di-GMP. This interference resulted in a declined alginate production in *P. aeruginosa*, which could potentially limit mucoid conversion and reduce a complication in CF patients [186]. Alginate oligomer (i.e., OligoG) inhibited

biofilm formation by inducing disruption of mucoid biofilm through interaction with both EPS and eDNA [161].

1.5.3 Immunotherapies

Bispecific monoclonal antibodies have been investigated as a promising agent to manage the bacterial infection. Anti-Psl, anti-PcrV (Type III Secretion System protein) and BiS4 α Pa (known as MEDI3902) have demonstrated their potential effectiveness towards both management and prevention of infection [187,188]. Monoclonal antibodies targeting a family of bacterial DNA-binding proteins (DNABII), a common component of biofilm which supports the structural stability, have been proved to be promising therapeutic candidates against *P. aeruginosa* biofilm in a mouse lung infection model [189].

1.5.4 Induction of biofilm dispersal

The signal molecule nitric oxide (NO) has been reported to induce biofilm dispersal through modification of intracellular c-di-GMP levels. However, biofilm dispersal was not enhanced by multiples treatments with NO due to the presence of flavohemoglobin in *P. aeruginosa* biofilms. To overcome this, imidazole was utilized to inhibit NO dioxygenase activity of flavohemoglobin produced in NO-pretreated biofilms and restored dispersal activity [162]. Furthermore, low dose NO gas can be used as an adjunctive strategy to potentiate antimicrobial efficacy by dispersing biofilm and exposing dispersed bacteria to antibiotic killing in ex vivo and clinical studies [190].

1.5.5 Inhibition of quorum sensing

Quorum sensing is an attractive target for inhibition and eradication of biofilm. Naturally occurring carotenoid zeaxanthin was found to inhibit biofilm and target LasIR and RhIR QS systems of wild-type PAO1 [191]. The plant flavonoid quercetin has been known for its their pharmacological effects such as reducing the production of pyocyanin and inhibiting the biofilm formation in *P. aeruginosa* [192]. A benzamide-benzimidazole

compound, M64, restricted biofilm development and improved antibiofilm properties of meropenem and tobramycin achieved by inhibiting the controller of QS system, MvfR [193]. Another quorum quenching molecule, *P. aeruginosa* periplasmic enzyme PvdQ acylase, was proved to be a hydrolyzer of *N*-acyl homoserine lactone (AHL), thereby attenuating virulence and alleviating infections *in vitro* and in a mouse pulmonary infection model [194]. Notably, terrein, a bioactive fungal metabolite isolated from *Aspergillus terreus*, has been revealed for the first time as an inhibitor with dual activities against both QS system and c-di-GMP without affecting bacterial viability, thus limiting the development of drug resistance [164]. A recent study identified a quorum quenching enzyme AqdC which decreased the production of alkylquinolone and pyocyanin while increasing levels of elastase. Interestingly, the co-presence of *Rhodococcus erythropolis* isolated QsdA and AqdC resulted in the decline of *N*-acylhomoserine lactone, rhamnolipid as well as elastase levels, suggesting that targeting a complex quorum sensing network may require more than a single enzyme. Indeed, the presence of both enzymes improved the survival of *Caenorhabditis elegans* upon *P. aeruginosa* exposure [163].

1.5.6 Targeting iron metabolism

Iron is known to play vital roles in a range of cellular processes including bacterial growth, DNA replication, biofilm formation and infection establishment [195,196]. Evidently, the enhanced concentration of sputum iron was observed in the lung of CF patients compared to healthy controls [197]. *P. aeruginosa* acquires extracellular iron via iron uptake systems such as the siderophores pyocyanin and pyochelin. Hence, targeting iron metabolism using iron analogues and chelators could be promising strategies to combat *P. aeruginosa* infections. Gallium, structurally similar to iron, was utilized as an iron substitute to impede iron uptake, disrupt iron-dependent pathways, influence bacterial viability and disturb biofilm formation [166]. Combination of tobramycin and FDA-approved iron chelation compounds, i.e., deferoxamine and deferasirox, is another effective approach to disperse pre-existing biofilms, enhance bactericidal activity and prevent biofilm development [167]. Treatment using novel deferoxamine conjugated gallium complexes alone exhibited planktonic killing and biofilm formation disturbance, and when

co-administered the complexes with gentamicin showed substantially enhanced antibiofilm actions [198].

1.5.7 Photodynamic therapy

Photodynamic therapy (PDT) has been demonstrated as a promising approach to tackle bacterial infections in both planktonic and biofilm lifestyles. Its antimicrobial effect relies on the activation of non-toxic photosensitizers (PS) upon exposing to harmless visible light of appropriate spectra in the presence of oxygen to produce cytotoxic reactive oxygen species (ROS) on site [199,200]. These oxygen species act on multiple targets including biofilm matrix, cell membranes and other cellular organelles as well as macromolecules such as lipids, protein, and nucleic acids [201]. Unlike conventional antimicrobials, the mechanism of PDT involves a distinct molecular pathway, hence unlikely inducing resistances [202]. As the efficacy of PDT mainly depends on the PS uptake by bacterial cells, different PS molecules have been employed to improve the cellular internalization [172,203]. Treating *P. aeruginosa* biofilms with the PS, tetracationic porphyrin [5,10,15,20-tetrakis (1-methylpyridinium-4-yl) porphyrin tetra-iodide, Tetra-Py⁺-Me], has resulted in a significant decline of EPS content, suggesting that the EPS may be the target of photoinactivation [204]. GD11, a member of a boron-dipyrrolemethene (BODIPY) dye family, has also been developed as PS against wild-type *P. aeruginosa* PAO1 biofilms [170]. After the irradiation, a substantial cell lethality was observed with minimal impact on biofilm structure and without recurrence of microbial growth after 24 h [170]. A glycosylated photosensitizer pGEMA-I derived from BODIPY has recently been developed to selectively bind to bacteria over human cells [206]. This improved selectivity has led to high bactericidal activity, effective biofilm suppression and reduction of side effects [205]. A recent study has revealed that curcumin mediated PDT was capable of efficiently decreasing viability of both planktonic and biofilm bacteria, and successfully repressing EPS production via inhibition of QS system [206]. Moreover, drug delivery systems such as nanoparticles are also utilized to enhance the stability and the diffusion of the PS into the biofilms. For example, the PS toluidine blue (TB) loaded in mesoporous silica

nanoparticles was capable of considerably reducing the cell viability and biofilm biomass as compared to free TB [172].

1.5.8. Photothermal therapy

Photothermal therapy (PTT) has emerged as an attractive therapeutic modality for combating antibiotic-resistant bacterial infections. PTT involves the use of the near-infrared (NIR) light in a wavelength ranging from 700 to 1100 nm for irradiation of nanomaterials to generate localized heat which causes irreversible damage to nearby bacterial cells [207]. Various photothermal nanomaterials, including carbon-based nanocomposites [208-210], gold and silver nanoparticles [211,212] and conducting polymers [207,213], have been optimized for PTT. For example, gold nanorods (AuNR) surface engineered with phospholipid-polyethylene (PEG) have been developed and utilized against *P. aeruginosa* suspension and biofilm cultures [173]. Upon continuous or pulse activation of laser, severe cell membrane destruction of planktonic cells and marked lethality of the biofilm population were observed [173]. Thiolated graphene (TG) sheet has also been developed for photothermal therapy by functionalizing with S-nitrosothiols, a heat-sensitive NO donor, along with boronic acid, which facilitates cell attachment due to its dense hydroxyl groups, to obtain a multifunctional photothermal agent [175]. Application of this agent with single NIR has led to the simultaneous release of NO and localized heat, both of which are required for effective ablation of bacteria and biofilms in vitro and in vivo with fewer side effects [175]. Recently, bacteriophage has been developed for treatment against antibiotic-resistant bacterial infections due to its high affinity toward bacteria. To overcome the cytotoxicity limitation of bacteriophage-based antibacterial approach, the bacteriophage was conjugated with AuNR [174]. This bioconjugate, phage-AuNR, has shown rapid killing of both planktonic and biofilm cells with minimal effect on mammalian epithelial cells and successful inhibition of phage replication. In addition, this strategy has offered improved specificity towards targeted pathogens via aggregation of phage-AuNR on bacteria, thus it is possibly used for diagnosis of bacterial infections as well [174].

Antimicrobial treatments of *P. aeruginosa* infections are still challenging which is mostly due to the ability of *P. aeruginosa* to form dense and persistent biofilms. Biofilms of *P. aeruginosa* are composed of polysaccharides (Pel, Psl and alginate) and extracellular DNA that play critical roles in protecting the bacterial communities from exogenous stresses caused by antimicrobial agents. This extraordinary ability of *P. aeruginosa* to form biofilms is promoted by sophisticated cell communication system called quorum sensing that function in a hierarchical manner and are actively inducible upon an increase in cell density or via limitation of nutrients (e.g., iron and phosphate). The complexity of antimicrobial treatments for *P. aeruginosa* biofilm is compounded when multiple species are also involved in forming polymicrobial communities within the biofilms. Molecular diagnosis methods have been developed to detect and identify *P. aeruginosa*. These methods are heavily relied on the *P. aeruginosa* characteristics in terms of its genetic, microbial physiology and biochemical markers that can be characterized using, for example, polymerase chain reaction, cell cultures for antibiotic-resistance profiling, and nanoparticle biosensor, respectively. Despite the diagnosis advancement, major challenges include the enrichment of bacterial cells and biochemical markers for detection and the lack of biomarker database, as well as the high cost and/or time-consuming. In the perspective of therapeutic strategies, more targeted approaches for the treatment of *P. aeruginosa* infections have been developed in the past years in efforts to target different components governing biofilm structure, biofilm dispersal, quorum sensing, and iron metabolism. Although promising results have been demonstrated, translation to clinical trials seems to be challenging due to the variation in biofilm lifestyle, composition and phenotypes which depend on various parameters such as nutrition conditions and the presence of other bacterial species. Future studies are required on the development of more advance techniques, aiming at providing high-throughput and specific diagnosis at an early stage of *P. aeruginosa* growth prior to biofilm development. On the other hand, more thorough understanding on genetic pathways that are responsible for all biofilm lifestyle cycles of *P. aeruginosa* warrants further investigation, which could provide informed decision to design therapeutic strategies that could impair the bacterial attachment and biofilm maturation capabilities.

1.6. Natural products

Natural products are biological molecules including primary and secondary metabolites, originated from natural sources such as plants, microorganisms, and animals. Primary metabolites are proteins, nucleic acid, amino acids, and polysaccharides, which directly contribute to the fundamental process of organisms' life - growth, metabolism, and reproduction. In contrast, secondary metabolites, *i.e.*, toxins, pheromones, attractants, and repellents, typically offer specific advantages for the adaptation and survival of organisms in ecological interactions with other organisms [214].

Natural products have been invaluable sources of medicinal agents for millennia. Indeed, their uses have been documented throughout history for the treatment of diseases including inflammations [215], cancer, cardiovascular diseases [216], neurological conditions [217], and infectious diseases [218,219]. The “Golden Age” of antibiotics beginning with the discovery of penicillin in 1929, has attracted the most significant attention for using natural products as antimicrobials [220]. The interest continues to rise as the incidence of highly antibiotic-resistant bacteria and persistent biofilm bacteria increases. The compounds isolated from plants, microbes, and marine organisms with antibiofilm properties will be discussed.

1.6.1. Plant-derived antibiofilm molecules

Historically, plants have been well-known sources of novel drug compounds with a broad range of valuable bioactivities for human health beneficial [221]. Plants contain many secondary metabolites, including terpenoids, flavonoids, alkaloids, and phenols which serve as plants' defense mechanisms against herbivores and infecting organisms [222,223]. Despite the diverse therapeutic values of these compounds and advancements in modern medicines and synthetic chemistry techniques, none of the plant-derived substances are approved antimicrobials. Extensive studies of plant utility as antibiotic potentiators and biofilm modulators (by attenuating virulence factors or inhibiting quorum sensing) have been recently reported in response to the rapid emergence of multi-drug resistant bacteria

[224-226]. Examples of plant-derived natural products as modulators of *P. aeruginosa* biofilms are described in **Table 1.2**.

Table 1. 2 Plant-derived natural products as modulators of *P. aeruginosa* biofilms

Phytochemical	Source	Mode of Action	Reference
Flavonoids	<i>Vaccinium macrocarpon</i> (cranberry)	Inhibit biofilm formation	[227]
	Grapefruit	Deplete biofilm EPS Enhance antibiotic penetration	[228]
Organosulfur	Garlic extracts	Increase tobramycin susceptibility Inhibit quorum sensing	[229,230]
	Horseradish	Inhibit biofilm formation Inhibit quorum sensing	[231]
Peptides	<i>Moringa oleifera</i>	Destabilize bacterial membrane	[232]
Essential oils	<i>Salvia officinalis</i>	Inhibit biofilm formation	[233]
	<i>Salvia transsylvanica</i>	Reduce pyocyanin production	

1.6.2. Antibiofilm substances from microorganisms

Another well-documented source of structurally diverse bioactive natural products is microorganisms. These secondary metabolites are critical for cell-cell communication, adaptation, and survival, which enable microbes to thrive in competitive communities [234]. They have been proven therapeutically effective as antimicrobial, antitumor, antidepressant, immunosuppressive agents [235], and especially as biofilm modifiers [236]. The latter is of particular interest as multifaceted microbial biofilms are challenging targets to combat and eradicate. Microorganisms derived antibiofilm molecules that have been shown to inhibit *P. aeruginosa* biofilms are listed in **Table 1.3**.

Table 1. 3 Microorganisms derived antibiofilm molecules against *P. aeruginosa* biofilms

Compound	Producing organism/Origin	Mode of Action	Reference(s)
<i>Cis</i> -2-dodecenoic acid (Diffusible signal factor (DSF))	<i>P. aeruginosa</i>	Disperse pre-formed biofilm	[237]
Skyllamycin B Skyllamycin C	<i>Streptomyces sp.</i>	Disperse pre-formed biofilm Enhance azithromycin activity	[238]
Promysalin	<i>Pseudomonas putida</i> RW10S1	Inhibit bacterial activity Disperse pre-formed biofilm	[239,240]
Ethyl acetate extract	Extremophilic <i>Natrinemaversi forme</i>	Inhibit biofilm formation Inhibit quorum sensing	[241]

1.6.3. Antibiofilm molecules extracted from marine natural products

The marine environment is a distinct home to a diverse range of living organisms, including sponges, tunicates, fishes, soft corals, bryozoans, sea hares, and marine microorganisms [242]. Marine species represent enormous resources of bioactive secondary metabolites with unique chemical structures and potent activity that cannot be obtained in terrestrial natural products [243]. The organisms, particularly sessile animals such as sponges and corals, are required to develop chemical defense mechanisms to compete for space and protect them from predators, bacteria, and fouling [244]. Many of these molecules from this line of defense have been demonstrated to possess antibiofilm attributes. To mitigate antibiotic resistance, antibiofilm compounds are expected to interfere with biofilm formation without affecting cellular viability. For instance, marine sponges-derived terpenoids [245] and pyrrole-imidazoles [246] have been reported to be nonantibiotic antibiofilm modifiers. Marine natural products that have been shown to modulate *P. aeruginosa* biofilms are included in **Table 1.4**.

Table 1. 4 Marine natural products modulating *P. aeruginosa* biofilms

Compound	Producing organism/Origin	Mode of Action	Reference(s)
Manoalides	<i>Luffariella variabilis</i>	Inhibit quorum sensing	[245]
Bromoageliferin and its derivatives	<i>Agelas conifera</i>	Inhibit biofilm formation Disperse pre-formed biofilm	[246-248]
Brominated furanones and their analogues	Red alga <i>Delisea pulchra</i>	Inhibit biofilm formation Inhibit quorum sensing	[249,250]
Butenolide	Marine <i>Streptomyces sp</i>	Inhibit biofilm formation Disperse pre-formed biofilm	[251]
Exopolysaccharide EPS273	Marine bacterium <i>P. stutzeri</i> 273	Inhibit biofilm formation Disperse pre-formed biofilm	[252]

1.7. Aims and objectives

(1) Develop biofilm dispersal assay to evaluate antibiofilm properties of fractions and pure compounds

- Establish growth curves of wild-type *P. aeruginosa* PAO1 and its isogenic mutants such as PDO300 and PDO300 Δ alg8.
- Establish biofilm growth curves of wild-type *P. aeruginosa* PAO1 and its isogenic mutants such as PDO300 and PDO300 Δ alg8.
- Determine the DMSO concentration used in the assay without detrimentally impacting bacterial cell growth.
- Determine antibiotics and the concentrations for using as positive controls in the assay.
- Develop and optimize liquid handling protocols for automatic liquid handler, which is used for the screening.

(2) Assess the activity of fractions on preformed *P. aeruginosa* biofilms

- Screen 1535 fractions using biofilm dispersal assay
- Biotas originated active fractions will be refractionated (5 fractions per biota) to confirm the activity of initial fractions.
- To identify active compounds, confirmed fractions will be subjected to further separation (60 fractions per biota).

(3) Determine the activity of two libraries of compounds

- Screen 54 NatureBank compounds using biofilm dispersal assay
- Screen 505 known natural products and their analogues using biofilm dispersal assay

(4) Evaluate the effects of Ianthelliformisamines A-C on *P. aeruginosa* biofilms

- Screen Ianthelliformisamine A-C against wild-type PAO1 and its isogenic mutants such as PAO1 Δ pslA, PAO1 Δ pelF, PDO300 and PDO300 Δ alg8 using biofilm dispersal and biofilm inhibition assays

- Conduct cytotoxicity assay using HEK-293 cell line.
- Explore possible mechanisms of action of these compounds
- Perform bacterial staining to obtain representative images of treated and untreated bacteria.

1.8. References

1. Gale, M.J.; Maritato, M.S.; Chen, Y.-L.; Abdulateef, S.S.; Ruiz, J.E. *Pseudomonas aeruginosa* causing inflammatory mass of the nasopharynx in an immunocompromised HIV infected patient: A mimic of malignancy. *IDCases* **2015**, *2*, 40-43, doi:<https://doi.org/10.1016/j.idcr.2015.01.004>.
2. Wu, W.; Jin, Y.; Bai, F.; Jin, S. Chapter 41 - *Pseudomonas aeruginosa*. In *Molecular Medical Microbiology (Second Edition)*, Tang, Y.-W., Sussman, M., Liu, D., Poxton, I., Schwartzman, J., Eds. Academic Press: Boston, 2015; <https://doi.org/10.1016/B978-0-12-397169-2.00041-Xpp>. 753-767.
3. Gomila, A.; Carratalà, J.; Badia, J.M.; Camprubí, D.; Piriz, M.; Shaw, E.; Diaz-Brito, V.; Espejo, E.; Nicolás, C.; Brugués, M., et al. Preoperative oral antibiotic prophylaxis reduces *Pseudomonas aeruginosa* surgical site infections after elective colorectal surgery: a multicenter prospective cohort study. *BMC Infect Dis* **2018**, *18*, 507-507, doi:10.1186/s12879-018-3413-1.
4. WHO. Prioritization of pathogens to guide discovery, research and development of new antibiotics for drug-resistant bacterial infections, including tuberculosis. **2017**.
5. Pang, Z.; Raudonis, R.; Glick, B.R.; Lin, T.J.; Cheng, Z. Antibiotic resistance in *Pseudomonas aeruginosa*: mechanisms and alternative therapeutic strategies. *Biotechnol Adv* **2019**, *37*, 177-192, doi:10.1016/j.biotechadv.2018.11.013.
6. Moradali, M.F.; Ghods, S.; Rehm, B.H. *Pseudomonas aeruginosa* Lifestyle: A Paradigm for Adaptation, Survival, and Persistence. *Front Cell Infect Microbiol* **2017**, *7*, 39, doi:10.3389/fcimb.2017.00039.
7. Romling, U.; Balsalobre, C. Biofilm infections, their resilience to therapy and innovative treatment strategies. *J Intern Med* **2012**, *272*, 541-561, doi:10.1111/joim.12004.
8. Sen, C.K.; Gordillo, G.M.; Roy, S.; Kirsner, R.; Lambert, L.; Hunt, T.K.; Gottrup, F.; Gurtner, G.C.; Longaker, M.T. Human skin wounds: a major and snowballing threat to public health and the economy. *Wound Repair Regen* **2009**, *17*, 763-771, doi:10.1111/j.1524-475X.2009.00543.x.
9. Donlan, R.M. Biofilms: microbial life on surfaces. *Emerg Infect Dis* **2002**, *8*, 881-890, doi:10.3201/eid0809.020063.

10. Rollet, C.; Gal, L.; Guzzo, J. Biofilm-detached cells, a transition from a sessile to a planktonic phenotype: a comparative study of adhesion and physiological characteristics in *Pseudomonas aeruginosa*. *FEMS Microbiol Lett* **2009**, *290*, 135-142, doi:10.1111/j.1574-6968.2008.01415.x.
11. Lewis, K. Riddle of biofilm resistance. *Antimicrob Agents Chemother* **2001**, *45*, 999-1007, doi:10.1128/AAC.45.4.999-1007.2001.
12. Ghafoor, A.; Hay, I.D.; Rehm, B.H. Role of exopolysaccharides in *Pseudomonas aeruginosa* biofilm formation and architecture. *Appl Environ Microbiol* **2011**, *77*, 5238-5246, doi:10.1128/AEM.00637-11.
13. Crespo, A.; Blanco-Cabra, N.; Torrents, E. Aerobic Vitamin B12 Biosynthesis Is Essential for *Pseudomonas aeruginosa* Class II Ribonucleotide Reductase Activity During Planktonic and Biofilm Growth. *Front Microbiol* **2018**, *9*, 986, doi:10.3389/fmicb.2018.00986.
14. Oluyombo, O.; Penfold, C.N.; Diggle, S.P. Competition in Biofilms between Cystic Fibrosis Isolates of *Pseudomonas aeruginosa* Is Shaped by R-Pyocins. *mBio* **2019**, *10*, e01828-01818, doi:10.1128/mBio.01828-18.
15. Coughlan, L.M.; Cotter, P.D.; Hill, C.; Alvarez-Ordenez, A. New Weapons to Fight Old Enemies: Novel Strategies for the (Bio)control of Bacterial Biofilms in the Food Industry. *Front Microbiol* **2016**, *7*, 1641, doi:10.3389/fmicb.2016.01641.
16. Moradali, M.F.; Rehm, B.H.A. Bacterial biopolymers: from pathogenesis to advanced materials. *Nat Rev Microbiol* **2020**, *18*, 195-210, doi:10.1038/s41579-019-0313-3.
17. Rehm, B.H.A. Bacterial polymers: biosynthesis, modifications and applications. *Nat Rev Microbiol* **2010**, *8*, 578-592, doi:10.1038/nrmicro2354.
18. Strempel, N.; Neidig, A.; Nusser, M.; Geffers, R.; Vieillard, J.; Lesouhaitier, O.; Brenner-Weiss, G.; Overhage, J. Human host defense peptide LL-37 stimulates virulence factor production and adaptive resistance in *Pseudomonas aeruginosa*. *PLoS One* **2013**, *8*, e82240, doi:10.1371/journal.pone.0082240.
19. Jackson, K.D.; Starkey, M.; Kremer, S.; Parsek, M.R.; Wozniak, D.J. Identification of *psl*, a locus encoding a potential exopolysaccharide that is essential for *Pseudomonas aeruginosa* PAO1 biofilm formation. *J Bacteriol* **2004**, *186*, 4466-4475, doi:10.1128/JB.186.14.4466-4475.2004.

20. Ryder, C.; Byrd, M.; Wozniak, D.J. Role of polysaccharides in *Pseudomonas aeruginosa* biofilm development. *Curr Opin Microbiol* **2007**, *10*, 644-648, doi:10.1016/j.mib.2007.09.010.
21. Billings, N.; Millan, M.; Caldara, M.; Rusconi, R.; Tarasova, Y.; Stocker, R.; Ribbeck, K. The extracellular matrix Component Psl provides fast-acting antibiotic defense in *Pseudomonas aeruginosa* biofilms. *PLoS Pathog* **2013**, *9*, e1003526, doi:10.1371/journal.ppat.1003526.
22. Ma, L.; Conover, M.; Lu, H.; Parsek, M.R.; Bayles, K.; Wozniak, D.J. Assembly and development of the *Pseudomonas aeruginosa* biofilm matrix. *PLoS Pathog* **2009**, *5*, e1000354, doi:10.1371/journal.ppat.1000354.
23. Byrd, M.S.; Sadovskaya, I.; Vinogradov, E.; Lu, H.; Sprinkle, A.B.; Richardson, S.H.; Ma, L.; Ralston, B.; Parsek, M.R.; Anderson, E.M., et al. Genetic and biochemical analyses of the *Pseudomonas aeruginosa* Psl exopolysaccharide reveal overlapping roles for polysaccharide synthesis enzymes in Psl and LPS production. *Mol Microbiol* **2009**, *73*, 622-638, doi:10.1111/j.1365-2958.2009.06795.x.
24. Ma, L.; Wang, S.; Wang, D.; Parsek, M.R.; Wozniak, D.J. The roles of biofilm matrix polysaccharide Psl in mucoid *Pseudomonas aeruginosa* biofilms. *FEMS Immunol Med Microbiol* **2012**, *65*, 377-380, doi:10.1111/j.1574-695X.2012.00934.x.
25. Jones, C.J.; Wozniak, D.J. Psl Produced by Mucoid *Pseudomonas aeruginosa* Contributes to the Establishment of Biofilms and Immune Evasion. *mBio* **2017**, *8*, e00864-00817, doi:10.1128/mBio.00864-17.
26. Irie, Y.; Roberts, A.E.L.; Kragh, K.N.; Gordon, V.D.; Hutchison, J.; Allen, R.J.; Melaugh, G.; Bjarnsholt, T.; West, S.A.; Diggle, S.P. The *Pseudomonas aeruginosa* PSL Polysaccharide Is a Social but Noncheatable Trait in Biofilms. *mBio* **2017**, *8*, e00374-00317, doi:10.1128/mBio.00374-17.
27. Staudinger, B.J.; Muller, J.F.; Halldórsson, S.; Boles, B.; Angermeyer, A.; Nguyen, D.; Rosen, H.; Baldursson, O.; Gottfreðsson, M.; Guðmundsson, G.H., et al. Conditions associated with the cystic fibrosis defect promote chronic *Pseudomonas aeruginosa* infection. *Am J Respir Crit Care Med* **2014**, *189*, 812-824, doi:10.1164/rccm.201312-2142OC.
28. Irie, Y.; Borlee, B.R.; O'Connor, J.R.; Hill, P.J.; Harwood, C.S.; Wozniak, D.J.; Parsek, M.R. Self-produced exopolysaccharide is a signal that stimulates biofilm

- formation in *Pseudomonas aeruginosa*. *Proc Natl Acad Sci U S A* **2012**, *109*, 20632-20636, doi:10.1073/pnas.1217993109.
29. Mishra, M.; Byrd, M.S.; Sergeant, S.; Azad, A.K.; Parsek, M.R.; McPhail, L.; Schlesinger, L.S.; Wozniak, D.J. *Pseudomonas aeruginosa* Psl polysaccharide reduces neutrophil phagocytosis and the oxidative response by limiting complement-mediated opsonization. *Cell Microbiol* **2012**, *14*, 95-106, doi:10.1111/j.1462-5822.2011.01704.x.
 30. Colvin, K.M.; Alnabelseya, N.; Baker, P.; Whitney, J.C.; Howell, P.L.; Parsek, M.R. PelA deacetylase activity is required for Pel polysaccharide synthesis in *Pseudomonas aeruginosa*. *J Bacteriol* **2013**, *195*, 2329-2339, doi:10.1128/JB.02150-12.
 31. Jennings, L.K.; Storek, K.M.; Ledvina, H.E.; Coulon, C.; Marmont, L.S.; Sadovskaya, I.; Secor, P.R.; Tseng, B.S.; Scian, M.; Filloux, A., et al. Pel is a cationic exopolysaccharide that cross-links extracellular DNA in the *Pseudomonas aeruginosa* biofilm matrix. *Proc Natl Acad Sci U S A* **2015**, *112*, 11353-11358, doi:10.1073/pnas.1503058112.
 32. Friedman, L.; Kolter, R. Genes involved in matrix formation in *Pseudomonas aeruginosa* PA14 biofilms. *Mol Microbiol* **2004**, *51*, 675-690.
 33. Colvin, K.M.; Irie, Y.; Tart, C.S.; Urbano, R.; Whitney, J.C.; Ryder, C.; Howell, P.L.; Wozniak, D.J.; Parsek, M.R. The Pel and Psl polysaccharides provide *Pseudomonas aeruginosa* structural redundancy within the biofilm matrix. *Enviro Microbiol* **2012**, *14*, 1913-1928, doi:10.1111/j.1462-2920.2011.02657.x.
 34. Yang, L.; Hu, Y.; Liu, Y.; Zhang, J.; Ulstrup, J.; Molin, S. Distinct roles of extracellular polymeric substances in *Pseudomonas aeruginosa* biofilm development. *Environ Microbiol* **2011**, *13*, 1705-1717, doi:10.1111/j.1462-2920.2011.02503.x.
 35. Baker, P.; Hill, P.J.; Snarr, B.D.; Alnabelseya, N.; Pestrak, M.J.; Lee, M.J.; Jennings, L.K.; Tam, J.; Melnyk, R.A.; Parsek, M.R., et al. Exopolysaccharide biosynthetic glycoside hydrolases can be utilized to disrupt and prevent *Pseudomonas aeruginosa* biofilms. *Sci Adv* **2016**, *2*, e1501632-e1501632, doi:10.1126/sciadv.1501632.
 36. Ciofu, O.; Tolker-Nielsen, T.; Jensen, P.O.; Wang, H.; Hoiby, N. Antimicrobial resistance, respiratory tract infections and role of biofilms in lung infections in cystic fibrosis patients. *Adv Drug Deliv Rev* **2015**, *85*, 7-23, doi:10.1016/j.addr.2014.11.017.

37. Folkesson, A.; Jelsbak, L.; Yang, L.; Johansen, H.K.; Ciofu, O.; Hoiby, N.; Molin, S. Adaptation of *Pseudomonas aeruginosa* to the cystic fibrosis airway: an evolutionary perspective. *Nat Rev Microbiol* **2012**, *10*, 841-851, doi:10.1038/nrmicro2907.
38. Evans, L.R.; Linker, A. Production and characterization of the slime polysaccharide of *Pseudomonas aeruginosa*. *J Bacteriol* **1973**, *116*, 915-924.
39. Tseng, B.S.; Zhang, W.; Harrison, J.J.; Quach, T.P.; Song, J.L.; Penterman, J.; Singh, P.K.; Chopp, D.L.; Packman, A.I.; Parsek, M.R. The extracellular matrix protects *Pseudomonas aeruginosa* biofilms by limiting the penetration of tobramycin. *Environ Microbiol* **2013**, *15*, 2865-2878, doi:10.1111/1462-2920.12155.
40. Hay, I.D.; Rehman, Z.U.; Moradali, M.F.; Wang, Y.; Rehm, B.H.A. Microbial alginate production, modification and its applications. *Microb Biotechnol* **2013**, *6*, 637-650, doi:10.1111/1751-7915.12076.
41. Hay, I.D.; Ur Rehman, Z.; Ghafoor, A.; Rehm, B.H.A. Bacterial biosynthesis of alginates. *J Chem Technol Biotechnol* **2010**, *85*, 752-759, doi:10.1002/jctb.2372.
42. Gloag, E.S.; German, G.K.; Stoodley, P.; Wozniak, D.J. Viscoelastic properties of *Pseudomonas aeruginosa* variant biofilms. *Sci Rep* **2018**, *8*, 9691, doi:10.1038/s41598-018-28009-5.
43. Wloka, M.; Rehage, H.; Flemming, H.C.; Wingender, J. Structure and rheological behaviour of the extracellular polymeric substance network of mucoid *Pseudomonas aeruginosa* biofilms. *Biofilms* **2005**, *2*, 275-283, doi:10.1017/S1479050506002031.
44. Rehm, B.H.A.; Valla, S. Bacterial alginates: biosynthesis and applications. *Appl Microbiol Biotechnol* **1997**, *48*, 281-288, doi:10.1007/s002530051051.
45. Turnbull, L.; Toyofuku, M.; Hynen, A.L.; Kurosawa, M.; Pessi, G.; Petty, N.K.; Osvath, S.R.; Carcamo-Oyarce, G.; Gloag, E.S.; Shimoni, R., et al. Explosive cell lysis as a mechanism for the biogenesis of bacterial membrane vesicles and biofilms. *Nat Commun* **2016**, *7*, 11220, doi:10.1038/ncomms11220.
46. Chiang, W.-C.; Nilsson, M.; Jensen, P.Ø.; Høiby, N.; Nielsen, T.E.; Givskov, M.; Tolker-Nielsen, T. Extracellular DNA shields against aminoglycosides in *Pseudomonas aeruginosa* biofilms. *Antimicrob Agents Chemother* **2013**, *57*, 2352-2361, doi:10.1128/AAC.00001-13.
47. Allesen-Holm, M.; Barken, K.B.; Yang, L.; Klausen, M.; Webb, J.S.; Kjelleberg, S.; Molin, S.; Givskov, M.; Tolker-Nielsen, T. A characterization of DNA release in

- Pseudomonas aeruginosa* cultures and biofilms. *Mol Microbiol* **2006**, *59*, 1114-1128, doi:10.1111/j.1365-2958.2005.05008.x.
48. Wilton, M.; Charron-Mazenod, L.; Moore, R.; Lewenza, S. Extracellular DNA Acidifies Biofilms and Induces Aminoglycoside Resistance in *Pseudomonas aeruginosa*. *Antimicrob Agents Chemother* **2015**, *60*, 544-553, doi:10.1128/AAC.01650-15.
 49. Wilton, M.; Wong, M.J.Q.; Tang, L.; Liang, X.; Moore, R.; Parkins, M.D.; Lewenza, S.; Dong, T.G. Chelation of Membrane-Bound Cations by Extracellular DNA Activates the Type VI Secretion System in *Pseudomonas aeruginosa*. *Infect Immun* **2016**, *84*, 2355, doi:10.1128/IAI.00233-16.
 50. Gloag, E.S.; Turnbull, L.; Huang, A.; Vallotton, P.; Wang, H.; Nolan, L.M.; Mililli, L.; Hunt, C.; Lu, J.; Osvath, S.R., et al. Self-organization of bacterial biofilms is facilitated by extracellular DNA. *Proc Natl Acad Sci U S A* **2013**, *110*, 11541-11546, doi:10.1073/pnas.1218898110.
 51. Fuxman Bass, J.I.; Russo, D.M.; Gabelloni, M.L.; Geffner, J.R.; Giordano, M.; Catalano, M.; Zorreguieta, Á.; Trevani, A.S. Extracellular DNA: A Major Proinflammatory Component of *Pseudomonas aeruginosa* Biofilms. *J Immunol* **2010**, *184*, 6386, doi:10.4049/jimmunol.0901640.
 52. Pham, T.H.; Webb, J.S.; Rehm, B.H. The role of polyhydroxyalkanoate biosynthesis by *Pseudomonas aeruginosa* in rhamnolipid and alginate production as well as stress tolerance and biofilm formation. *Microbiology (Reading)* **2004**, *150*, 3405-3413, doi:10.1099/mic.0.27357-0.
 53. Sonderholm, M.; Kragh, K.N.; Koren, K.; Jakobsen, T.H.; Darch, S.E.; Alhede, M.; Jensen, P.O.; Whiteley, M.; Kuhl, M.; Bjarnsholt, T. *Pseudomonas aeruginosa* Aggregate Formation in an Alginate Bead Model System Exhibits In Vivo-Like Characteristics. *Appl Environ Microbiol* **2017**, *83*, doi:10.1128/AEM.00113-17.
 54. O'Toole, G.A.; Kolter, R. Flagellar and twitching motility are necessary for *Pseudomonas aeruginosa* biofilm development. *Mol. Microbiol* **1998**, *30*, 295-304, doi:10.1046/j.1365-2958.1998.01062.x.
 55. Klausen, M.; Aaes-Jørgensen, A.; Molin, S.; Tolker-Nielsen, T. Involvement of bacterial migration in the development of complex multicellular structures in *Pseudomonas aeruginosa* biofilms. *Mol. Microbiol* **2003**, *50*, 61-68, doi:10.1046/j.1365-2958.2003.03677.x.

56. Hickman, J.W.; Harwood, C.S. Identification of FleQ from *Pseudomonas aeruginosa* as a c-di-GMP-responsive transcription factor. *Mol. Microbiol* **2008**, *69*, 376-389, doi:10.1111/j.1365-2958.2008.06281.x.
57. Guilbaud, M.; Bruzard, J.; Bouffartigues, E.; Orange, N.; Guillot, A.; Aubert-Frambourg, A.; Monnet, V.; Herry, J.M.; Chevalier, S.; Bellon-Fontaine, M.N. Proteomic Response of *Pseudomonas aeruginosa* PAO1 Adhering to Solid Surfaces. *Front Microbiol* **2017**, *8*, 1465, doi:10.3389/fmicb.2017.01465.
58. Rasamiravaka, T.; Labtani, Q.; Duez, P.; El Jaziri, M. The formation of biofilms by *Pseudomonas aeruginosa*: a review of the natural and synthetic compounds interfering with control mechanisms. *Biomed Res Int* **2015**, *2015*, 759348-759348, doi:10.1155/2015/759348.
59. Cherny, K.E.; Sauer, K. *Pseudomonas aeruginosa* requires the DNA-specific endonuclease EndA to degrade eDNA to disperse from the biofilm. *J Bacteriol* **2019**, 10.1128/JB.00059-19, JB.00059-00019, doi:10.1128/JB.00059-19.
60. Shrout, J.D.; Chopp, D.L.; Just, C.L.; Hentzer, M.; Givskov, M.; Parsek, M.R. The impact of quorum sensing and swarming motility on *Pseudomonas aeruginosa* biofilm formation is nutritionally conditional. *Mol Microbiol* **2006**, *62*, 1264-1277, doi:10.1111/j.1365-2958.2006.05421.x.
61. Chua, S.L.; Tan, S.Y.-Y.; Rybtke, M.T.; Chen, Y.; Rice, S.A.; Kjelleberg, S.; Tolker-Nielsen, T.; Yang, L.; Givskov, M. Bis-(3'-5')-cyclic dimeric GMP regulates antimicrobial peptide resistance in *Pseudomonas aeruginosa*. *Antimicrob Agents Chemother* **2013**, *57*, 2066-2075, doi:10.1128/AAC.02499-12.
62. Chua, S.L.; Hultqvist, L.D.; Yuan, M.; Rybtke, M.; Nielsen, T.E.; Givskov, M.; Tolker-Nielsen, T.; Yang, L. In vitro and in vivo generation and characterization of *Pseudomonas aeruginosa* biofilm-dispersed cells via c-di-GMP manipulation. *Nat Protoc* **2015**, *10*, 1165-1180, doi:10.1038/nprot.2015.067.
63. Chua, S.L.; Liu, Y.; Yam, J.K.H.; Chen, Y.; Vejborg, R.M.; Tan, B.G.C.; Kjelleberg, S.; Tolker-Nielsen, T.; Givskov, M.; Yang, L. Dispersed cells represent a distinct stage in the transition from bacterial biofilm to planktonic lifestyles. *Nat Commun* **2014**, *5*, 4462, doi:10.1038/ncomms5462.
64. Chambers, J.R.; Cherny, K.E.; Sauer, K. Susceptibility of *Pseudomonas aeruginosa* Dispersed Cells to Antimicrobial Agents Is Dependent on the Dispersion Cue and

- Class of the Antimicrobial Agent Used. *Antimicrob Agents Chemother* **2017**, *61*, e00846-00817, doi:10.1128/AAC.00846-17.
65. Li, Y.; Petrova, O.E.; Su, S.; Lau, G.W.; Panmanee, W.; Na, R.; Hassett, D.J.; Davies, D.G.; Sauer, K. BdlA, DipA and induced dispersion contribute to acute virulence and chronic persistence of *Pseudomonas aeruginosa*. *PLoS Pathog* **2014**, *10*, e1004168-e1004168, doi:10.1371/journal.ppat.1004168.
 66. Fleming, D.; Rumbaugh, K. The Consequences of Biofilm Dispersal on the Host. *Sci Rep* **2018**, *8*, 10738, doi:10.1038/s41598-018-29121-2.
 67. Mashburn, L.M.; Jett, A.M.; Akins, D.R.; Whiteley, M. *Staphylococcus aureus* Serves as an Iron Source for *Pseudomonas aeruginosa* during In Vivo Coculture. *J Bacteriol* **2005**, *187*, 554, doi:10.1128/JB.187.2.554-566.2005.
 68. Korgaonkar, A.; Trivedi, U.; Rumbaugh, K.P.; Whiteley, M. Community surveillance enhances *Pseudomonas aeruginosa* virulence during polymicrobial infection. *Proc Natl Acad Sci U S A* **2013**, *110*, 1059-1064, doi:10.1073/pnas.1214550110.
 69. Willner, D.; Haynes, M.R.; Furlan, M.; Schmieder, R.; Lim, Y.W.; Rainey, P.B.; Rohwer, F.; Conrad, D. Spatial distribution of microbial communities in the cystic fibrosis lung. *ISME J* **2012**, *6*, 471-474, doi:10.1038/ismej.2011.104.
 70. Hall-Stoodley, L.; Costerton, J.W.; Stoodley, P. Bacterial biofilms: from the Natural environment to infectious diseases. *Nat Rev Microbiol* **2004**, *2*, 95-108, doi:10.1038/nrmicro821.
 71. Weaver, V.B.; Kolter, R. Burkholderia spp. Alter *Pseudomonas aeruginosa* Physiology through Iron Sequestration. *J Bacteriol* **2004**, *186*, 2376, doi:10.1128/JB.186.8.2376-2384.2004.
 72. Limoli, D.H.; Whitfield, G.B.; Kitao, T.; Ivey, M.L.; Davis, M.R., Jr.; Grahl, N.; Hogan, D.A.; Rahme, L.G.; Howell, P.L.; O'Toole, G.A., et al. *Pseudomonas aeruginosa* Alginate Overproduction Promotes Coexistence with *Staphylococcus aureus* in a Model of Cystic Fibrosis Respiratory Infection. *mBio* **2017**, *8*, doi:10.1128/mBio.00186-17.
 73. Armbruster, C.R.; Wolter, D.J.; Mishra, M.; Hayden, H.S.; Radey, M.C.; Merrihew, G.; MacCoss, M.J.; Burns, J.; Wozniak, D.J.; Parsek, M.R., et al. *Staphylococcus aureus* Protein A Mediates Interspecies Interactions at the Cell Surface of *Pseudomonas aeruginosa*. *mBio* **2016**, *7*, doi:10.1128/mBio.00538-16.

74. Chew, S.C.; Yam, J.K.H.; Matysik, A.; Seng, Z.J.; Klebensberger, J.; Givskov, M.; Doyle, P.; Rice, S.A.; Yang, L.; Kjelleberg, S. Matrix Polysaccharides and SiaD Diguanylate Cyclase Alter Community Structure and Competitiveness of *Pseudomonas aeruginosa* during Dual-Species Biofilm Development with *Staphylococcus aureus*. *mBio* **2018**, *9*, doi:10.1128/mBio.00585-18.
75. Bragonzi, A.; Farulla, I.; Paroni, M.; Twomey, K.B.; Pirone, L.; Lore, N.I.; Bianconi, I.; Dalmastri, C.; Ryan, R.P.; Bevivino, A. Modelling co-infection of the cystic fibrosis lung by *Pseudomonas aeruginosa* and *Burkholderia cenocepacia* reveals influences on biofilm formation and host response. *PLoS One* **2012**, *7*, e52330, doi:10.1371/journal.pone.0052330.
76. Filkins, L.M.; Hampton, T.H.; Gifford, A.H.; Gross, M.J.; Hogan, D.A.; Sogin, M.L.; Morrison, H.G.; Paster, B.J.; O'Toole, G.A. Prevalence of streptococci and increased polymicrobial diversity associated with cystic fibrosis patient stability. *J Bacteriol* **2012**, *194*, 4709-4717, doi:10.1128/JB.00566-12.
77. Scoffield, J.A.; Wu, H. Oral streptococci and nitrite-mediated interference of *Pseudomonas aeruginosa*. *Infect Immun* **2015**, *83*, 101-107, doi:10.1128/IAI.02396-14.
78. Scoffield, J.A.; Duan, D.; Zhu, F.; Wu, H. A commensal streptococcus hijacks a *Pseudomonas aeruginosa* exopolysaccharide to promote biofilm formation. *PLoS Pathog* **2017**, *13*, e1006300, doi:10.1371/journal.ppat.1006300.
79. Yan, S.; Wu, G. Can biofilm be reversed through quorum sensing in *Pseudomonas aeruginosa*? *Front Microbiol* **2019**, *10*, doi:10.3389/fmicb.2019.01582.
80. Mukherjee, S.; Bassler, B.L. Bacterial quorum sensing in complex and dynamically changing environments. *Nat Rev Microbiol* **2019**, *17*, 371-382, doi:10.1038/s41579-019-0186-5.
81. Fuqua, W.C.; Winans, S.C.; Greenberg, E.P. Quorum sensing in bacteria: the LuxR-LuxI family of cell density-responsive transcriptional regulators. *J Bacteriol* **1994**, *176*, 269, doi:10.1128/jb.176.2.269-275.1994.
82. Lee, J.; Zhang, L. The hierarchy quorum sensing network in *Pseudomonas aeruginosa*. *Protein Cell* **2015**, *6*, 26-41, doi:10.1007/s13238-014-0100-x.
83. Choi, Y.; Park, H.-Y.; Park, S.J.; Park, S.-J.; Kim, S.-K.; Ha, C.; Im, S.-J.; Lee, J.-H. Growth phase-differential quorum sensing regulation of anthranilate metabolism in

- Pseudomonas aeruginosa*. *Mol Cells* **2011**, 32, 57-65, doi:10.1007/s10059-011-2322-6.
84. Oglesby, A.G.; Farrow, J.M.; Lee, J.-H.; Tomaras, A.P.; Greenberg, E.P.; Pesci, E.C.; Vasil, M.L. The influence of iron on *Pseudomonas aeruginosa* physiology: a regulatory link between iron and quorum sensing. *J Biol Chem* **2008**, 283, 15558-15567, doi:10.1074/jbc.M707840200.
 85. Rampioni, G.; Falcone, M.; Heeb, S.; Frangipani, E.; Fletcher, M.P.; Dubern, J.-F.; Visca, P.; Leoni, L.; Cámara, M.; Williams, P. Unravelling the genome-wide contributions of specific 2-alkyl-4-quinolones and PqsE to quorum sensing in *Pseudomonas aeruginosa*. *PLoS Pathog* **2016**, 12, e1006029, doi:10.1371/journal.ppat.1006029.
 86. Mashburn, L.M.; Whiteley, M. Membrane vesicles traffic signals and facilitate group activities in a prokaryote. *Nature* **2005**, 437, 422-425, doi:10.1038/nature03925.
 87. Seed, P.C.; Passador, L.; Iglewski, B.H. Activation of the *Pseudomonas aeruginosa* lasI gene by LasR and the *Pseudomonas* autoinducer PAI: an autoinduction regulatory hierarchy. *J Bacteriol* **1995**, 177, 654, doi:10.1128/jb.177.3.654-659.1995.
 88. Déziel, E.; Lépine, F.; Milot, S.; He, J.; Mindrinos, M.N.; Tompkins, R.G.; Rahme, L.G. Analysis of *Pseudomonas aeruginosa* 4-hydroxy-2-alkylquinolines (HAQs) reveals a role for 4-hydroxy-2-heptylquinoline in cell-to-cell communication. *Proc Natl Acad Sci U S A* **2004**, 101, 1339, doi:10.1073/pnas.0307694100.
 89. Winson, M.K.; Camara, M.; Latifi, A.; Foglino, M.; Chhabra, S.R.; Daykin, M.; Bally, M.; Chapon, V.; Salmond, G.P.; Bycroft, B.W. Multiple N-acyl-L-homoserine lactone signal molecules regulate production of virulence determinants and secondary metabolites in *Pseudomonas aeruginosa*. *Proc Natl Acad Sci U S A* **1995**, 92, 9427, doi:10.1073/pnas.92.20.9427.
 90. McKnight, S.L.; Iglewski, B.H.; Pesci, E.C. The *Pseudomonas* quinolone signal regulates *rhl* quorum sensing in *Pseudomonas aeruginosa*. *J Bacteriol* **2000**, 182, 2702, doi:10.1128/JB.182.10.2702-2708.2000.
 91. Cao, H.; Krishnan, G.; Goumnerov, B.; Tsongalis, J.; Tompkins, R.; Rahme, L.G. A quorum sensing-associated virulence gene of *Pseudomonas aeruginosa* encodes a LysR-like transcription regulator with a unique self-regulatory mechanism. *Proc Natl Acad Sci* **2001**, 98, 14613-14618, doi:10.1073/pnas.251465298.

92. Lee, J.; Wu, J.; Deng, Y.; Wang, J.; Wang, C.; Wang, J.; Chang, C.; Dong, Y.; Williams, P.; Zhang, L.-H. A cell-cell communication signal integrates quorum sensing and stress response. *Nat Chem Biol* **2013**, *9*, 339-343, doi:10.1038/nchembio.1225.
93. Meng, X.; Ahator, S.D.; Zhang, L.-H. Molecular Mechanisms of Phosphate Stress Activation of *Pseudomonas aeruginosa* Quorum Sensing Systems. *mSphere* **2020**, *5*, e00119-00120, doi:10.1128/mSphere.00119-20.
94. Ye, L.; Cornelis, P.; Guillemyn, K.; Ballet, S.; Hammerich, O. Structure revision of N-mercapto-4-formylcarbostyryl produced by *Pseudomonas fluorescens* G308 to 2-(2-hydroxyphenyl)thiazole-4-carbaldehyde [aeruginaldehyde]. *Nat Prod Commun* **2014**, *9*, 789-794.
95. Trottmann, F.; Franke, J.; Ishida, K.; García-Altares, M.; Hertweck, C. A Pair of Bacterial Siderophores Releases and Traps an Intercellular Signal Molecule: An Unusual Case of Natural Nitrone Bioconjugation. *Angew Chem Int Ed Engl* **2019**, *58*, 200-204, doi:10.1002/anie.201811131.
96. Rojas Murcia, N.; Lee, X.; Waridel, P.; Maspoli, A.; Imker, H.J.; Chai, T.; Walsh, C.T.; Reimmann, C. The *Pseudomonas aeruginosa* antimetabolite L -2-amino-4-methoxy-trans-3-butenoic acid (AMB) is made from glutamate and two alanine residues via a thiotemplate-linked tripeptide precursor. *Front Microbiol* **2015**, *6*, 170.
97. Pamp, S.J.; Tolker-Nielsen, T. Multiple roles of biosurfactants in structural biofilm development by *Pseudomonas aeruginosa*. *J Bacteriol* **2007**, *189*, 2531, doi:10.1128/JB.01515-06.
98. Pearson, J.P.; Pesci, E.C.; Iglewski, B.H. Roles of *Pseudomonas aeruginosa* las and rhl quorum-sensing systems in control of elastase and rhamnolipid biosynthesis genes. *J Bacteriol* **1997**, *179*, 5756, doi:10.1128/jb.179.18.5756-5767.1997.
99. Banin, E.; Vasil, M.L.; Greenberg, E.P. Iron and *Pseudomonas aeruginosa* biofilm formation. *Proc Natl Acad Sci U S A* **2005**, *102*, 11076, doi:10.1073/pnas.0504266102.
100. Das, T.; Kutty, S.K.; Kumar, N.; Manefield, M. Pyocyanin facilitates extracellular DNA binding to *Pseudomonas aeruginosa* influencing cell surface properties and aggregation. *PLoS One* **2013**, *8*, e58299, doi:10.1371/journal.pone.0058299.
101. Das, T.; Kutty, S.K.; Tavallaie, R.; Ibugo, A.I.; Panchompoo, J.; Sehar, S.; Aldous, L.; Yeung, A.W.S.; Thomas, S.R.; Kumar, N., et al. Phenazine virulence factor

- binding to extracellular DNA is important for *Pseudomonas aeruginosa* biofilm formation. *Sci Rep* **2015**, 5, 8398, doi:10.1038/srep08398.
102. Sakuragi, Y.; Kolter, R. Quorum-sensing regulation of the biofilm matrix genes *pel* of *Pseudomonas aeruginosa*. *J Bacteriol* **2007**, 189, 5383, doi:10.1128/JB.00137-07.
 103. Passos da Silva, D.; Matwichuk, M.L.; Townsend, D.O.; Reichhardt, C.; Lamba, D.; Wozniak, D.J.; Parsek, M.R. The *Pseudomonas aeruginosa* lectin LecB binds to the exopolysaccharide Psl and stabilizes the biofilm matrix. *Nat Commun* **2019**, 10, 2183, doi:10.1038/s41467-019-10201-4.
 104. Diggle, S.P.; Stacey, R.E.; Dodd, C.; Cámara, M.; Williams, P.; Winzer, K. The galactophilic lectin, LecA, contributes to biofilm development in *Pseudomonas aeruginosa*. *Environ Microbiol* **2006**, 8, 1095-1104, doi:10.1111/j.1462-2920.2006.001001.x.
 105. Visca, P.; Imperi, F.; Lamont, I.L. Pyoverdine siderophores: from biogenesis to biosignificance. *Trends Microbiol* **2007**, 15, 22-30, doi:10.1016/j.tim.2006.11.004.
 106. Kirisits, M.J.; Prost, L.; Starkey, M.; Parsek, M.R. Characterization of colony morphology variants isolated from *Pseudomonas aeruginosa* biofilms. *J Appl Environ Microbiol* **2005**, 71, 4809-4821, doi:10.1128/AEM.71.8.4809-4821.2005.
 107. Whistler, T.; Sangwichian, O.; Jorakate, P.; Sawatwong, P.; Surin, U.; Piralam, B.; Thamthitiwat, S.; Promkong, C.; Peruski, L. Identification of Gram negative non-fermentative bacteria: How hard can it be? *PLoS Negl Trop Dis* **2019**, 13, e0007729-e0007729, doi:10.1371/journal.pntd.0007729.
 108. Abayasekara, L.M.; Perera, J.; Chandrasekharan, V.; Gnanam, V.S.; Udunuwara, N.A.; Liyanage, D.S.; Bulathsinhala, N.E.; Adikary, S.; Aluthmuhandiram, J.V.S.; Thanaseelan, C.S., et al. Detection of bacterial pathogens from clinical specimens using conventional microbial culture and 16S metagenomics: a comparative study. *BMC Infect Dis* **2017**, 17, 631-631, doi:10.1186/s12879-017-2727-8.
 109. Bobenchik, A.M.; Deak, E.; Hindler, J.A.; Charlton, C.L.; Humphries, R.M. Performance of Vitek 2 for Antimicrobial Susceptibility Testing of *Acinetobacter baumannii*, *Pseudomonas aeruginosa*, and *Stenotrophomonas maltophilia* with Vitek 2 (2009 FDA) and CLSI M100S 26th Edition Breakpoints. *J Clin Microbiol* **2017**, 55, 450-456, doi:10.1128/JCM.01859-16.
 110. Sader, H.S.; Fritsche, T.R.; Jones, R.N. Accuracy of three automated systems (MicroScan WalkAway, VITEK, and VITEK 2) for susceptibility testing of

- Pseudomonas aeruginosa* against five broad-spectrum beta-lactam agents. *J Clin Microbiol* **2006**, *44*, 1101-1104, doi:10.1128/JCM.44.3.1101-1104.2006.
111. O'Hara, C.M. Evaluation of the Phoenix 100 ID/AST system and NID panel for identification of *Enterobacteriaceae*, *Vibrionaceae*, and commonly isolated nonenteric gram-negative bacilli. *J Clin Microbiol* **2006**, *44*, 928-933, doi:10.1128/JCM.44.3.928-933.2006.
 112. McGregor, A.; Schio, F.; Beaton, S.; Boulton, V.; Perman, M.; Gilbert, G. The MicroScan WalkAway diagnostic microbiology system--an evaluation. *Pathology* **1995**, *27*, 172-176, doi:10.1080/00313029500169822.
 113. Ligozzi, M.; Bernini, C.; Bonora, M.G.; De Fatima, M.; Zuliani, J.; Fontana, R. Evaluation of the VITEK 2 system for identification and antimicrobial susceptibility testing of medically relevant gram-positive cocci. *J Clin Microbiol* **2002**, *40*, 1681-1686, doi:10.1128/jcm.40.5.1681-1686.2002.
 114. Osei Sekyere, J.; Sephofane, A.K.; Mbelle, N.M. Comparative Evaluation of CHROMagar COL-APSE, MicroScan Walkaway, ComASP Colistin, and Colistin MAC Test in Detecting Colistin-resistant Gram-Negative Bacteria. *Sci Rep* **2020**, *10*, 6221, doi:10.1038/s41598-020-63267-2.
 115. Qin, X.; Emerson, J.; Stapp, J.; Stapp, L.; Abe, P.; Burns, J.L. Use of Real-Time PCR with Multiple Targets To Identify *Pseudomonas aeruginosa* and Other Nonfermenting Gram-Negative Bacilli from Patients with Cystic Fibrosis. *J Clin Microbiol* **2003**, *41*, 4312, doi:10.1128/JCM.41.9.4312-4317.2003.
 116. Anuj, S.N.; Whiley, D.M.; Kidd, T.J.; Bell, S.C.; Wainwright, C.E.; Nissen, M.D.; Sloots, T.P. Identification of *Pseudomonas aeruginosa* by a duplex real-time polymerase chain reaction assay targeting the *ecfX* and the *gyrB* genes. *Diagn Microbiol Infect Dis* **2009**, *63*, 127-131, doi:10.1016/j.diagmicrobio.2008.09.018.
 117. Aghamollaei, H.; Moghaddam, M.M.; Kooshki, H.; Heiat, M.; Mirnejad, R.; Barzi, N.S. Detection of *Pseudomonas aeruginosa* by a triplex polymerase chain reaction assay based on *lasI/R* and *gyrB* genes. *J Infect Public Health* **2015**, *8*, 314-322, doi:10.1016/j.jiph.2015.03.003.
 118. Motoshima, M.; Yanagihara, K.; Fukushima, K.; Matsuda, J.; Sugahara, K.; Hirakata, Y.; Yamada, Y.; Kohno, S.; Kamihira, S. Rapid and accurate detection of *Pseudomonas aeruginosa* by real-time polymerase chain reaction with melting curve

- p analysis targeting
- gyrB*
- gene.
- Diagn Microbiol Infect Dis*
- 2007**
- , 58, 53-58, doi:10.1016/j.diagmicrobio.2006.11.007.
119. Le Gall, F.; Le Berre, R.; Rosec, S.; Hardy, J.; Gouriou, S.; Boisramé-Gastrin, S.; Vallet, S.; Rault, G.; Payan, C.; Héry-Arnaud, G. Proposal of a quantitative PCR-based protocol for an optimal *Pseudomonas aeruginosa* detection in patients with cystic fibrosis. *BMC Microbiol* **2013**, 13, 143, doi:10.1186/1471-2180-13-143.
 120. Dong, D.; Zou, D.; Liu, H.; Yang, Z.; Huang, S.; Liu, N.; He, X.; Liu, W.; Huang, L. Rapid detection of *Pseudomonas aeruginosa* targeting the *toxA* gene in intensive care unit patients from Beijing, China. *Front Microbiol* **2015**, 6, 1100, doi:10.3389/fmicb.2015.01100.
 121. Oumeraci, T.; Jensen, V.; Talbot, S.R.; Hofmann, W.; Kostrzewa, M.; Schlegelberger, B.; von Neuhoff, N.; Häussler, S. Comprehensive MALDI-TOF biotyping of the non-redundant Harvard *Pseudomonas aeruginosa* PA14 transposon insertion mutant library. *PloS one* **2015**, 10, e0117144-e0117144, doi:10.1371/journal.pone.0117144.
 122. Singhal, N.; Kumar, M.; Kanaujia, P.K.; Viridi, J.S. MALDI-TOF mass spectrometry: an emerging technology for microbial identification and diagnosis. *Front Microbiol* **2015**, 6, 791, doi:10.3389/fmicb.2015.00791.
 123. He, Y.; Li, H.; Lu, X.; Stratton, C.W.; Tang, Y.W. Mass spectrometry biotyper system identifies enteric bacterial pathogens directly from colonies grown on selective stool culture media. *J Clin Microbiol* **2010**, 48, 3888-3892, doi:10.1128/JCM.01290-10.
 124. Carbonnelle, E.; Beretti, J.L.; Cottyn, S.; Quesne, G.; Berche, P.; Nassif, X.; Ferroni, A. Rapid identification of Staphylococci isolated in clinical microbiology laboratories by matrix-assisted laser desorption ionization-time of flight mass spectrometry. *J Clin Microbiol* **2007**, 45, 2156-2161, doi:10.1128/JCM.02405-06.
 125. Sogawa, K.; Watanabe, M.; Sato, K.; Segawa, S.; Ishii, C.; Miyabe, A.; Murata, S.; Saito, T.; Nomura, F. Use of the MALDI BioTyper system with MALDI-TOF mass spectrometry for rapid identification of microorganisms. *Anal and Bioanal Chem* **2011**, 400, 1905, doi:10.1007/s00216-011-4877-7.
 126. Cabroler, N.; Sauget, M.; Bertrand, X.; Hocquet, D. Matrix-assisted laser desorption ionization-time of flight mass spectrometry identifies *Pseudomonas aeruginosa* high-risk clones. *J Clin Microbiol* **2015**, 53, 1395-1398, doi:10.1128/JCM.00210-15.

127. Flores-Trevino, S.; Garza-Gonzalez, E.; Mendoza-Olazarán, S.; Morfin-Otero, R.; Camacho-Ortiz, A.; Rodríguez-Noriega, E.; Martínez-Melendez, A.; Bocanegra-Ibarras, P. Screening of biomarkers of drug resistance or virulence in ESCAPE pathogens by MALDI-TOF mass spectrometry. *Sci Rep* **2019**, *9*, 18945, doi:10.1038/s41598-019-55430-1.
128. Pereira, F.D.; Bonatto, C.C.; Lopes, C.A.; Pereira, A.L.; Silva, L.P. Use of MALDI-TOF mass spectrometry to analyze the molecular profile of *Pseudomonas aeruginosa* biofilms grown on glass and plastic surfaces. *Microb Pathog* **2015**, *86*, 32-37, doi:10.1016/j.micpath.2015.07.005.
129. DeBritto, S.; Gajbar, T.D.; Satapute, P.; Sundaram, L.; Lakshmikantha, R.Y.; Jogaiah, S.; Ito, S.-i. Isolation and characterization of nutrient dependent pyocyanin from *Pseudomonas aeruginosa* and its dye and agrochemical properties. *Sci Rep* **2020**, *10*, 1542, doi:10.1038/s41598-020-58335-6.
130. Barequet, I.S.; Ben Simon, G.J.; Safrin, M.; Ohman, D.E.; Kessler, E. *Pseudomonas aeruginosa* LasA Protease in Treatment of Experimental Staphylococcal Keratitis. *Antimicrob Agents Chemother* **2004**, *48*, 1681-1687, doi:10.1128/aac.48.5.1681-1687.2004.
131. Elkhawaga, A.A.; Khalifa, M.M.; El-Badawy, O.; Hassan, M.A.; El-Said, W.A. Rapid and highly sensitive detection of pyocyanin biomarker in different *Pseudomonas aeruginosa* infections using gold nanoparticles modified sensor. *PLoS One* **2019**, *14*, e0216438, doi:10.1371/journal.pone.0216438.
132. Alhogail, S.; Suaifan, G.; Bikker, F.J.; Kaman, W.E.; Weber, K.; Cialla-May, D.; Popp, J.; Zourob, M.M. Rapid Colorimetric Detection of *Pseudomonas aeruginosa* in Clinical Isolates Using a Magnetic Nanoparticle Biosensor. *ACS Omega* **2019**, *4*, 21684-21688, doi:10.1021/acsomega.9b02080.
133. Breidenstein, E.B.; de la Fuente-Nunez, C.; Hancock, R.E. *Pseudomonas aeruginosa*: all roads lead to resistance. *Trends Microbiol* **2011**, *19*, 419-426, doi:10.1016/j.tim.2011.04.005.
134. Koo, H.; Yamada, K.M. Dynamic cell-matrix interactions modulate microbial biofilm and tissue 3D microenvironments. *Curr Opin Cell Biol* **2016**, *42*, 102-112, doi:10.1016/j.ceb.2016.05.005.
135. Hajishengallis, G.; Hajishengallis, E.; Kajikawa, T.; Wang, B.; Yancopoulou, D.; Ricklin, D.; Lambris, J.D. Complement inhibition in pre-clinical models of

- periodontitis and prospects for clinical application. *Semin Immunol* **2016**, 28, 285-291, doi:10.1016/j.smim.2016.03.006.
136. Watters, C.; Everett, J.A.; Haley, C.; Clinton, A.; Rumbaugh, K.P. Insulin treatment modulates the host immune system to enhance *Pseudomonas aeruginosa* wound biofilms. *Infect Immun* **2014**, 82, 92-100, doi:10.1128/IAI.00651-13.
 137. Maliniak, M.L.; Stecenko, A.A.; McCarty, N.A. A longitudinal analysis of chronic MRSA and *Pseudomonas aeruginosa* co-infection in cystic fibrosis: A single-center study. *J Cyst Fibros* **2016**, 15, 350-356, doi:10.1016/j.jcf.2015.10.014.
 138. Reffuveille, F.; Fuente-Nunez Cde, L.; Fairfull-Smith, K.E.; Hancock, R.E. Potentiation of ciprofloxacin action against Gram-negative bacterial biofilms by a nitroxide. *Pathog Dis* **2015**, 73, doi:10.1093/femspd/ftv016.
 139. Aoki, W.; Ueda, M. Characterization of Antimicrobial Peptides toward the Development of Novel Antibiotics. *Pharmaceuticals (Basel)* **2013**, 6, 1055-1081, doi:10.3390/ph6081055.
 140. Dosler, S.; Karaaslan, E. Inhibition and destruction of *Pseudomonas aeruginosa* biofilms by antibiotics and antimicrobial peptides. *Peptides* **2014**, 62, 32-37, doi:10.1016/j.peptides.2014.09.021.
 141. Gordon, Y.J.; Romanowski, E.G.; McDermott, A.M. A Review of Antimicrobial Peptides and Their Therapeutic Potential as Anti-Infective Drugs. *Curr Eye Res* **2005**, 30, 505-515, doi:10.1080/02713680590968637.
 142. Papareddy, P.; Kasetty, G.; Kalle, M.; Bhongir, R.K.V.; Mörgelin, M.; Schmidtchen, A.; Malmsten, M. NLF20: an antimicrobial peptide with therapeutic potential against invasive *Pseudomonas aeruginosa* infection. *J Antimicrob Chemother* **2016**, 71, 170-180, doi:10.1093/jac/dkv322.
 143. Shin, S.C.; Ahn, I.H.; Ahn, D.H.; Lee, Y.M.; Lee, J.; Lee, J.H.; Kim, H.-W.; Park, H. Characterization of Two Antimicrobial Peptides from Antarctic Fishes (*Notothenia coriiceps* and *Parachaenichthys charcoti*). *Plos One* **2017**, 12, e0170821, doi:10.1371/journal.pone.0170821.
 144. Wnorowska, U.; Niemirowicz, K.; Myint, M.; Diamond, S.L.; Wróblewska, M.; Savage, P.B.; Janmey, P.A.; Bucki, R. Bactericidal Activities of Cathelicidin LL-37 and Select Cationic Lipids against the Hypervirulent *Pseudomonas aeruginosa* Strain LESB58. *Antimicrob Agents Chemother* **2015**, 59, 3808, doi:10.1128/AAC.00421-15.

145. Flume, P.A.; VanDevanter, D.R.; Morgan, E.E.; Dudley, M.N.; Loutit, J.S.; Bell, S.C.; Kerem, E.; Fischer, R.; Smyth, A.R.; Aaron, S.D., et al. A phase 3, multi-center, multinational, randomized, double-blind, placebo-controlled study to evaluate the efficacy and safety of levofloxacin inhalation solution (APT-1026) in stable cystic fibrosis patients. *J Cyst Fibros* **2016**, *15*, 495-502, doi:10.1016/j.jcf.2015.12.004.
146. Wagner, S.; Hauck, D.; Hoffmann, M.; Sommer, R.; Joachim, I.; Müller, R.; Imberty, A.; Varrot, A.; Titz, A. Covalent Lectin Inhibition and Application in Bacterial Biofilm Imaging. *Angew Chem Int Ed Engl* **2017**, *56*, 16559-16564, doi:10.1002/anie.201709368.
147. Johansson, E.M.V.; Crusz, S.A.; Kolomiets, E.; Buts, L.; Kadam, R.U.; Cacciarini, M.; Bartels, K.-M.; Diggle, S.P.; Cámara, M.; Williams, P., et al. Inhibition and Dispersion of *Pseudomonas aeruginosa* Biofilms by Glycopeptide Dendrimers Targeting the Fucose-Specific Lectin LecB. *Chemistry & Biology* **2008**, *15*, 1249-1257, doi:<https://doi.org/10.1016/j.chembiol.2008.10.009>.
148. Krachler, A.M.; Orth, K. Targeting the bacteria–host interface. *Virulence* **2013**, *4*, 284-294, doi:10.4161/viru.24606.
149. Chatain-ly, M.H. The factors affecting effectiveness of treatment in phages therapy. *Front Microbiol* **2014**, *5*, doi:10.3389/fmicb.2014.00051.
150. Pires, D.P.; Vilas Boas, D.; Sillankorva, S.; Azeredo, J. Phage Therapy: a Step Forward in the Treatment of *Pseudomonas aeruginosa* Infections. *J Virol* **2015**, *89*, 7449, doi:10.1128/JVI.00385-15.
151. Vandenheuvel, D.; Lavigne, R.; Brüßow, H. Bacteriophage Therapy: Advances in Formulation Strategies and Human Clinical Trials. *Annu Rev Virol* **2015**, *2*, 599-618, doi:10.1146/annurev-virology-100114-054915.
152. Penadés, J.R.; Chen, J.; Quiles-Puchalt, N.; Carpena, N.; Novick, R.P. Bacteriophage-mediated spread of bacterial virulence genes. *Curr Opin Microbiol* **2015**, *23*, 171-178, doi:<https://doi.org/10.1016/j.mib.2014.11.019>.
153. Hesse, S.; Adhya, S. Phage Therapy in the Twenty-First Century: Facing the Decline of the Antibiotic Era; Is It Finally Time for the Age of the Phage? *Annu Rev Microbiol* **2019**, *73*, 155-174, doi:10.1146/annurev-micro-090817-062535.
154. Melander, R.J.; Basak, A.K.; Melander, C. Natural products as inspiration for the development of bacterial antibiofilm agents. *Nat Prod Rep* **2020**, 10.1039/d0np00022a, doi:10.1039/d0np00022a.

155. Salomoni, R.; Leo, P.; Montemor, A.F.; Rinaldi, B.G.; Rodrigues, M. Antibacterial effect of silver nanoparticles in *Pseudomonas aeruginosa*. *Nanotechnol Sci Appl* **2017**, *10*, 115-121, doi:10.2147/NSA.S133415.
156. Chen, Q.; Shah, K.N.; Zhang, F.; Salazar, A.J.; Shah, P.N.; Li, R.; Sacchettini, J.C.; Wooley, K.L.; Cannon, C.L. Minocycline and Silver Dual-Loaded Polyphosphoester-Based Nanoparticles for Treatment of Resistant *Pseudomonas aeruginosa*. *Mol Pharm* **2019**, *16*, 1606-1619, doi:10.1021/acs.molpharmaceut.8b01288.
157. Gunday Tureli, N.; Torge, A.; Juntke, J.; Schwarz, B.C.; Schneider-Daum, N.; Tureli, A.E.; Lehr, C.M.; Schneider, M. Ciprofloxacin-loaded PLGA nanoparticles against cystic fibrosis *P. aeruginosa* lung infections. *Eur J Pharm Biopharm* **2017**, *117*, 363-371, doi:10.1016/j.ejpb.2017.04.032.
158. Deacon, J.; Abdelghany, S.M.; Quinn, D.J.; Schmid, D.; Megaw, J.; Donnelly, R.F.; Jones, D.S.; Kissenpfennig, A.; Elborn, J.S.; Gilmore, B.F., et al. Antimicrobial efficacy of tobramycin polymeric nanoparticles for *Pseudomonas aeruginosa* infections in cystic fibrosis: formulation, characterisation and functionalisation with dornase alfa (DNase). *J Control Release* **2015**, *198*, 55-61, doi:10.1016/j.jconrel.2014.11.022.
159. d'Angelo, I.; Casciaro, B.; Miro, A.; Quaglia, F.; Mangoni, M.L.; Ungaro, F. Overcoming barriers in *Pseudomonas aeruginosa* lung infections: Engineered nanoparticles for local delivery of a cationic antimicrobial peptide. *Colloids Surf B Biointerfaces* **2015**, *135*, 717-725, doi:10.1016/j.colsurfb.2015.08.027.
160. Baelo, A.; Levato, R.; Julian, E.; Crespo, A.; Astola, J.; Gavalda, J.; Engel, E.; Mateos-Timoneda, M.A.; Torrents, E. Disassembling bacterial extracellular matrix with DNase-coated nanoparticles to enhance antibiotic delivery in biofilm infections. *J Control Release* **2015**, *209*, 150-158, doi:10.1016/j.jconrel.2015.04.028.
161. Powell, L.C.; Pritchard, M.F.; Ferguson, E.L.; Powell, K.A.; Patel, S.U.; Rye, P.D.; Sakellakou, S.M.; Buurma, N.J.; Brilliant, C.D.; Copping, J.M., et al. Targeted disruption of the extracellular polymeric network of *Pseudomonas aeruginosa* biofilms by alginate oligosaccharides. *NPJ Biofilms Microbiomes* **2018**, *4*, 13, doi:10.1038/s41522-018-0056-3.
162. Zhu, X.; Oh, H.-S.; Ng, Y.C.B.; Tang, P.Y.P.; Barraud, N.; Rice, S.A. Nitric Oxide-Mediated Induction of Dispersal in *Pseudomonas aeruginosa* Biofilms Is Inhibited by

- Flavohemoglobin Production and Is Enhanced by Imidazole. *Antimicrob Agents Chemother* **2018**, 62, e01832-01817, doi:10.1128/AAC.01832-17.
163. Birmes, F.S.; Säring, R.; Hauke, M.C.; Ritzmann, N.H.; Drees, S.L.; Daniel, J.; Treffon, J.; Liebau, E.; Kahl, B.C.; Fetzner, S. Interference with *Pseudomonas aeruginosa* Quorum Sensing and Virulence by the Mycobacterial *Pseudomonas* Quinolone Signal Dioxygenase AqdC in Combination with the N-Acylhomoserine Lactone Lactonase QsdA. *Infect Immun* **2019**, 87, e00278-00219, doi:10.1128/IAI.00278-19.
 164. Kim, B.; Park, J.S.; Choi, H.Y.; Yoon, S.S.; Kim, W.G. Terrein is an inhibitor of quorum sensing and c-di-GMP in *Pseudomonas aeruginosa*: a connection between quorum sensing and c-di-GMP. *Sci Rep* **2018**, 8, 8617, doi:10.1038/s41598-018-26974-5.
 165. Kiymaci, M.E.; Altanlar, N.; Gumustas, M.; Ozkan, S.A.; Akin, A. Quorum sensing signals and related virulence inhibition of *Pseudomonas aeruginosa* by a potential probiotic strain's organic acid. *Microb Pathog* **2018**, 121, 190-197, doi:10.1016/j.micpath.2018.05.042.
 166. Kaneko, Y.; Thoendel, M.; Olakanmi, O.; Britigan, B.E.; Singh, P.K. The transition metal gallium disrupts *Pseudomonas aeruginosa* iron metabolism and has antimicrobial and antibiofilm activity. *J Clin Invest* **2007**, 117, 877-888, doi:10.1172/JCI30783.
 167. Moreau-Marquis, S.; O'Toole, G.A.; Stanton, B.A. Tobramycin and FDA-approved iron chelators eliminate *Pseudomonas aeruginosa* biofilms on cystic fibrosis cells. *Am J Respir Cell Mol Biol* **2009**, 41, 305-313, doi:10.1165/rcmb.2008-0299OC.
 168. Soukos, N.S.; Goodson, J.M. Photodynamic therapy in the control of oral biofilms. *Periodontol 2000* **2011**, 55, 143-166, doi:10.1111/j.1600-0757.2010.00346.x.
 169. Kübler, A.C. Photodynamic therapy. *Med Laser Appl* **2005**, 20, 37-45, doi:<https://doi.org/10.1016/j.mla.2005.02.001>.
 170. Orlandi, V.T.; Rybtke, M.; Caruso, E.; Banfi, S.; Tolker-Nielsen, T.; Barbieri, P. Antimicrobial and anti-biofilm effect of a novel BODIPY photosensitizer against *Pseudomonas aeruginosa* PAO1. *Biofouling* **2014**, 30, 883-891, doi:10.1080/08927014.2014.940921.
 171. Vassena, C.; Fenu, S.; Giuliani, F.; Fantetti, L.; Roncucci, G.; Simonutti, G.; Romano, C.L.; De Francesco, R.; Drago, L. Photodynamic antibacterial and antibiofilm activity

- of RLP068/Cl against *Staphylococcus aureus* and *Pseudomonas aeruginosa* forming biofilms on prosthetic material. *Int J Antimicrob Agents* **2014**, *44*, 47-55, doi:10.1016/j.ijantimicag.2014.03.012.
172. Parasuraman, P.; Antony, A.P.; B, S.L.S.; Sharan, A.; Siddhardha, B.; Kasinathan, K.; Bahkali, N.A.; Dawoud, T.M.S.; Syed, A. Antimicrobial photodynamic activity of toluidine blue encapsulated in mesoporous silica nanoparticles against *Pseudomonas aeruginosa* and *Staphylococcus aureus*. *Biofouling* **2019**, *35*, 89-103, doi:10.1080/08927014.2019.1570501.
 173. Al-Bakri, A.G.; Mahmoud, N.N. Photothermal-Induced Antibacterial Activity of Gold Nanorods Loaded into Polymeric Hydrogel against *Pseudomonas aeruginosa* Biofilm. *Molecules* **2019**, *24*, doi:10.3390/molecules24142661.
 174. Peng, H.; Borg, R.E.; Dow, L.P.; Pruitt, B.L.; Chen, I.A. Controlled phage therapy by photothermal ablation of specific bacterial species using gold nanorods targeted by chimeric phages. *Proc Natl Acad Sci U S A* **2020**, *117*, 1951-1961, doi:10.1073/pnas.1913234117.
 175. Zhao, B.; Wang, H.; Dong, W.; Cheng, S.; Li, H.; Tan, J.; Zhou, J.; He, W.; Li, L.; Zhang, J., et al. A multifunctional platform with single-NIR-laser-triggered photothermal and NO release for synergistic therapy against multidrug-resistant Gram-negative bacteria and their biofilms. *J Nanobiotechnology* **2020**, *18*, 59, doi:10.1186/s12951-020-00614-5.
 176. Bilici, K.; Atac, N.; Muti, A.; Baylam, I.; Dogan, O.; Sennaroglu, A.; Can, F.; Yagci Acar, H. Broad spectrum antibacterial photodynamic and photothermal therapy achieved with indocyanine green loaded SPIONs under near infrared irradiation. *Biomater Sci* **2020**, *8*, 4616-4625, doi:10.1039/d0bm00821d.
 177. Wong, J.P.; Yang, H.; Blasetti, K.L.; Schnell, G.; Conley, J.; Schofield, L.N. Liposome delivery of ciprofloxacin against intracellular *Francisella tularensis* infection. *J Control Release* **2003**, *92*, 265-273, doi:10.1016/s0168-3659(03)00358-4.
 178. Ghaffari, S.; Varshosaz, J.; Saadat, A.; Atyabi, F. Stability and antimicrobial effect of amikacin-loaded solid lipid nanoparticles. *Int J Nanomedicine* **2010**, *6*, 35-43, doi:10.2147/IJN.S13671.
 179. Bargoni, A.; Cavalli, R.; Zara, G.P.; Fundaro, A.; Caputo, O.; Gasco, M.R. Transmucosal transport of tobramycin incorporated in solid lipid nanoparticles (SLN)

- after duodenal administration to rats. Part II--tissue distribution. *Pharmacol Res* **2001**, 43, 497-502, doi:10.1006/phrs.2001.0813.
180. Alizadeh, A.; Salouti, M.; Alizadeh, H.; Kazemizadeh, A.R.; Safari, A.A.; Mahmazi, S. Enhanced antibacterial effect of azlocillin in conjugation with silver nanoparticles against *Pseudomonas aeruginosa*. *IET Nanobiotechnol* **2017**, 11, 942-947, doi:10.1049/iet-nbt.2017.0009.
 181. Lamppa, J.W.; Griswold, K.E. Alginate lyase exhibits catalysis-independent biofilm dispersion and antibiotic synergy. *Antimicrob Agents Chemother* **2013**, 57, 137-145, doi:10.1128/AAC.01789-12.
 182. Pleszczynska, M.; Wiater, A.; Janczarek, M.; Szczodrak, J. (1-->3)-alpha-D-Glucan hydrolases in dental biofilm prevention and control: A review. *Int J Biol Macromol* **2015**, 79, 761-778, doi:10.1016/j.ijbiomac.2015.05.052.
 183. Eckhart, L.; Fischer, H.; Barken, K.B.; Tolker-Nielsen, T.; Tschachler, E. DNase1L2 suppresses biofilm formation by *Pseudomonas aeruginosa* and *Staphylococcus aureus*. *Br J Dermatol* **2007**, 156, 1342-1345, doi:10.1111/j.1365-2133.2007.07886.x.
 184. Okshevsky, M.; Regina, V.R.; Meyer, R.L. Extracellular DNA as a target for biofilm control. *Curr Opin Biotechnol* **2015**, 33, 73-80, doi:<https://doi.org/10.1016/j.copbio.2014.12.002>.
 185. Liu, Y.; Kamesh, A.C.; Xiao, Y.; Sun, V.; Hayes, M.; Daniell, H.; Koo, H. Topical delivery of low-cost protein drug candidates made in chloroplasts for biofilm disruption and uptake by oral epithelial cells. *Biomaterials* **2016**, 105, 156-166, doi:10.1016/j.biomaterials.2016.07.042.
 186. Zhou, E.; Seminara, A.B.; Kim, S.K.; Hall, C.L.; Wang, Y.; Lee, V.T. Thiol-benzotriazolo-quinazolinone Inhibits Alg44 Binding to c-di-GMP and Reduces Alginate Production by *Pseudomonas aeruginosa*. *ACS Chem Biol* **2017**, 12, 3076-3085, doi:10.1021/acschembio.7b00826.
 187. Warrenner, P.; Varkey, R.; Bonnell, J.C.; DiGiandomenico, A.; Camara, M.; Cook, K.; Peng, L.; Zha, J.; Chowdury, P.; Sellman, B., et al. A novel anti-PcrV antibody providing enhanced protection against *Pseudomonas aeruginosa* in multiple animal infection models. *Antimicrob Agents Chemother* **2014**, 58, 4384-4391, doi:10.1128/AAC.02643-14.
 188. DiGiandomenico, A.; Warrenner, P.; Hamilton, M.; Guillard, S.; Ravn, P.; Minter, R.; Camara, M.M.; Venkatraman, V.; Macgill, R.S.; Lin, J., et al. Identification of

- broadly protective human antibodies to *Pseudomonas aeruginosa* exopolysaccharide Psl by phenotypic screening. *J Exp Med* **2012**, 209, 1273-1287, doi:10.1084/jem.20120033.
189. Novotny, L.A.; Jurcisek, J.A.; Goodman, S.D.; Bakaletz, L.O. Monoclonal antibodies against DNA-binding tips of DNABII proteins disrupt biofilms in vitro and induce bacterial clearance in vivo. *EBioMedicine* **2016**, 10, 33-44, doi:10.1016/j.ebiom.2016.06.022.
 190. Howlin, R.P.; Cathie, K.; Hall-Stoodley, L.; Cornelius, V.; Duignan, C.; Allan, R.N.; Fernandez, B.O.; Barraud, N.; Bruce, K.D.; Jefferies, J., et al. Low-Dose Nitric Oxide as Targeted Anti-biofilm Adjunctive Therapy to Treat Chronic *Pseudomonas aeruginosa* Infection in Cystic Fibrosis. *Mol Ther* **2017**, 25, 2104-2116, doi:10.1016/j.ymthe.2017.06.021.
 191. Lin Chua, S.; Liu, Y.; Li, Y.; Jun Ting, H.; Kohli, G.S.; Cai, Z.; Suwanchaikasem, P.; Kau Kit Goh, K.; Pin Ng, S.; Tolker-Nielsen, T., et al. Reduced Intracellular c-di-GMP Content Increases Expression of Quorum Sensing-Regulated Genes in *Pseudomonas aeruginosa*. *Front Cell Infect Microbiol* **2017**, 7, 451, doi:10.3389/fcimb.2017.00451.
 192. Ouyang, J.; Sun, F.; Feng, W.; Sun, Y.; Qiu, X.; Xiong, L.; Liu, Y.; Chen, Y. Quercetin is an effective inhibitor of quorum sensing, biofilm formation and virulence factors in *Pseudomonas aeruginosa*. *J Appl Microbiol* **2016**, 120, 966-974, doi:10.1111/jam.13073.
 193. Maura, D.; Rahme, L.G. Pharmacological Inhibition of the *Pseudomonas aeruginosa* MvfR Quorum-Sensing System Interferes with Biofilm Formation and Potentiates Antibiotic-Mediated Biofilm Disruption. *Antimicrob Agents Chemother* **2017**, 61, doi:10.1128/AAC.01362-17.
 194. Utari, P.D.; Setroikromo, R.; Melgert, B.N.; Quax, W.J. PvdQ Quorum Quenching Acylase Attenuates *Pseudomonas aeruginosa* Virulence in a Mouse Model of Pulmonary Infection. *Front Cell Infect Microbiol* **2018**, 8, doi:10.3389/fcimb.2018.00119.
 195. Oglesby-Sherrouse, A.G.; Djapgne, L.; Nguyen, A.T.; Vasil, A.I.; Vasil, M.L. The complex interplay of iron, biofilm formation, and mucoidy affecting antimicrobial resistance of *Pseudomonas aeruginosa*. *Pathog Dis* **2014**, 70, 307-320, doi:10.1111/2049-632X.12132.

196. Ma, L.; Terwilliger, A.; Maresso, A.W. Iron and zinc exploitation during bacterial pathogenesis. *Metallomics* **2015**, *7*, 1541-1554, doi:10.1039/c5mt00170f.
197. Reid, D.W.; Carroll, V.; May, C.; Champion, A.; Kirov, S.M. Increased airway iron as a potential factor in the persistence of *Pseudomonas aeruginosa* infection in cystic fibrosis. *Eur Respir J* **2007**, *30*, 286, doi:10.1183/09031936.00154006.
198. Banin, E.; Lozinski, A.; Brady, K.M.; Berenshtein, E.; Butterfield, P.W.; Moshe, M.; Chevion, M.; Greenberg, E.P.; Banin, E. The potential of desferrioxamine-gallium as an anti-*Pseudomonas* therapeutic agent. *Proc Natl Acad Sci U S A* **2008**, *105*, 16761-16766, doi:10.1073/pnas.0808608105.
199. Darabpour, E.; Kashef, N.; Mashayekhan, S. Chitosan nanoparticles enhance the efficiency of methylene blue-mediated antimicrobial photodynamic inactivation of bacterial biofilms: An in vitro study. *Photodiagnosis Photodyn Ther* **2016**, *14*, 211-217, doi:<https://doi.org/10.1016/j.pdpdt.2016.04.009>.
200. Wainwright, M.; Phoenix, D.A.; Laycock, S.L.; Wareing, D.R.; Wright, P.A. Photobactericidal activity of phenothiazinium dyes against methicillin-resistant strains of *Staphylococcus aureus*. *FEMS Microbiol Lett* **1998**, *160*, 177-181, doi:10.1111/j.1574-6968.1998.tb12908.x.
201. Vatansever, F.; de Melo, W.C.; Avci, P.; Vecchio, D.; Sadasivam, M.; Gupta, A.; Chandran, R.; Karimi, M.; Parizotto, N.A.; Yin, R., et al. Antimicrobial strategies centered around reactive oxygen species--bactericidal antibiotics, photodynamic therapy, and beyond. *FEMS Microbiol Rev* **2013**, *37*, 955-989, doi:10.1111/1574-6976.12026.
202. Tavares, A.; Carvalho, C.M.; Faustino, M.A.; Neves, M.G.; Tome, J.P.; Tome, A.C.; Cavaleiro, J.A.; Cunha, A.; Gomes, N.C.; Alves, E., et al. Antimicrobial photodynamic therapy: study of bacterial recovery viability and potential development of resistance after treatment. *Mar Drugs* **2010**, *8*, 91-105, doi:10.3390/md8010091.
203. Misba, L.; Zaidi, S.; Khan, A.U. A comparison of antibacterial and antibiofilm efficacy of phenothiazinium dyes between Gram positive and Gram negative bacterial biofilm. *Photodiagnosis Photodyn Ther* **2017**, *18*, 24-33, doi:<https://doi.org/10.1016/j.pdpdt.2017.01.177>.
204. Beirao, S.; Fernandes, S.; Coelho, J.; Faustino, M.A.; Tome, J.P.; Neves, M.G.; Tome, A.C.; Almeida, A.; Cunha, A. Photodynamic inactivation of bacterial and yeast

- biofilms with a cationic porphyrin. *Photochem Photobiol* **2014**, 90, 1387-1396, doi:10.1111/php.12331.
205. Zhao, Y.; Lu, Z.; Dai, X.; Wei, X.; Yu, Y.; Chen, X.; Zhang, X.; Li, C. Glycomimetic-Conjugated Photosensitizer for Specific *Pseudomonas aeruginosa* Recognition and Targeted Photodynamic Therapy. *Bioconjug Chem* **2018**, 29, 3222-3230, doi:10.1021/acs.bioconjchem.8b00600.
 206. Abdulrahman, H.; Misba, L.; Ahmad, S.; Khan, A.U. Curcumin induced photodynamic therapy mediated suppression of quorum sensing pathway of *Pseudomonas aeruginosa*: An approach to inhibit biofilm in vitro. *Photodiagnosis Photodyn Ther* **2020**, 30, 101645, doi:10.1016/j.pdpdt.2019.101645.
 207. Korupalli, C.; Huang, C.-C.; Lin, W.-C.; Pan, W.-Y.; Lin, P.-Y.; Wan, W.-L.; Li, M.-J.; Chang, Y.; Sung, H.-W. Acidity-triggered charge-convertible nanoparticles that can cause bacterium-specific aggregation in situ to enhance photothermal ablation of focal infection. *Biomaterials* **2017**, 116, 1-9, doi:<https://doi.org/10.1016/j.biomaterials.2016.11.045>.
 208. Murali, V.S.; Wang, R.; Mikoryak, C.A.; Pantano, P.; Draper, R.K. The impact of subcellular location on the near infrared-mediated thermal ablation of cells by targeted carbon nanotubes. *Nanotechnology* **2016**, 27, 425102-425102, doi:10.1088/0957-4484/27/42/425102.
 209. Qian, W.; Yan, C.; He, D.; Yu, X.; Yuan, L.; Liu, M.; Luo, G.; Deng, J. pH-triggered charge-reversible of glycol chitosan conjugated carboxyl graphene for enhancing photothermal ablation of focal infection. *Acta Biomater* **2018**, 69, 256-264, doi:<https://doi.org/10.1016/j.actbio.2018.01.022>.
 210. Behzadpour, N.; Sattarahmady, N.; Akbari, N. Antimicrobial Photothermal Treatment of *Pseudomonas Aeruginosa* by a Carbon Nanoparticles-Polypyrrole Nanocomposite. *J Biomed Phys Eng* **2019**, 9, 661-672, doi:10.31661/jbpe.v0i0.1024.
 211. Dickerson, E.B.; Dreaden, E.C.; Huang, X.; El-Sayed, I.H.; Chu, H.; Pushpanketh, S.; McDonald, J.F.; El-Sayed, M.A. Gold nanorod assisted near-infrared plasmonic photothermal therapy (PPTT) of squamous cell carcinoma in mice. *Cancer Lett* **2008**, 269, 57-66, doi:10.1016/j.canlet.2008.04.026.
 212. Huang, J.; Zhou, J.; Zhuang, J.; Gao, H.; Huang, D.; Wang, L.; Wu, W.; Li, Q.; Yang, D.-P.; Han, M.-Y. Strong Near-Infrared Absorbing and Biocompatible CuS Nanoparticles for Rapid and Efficient Photothermal Ablation of Gram-Positive and -

- Negative Bacteria. *ACS Appl Mater Interfaces* **2017**, 9, 36606-36614, doi:10.1021/acsami.7b11062.
213. Bongiovanni Abel, S.; Gallarato, L.A.; Dardanelli, M.S.; Barbero, C.A.; Rivarola, C.R.; Yslas, E.I. Photothermal lysis of *Pseudomonas aeruginosa* by polyaniline nanoparticles under near infrared irradiation. *Biomed Phys Eng Express* **2018**, 4, doi:10.1088/2057-1976/aacf33.
214. Dias, D.A.; Urban, S.; Roessner, U. A historical overview of natural products in drug discovery. *Metabolites* **2012**, 2, 303-336, doi:10.3390/metabo2020303.
215. Cragg, G.M.; Newman, D.J. Natural products: a continuing source of novel drug leads. *Biochim Biophys Acta* **2013**, 1830, 3670-3695, doi:10.1016/j.bbagen.2013.02.008.
216. Zjawiony, J.K. Biologically active compounds from Aphyllophorales (polypore) fungi. *J Nat Prod* **2004**, 67, 300-310, doi:10.1021/np030372w.
217. Heinrich, M.; Lee Teoh, H. Galanthamine from snowdrop—the development of a modern drug against Alzheimer's disease from local Caucasian knowledge. *Journal of Ethnopharmacology* **2004**, 92, 147-162, doi:<https://doi.org/10.1016/j.jep.2004.02.012>.
218. Ojima, I. Modern natural products chemistry and drug discovery. *J Med Chem* **2008**, 51, 2587-2588, doi:10.1021/jm701291u.
219. Butler, M.S.; Robertson, A.A.; Cooper, M.A. Natural product and natural product derived drugs in clinical trials. *Nat Prod Rep* **2014**, 31, 1612-1661, doi:10.1039/c4np00064a.
220. Hoff, B.; Poggeler, S.; Kuck, U. Eighty years after its discovery, Fleming's *Penicillium* strain discloses the secret of its sex. *Eukaryot Cell* **2008**, 7, 465-470, doi:10.1128/EC.00430-07.
221. Mazumder, K.; Tanaka, K.; Fukase, K. Cytotoxic activity of ursolic acid derivatives obtained by isolation and oxidative derivatization. *Molecules* **2013**, 18, 8929-8944, doi:10.3390/molecules18088929.
222. Salam, A.M.; Quave, C.L. Opportunities for plant natural products in infection control. *Curr Opin Microbiol* **2018**, 45, 189-194, doi:10.1016/j.mib.2018.08.004.
223. Cowan, M.M. Plant products as antimicrobial agents. *Clin Microbiol Rev* **1999**, 12, 564-582, doi:10.1128/CMR.12.4.564.
224. Borges, A.; Abreu, A.C.; Dias, C.; Saavedra, M.J.; Borges, F.; Simoes, M. New Perspectives on the Use of Phytochemicals as an Emergent Strategy to Control

- Bacterial Infections Including Biofilms. *Molecules* **2016**, *21*, doi:10.3390/molecules21070877.
225. AlSheikh, H.M.A.; Sultan, I.; Kumar, V.; Rather, I.A.; Al-Sheikh, H.; Tasleem Jan, A.; Haq, Q.M.R. Plant-Based Phytochemicals as Possible Alternative to Antibiotics in Combating Bacterial Drug Resistance. *Antibiotics (Basel)* **2020**, *9*, doi:10.3390/antibiotics9080480.
 226. González-Lamothe, R.; Mitchell, G.; Gattuso, M.; Diarra, M.S.; Malouin, F.; Bouarab, K. Plant Antimicrobial Agents and Their Effects on Plant and Human Pathogens. *International Journal of Molecular Sciences* **2009**, *10*, doi:10.3390/ijms10083400.
 227. Ulrey, R.K.; Barksdale, S.M.; Zhou, W.; van Hoek, M.L. Cranberry proanthocyanidins have anti-biofilm properties against *Pseudomonas aeruginosa*. *BMC Complement Altern Med* **2014**, *14*, 499-499, doi:10.1186/1472-6882-14-499.
 228. Dey, P.; Parai, D.; Banerjee, M.; Hossain, S.T.; Mukherjee, S.K. Naringin sensitizes the antibiofilm effect of ciprofloxacin and tetracycline against *Pseudomonas aeruginosa* biofilm. *International Journal of Medical Microbiology* **2020**, *310*, 151410, doi:<https://doi.org/10.1016/j.ijmm.2020.151410>.
 229. Bjarnsholt, T.; Jensen, P.O.; Rasmussen, T.B.; Christophersen, L.; Calum, H.; Hentzer, M.; Hougen, H.P.; Rygaard, J.; Moser, C.; Eberl, L., et al. Garlic blocks quorum sensing and promotes rapid clearing of pulmonary *Pseudomonas aeruginosa* infections. *Microbiology (Reading)* **2005**, *151*, 3873-3880, doi:10.1099/mic.0.27955-0.
 230. Nakamoto, M.; Kunitura, K.; Suzuki, J.-I.; Koda, Y. Antimicrobial properties of hydrophobic compounds in garlic: Allicin, vinylthiin, ajoene and diallyl polysulfides. *Exp Ther Med* **2020**, *19*, 1550-1553, doi:10.3892/etm.2019.8388.
 231. Tan, S.Y.-Y.; Liu, Y.; Chua, S.L.; Vejborg, R.M.; Jakobsen, T.H.; Chew, S.C.; Li, Y.; Nielsen, T.E.; Tolker-Nielsen, T.; Yang, L., et al. Comparative systems biology analysis to study the mode of action of the isothiocyanate compound Iberin on *Pseudomonas aeruginosa*. *Antimicrob Agents Chemother* **2014**, *58*, 6648-6659, doi:10.1128/AAC.02620-13.
 232. Suarez, M.; Haenni, M.; Canarelli, S.; Fisch, F.; Chodanowski, P.; Servis, C.; Michielin, O.; Freitag, R.; Moreillon, P.; Mermoud, N. Structure-function

- characterization and optimization of a plant-derived antibacterial peptide. *Antimicrob Agents Chemother* **2005**, *49*, 3847-3857, doi:10.1128/AAC.49.9.3847-3857.2005.
233. Mocan, A.; Babotă, M.; Pop, A.; Fizeșan, I.; Diuzheva, A.; Locatelli, M.; Carradori, S.; Campestre, C.; Menghini, L.; Sisea, C.R., et al. Chemical Constituents and Biologic Activities of Sage Species: A Comparison between *Salvia officinalis* L., *S. glutinosa* L. and *S. transsylvanica* (Schur ex Griseb. & Schenk) Schur. *Antioxidants* **2020**, *9*, doi:10.3390/antiox9060480.
 234. Stubbendieck, R.M.; Straight, P.D. Multifaceted Interfaces of Bacterial Competition. *J Bacteriol* **2016**, *198*, 2145-2155, doi:10.1128/JB.00275-16.
 235. Wright, G.D. Unlocking the potential of natural products in drug discovery. *Microb Biotechnol* **2019**, *12*, 55-57, doi:10.1111/1751-7915.13351.
 236. Townsley, L.; Shank, E.A. Natural-Product Antibiotics: Cues for Modulating Bacterial Biofilm Formation. *Trends Microbiol* **2017**, *25*, 1016-1026, doi:10.1016/j.tim.2017.06.003.
 237. Davies, D.G.; Marques, C.N.H. A fatty acid messenger is responsible for inducing dispersion in microbial biofilms. *J Bacteriol* **2009**, *191*, 1393-1403, doi:10.1128/JB.01214-08.
 238. Navarro, G.; Cheng, A.T.; Peach, K.C.; Bray, W.M.; Bernan, V.S.; Yildiz, F.H.; Linington, R.G. Image-based 384-well high-throughput screening method for the discovery of skyllamycins A to C as biofilm inhibitors and inducers of biofilm detachment in *Pseudomonas aeruginosa*. *Antimicrob Agents Chemother* **2014**, *58*, 1092-1099, doi:10.1128/AAC.01781-13.
 239. Steele, A.D.; Knouse, K.W.; Keohane, C.E.; Wuest, W.M. Total Synthesis and Biological Investigation of (–)-Promysalin. *Journal of the American Chemical Society* **2015**, *137*, 7314-7317, doi:10.1021/jacs.5b04767.
 240. Steele, A.D.; Keohane, C.E.; Knouse, K.W.; Rossiter, S.E.; Williams, S.J.; Wuest, W.M. Diverted Total Synthesis of Promysalin Analogs Demonstrates That an Iron-Binding Motif Is Responsible for Its Narrow-Spectrum Antibacterial Activity. *Journal of the American Chemical Society* **2016**, *138*, 5833-5836, doi:10.1021/jacs.6b03373.
 241. Basaran, T.I.; Berber, D.; Gokalsin, B.; Tramice, A.; Tommonaro, G.; Abbamondi, G.R.; Erginer Haskoylu, M.; Toksoy Oner, E.; Iodice, C.; Sesal, N.C. Extremophilic *Natrinema versiforme* Against *Pseudomonas aeruginosa* Quorum Sensing and Biofilm. *Front Microbiol* **2020**, *11*, 79, doi:10.3389/fmicb.2020.00079.

242. Donia, M.; Hamann, M.T. Marine natural products and their potential applications as anti-infective agents. *Lancet Infect Dis* **2003**, *3*, 338-348, doi:10.1016/s1473-3099(03)00655-8.
243. Malve, H. Exploring the ocean for new drug developments: Marine pharmacology. *J Pharm Bioallied Sci* **2016**, *8*, 83-91, doi:10.4103/0975-7406.171700.
244. Ruzicka, R.; Gleason, D.F. Latitudinal variation in spongivorous fishes and the effectiveness of sponge chemical defenses. *Oecologia* **2008**, *154*, 785-794, doi:10.1007/s00442-007-0874-0.
245. Skindersoe, M.E.; Ettinger-Epstein, P.; Rasmussen, T.B.; Bjarnsholt, T.; de Nys, R.; Givskov, M. Quorum sensing antagonism from marine organisms. *Mar Biotechnol (NY)* **2008**, *10*, 56-63, doi:10.1007/s10126-007-9036-y.
246. Huigens, R.W., 3rd; Richards, J.J.; Parise, G.; Ballard, T.E.; Zeng, W.; Deora, R.; Melander, C. Inhibition of *Pseudomonas aeruginosa* biofilm formation with Bromoageliferin analogues. *J Am Chem Soc* **2007**, *129*, 6966-6967, doi:10.1021/ja069017t.
247. Huigens, R.W., 3rd; Ma, L.; Gambino, C.; Moeller, P.D.; Basso, A.; Cavanagh, J.; Wozniak, D.J.; Melander, C. Control of bacterial biofilms with marine alkaloid derivatives. *Mol Biosyst* **2008**, *4*, 614-621, doi:10.1039/b719989a.
248. Trang, T.T.T.; Dieltjens, L.; Hooyberghs, G.; Waldrant, K.; Ermolat'ev, D.S.; Van der Eycken, E.V.; Steenackers, H.P.L. Enhancing the anti-biofilm activity of 5-aryl-2-aminoimidazoles through nature inspired dimerisation. *Bioorganic & Medicinal Chemistry* **2018**, *26*, 1470-1480, doi:<https://doi.org/10.1016/j.bmc.2018.01.005>.
249. Hentzer, M.; Wu, H.; Andersen, J.B.; Riedel, K.; Rasmussen, T.B.; Bagge, N.; Kumar, N.; Schembri, M.A.; Song, Z.; Kristoffersen, P., et al. Attenuation of *Pseudomonas aeruginosa* virulence by quorum sensing inhibitors. *EMBO J* **2003**, *22*, 3803-3815, doi:10.1093/emboj/cdg366.
250. Wu, H.; Song, Z.; Hentzer, M.; Andersen, J.B.; Molin, S.; Givskov, M.; Høiby, N. Synthetic furanones inhibit quorum-sensing and enhance bacterial clearance in *Pseudomonas aeruginosa* lung infection in mice. *Journal of Antimicrobial Chemotherapy* **2004**, *53*, 1054-1061, doi:10.1093/jac/dkh223.
251. Yin, Q.; Liang, J.; Zhang, W.; Zhang, L.; Hu, Z.L.; Zhang, Y.; Xu, Y. Butenolide, a Marine-Derived Broad-Spectrum Antibiofilm Agent Against Both Gram-Positive and

- Gram-Negative Pathogenic Bacteria. *Mar Biotechnol (NY)* **2019**, *21*, 88-98, doi:10.1007/s10126-018-9861-1.
252. Wu, S.; Liu, G.; Jin, W.; Xiu, P.; Sun, C. Antibiofilm and Anti-Infection of a Marine Bacterial Exopolysaccharide Against *Pseudomonas aeruginosa*. *Frontiers in Microbiology* **2016**, *7*.

CHAPTER 2: General materials and methods

2.1 Experimental design

This chapter describes the design, development and optimization of biofilm dispersal assay to identify fractions and pure compounds with antibiofilm properties against *P. aeruginosa* strains. There are four steps within the assay design. First to consider was the choice of an assay format. The microtiter plate format (384 well-plates) was chosen as it not only saves reagents and fractions/testing compounds but also allows rapid testing of many molecules of interest at multiple concentrations at once. The biological relevance of *in vitro* biofilm model to *in vivo* lung infection is crucial. The choice of medium used to mimic physiology conditions of the lung was made. The fluorescent labels were chosen as the detection method. The availability of equipment was, as well, considered. The process of assay development and optimization includes a series of steps as outlined in **Figure 2.1**. Bacterial culture conditions were determined including bacterial growth phase, inoculum size, and the tolerability of bacterial cells to dimethyl sulfoxide (DMSO). Since fractions are dissolved in DMSO 100% (v/v), the effect of DMSO concentrations on the metabolic activity of both planktonic and biofilm cells should be considered. The timeline and the timescale of biofilm formation in microtiter plate format were defined. The selection of positive control, *i.e.*, antibiotic, and the determination of suitable time for fraction addition and incubation times were performed. Staining conditions were optimized to determine appropriate concentrations and incubation time. Appropriate magnification, the focus and microscopic setting are required to obtain good images which are essential for subsequent image analysis. The reproducibility of the assay and the intra-plate and inter-plate variability were assessed using the coefficient of variation and Z' factor.

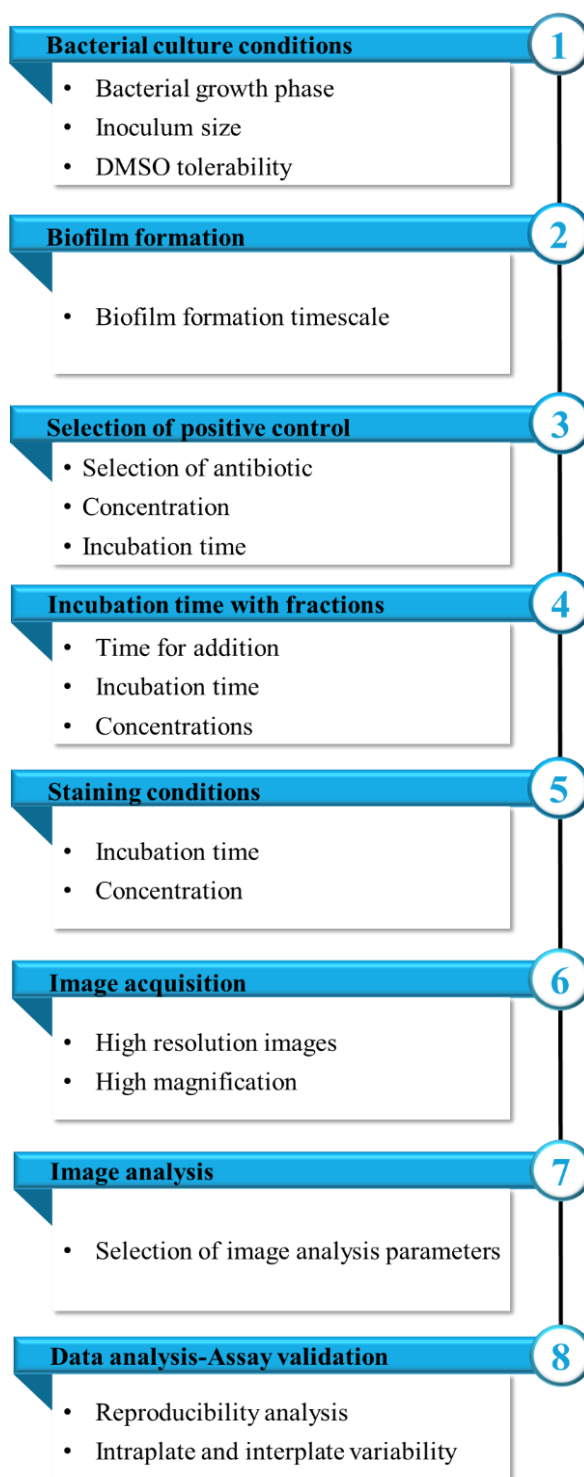


Figure 2.1 The development and optimization of biofilm dispersal assay

2.2 Materials and methods

2.2.1 Bacterial strains

Twelve *P. aeruginosa* strains will be used in this study.

Table 2. 1 List of *P. aeruginosa* strains used in this study

Strain	Characteristics	Reference
<i>Pseudomonas aeruginosa</i> PAO1	Prototroph, non-mucoid	ATCC 15692
PAO1 Δ <i>alg8</i>	PAO1 containing a deletion of <i>alg8</i> gene	[1]
PAO1 Δ <i>pslA</i>	PAO1 containing deletion of <i>pslA</i> gene	[1]
PAO1 Δ <i>pelF</i>	PAO1 containing deletion of <i>pelF</i> gene	[1]
PAO1 Δ <i>pslA</i> Δ <i>alg8</i>	PAO1 containing a deletion of <i>pslA</i> and <i>alg8</i> genes	[1]
PAO1 Δ <i>phaC1ZC2</i>	PAO1 containing a chromosomal deletion of <i>phaC1-Z-C2</i> genes	[2]
PAO1 Δ <i>phaC1ZC2</i> Δ <i>pslA</i> Δ <i>alg8</i> Δ <i>pelF</i>	PAO1 containing a deletion of <i>phaC1-Z-C2</i> , <i>pslA</i> , <i>alg8</i> and <i>pelF</i> genes Quadruple mutant	Jason Lee, Massey University, New Zealand
PDO300	Isogenic <i>mucA22</i> mutant derived from PAO1	[3]
PDO300 Δ <i>alg8</i>	PDO300 containing a deletion of <i>alg8</i> gene	[4]
PDO300 Δ <i>pslA</i>	PDO300 containing a deletion of <i>pslA</i> gene	[1]
PDO300 Δ <i>pslA</i> Δ <i>alg8</i>	PDO300 containing a deletion of <i>pslA</i> and <i>alg8</i> gene	[1]
FRD1	Cystic fibrosis isolate	[5]

2.2.2 Medium

The artificial sputum medium (ASM) mimics the sputum of cystic fibrosis (CF) patients, providing physiochemical properties required for *P. aeruginosa* to express genes associated with biofilm formation and to form biofilm architectures (i.e., microcolonies, microcolonies and unattached cell aggregates) [6,7]. The medium was prepared as previously described [6]. Its components are listed in **Table 2.2**. Briefly, mucin, DNA, DTPA, NaCl, KCl, Tris Base and Hy-Case® SF were dissolved slowly one by one into 800 mL of Milli-Q water. Adjustment and stabilization of pH at 7.0 was achieved using Tris Base. MilliQ water was added to make up to the total volume of 1 L. The medium was autoclaved at 110°C for 15 min. 5 mL of egg yolk emulsion was added when the medium was cool down, and the medium was kept at 4°C.

Table 2. 2 Components of Artificial Sputum Medium

Components	Supplier	Concentrations
Mucin	Sigma Aldrich	5 g/L
Deoxyribonucleic acid from herring sperm (DNA)	Sigma Aldrich	4 g/L
Diethylene triamine pentaacetic acid (DTPA)	Sigma Aldrich	5.9 mg/L
NaCl	Chem-Supply	5 g/L
KCl	Chem-Supply	2.2 g/L
Tris Base	Formedium	1.81 g/L
Egg yolk emulsion	Oxoid	5 mL/L
Hy-Case® SF	Sigma Aldrich	5 g/L

2.2.3 Growth curve

Frozen bacterial stocks (PAO1, PDO300 and PDO300 Δ alg8) were streaked directly on *Pseudomonas* Isolation Agar (PIA; Difco) and incubated at 37°C for 20 – 24 h. Single colonies were transferred into fresh 50 mL of Luria-Bertani medium (LB; 10g/L peptone, 10g/L NaCl, 5 g/L yeast extract and incubated overnight at 37°C and 200 rpm. The pre-cultures were washed once with sterile saline 0.9 % (w/v) followed by resuspending in saline 0.9 % (w/v) and diluting to an optical density at 600 nm (OD₆₀₀) of 0.05. A 1% inoculum was inoculated into 50 mL of LB medium and OD₆₀₀ of the samples were measured every hour for 24 h. Additional data points were obtained at 28 h, 44 h, 48 h, 69 h, 72 h and 96 h. The experiment was set up in duplicate.

Exponential (log) phase was determined by visual examination of a plot with time course on x-axis and OD₆₀₀ on y-axis followed by identification of the doubling time when OD₆₀₀ increased by a factor of 2. The growth rate between two time points within the doubling period was computed using the following equation [8]:

$$\mu = \frac{\ln OD_2 - \ln OD_1}{(t_2 - t_1)} \quad (1)$$

where μ is the growth rate; t_1 and t_2 are the corresponding time points when OD₁ and OD₂ are obtained, respectively. The maximum growth rate was chosen. A line was drawn between the respective time interval of the maximum growth rate on the abscissa and the plotted line of the growth curve to determine the time for cell seeding in 96 and/or 384 well plates.

2.2.4 xCELLigence - Real-Time Cell Analyzer (RTCA) SP

The RTCA SP (Acea Biosciences, San Diego, CA, USA) system was used in various studies on monitoring responses of eukaryotic cell lines to different treatments such as tumour targeting drugs and cancer immunotherapy and evaluate bacterial biofilms and potency of antimicrobials without labels or reporters [9,10]. The instrument measures impedance changes in 96 well plate

(E-plate® 96) whose bottom is fused with gold microelectrodes. A weak electric current travel across these microelectrodes when they are in contact with the solution of electrical conductivity (buffer or growth medium). Cell attachment to the electrodes results in current impedance and its magnitude depends on the size of the cells and the cell density [11]. Association of extracellular polymeric substances such as bacterial biofilm to the electrodes also contributes to changes in impedance signals [12] (**Figure 2.2**).

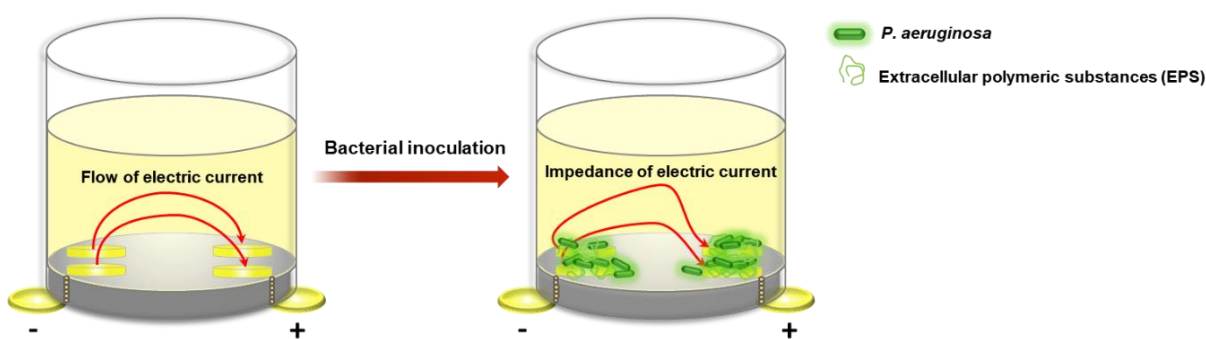


Figure 2.2 Generation of the impedance signals. The electric current travels unrestrictedly from negative to positive terminals in the absence of bacterial cells. When bacterial attachment and cell division occur, the electric current is hindered, giving rise to the impedance signals whose magnitude depends on the size of the cells and cell density.

➤ Measurement of background impedance

100 μ L of either LB medium or ASM was added to each well of the E-Plate and the plate was placed back into RTCA SP station in a 37°C incubator. The background impedance of culture medium in the absence of the cells was recorded.

➤ Data acquisition and plotting

100 μ L of pre-cultures were inoculated into wells that previously contained 100 μ L of culture medium to achieve OD₆₀₀ of 0.05. Experiment was performed in triplicate. The

plate was placed back into RTCA SP station and the all 3-frequency impedance signal represented by Cell Index (CI) was recorded every 5 minutes for 72 h. The background impedance was subtracted from impedance measurement so that $CI = 0$ at the time background was measured. The parameter CI is calculated as follows:

$$\text{Cell Index} = [(R, t_n) - (R, t_0)] / F_i \quad (2)$$

where (R, t_n) is the impedance signal measured at three frequencies (10 kHz, 25 kHz and 50 kHz) at a time point t_n ; (R, t_0) is the impedance signal measured at three frequencies (10 kHz, 25 kHz and 50 kHz) at a time point t_0 ; F_i is the corresponding impedance values (15 Ω ; 12 Ω ; 10 Ω) [10,11].

2.2.5 Crystal violet assay

2.2.5.1 Biofilm growth curve

The pre-cultures (mid-log phase) at 37°C in LB medium were washed once with sterile saline 0.9 % (w/v) and adjusted to an OD_{600} of 0.05, and 1% inoculum was transferred into fresh LB medium. Following the incubation at 37°C, 200 rpm for the respective times for each strain to reach exponential phase, the cells were washed once with sterile saline 0.9 % (w/v) and diluted to an OD_{600} of 0.05 in either LB or ASM. Two hundred microliter-aliquots were added to each well of 96 well plates and/or E-Plate. The experiment with six technical replicates was carried out parallelly with impedance measurement using xCELLigence.

To quantify biofilm formation, crystal violet (CV) staining was performed as previously described with modification [13]. After incubation for a specified period (4 h, 14 h, 20 h, 24 h, 38 h, 48 h and 72 h), planktonic cultures were withdrawn followed by three washes with sterile water using gentle suction or the plate washer ELx405 Select CW (BioTek). The plates were heat-fixed at 60°C for 1 h and biofilm bacteria were stained with crystal violet 1 % (m/v in water) for 20 min at room temperature. The excess CV was removed, and the plates were rinsed as mentioned above. The plates were then dried at room temperature and bound CV was

solubilized in dimethyl sulfoxide (DMSO) 100 % (v/v) for 30 minutes. Subsequently, the measurement of the absorbance signal at 595 nm was performed using the plate reader (BioTek).

2.2.5.2 Antibiotic test

All antibiotics were dissolved in water and filter sterilized.

Table 2. 3 Antibiotic used in this study

Antibiotic	Supplier	Final concentrations
Ciprofloxacin (CIP)	Acros Organics	1.6 µg/mL; 3.2 µg/mL; 6.4 µg/mL; 12.8 µg/mL
Tobramycin (TOB)	Alfa Aesar [®]	2 µg/mL; 4 µg/mL; 8 µg/mL; 16 µg/mL; 32 µg/mL
Meropenem (MEM)	Sigma Aldrich	0.25 µg/mL; 0.5 µg/mL; 1 µg/mL; 2 µg/mL

Abbreviation: ciprofloxacin (CIP), tobramycin (TOB), and meropenem (MEM).

Preparation of exponential phase cultures and CV staining were carried out as described in **Section 2.2.5.1**.

Briefly, after 96 well plates were inoculated with exponential phase cultures at 37°C for 14 h, antibiotics were added to each well to achieve final concentrations (**Table 2.3**) and the plates were further incubated for 24 h. Biofilm biomass was quantified using CV staining. The experiments were carried out with six technical replicates.

2.2.6 Resazurin metabolic assay

Resazurin (RSZ) is a non-toxic and non-fluorescent blue compound which is irreversibly reduced by living cells through electron transfer reactions to highly fluorescent resorufin derivative. The resorufin can be further reduced to colorless and non-fluorescent hydroresorufin

[14]. RSZ has been extensively used for assessment of antibacterial and anti-parasite activities and as an indicator for cell viability [14-16].

DMSO is a common solvent used to dissolve compounds that are insoluble in water [17]. Since the assay was going to be implemented with fractions dissolved in DMSO 100% (v/v), the effect of DMSO concentrations on the metabolic activity of both planktonic and biofilm cells should be considered. This was examined using RSZ assay as previously described [18]. RSZ 0.2 % (w/v) was dissolved in water, filtered, protected from light and kept at -20°C. Experimentally, exponential phase cultures (**Section 2.2.5.1**) were inoculated into 384 well plates followed by incubation at 37°C for 14 h. DMSO was added to each well to achieve final concentrations 2%, 4%, 6%, 8% and 10% (v/v). After further incubation at 37°C for 24 h, cultures were withdrawn by gentle suction and RSZ containing culture medium was added to each well at final concentration 0.004% (v/v). Fluorescence was measured (excitation 570 nm, emission 615 nm) using the plate reader (BioTek) after 5 h incubation at 37°C.

2.2.7 LIVE/DEAD staining

Preparation of exponential phase cultures was carried out as described in **Section 2.2.5.1**.

Briefly, after 384 well plates were inoculated with exponential phase cultures at 37°C 14 h, antibiotics were added to each well to achieve final concentrations (**Table 2.3**) and the plates were further incubated for 24 h. Staining of biofilm cells was performed as previously described [1]. The cultures were removed, and the plates were washed once with sterile water. Addition of 25 µL of staining solution containing Syto9 and propidium iodide (PI) at a final concentration of 5 µM and 30 µM, respectively (LIVE/DEAD BacLight Bacterial Viability Kit, Molecular Probes/Life Technologies) followed by incubation for 15 min. Biofilms were visualized using automatic confocal laser scanning microscopy equipped with a 60X objective (FV-3000, Olympus) or high content imaging system In Cell Analyzer 6500HS with a 60X objective (GE Healthcare Life Sciences).

2.2.8 Nile Red staining

Nile Red (9-diethylamino-5H-benzo[α]phenoxazine-5-one) is a non-cytotoxic dye which displays weak fluorescence in water and intense fluorescence in lipid environment. It is widely used to detect intracellular lipid droplets [19]. Nile Red powder (Sigma) was dissolved in DMSO at a concentration 0.25 mg/mL and diluted to a final concentration of 2.5 μ g/mL for staining. The staining procedure was performed as mentioned in **Section 2.2.7**. Antibiotic utilized for Nile Red staining was meropenem (2 μ g/mL). Biofilm images were acquired by high content imaging system In Cell Analyzer 6500HS with a 60X objective (GE Healthcare Life Sciences).

2.2.9 Data analysis

The assay reproducibility and signal variation were assessed using the coefficient of variation (CV):

$$CV (\%) = \left(\frac{SD}{\mu} \right) \times 100 \quad (3)$$

where SD is the standard deviation of the sample replicates and μ is the average of the replicates.

To evaluate the quality of the assay without considering test samples, Z' factor, a dimensionless statistical parameter, is utilized:

$$Z' = 1 - \frac{(3MAD_{c+} + 3MAD_{c-})}{|M_{c+} - M_{c-}|} \quad (4)$$

where MAD_{c+} and MAD_{c-} are the median absolute deviation of positive and negative controls, respectively; M_{c+} and M_{c-} are the median of positive and negative controls, accordingly. An assay with $0.5 < Z' < 1$ is considered as a good assay, with $Z' > 0$ as an acceptable assay and < 0 as unacceptable assay [20-22].

2.2.10 Biofilm assay

Preparation of exponential phase cultures in ASM was performed as described in Section 2.2.5.1. The plate layout of fractions used in the screening was outlined in **Figure 2.3**. Columns 1, 24 and rows A, P contain sterile water only to prevent edge effect. Each assay plate comprises negative control (DMSO 2% (v/v); columns 2 and 22) and positive control (Tobramycin 16 µg/mL; columns 3 and 23). For biofilm dispersal assay, cells (start OD₆₀₀ was 0.01) were inoculated into 384 well plates (45 µL per well) using the automatic liquid handler Opentrons OT-2 or Bravo (Agilent) followed by incubation at 37°C for 14 h. The test fractions, positive control (Tobramycin (TOB), final concentration: 16 µg/mL) and negative control (DMSO, final concentration: 2% (v/v)) (5 µL per well) were next transferred into the above plates by the OT-2, and the plates were incubated further at 37°C for 24 h. The initial OD₆₀₀ and final OD₆₀₀ were read before incubation at 37°C and after 24 h incubation, respectively, followed by assessment of biofilm viability by resazurin staining. Next, media and non-attached cells were washed off with sterile water. Staining of biofilm cells with RSZ was performed as previously described in **Section 2.2.6**. For biofilm inhibition assay, the cells and the fractions were added to the plates concurrently. The optical density at 600nm was recorded before incubation and after 24 h incubation. The plates were then washed and stained with RSZ.

The growth inhibition was calculated as a function of the percentage of the total bacterial inhibition using equation (1) where A_B is the OD₆₀₀ of LB medium, and A_{T0} and A_{Tf} are the OD₆₀₀ recorded at inoculating time and at the end of the assay.

$$\% \text{ Inhibition} = 100 \times \left[1 - \frac{OD_{600} (A_{\text{sample Tf}} - A_{\text{sample T0}}) - (A_B \text{ Tf} - A_B \text{ T0})}{OD_{600} (A_{\text{negative control Tf}} - A_{\text{negative control T0}}) - (A_B \text{ Tf} - A_B \text{ T0})} \right] \quad (1)$$

The viability of biofilm bacteria was determined as a function of fluorescence percentage using equation (2) where F_B is the fluorescence of the diluted RSZ solution in LB medium in the absence of *P. aeruginosa* cells.

$$\% \text{ Inhibition} = \left[\frac{(F_{\text{negative control}} - F_B) - (F_{\text{sample}} - F_B)}{(F_{\text{negative control}} - F_B)} \right] \times 100 \quad (2)$$

	1	2	3	4	5	6	7	8	9	10	11	12	13	14	15	16	17	18	19	20	21	22	23	24
A																								
B		DMSO	Tobramycin	Sample 1			Sample 15			Sample 29			Sample 43			Sample 57			Sample 71	DMSO	Tobramycin			
C		DMSO	Tobramycin	Sample 2			Sample 16			Sample 30			Sample 44			Sample 58			Sample 72	DMSO	Tobramycin			
D		DMSO	Tobramycin	Sample 3			Sample 17			Sample 31			Sample 45			Sample 59			Sample 73	DMSO	Tobramycin			
E		DMSO	Tobramycin	Sample 4			Sample 18			Sample 32			Sample 46			Sample 60			Sample 74	DMSO	Tobramycin			
F		DMSO	Tobramycin	Sample 5			Sample 19			Sample 33			Sample 47			Sample 61			Sample 75	DMSO	Tobramycin			
G		DMSO	Tobramycin	Sample 6			Sample 20			Sample 34			Sample 48			Sample 62			Sample 76	DMSO	Tobramycin			
H		DMSO	Tobramycin	Sample 7			Sample 21			Sample 35			Sample 49			Sample 63			Sample 77	DMSO	Tobramycin			
I		DMSO	Tobramycin	Sample 8			Sample 22			Sample 36			Sample 50			Sample 64			Sample 78	DMSO	Tobramycin			
J		DMSO	Tobramycin	Sample 9			Sample 23			Sample 37			Sample 51			Sample 65			Sample 79	DMSO	Tobramycin			
K		DMSO	Tobramycin	Sample 10			Sample 24			Sample 38			Sample 52			Sample 66			Sample 80	DMSO	Tobramycin			
L		DMSO	Tobramycin	Sample 11			Sample 25			Sample 39			Sample 53			Sample 67			Sample 81	DMSO	Tobramycin			
M		DMSO	Tobramycin	Sample 12			Sample 26			Sample 40			Sample 54			Sample 68			Sample 82	DMSO	Tobramycin			
N		DMSO	Tobramycin	Sample 13			Sample 27			Sample 41			Sample 55			Sample 69			Sample 83	DMSO	Tobramycin			
O		DMSO	Tobramycin	Sample 14			Sample 28			Sample 42			Sample 56			Sample 70			Sample 84	DMSO	Tobramycin			
P																								

Figure 2.3 The plate template of fractions used in biofilm dispersal assay. Columns 1, 24 and rows A, P contain sterile water only. Each assay plate includes negative control (DMSO 2% (v/v); columns 2 and 22) and positive control (Tobramycin 16 µg/mL; columns 3 and 23).

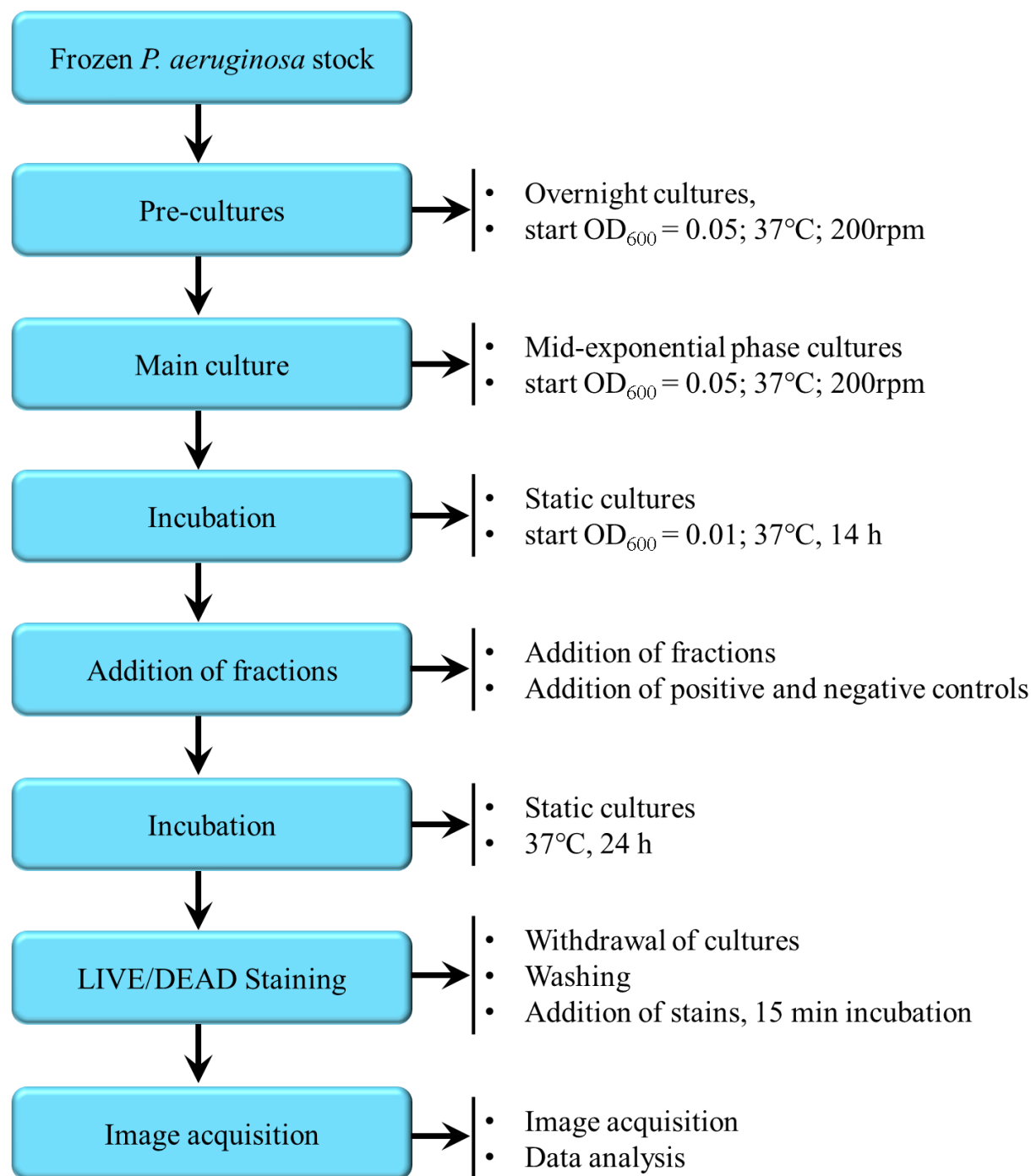


Figure 2. 4. Overview of screening approach used in this study

2.3 References

1. Ghafoor, A.; Hay, I.D.; Rehm, B.H. Role of exopolysaccharides in *Pseudomonas aeruginosa* biofilm formation and architecture. *Appl Environ Microbiol* **2011**, *77*, 5238-5246, doi:10.1128/AEM.00637-11.
2. Pham, T.H.; Webb, J.S.; Rehm, B.H. The role of polyhydroxyalkanoate biosynthesis by *Pseudomonas aeruginosa* in rhamnolipid and alginate production as well as stress tolerance and biofilm formation. *Microbiology* **2004**, *150*, 3405-3413, doi:10.1099/mic.0.27357-0.
3. Mathee, K.; Ciofu, O.; Sternberg, C.; Lindum, P.W.; Campbell, J.I.; Jensen, P.; Johnsen, A.H.; Givskov, M.; Ohman, D.E.; Molin, S., et al. Mucoid conversion of *Pseudomonas aeruginosa* by hydrogen peroxide: a mechanism for virulence activation in the cystic fibrosis lung. *Microbiology* **1999**, *145* (Pt 6), 1349-1357, doi:10.1099/13500872-145-6-1349.
4. Remminghorst, U.; Rehm, B.H. In vitro alginate polymerization and the functional role of Alg8 in alginate production by *Pseudomonas aeruginosa*. *Appl Environ Microbiol* **2006**, *72*, 298-305, doi:10.1128/AEM.72.1.298-305.2006.
5. Ohman, D.E.; Chakrabarty, A.M. Genetic mapping of chromosomal determinants for the production of the exopolysaccharide alginate in a *Pseudomonas aeruginosa* cystic fibrosis isolate. *Infect Immun* **1981**, *33*, 142-148.
6. Sriramulu, D.D.; Lunsdorf, H.; Lam, J.S.; Romling, U. Microcolony formation: a novel biofilm model of *Pseudomonas aeruginosa* for the cystic fibrosis lung. *J Med Microbiol* **2005**, *54*, 667-676, doi:10.1099/jmm.0.45969-0.
7. Fothergill, J.L.; Neill, D.R.; Loman, N.; Winstanley, C.; Kadioglu, A. *Pseudomonas aeruginosa* adaptation in the nasopharyngeal reservoir leads to migration and persistence in the lungs. *Nat Commun* **2014**, *5*, 4780, doi:10.1038/ncomms5780.
8. Hall, B.G.; Acar, H.; Nandipati, A.; Barlow, M. Growth rates made easy. *Mol Biol Evol* **2014**, *31*, 232-238, doi:10.1093/molbev/mst187.
9. Hamidi, H.; Lilja, J.; Ivaska, J. Using xCELLigence RTCA Instrument to Measure Cell Adhesion. *Bio Protoc* **2017**, *7*, doi:10.21769/BioProtoc.2646.

10. van Duuren, J.; Musken, M.; Karge, B.; Tomasch, J.; Wittmann, C.; Haussler, S.; Bronstrup, M. Use of Single-Frequency Impedance Spectroscopy to Characterize the Growth Dynamics of Biofilm Formation in *Pseudomonas aeruginosa*. *Sci Rep* **2017**, *7*, 5223, doi:10.1038/s41598-017-05273-5.
11. Maria D. Ferrer, B.L., Alex Mira. Studying Bacterial Biofilms Using Cellular Impedance. *ACEA Biosciences, Inc.* **2017**.
12. Gutierrez, D.; Hidalgo-Cantabrana, C.; Rodriguez, A.; Garcia, P.; Ruas-Madiedo, P. Monitoring in Real Time the Formation and Removal of Biofilms from Clinical Related Pathogens Using an Impedance-Based Technology. *PLoS One* **2016**, *11*, e0163966, doi:10.1371/journal.pone.0163966.
13. Hay, I.D.; Gatland, K.; Campisano, A.; Jordens, J.Z.; Rehm, B.H. Impact of alginate overproduction on attachment and biofilm architecture of a supermucoid *Pseudomonas aeruginosa* strain. *Appl Environ Microbiol* **2009**, *75*, 6022-6025, doi:10.1128/AEM.01078-09.
14. O'Brien, J.; Wilson, I.; Orton, T.; Pognan, F. Investigation of the Alamar Blue (resazurin) fluorescent dye for the assessment of mammalian cell cytotoxicity. *Eur J Biochem* **2000**, *267*, 5421-5426, doi:10.1046/j.1432-1327.2000.01606.x.
15. Sarker, S.D.; Nahar, L.; Kumarasamy, Y. Microtitre plate-based antibacterial assay incorporating resazurin as an indicator of cell growth, and its application in the in vitro antibacterial screening of phytochemicals. *Methods* **2007**, *42*, 321-324, doi:10.1016/j.ymeth.2007.01.006.
16. Bowling, T.; Mercer, L.; Don, R.; Jacobs, R.; Nare, B. Application of a resazurin-based high-throughput screening assay for the identification and progression of new treatments for human African trypanosomiasis. *International Journal for Parasitology: Drugs and Drug Resistance* **2012**, *2*, 262-270, doi:<https://doi.org/10.1016/j.ijpddr.2012.02.002>.
17. Guo, Q.; Wu, Q.; Bai, D.; Liu, Y.; Chen, L.; Jin, S.; Wu, Y.; Duan, K. Potential Use of Dimethyl Sulfoxide in Treatment of Infections Caused by *Pseudomonas aeruginosa*. *Antimicrobial agents and chemotherapy* **2016**, *60*, 7159-7169, doi:10.1128/AAC.01357-16.
18. Paytubi, S.; de La Cruz, M.; Tormo, J.R.; Martin, J.; Gonzalez, I.; Gonzalez-Menendez, V.; Genilloud, O.; Reyes, F.; Vicente, F.; Madrid, C., et al. A High-Throughput

- Screening Platform of Microbial Natural Products for the Discovery of Molecules with Antibiofilm Properties against Salmonella. *Front Microbiol* **2017**, 8, 326, doi:10.3389/fmicb.2017.00326.
19. Greenspan, P.; Mayer, E.P.; Fowler, S.D. Nile red: a selective fluorescent stain for intracellular lipid droplets. *J Cell Biol* **1985**, 100, 965-973, doi:10.1083/jcb.100.3.965.
 20. Zhang, J.-H.; Chung, T.D.Y.; Oldenburg, K.R. A Simple Statistical Parameter for Use in Evaluation and Validation of High Throughput Screening Assays. *Journal of Biomolecular Screening* **1999**, 4, 67-73, doi:10.1177/108705719900400206.
 21. Birmingham, A.; Selfors, L.M.; Forster, T.; Wrobel, D.; Kennedy, C.J.; Shanks, E.; Santoyo-Lopez, J.; Dunican, D.J.; Long, A.; Kelleher, D., et al. Statistical methods for analysis of high-throughput RNA interference screens. *Nat Methods* **2009**, 6, 569-575, doi:10.1038/nmeth.1351.
 22. Sui, Y.; Wu, Z. Alternative Statistical Parameter for High-Throughput Screening Assay Quality Assessment. *Journal of Biomolecular Screening* **2007**, 12, 229-234, doi:10.1177/1087057106296498.

CHAPTER 3: Screening of natural product libraries

3.1. Introduction

The ongoing challenge of antibiotic resistance has prompted the search for novel antibacterial molecules. Among Gram-negative bacteria, *P. aeruginosa* has become one of the most life-threatening bacteria due to its rapid adaptability, high intrinsic antibiotic resistance, and especially the ability to form biofilms. Biofilm matrix protects encased bacteria from surrounding environmental stresses, impedes phagocytosis, and hinders antimicrobial diffusion [1,2]. In this study, a biofilm dispersal assay was developed and optimized. This assay employed an artificial sputum medium (ASM) that mimics cystic fibrosis (CF) lung physiology to grow biofilms. The effects of a library of 1535 fractions on established biofilms of wild-type PAO1 and alginate overproducing mutant PDO300 (an isogenic derivative of PAO1 generated to replicate clinical CF isolates) were investigated using the developed biofilm dispersal assay. These fractions were previously reported to have antibacterial activity against planktonic *P. aeruginosa* PAO1 [3,4]. Additionally, this assay was utilized to determine the antibiofilm properties of 54 NatureBank compounds.

3.2. Materials and Methods

3.2.1 Natural product library

The library contains 1535 fractions from plants and marine organisms, which were obtained from Nature Bank and stored in Compound Australia facility under robust environmental conditions and supplied in assay-ready plate format. They were previously identified as anti-*P. aeruginosa* molecules.

3.2.2 Library of pure compounds

The library of 54 NatureBank compounds was kindly provided by Associated Professor Rohan Davis (Nature Bank). This is a new compound collection, and their activity has not been investigated.

3.2.3 Fraction refractionation

Small-scale and large-scale isolation and refractionation were carried out by Dr. Russell Addison and Miss Sasha Hayes (Nature Bank).

3.2.4 Biofilm assay

Please refer to **Chapter 2 – General Materials and Methods, section 2.2.10**.

3.2.5 Statistical analysis

Results were analyzed by A one-way ANOVA using Kruskal-Wallis test followed by Dunnett's multiple comparison post-hoc test was carried out to determine statistical significance between each treatment and the negative control. *, $p < 0.05$; **, $p < 0.01$; ***, $p < 0.001$; ****, $p < 0.0001$, ns, not significant.

3.3. Results and discussion

3.3.1 Assay development

3.3.1.1 Physiology state of *P. aeruginosa*

It was previously demonstrated that the physiological state of bacterial cells affects their surface attachment level [5]. *P. aeruginosa* cells in the exponential growth phase exhibited progressively enhanced adhesion compared to their stationary phase counterparts [6]. Hence, mid-exponentially growing cells were chosen to generate the biofilms for subsequent experiments. Physiological states of *P. aeruginosa* cells in LB medium were determined using growth curves (**Figure 3.1**).

Examination of the plotted growth curves revealed that exponential phases of PAO1, PDO300 and PDO300 Δ alg8 were from 5 to 8 h. Next, the growth rate, μ , of three bacterial strains in the exponential phase was calculated. PAO1 and PDO300 had maximum growth rates 0.794/h and 0.684/h, respectively, between 6 and 7 h, while PDO300 Δ alg8 achieved maximum growth rate 0.801/h between 5 to 6 h. The time to grow the planktonic cells to

reach the mid-exponential phase was determined at 6 h for PAO1 and PDO300 Δ *alg8* and 6.5 h for PDO300.

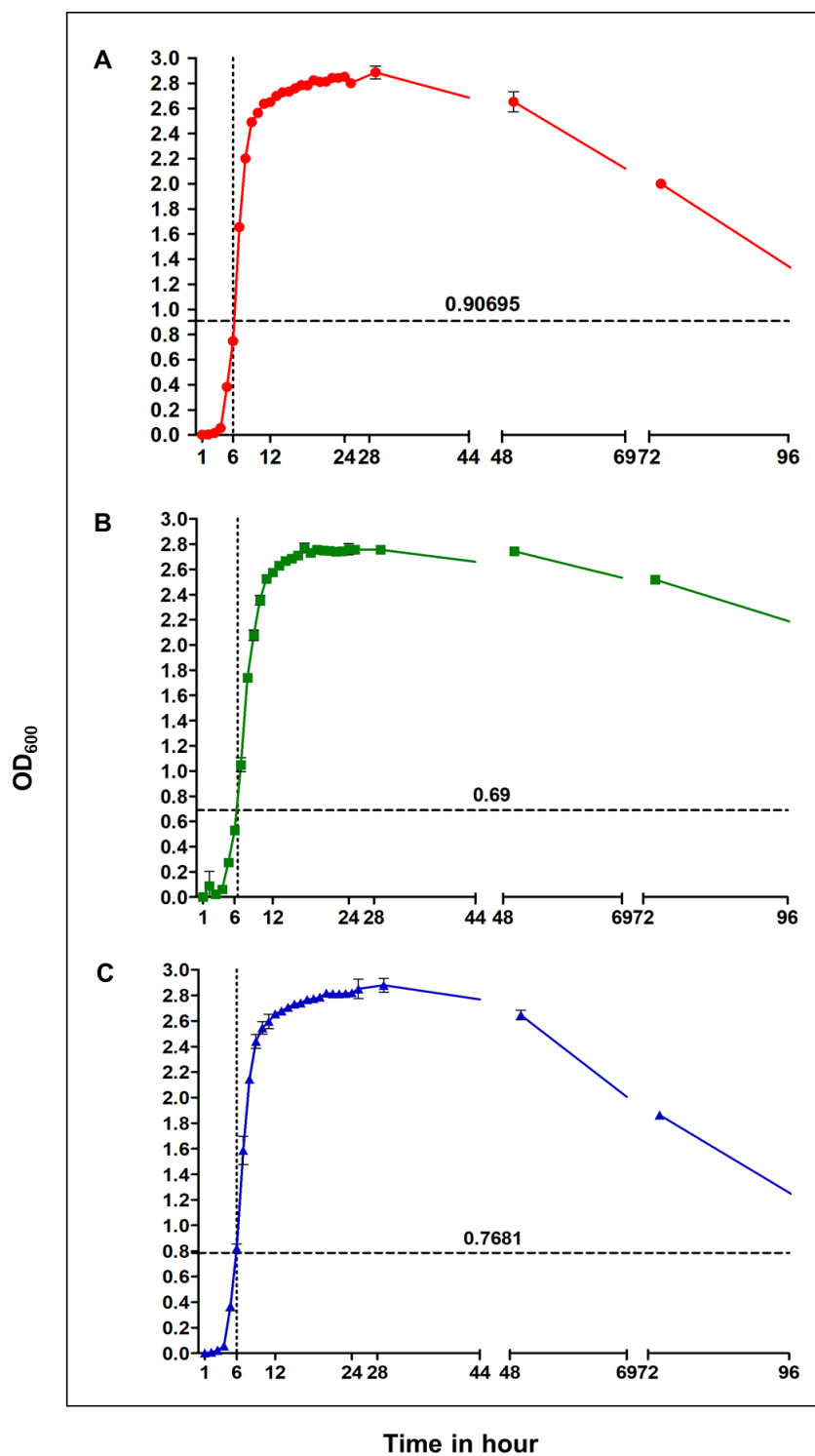


Figure 3.1 Growth curves of PAO1 (wild-type) (A), PDO300 (alginate overproducing mutant) (B) and PDO300 Δ *alg8* (alginate knock-out mutant) (C) Values are the mean and

standard deviation of two technical replicates. The time to grow planktonic cells to the mid-exponential phase was 6h for PAO1 and PDO300 Δ *alg8*; and 6.5h for PDO300.

3.3.1.2 DMSO tolerability

The metabolic activity of planktonic and biofilm cells in the presence of different concentrations of DMSO ranging from 2% to 10% is shown in **Figure 3.2**. The DMSO exhibited effect on planktonic and biofilm cells in a strain-dependent manner. DMSO at 4% (v/v) promoted the metabolic activity of PAO1 (planktonic and biofilm cells) significantly (p value: 0.0254) while showing no significant effect at other examined concentrations compared to untreated cells. DMSO at 8% and 10% (v/v) substantially reduced metabolic activity of planktonic and biofilm of PDO300 (p values: 0.022 (8% DMSO) and 0.0001 (10% DMSO)). Detrimental effect on free living and biofilm cells of PDO300 Δ *alg8* was only observed at 10% DMSO (p value: 0.0437) (**Figure 3.2A**). Metabolic activity of biofilm bacteria was not affected significantly by DMSO up to 8% (v/v). However, at 10%, DMSO considerably decreased metabolic activity of PAO1 biofilms (p value: 0.0466) and PDO300 biofilms (p value: 0.0033) (**Figure 3.2B**). Final concentration of DMSO at 2% (v/v) was chosen as it had low impact on three bacterial strains (PAO1, PDO300 and PDO300 Δ *alg8*) used in this study

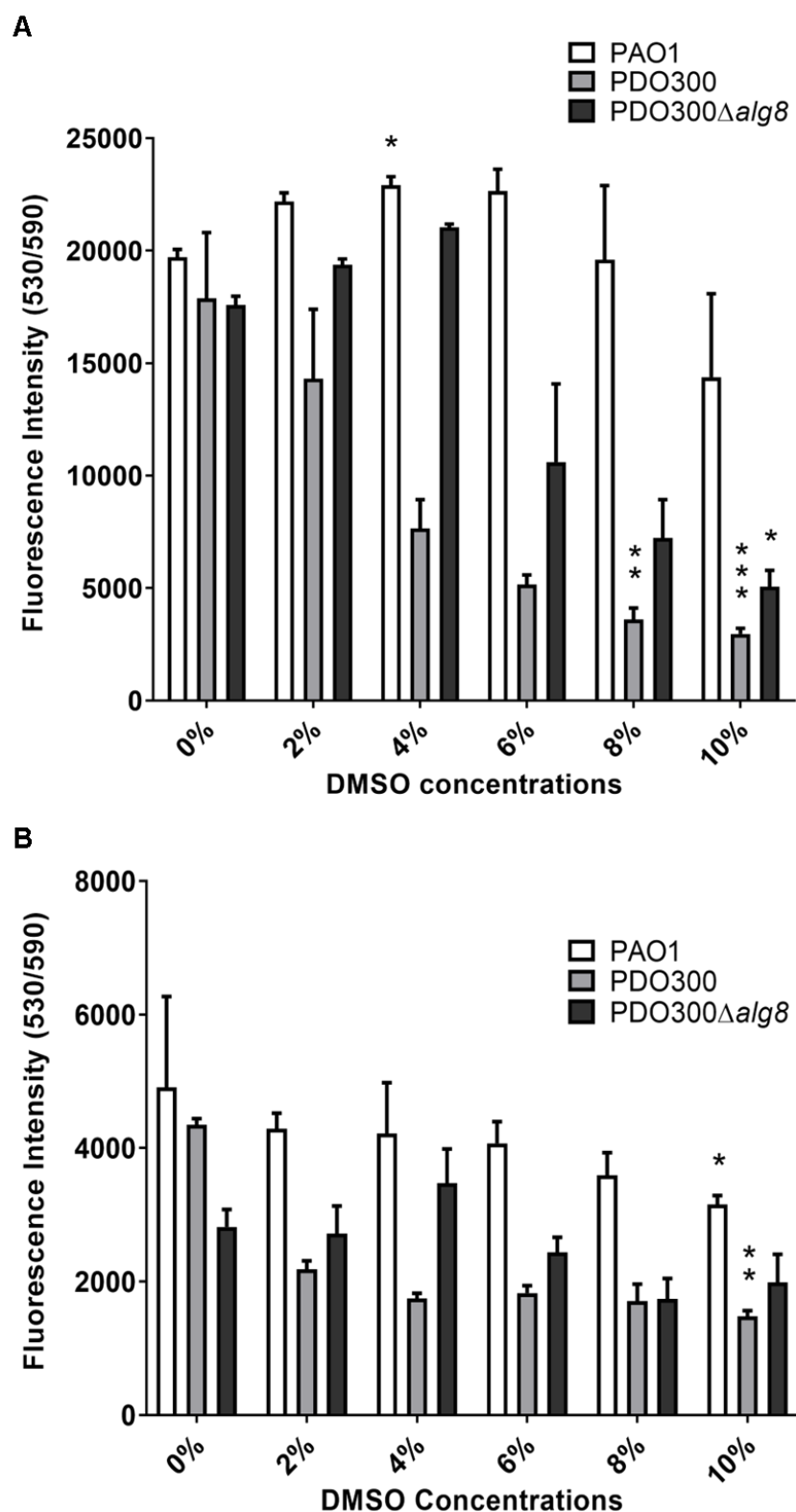


Figure 3.2 Metabolic activity of planktonic and biofilm cells in the presence of DMSO (0-10% (v/v)) using resazurin metabolic assay. **(A)** Metabolic activity of both planktonic and biofilm bacteria. **(B)** Metabolic activity of biofilm cells. The experiment was done in triplicate. Values represent the mean and the standard deviation of three technical replicates.

A one-way ANOVA using Kruskal-Wallis test followed by Dunnett's multiple comparison post-hoc test was carried out to determine statistical significance between DMSO treated cells and the negative control (untreated cells). *, $p < 0.05$; **, $p < 0.01$; ***, $p < 0.001$; ****, $p < 0.0001$.

3.3.1.3 Biofilm growth curve and antibiotic tests

3.3.1.3.1 Biofilm growth and the cell index

The suitability of the RTCA system to continuously monitor the biofilm formation of different *P. aeruginosa* strains PAO1, PDO300 and PDO300 Δ alg8 was investigated by measuring the impedance. Variations in the impedance signals are expressed as cell index (**Figure 3.3A**). The cell index values of LB medium increased to 0.05 after 1 h and then gradually decreased over 72 h with a minimum being -0.08 while the cell index of three strains steadily increased and peaked after 14 h of incubation for PAO1 at 0.160, PDO300 Δ alg8 at 0.164, and after 24 h for PDO300 at 0.12. Slowly declined curves were then observed for approximately 10 h for PDO300 Δ alg8, 12 h for PAO1, and 20 h for PDO300 with a minimum being 0.089, -0.01 and 0.03, respectively. After the decline, the signals constantly increased for PAO1 and PDO300 up to 0.38 and 0.3, correspondingly. In contrast, cell index values of PDO300 Δ alg8 remained unchanged at 0.58 for the last 12 h. Crystal violet staining under the same experimental conditions was used as a reference to the measurement of impedance signals (**Figure 3.3B**). Results obtained demonstrated the formation of biofilm and pellicle biofilm (4 h – 14 h for PAO1 and PDO300 Δ alg8; 4 h – 24 h for PDO300) which corresponded to the changes in impedance signals. The time point at 14 h was chosen to add fractions, positive controls, and negative controls to the plates previously containing bacterial cultures.

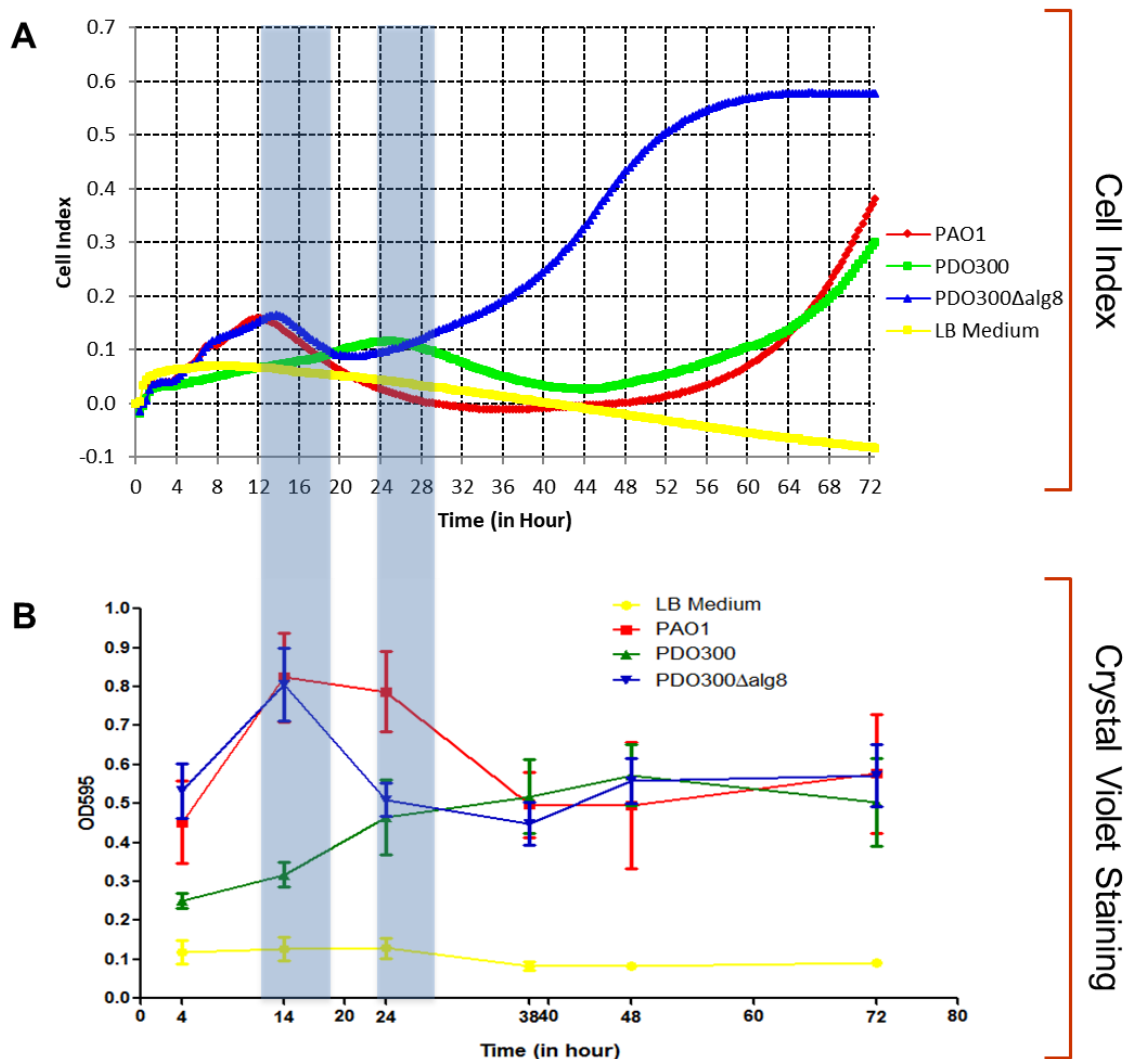


Figure 3. 3 (A) Changes in cell index (CI) during 72 h of biofilm formation at 37 °C (n=6). **(B)** Biofilm growth of PAO1, PDO300 and PDO300Δ*alg8* monitored by crystal violet staining over 72 h in LB medium (n=6). N represents the number of technical replicates. Blue bars highlight the peaks of CI values and maximum CV signals. Values represent the mean and standard deviation of six technical replicates.

3.3.1.3.2 Antibiotic treatments on established biofilms

Clinically used antibiotics ciprofloxacin (1.6 $\mu\text{g/mL}$ – 12.8 $\mu\text{g/mL}$), meropenem (0.25 $\mu\text{g/mL}$ – 2 $\mu\text{g/mL}$) and tobramycin (2 $\mu\text{g/mL}$ – 32 $\mu\text{g/mL}$) were tested against wild-type PAO1 using crystal violet assay. Ciprofloxacin (6.4 $\mu\text{g/mL}$ and 12.8 $\mu\text{g/mL}$) and meropenem (1 $\mu\text{g/mL}$ and 2 $\mu\text{g/mL}$) substantially affected existing biofilms (p values < 0.0001). Tobramycin showed the highest activity against preformed biofilms of PAO1 compared to ciprofloxacin and meropenem. At 16 $\mu\text{g/mL}$, tobramycin significantly dispersed established biofilms (p value < 0.0001) compared to other tested concentrations (**Figure 3.4**). Hence, it was used as positive control of subsequent experiments.

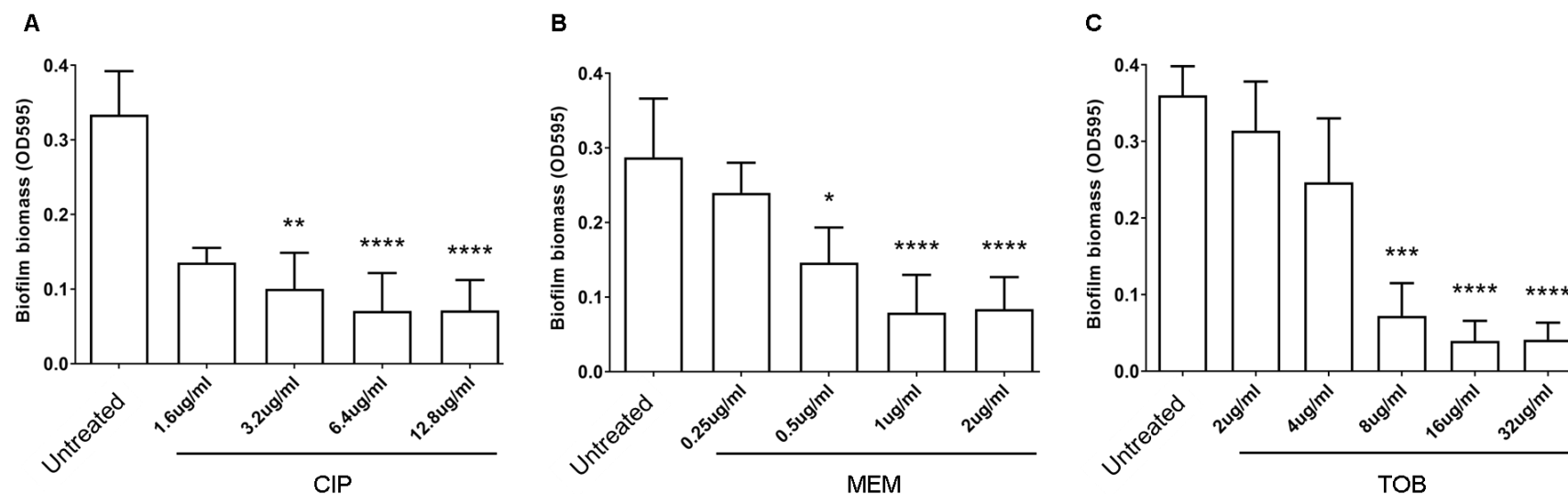


Figure 3. 4 Effect of antibiotics (A) ciprofloxacin (CIP), (B) meropenem (MEM) and (C) tobramycin (TOB) on pre-formed biofilms of wild-type PAO1 was determined using crystal violet assay. Values represent mean and standard deviation of ten technical replicates. A one-way ANOVA using Kruskal-Wallis test followed by Dunnett's multiple comparison post-hoc test was carried out to determine statistical significance between treated cells and untreated cells. *, $p < 0.05$; **, $p < 0.01$; ***, $p < 0.001$; ****, $p < 0.0001$.

Antimicrobial agents including ciprofloxacin (12.8 µg/mL), tobramycin (16 µg/mL), and meropenem (2 µg/mL) were tested against different *P. aeruginosa* strains using crystal violet staining (**Figure 3.5**). Three antibiotics showed cytotoxic effects, however, at different levels, on all tested bacterial strains. Ciprofloxacin significantly reduced biofilm biomass of PAO1Δ*pslA*, PAO1Δ*alg8ΔpslA*, FRD1, PAO1, PDO300, and PDO300Δ*pslA*, PDO300Δ*alg8ΔpslA*. Established biofilms of PAO1Δ*alg8*, PAO1Δ*pslA*, FRD1, PAO1, PDO300, PDO300Δ*alg8*, PDO300Δ*pslA*, PAO1Δ*phaC1ZC2*, and PAO1Δ*pslAΔalg8ΔphaC1ZC2ΔpelF*. Meropenem displayed weak impacts on tested strains compared to the other two antibiotics, except for PAO1Δ*alg8ΔpslA*, PDO300Δ*alg8ΔpslA*.and PAO1Δ*pslAΔalg8ΔphaC1ZC2ΔpelF*. Unexpectedly, PAO1Δ*alg8*, PAO1Δ*phaC1ZC2*, and PDO300Δ*alg8* treated with meropenem exhibited higher crystal violet intensities (higher biofilm biomass) than untreated cultures.

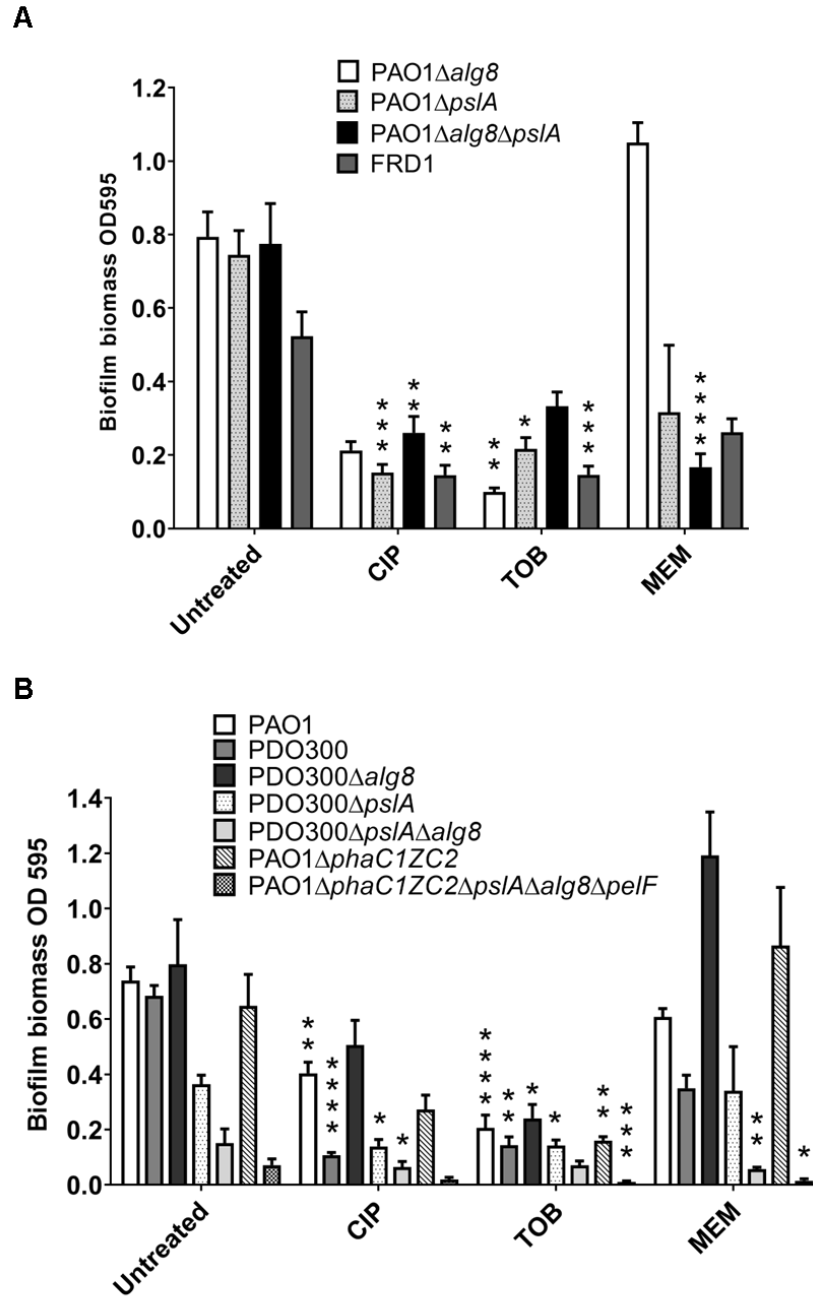


Figure 3. 5 The susceptibility of established biofilms to antimicrobial agents: ciprofloxacin (12.8 $\mu\text{g/mL}$), tobramycin (16 $\mu\text{g/mL}$), and meropenem (2 $\mu\text{g/mL}$). **(A)** Crystal violet staining of PAO1Δalg8, PAO1ΔpslA and PAO1Δalg8ΔpslA. **(B)** Crystal violet staining of PAO1, PDO300, PDO300Δalg8, PDO300ΔpslA, PDO300Δalg8ΔpslA, PAO1ΔphaC1ZC2 and PAO1ΔphaC1ZC2ΔplsAΔalg8ΔpelF. Values represent the mean and standard deviation of six technical replicates. A one-way ANOVA using Kruskal-Wallis test followed by Dunnett's multiple comparison post-hoc test was carried out to determine statistical significance between treated cells and untreated cells. *, $p < 0.05$; **, $p < 0.01$; ***, $p < 0.001$; ****, $p < 0.0001$.

To understand the enhancement of biofilm biomass upon meropenem exposure, biofilms of PAO1, PDO300, and PDO300 Δ alg8 were stained with LIVE/DEAD staining (**Figure 3.6**). The results of cells treated with up to 2% DMSO (v/v) were correlated with the metabolic measurement of biofilm cells and biofilm coverage (**Section 3.2**). It was observed that the presence of 2% DMSO (v/v) had effects on both metabolic activity and density of biofilm cells of alginate overproducing PDO300 mutant while exhibiting low impact on PAO1 and PDO300 Δ alg8. Exposure to ciprofloxacin and tobramycin resulted in biofilm dispersal and a significant reduction of viability on three of the tested strains, which corresponded with biofilm quantification determined by crystal violet staining (**Figure 3.5**). Moreover, treatment with ciprofloxacin induced morphological changes from rod-shaped to filamentous bacteria, whereas tobramycin treatment produced small rounded-shaped ones. Interestingly, exposure to meropenem, a member of the carbapenem antibiotic class, generated fewer dead cells, reduced bacterial size in PDO300; round-shaped PAO1; and round structures located proximal to the cytoplasmic membrane of PDO300 Δ alg8. These findings coincided with a previous report which showed that treatment with imipenem and β -lactam antibiotic ceftazidime produced rounded and long filamentous *P. aeruginosa* cells, respectively. In addition, the antibiotic exposure-derived morphological alteration was associated with phagocytosis susceptibility and different levels of endotoxin production [7].

Nile red staining was next applied to investigate if round structures observed upon meropenem treatment were intracellular spherical inclusions of polyhydroxyalkanoic acids (PHAs) that serve as carbon and energy source during nutrient limitation and starvation conditions [8]. Furthermore, it was demonstrated that alginate overproduction and PHA biosynthesis are competitive and associated with stress tolerance and biofilm formation [9]. In the presence of 2% DMSO (v/v), PAO1 and PDO300 Δ alg8 were stained positive with Nile red, whereas PDO300 showed Nile red negative. Once exposed to meropenem, the intensity of Nile red increased for PAO1 and PDO300 and significantly for PDO300 Δ alg8, indicating the formation of PHA inclusions (**Figure 3.7**). The results suggested that PDO300 Δ alg8 mutant defective in alginate markedly synthesized PHAs in response to meropenem stress. Similarly, PHA negative PAO1 Δ phaC1ZC2 excessively produced alginate as a defense mechanism against meropenem. Nonetheless, the underlying mechanism of the association between PHA accumulation and stress tolerance remain to be investigated. These findings may explain the enhanced crystal violet intensities of PAO1 Δ alg8,

PAO1 Δ *phaCIZC2* and PDO300 Δ *alg8* when treated with meropenem (**Figure 3.7B**) whereas more research is needed to confirm the observation.

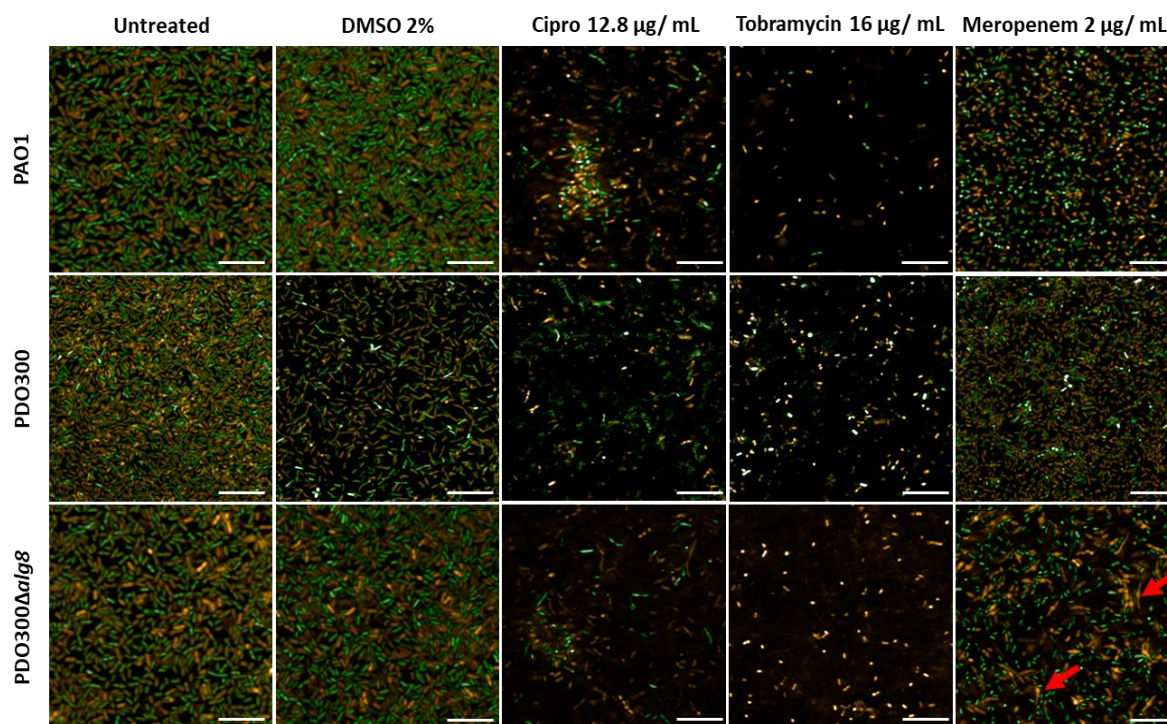


Figure 3.6 Impacts of DMSO and antibiotics on the viability of biofilm cells. Live and dead biofilm cells were stained with Syto9 (green) and propidium iodide (orange), respectively. Red arrows indicate meropenem-induced morphological changes. Four images per well were acquired by high content imaging system In Cell Analyzer 6 μ 0HS with a 60X objective (GE Healthcare Life Sciences). The experiment was performed in triplicate. The scale bar is 10 μ m.

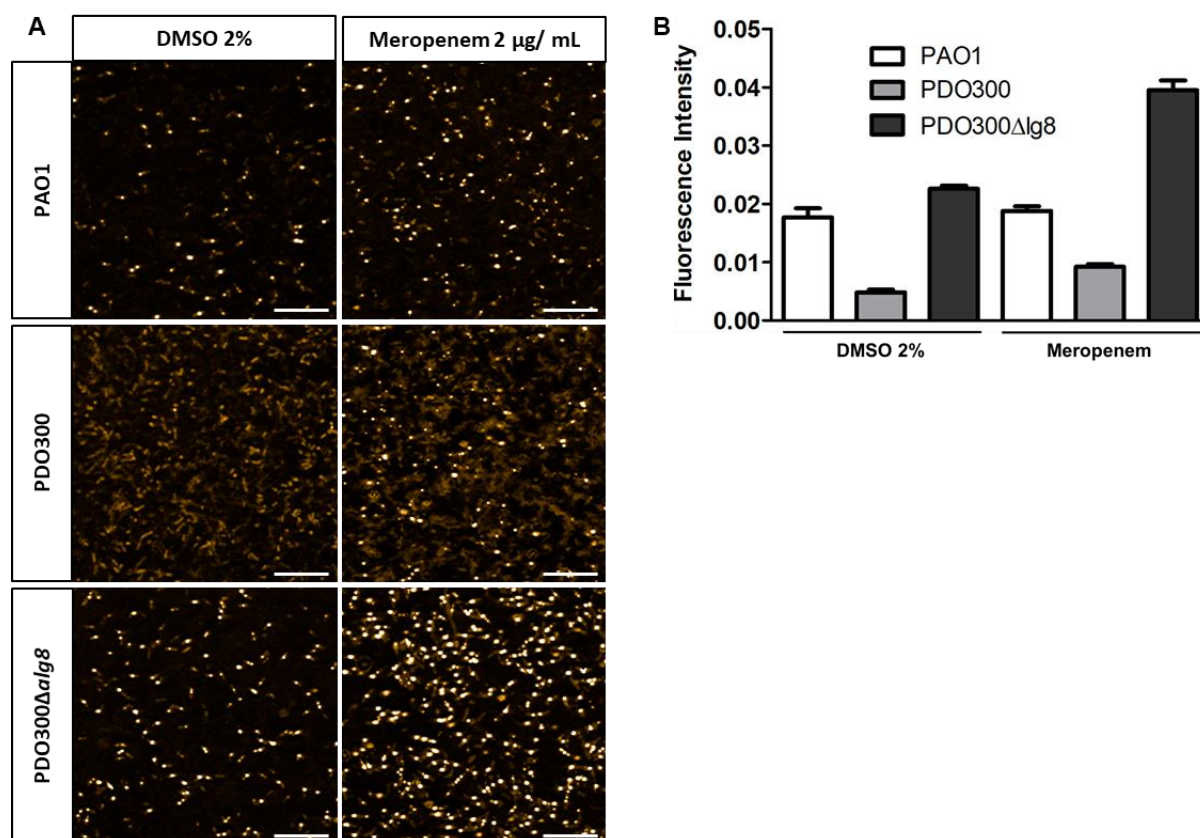


Figure 3.7 (A) Representative images of *P. aeruginosa* biofilms stained with Nile red. The biofilms were treated with 2% DMSO (v/v) and meropenem (2 μg/mL) and stained with Nile red. Four images per well were acquired by high content imaging system In Cell Analyzer 6500HS with a 60X objective (GE Healthcare Life Sciences). The scale bar is 10 μm. (B) Quantification of Nile red intensity using three representative images per well. Images were analyzed by free image analysis software CellProfiler 3 (Broad Institute, Cambridge, MA). The experiment was performed in triplicate. Values represent the mean and standard deviation of the three technical replicates.

3.3.2 Screening of natural product library

After all experimental conditions for biofilm dispersal assay were optimized, a library of 1535 fractions (stock concentration of 250 μg/μL) (**Section 2.2.10**) was screened at a concentration of 50 μg equivalent per μL (μg/μL) against established biofilms of PAO1 and PDO300. The concentration units, μg/μL, of the extracts/fractions used in screening are the ratio of (i) the quantity of dry material used for extraction and (ii) the amount of DMSO solvent required to dissolve the dry material [10]. These fractions have been previously

reported to have antibacterial activity against wild-type *P. aeruginosa* PAO1 [3,4]. These fractions were extracted from Queensland Herbarium, Queensland Marine, and China Biota by NatureBank and stored by Compound Australia under robust environmental conditions. The sample was diluted by the addition of 14 μ L of sterile water into 3.5 μ L of stock fractions in DMSO and supplied in assay ready format plate by Compound Australia. DMSO (20%) (v/v) control plate was also prepared by Compound Australia.

Syto9 is a green fluorescent nucleic acid dye that can penetrate intact cell membrane while PI is a red-fluorescent nucleic acid dye employed to stain only bacteria with the compromised membrane. When present together at appropriate concentrations, the replacement of Syto9 by PI gives rise to red fluorescent signals in dead cells. Although PI has been broadly used for decades, little is known about its limitations, especially in the context of evaluating biofilm viability. PI uptake by viable cells was physiological state-dependent, with a higher percentage of exponential phase cultures being stained by PI compared to bacteria in the stationary growth phase [11].

Images were obtained by confocal laser scanning microscope FV-3000 (Olympus). During image analysis, double-stained bacteria (bacteria were stained with both Syto 9 and PI) were identified. A biofilm experiment on PAO1, PDO300, and PDO300 Δ alg8 with the addition of 2% DMSO was conducted to investigate whether this phenomenon was reproducible and strain specific. Closely examining the obtained images revealed biofilm cells of three tested strains had dual signals with almost all PDO300 cells displaying this staining pattern (**Figure 3.8**). The extent of double staining was possibly specific for strains and biofilm constituents. Nevertheless, additional experiments are required to validate these results. The obtained results here were in line with a recent report in which bacterial cells in the biofilm were double-stained when both Syto9 and PI were present although these cells were able to form colonies on nutrient agar. The false PI-positive signals were attributed to the presence of eDNA in biofilm [12]. When co-staining with Syto9, PI overestimated the number of dead cells, which is an important parameter in examining the efficacy of antimicrobial and/or anti-biofilm agents. To resolve the issue, metabolic activity assessment of biofilm cells using resazurin (RSZ) was used as an alternative approach to LIVE/DEAD staining (**Figure 3.9**). In addition, Syto9 can solely be utilized to visualize changes in biofilm structures upon treatments.

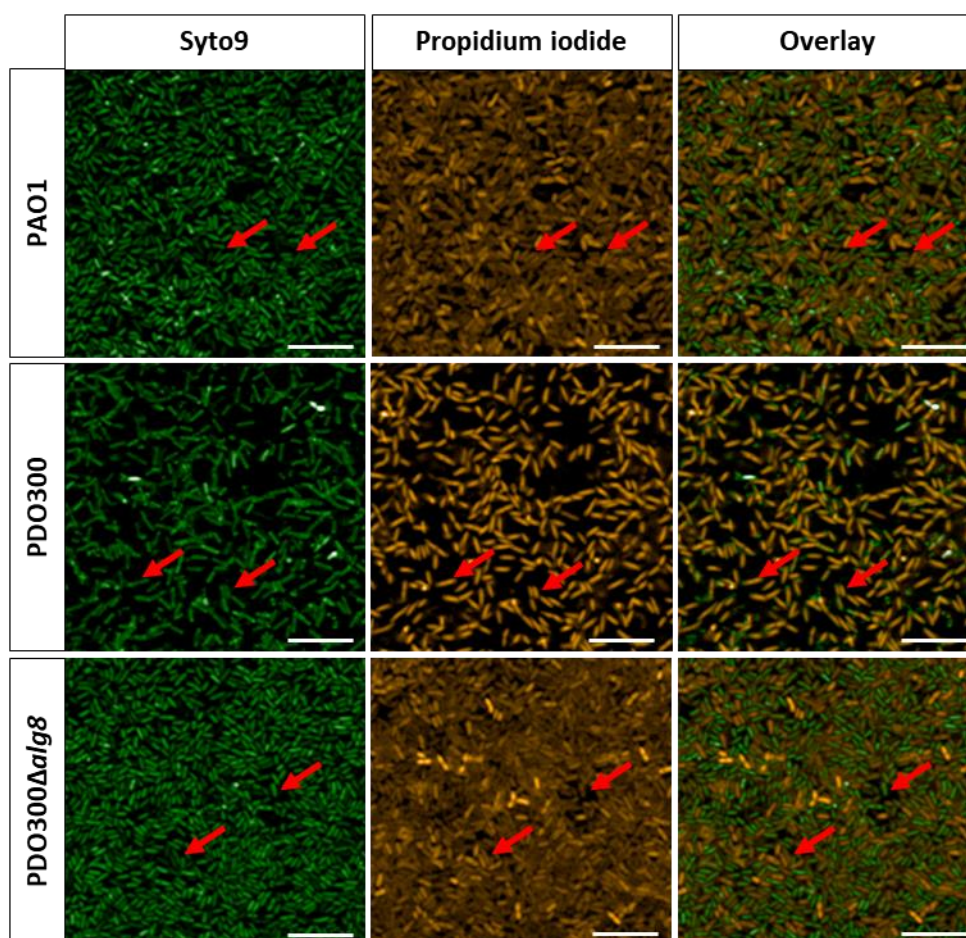


Figure 3.8. Confocal laser scanning microscopic images of PAO1, PDO300 and PDO300 Δ alg8 in the presence of 2% DMSO. Syto9 (green) and propidium iodide (orange) were utilized to stain live and dead bacteria, respectively. Red arrows indicate double-stained bacteria. The experiment was performed in triplicate. Four images per well were acquired by high content imaging system In Cell Analyzer 6500HS with a 60X objective (GE Healthcare Life Sciences). The scale bar is 10 μ m.

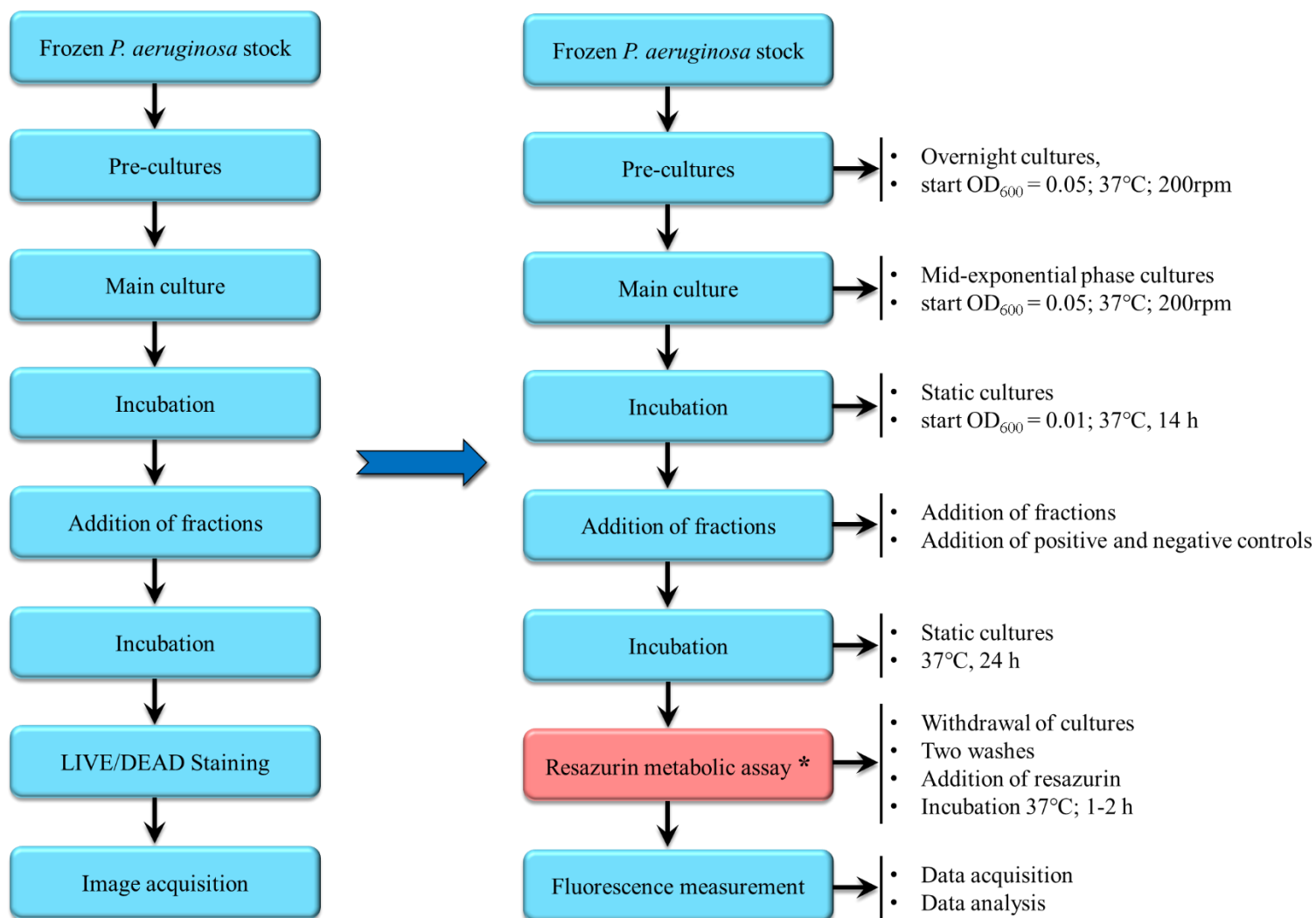


Figure 3.9 An alternative approach for biofilm assay. * Resazurin will be used to quantify the metabolic activity of biofilm cells instead of LIVE/DEAD staining and imaging.

3.3.3 Biofilm assay using resazurin as a viability indicator

1535 fractions plated by Compound Australia were re-screened against pre-existing biofilms of PAO1 using an alternative approach detailed in **Figure 3.9**. In the biofilm dispersal assay, the ratio between negative controls and positive controls was ~ 9 , indicating resazurin is an appropriate metabolic indicator of biofilm bacteria. Additionally, Z' factor was calculated to assess the screen's performance. The resulted Z' factor of 0.66 suggested that the assay had acceptable quality. In this study, preformed biofilm dispersing molecules are of particular interest. These molecules are classified into three categories: (i) disperse established biofilms without affecting the bacterial growth, (ii) disperse preexisting biofilms and kill bacteria, and (iii) disperse preformed biofilms and display bacteriostatic activity. In initial stage of the screening, fractions displayed the ability to disintegrate preformed biofilms were selected. Based on the data obtained in RSZ assay (up to 60% biofilm dispersal), the fractions exhibited at least 40% of biofilm dispersal relative to DMSO control with a coefficient of variation (CV) of less than 20% were chosen for subsequent experiments to confirm their activity. As a result, 78 fractions from a library of 1535 fractions (5%) were classified as biofilm dispersers (**Figure 3.10**).

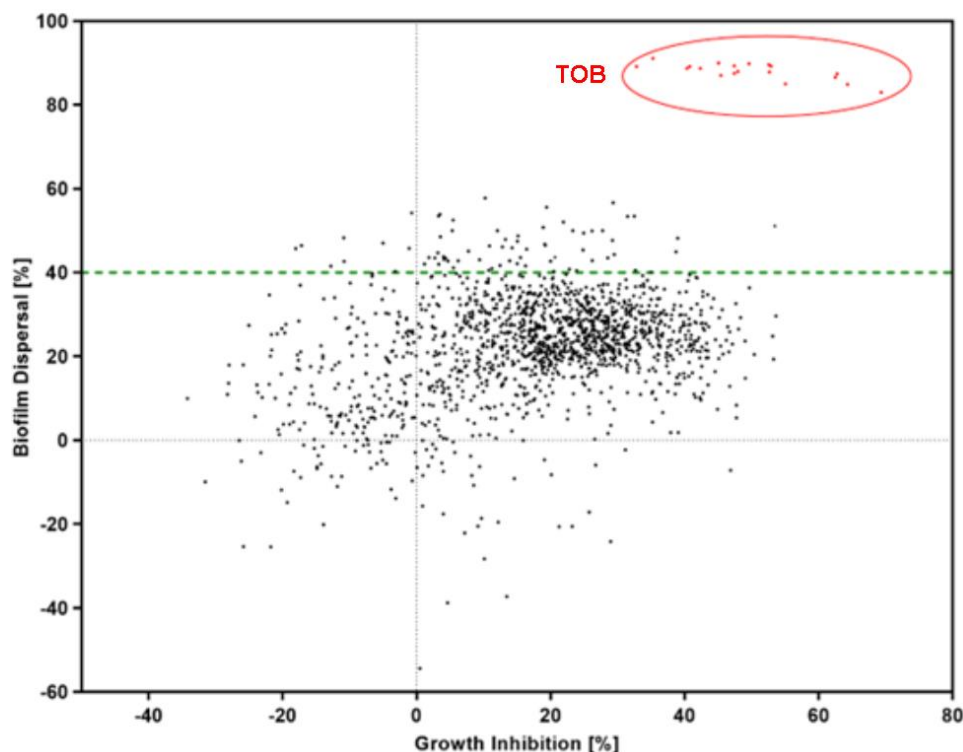


Figure 3.10 A scatter plot displays the percentage of growth inhibition and biofilm dispersal of screened fractions and tobramycin against wild-type PAO1. The activity of the fractions was compared to that of negative control (DMSO solvent). Fractions dispersed established biofilms by at least 40% were selected for further testing. Negative controls (DMSO solvent, 2% (v/v)) and positive controls (TOB, 16 $\mu\text{g/mL}$) were included in individual plates. Experiments were carried out in triplicate.

Alginate overproducing mutant PDO300, an isogenic derivative of PAO1, was generated to imitate clinical isolates from CF patient lungs. Alginate-rich biofilms have been shown to be highly resistant to antibiotics, thus resulting in poor treatment outcomes and infection recurrence. The library of 1535 fractions was screened against established biofilms of PDO300 (Z' factor = 0.7). As expected, levels of dispersing activity on preformed PDO300 biofilms were lower than those observed for preformed PAO1 biofilms. A threshold of 30% biofilm dispersal was utilized to select active fractions. Accordingly, 37 fractions with CV less than 20% were identified as biofilm dispersers (**Figure 3.11**).

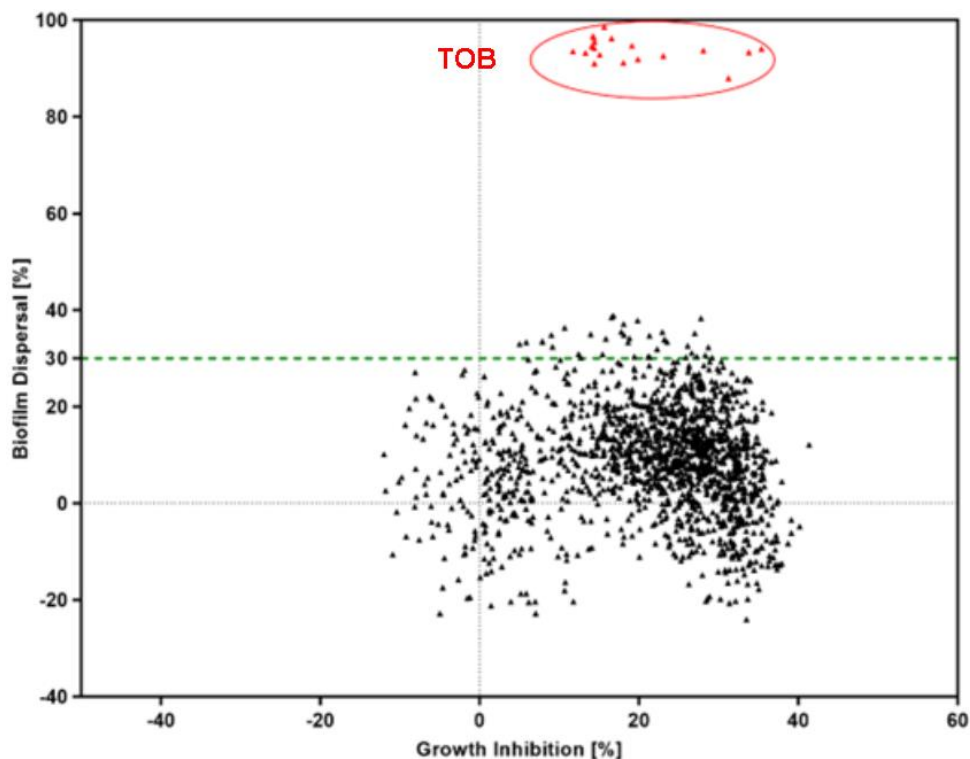


Figure 3.11 Effects of screened fractions on growth and established biofilms of PDO300 relative to the negative control. A threshold of 30% biofilm dispersal was used to select active fractions. Negative controls (DMSO solvent, 2% (v/v)) and positive controls (TOB, 16 $\mu\text{g/mL}$) were included in individual plates. Experiments were carried out in triplicate.

We next sought to evaluate the activity of selected fractions (78 active fractions from the PAO1 screen and 37 active fractions from the PDO300 screen) in inhibiting biofilm formation of PAO1. A biofilm inhibition assay was conducted, and the results indicated that these fractions had limited effects on the viability and biofilm formation of PAO1 (**Figure 3.12**).

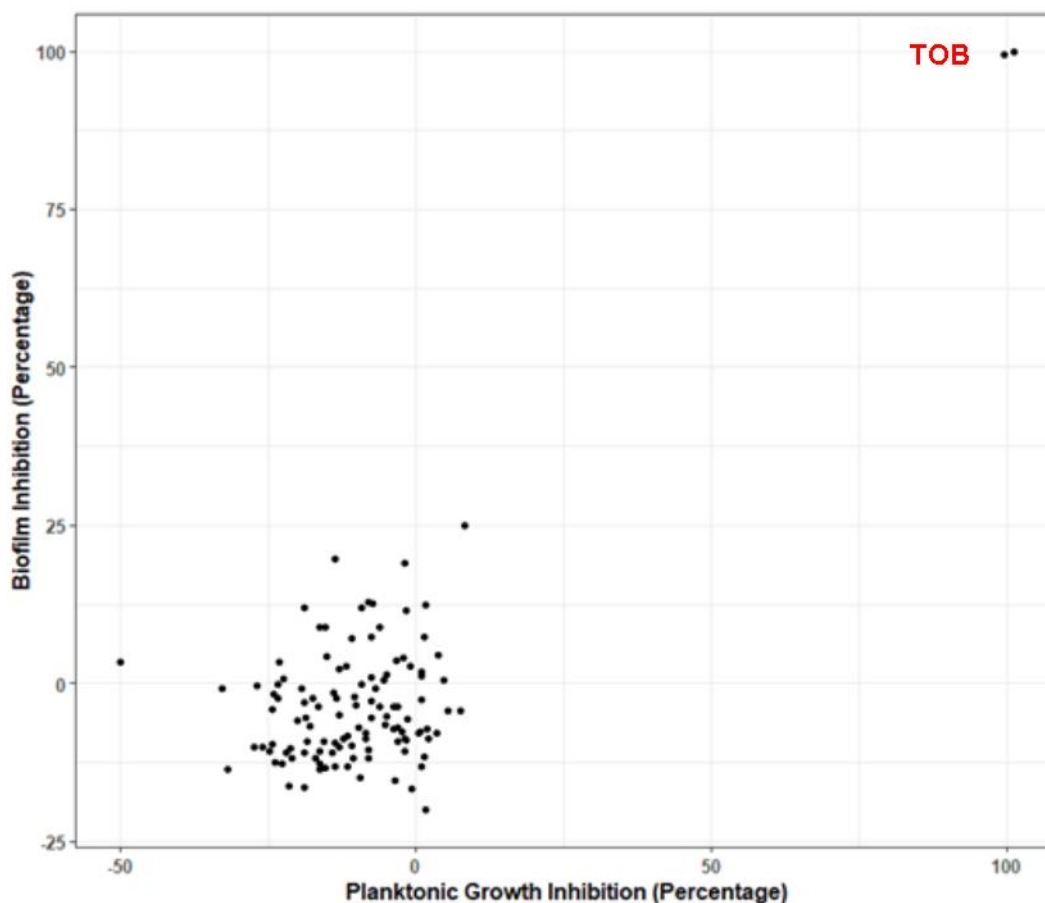


Figure 3.12 Activity of selected fractions on growth and biofilm formation of PAO1 relative to that of the negative control. Negative controls (DMSO solvent, 2%) and positive controls (TOB, 16 $\mu\text{g/mL}$) were included in individual plates. Experiments were carried out in triplicate.

Subsequently, 12 active fractions from the PAO1 primary screen and two active fractions from PDO300 primary screen were subjected to small-scale refractionation (5 fractions per biota) (**Figure 3.13**), followed by a secondary screen to validate the activity in dispersing existing biofilms of PAO1. There were fractions derived from the same biotas, *i.e.*, fractions 3 and 4 belong to biota 1; fractions 1 and 4 were derived from biota 8. Hence, a total of 12 biotas were used for refractionation. The origins of these fractions are provided in **Table 1**. The inhibition of PAO1 growth and the dispersal of PAO1 preformed biofilms induced by refractionated fractions were compared with the activity of initial fractions against established biofilms of PAO1 and PDO300 (**Figures 3.14 - 3.15**). A reduction in growth inhibition caused by refractionated fractions was observed for biota 1 - 3 and biota

1 - 4. Initial fractions biota 4 - 1 and biota 7 - 4 produced minimal inhibition on PAO1 growth while refractionated fractions stimulated the bacterial growth. Opposite effects were also observed for initial and refractionated biota 10 - 5. Likewise, initial biota 12 - 3 impeded the viability of PAO1 and PDO300 by ~20%, whereas refractionated fraction improved planktonic development (2.4%). Biofilm dispersing activity was decreased by ~50% when cells were treated with refractionated biota 5 - 3 and biota 12 - 3. Taken together, ten fractions of the initial hits were confirmed. Subsequently, three fractions, biota 6 - 1, biota 8 - 1, and biota 8 - 4, were chosen for large-scale refractionation (60 fractions per biota) to characterize compounds within the active fractions.

Table 3.1 Origins of selected fractions for small-scale refractionation

No.	Fraction (Biota ID - Fraction ID)	Library	Primary screen
1	Biota 1 - 3	Qld Herbarium	PAO1
2	Biota 1 - 4	Qld Herbarium	-
3	Biota 2 - 3	Qld Herbarium	-
4	Biota 3 - 3	Qld Marine	-
5	Biota 4 - 1	Qld Marine	-
6	Biota 5 - 3	Tas Marine	-
7	Biota 6 - 1	Tas Marine	-
8	Biota 7 - 4	Qld Marine	-
9	Biota 8 - 1	Qld Marine	-
10	Biota 8 - 4	Qld Marine	-
11	Biota 9 - 1	Qld Marine	-
12	Biota 10 - 5	Qld Marine	-
13	Biota 11 - 1	Qld Marine	PDO300
14	Biota 12 - 3	Tas Marine	PDO300

Abbreviation: QLD, Queensland; Tas, Tasmania.

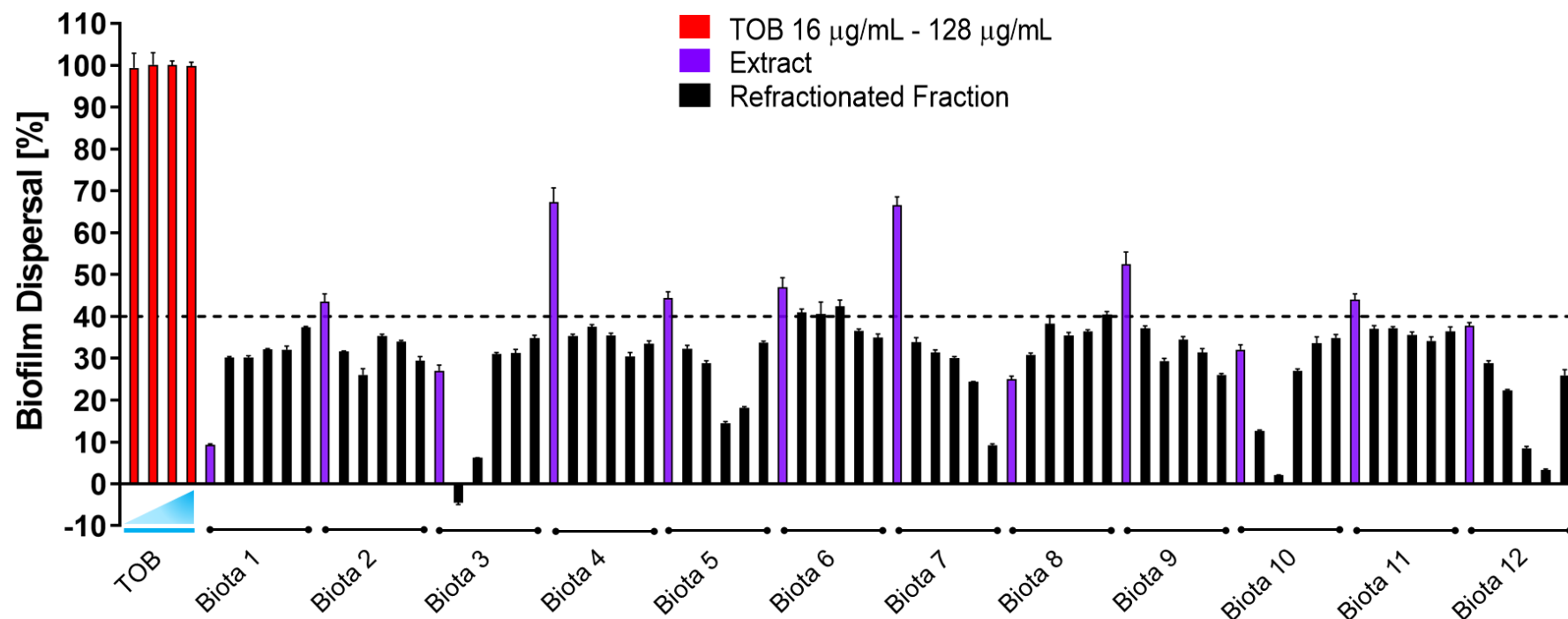


Figure 3.13 Antibiofilm efficiency of biotas isolated extracts and refractionated fractions in dispersing preformed biofilms of wild-type PAO1. In small-scale refractionation, two extracts (Hexane and DCM/MeOH) and five fractions were obtained from each biota. Plotted data were biofilm dispersing activity of DCM/MeOH extracts and five refractionated fractions. TOB 16 - 128 µg/mL were used as positive controls. The experiment was performed in triplicate. Values are the mean and standard deviation of three technical replicates. Abbreviations: DCM, Dichloromethane; MeOH, Methanol.

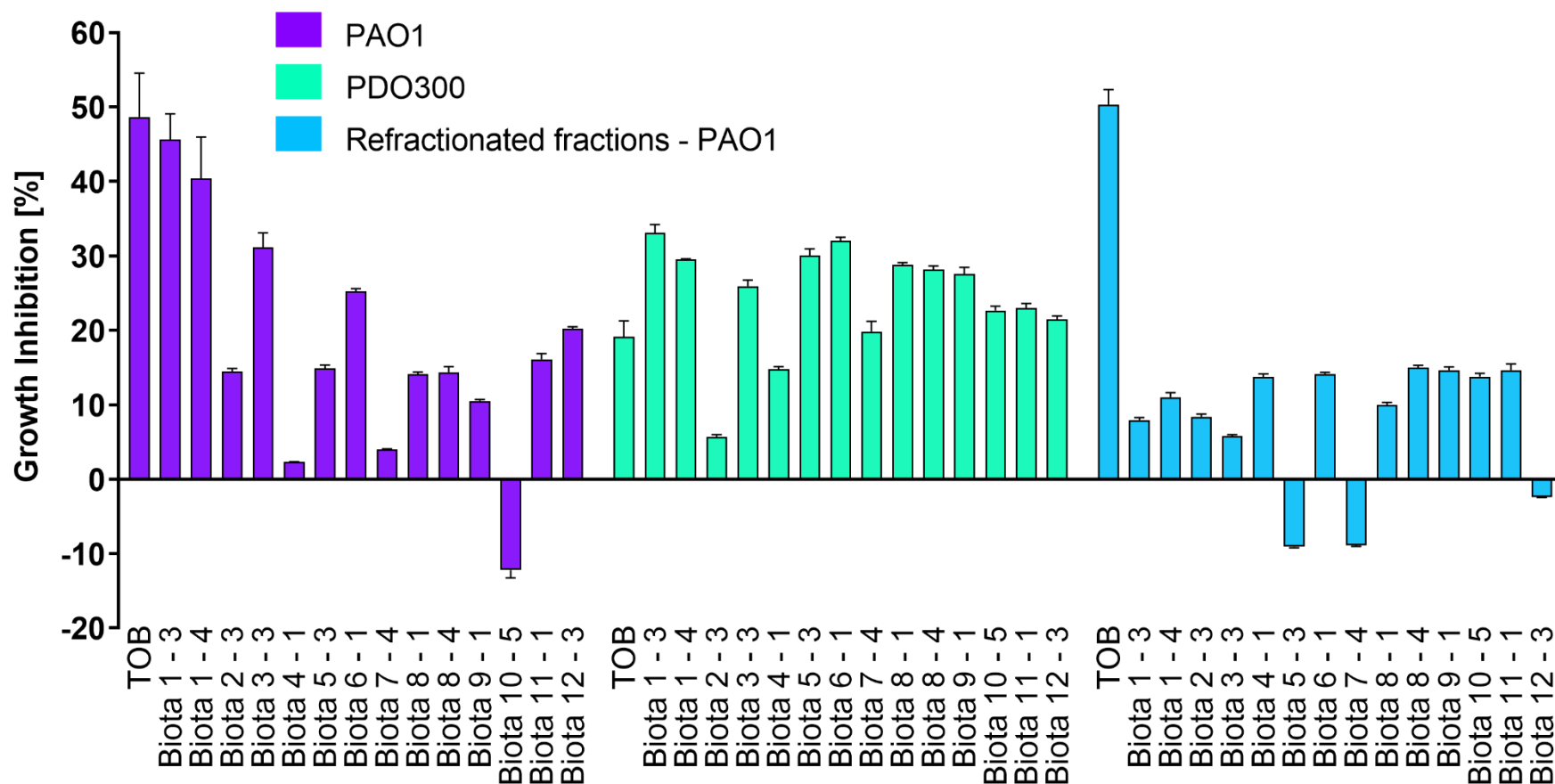


Figure 3.14 Impacts of 14 initial fractions and refractionated fractions on the viability of PAO1 and PDO300. DMSO solvent (2%, (v/v)) was negative control, and tobramycin (TOB, 16 μ g/mL) was positive control. Data were compared to negative controls and error bars were the coefficient of variation (CV%). Experiments were carried out in triplicate.

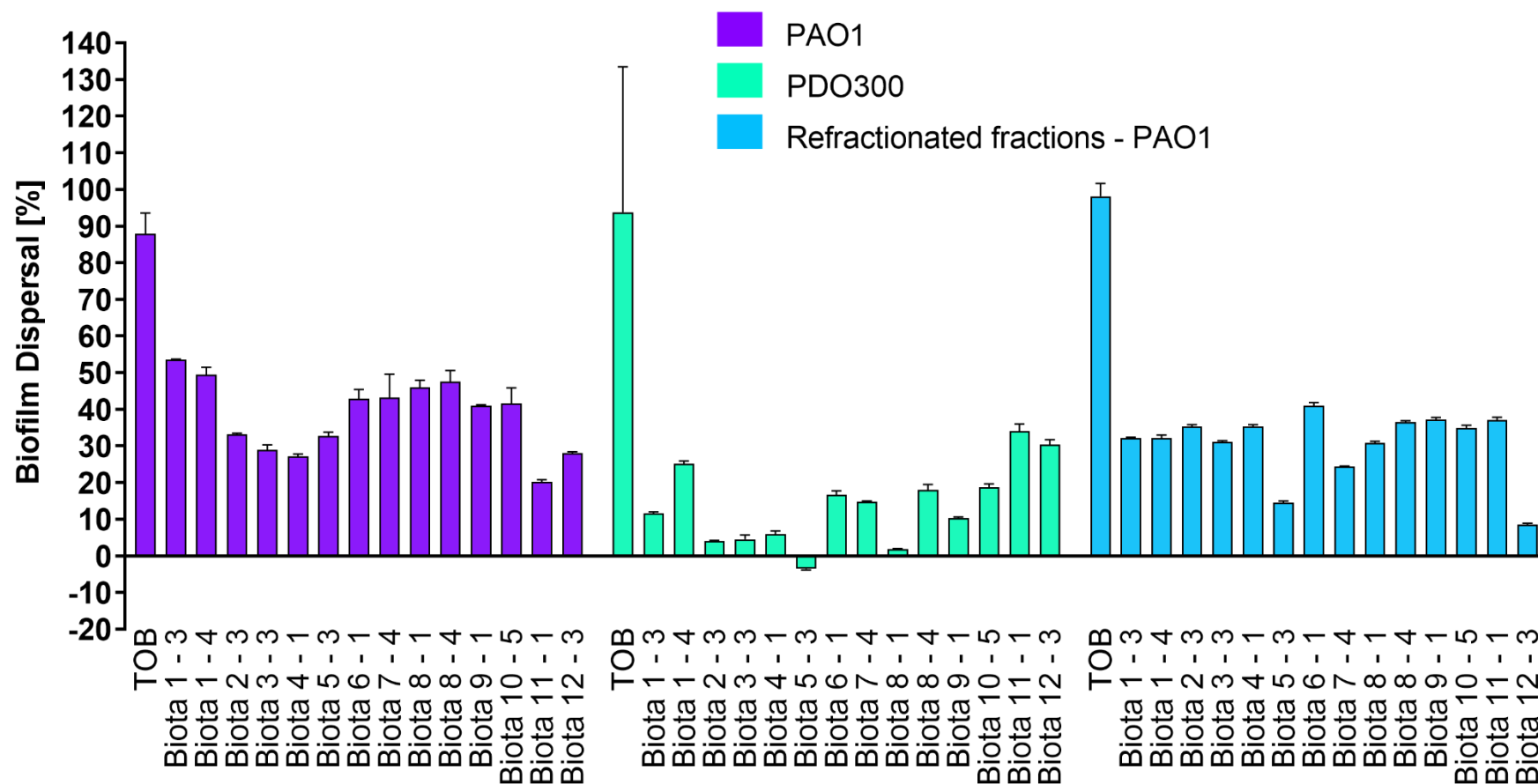


Figure 3.15 Viability of PAO1 and PDO300 biofilms upon exposure to 14 initial and refractionated fractions. Controls included in individual plates were negative controls (DMSO solvent, 2% (v/v)) and positive controls (TOB, 16 μ g/mL). Data were compared to negative controls, and error bars represented the coefficient of variation (CV%). Experiments were performed in triplicate.

Unexpectedly, the effects of fractions derived from large-scale refractionation dramatically reduced more than 50% as opposed to that originated from small-scale refractionation (**Figure 3.16**). We hypothesized that if there were synergistic effects between compounds within active fractions, further separation would reduce the antibiofilm activity and that fractions from small-scale refractionation would show reproducible effects. Fractions 18 - 48 are deemed to contain bioactive compounds; thus, they were chosen for the repeated screen. Additionally, these fractions were screened along with different tobramycin concentrations to evaluate their efficacy against PAO1 preformed biofilms. None of the fractions displayed antibiofilm activity as they previously did (**Figure 3.17**). It is unclear why these fractions were active in primary and secondary screens, but they only exhibit negligible effects after large-scale refractionation. Furthermore, fractions from small-scale refractionation did not show reproducible activity. It is also noteworthy that, porcine gastric mucin (PGM), one ingredient of artificial sputum medium (ASM), initially purchased from Sigma, was replaced by PGM from Lee Biosolutions due to a shortage of supply. Screening of fractions from large-scale refractionation and subsequent screens were carried out using ASM containing Lee Biosolutions PGM. A recent finding demonstrated that a high concentration of iron in commercial PGM promoted PAO1 growth and enhanced the production of phenazines (1-hydroxyphenazine, pyocyanin and phenazine-1-carboxylic acid) and reduced rhamnolipid and siderophore levels [13]. In addition, elevated pyocyanin production was found to associate with increased biofilm formation [14], which might further impede the penetration of screened fractions into the biofilms, thus possibly explaining the non-reproducible effectiveness of these fractions in dispersing established biofilms of PAO1.

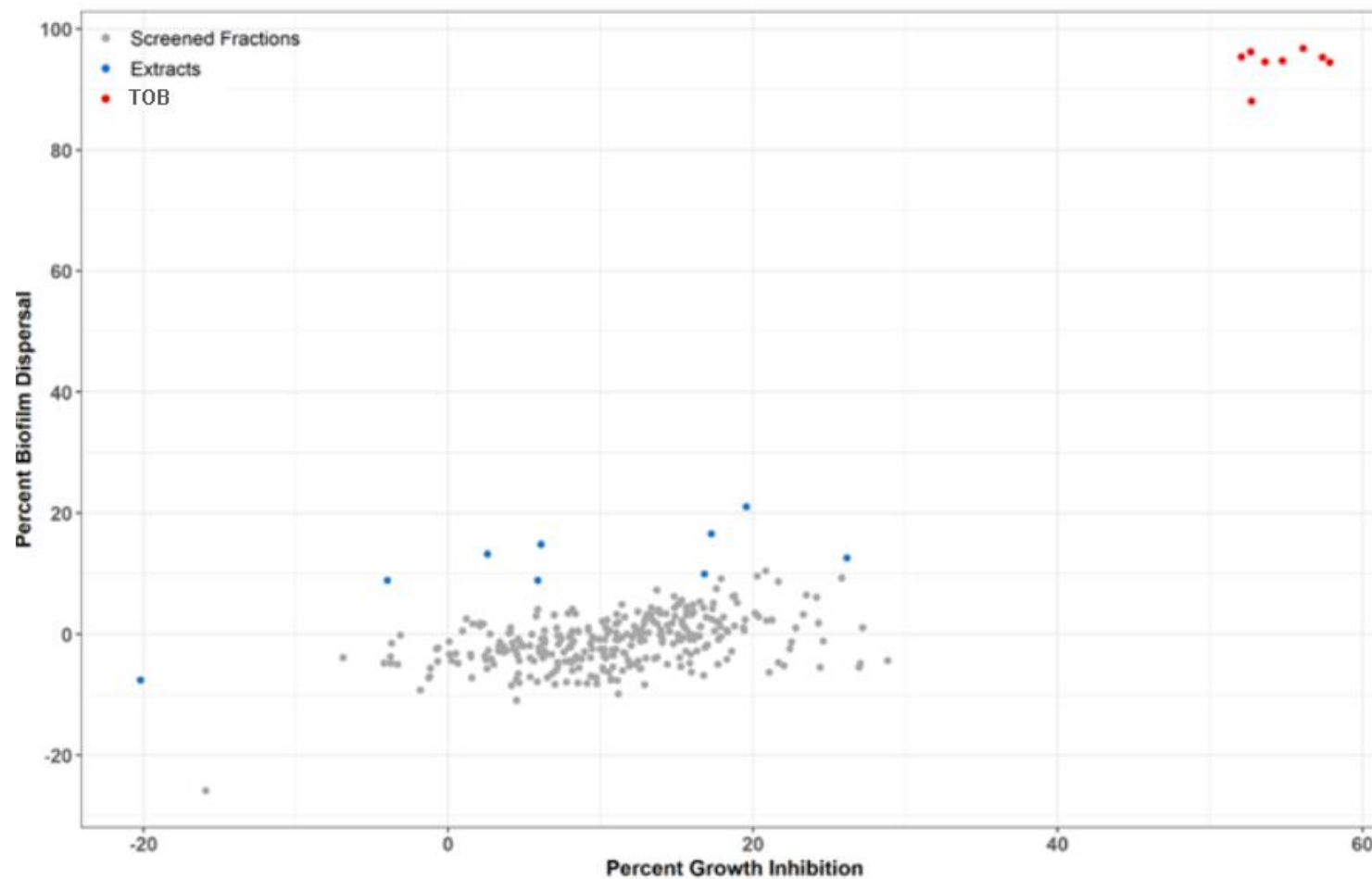


Figure 3.16 Biofilm dispersing effects of extracts and refractionated fractions (large-scale refractionation, 60 fractions per biota) on PAO1. TOB (16 - 128 $\mu\text{g/mL}$) was used as the positive control. Experiments were conducted with three technical replicates.

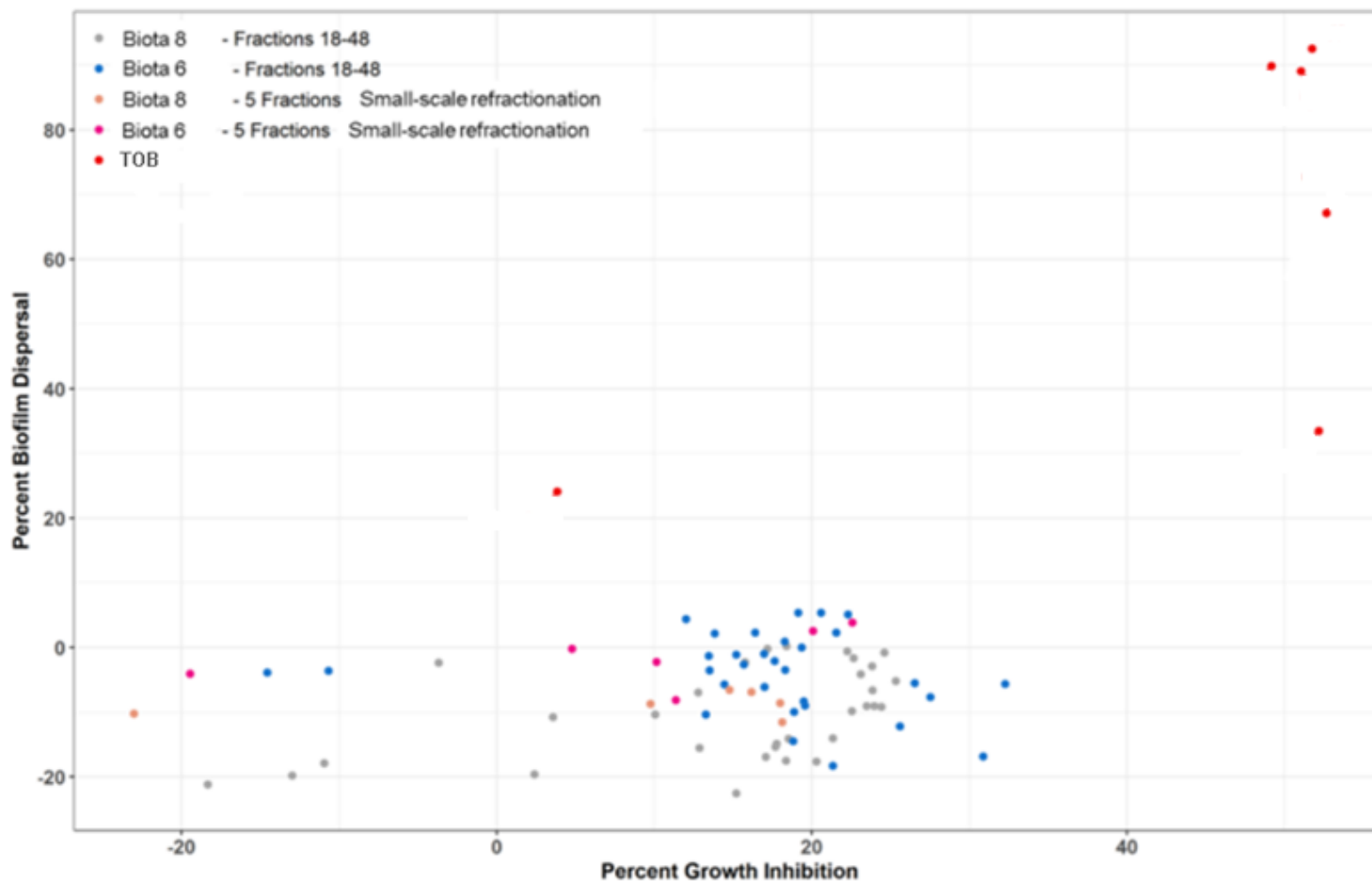


Figure 3.17 Viability of PAO1 preformed biofilms treated with selected fractions. Fractions 18 - 48 (large-scale refractionation, 60 fractions per biota) and fractions (small-scale refractionation, 5 fractions per biota) derived from biotas 6 and 8 were re-tested using biofilm dispersal assay. TOB (0.64 - 64 $\mu\text{g/mL}$) was positive controls. Experiments were carried out with three technical replicates.

3.3.4 Screening of the NatureBank library

In addition to the fraction library, a set of 54 NatureBank compounds were screened at 2 μ M and 20 μ M against existing biofilms of PAO1 using ASM containing Lee Biosolutions PGM. The data showed that these compounds had limited effects on dispersing preformed biofilms while impeding planktonic growth up to ~ 40%. However, we focused on identifying molecules with biofilm dispersing activity in this study. Hence, these compounds were not further investigated (**Figure 3.18**).

3.4 Conclusion

To develop a biofilm assay, several associated parameters including reference strain, assay format, growth medium, bacterial growth phase, biofilm stages, the tolerability of bacterial cells to dimethyl sulfoxide (DMSO) were considered. In addition, the selection of positive control, *i.e.*, antibiotic, and the determination of suitable time for fractions/compounds addition were also taken into account.

Wild-type *P. aeruginosa* PAO1 has been a reference strain for studies of *P. aeruginosa* physiology and metabolism for over 50 years [15]. PAO1 was chosen as representative strain for developing and optimizing biofilm assay for identification of molecules with biofilm dispersing activity. The microtiter plate format (384 well-plates) was chosen as it not only saves reagents and fractions/testing compounds but also allows rapid testing of many molecules of interest at multiple concentrations at once, thus making the assay more cost-effective. The biological relevance of *in vitro* biofilm model to *in vivo* lung infection is essential. ASM was selected as it was reported to mimic physiology conditions of the CF lungs [16]. Bacterial growth curve was established to determine growth phase of *P. aeruginosa*. It was demonstrated that cells in the exponential growth phase exhibited progressively enhanced adhesion compared to their stationary phase counterparts [6]. Hence, cells in mid-log were chosen to generate the biofilms for subsequent experiments. Suitable time for fraction addition was estimated using biofilm growth curve. Bacteria were allowed to growth biofilms for 14 h before addition of fractions since it was the peak of

crystal violet intensities-stained biofilm biomass. The tolerability of the bacteria to DMSO is essential as all fractions and compounds are dissolved in 100% DMSO (v/v). Effect of different concentrations of DMSO on the bacterial metabolism was evaluated using resazurin viability assay. A final concentration of 2% DMSO (v/v) was used since it had low impact on cell viability. For positive control, the efficacy of three clinically used antibiotics including tobramycin, ciprofloxacin and meropenem was assessed. Tobramycin at 16 $\mu\text{g/mL}$ was used as positive control since it decreased biofilm biomass significantly compared to ciprofloxacin and meropenem.

This assay was employed to screen a fraction library and a set of pure compounds. Screening of pure compounds did not produce any molecules with antibiofilm properties. In respect of the fraction library, active fractions in the primary screen were selected for small-scale refractionation, and their activities were confirmed in the secondary screen. However, a significant reduction of antibiofilm effects was observed when large-scale refractionation derived fractions were tested. Possibly the change in PGM suppliers led to non-reproducible results. Nonetheless, further experiments involving different PGM are required to understand how the ASM of different components influences the outcomes between experiments. Due to the time constrain, this project was put on hold.

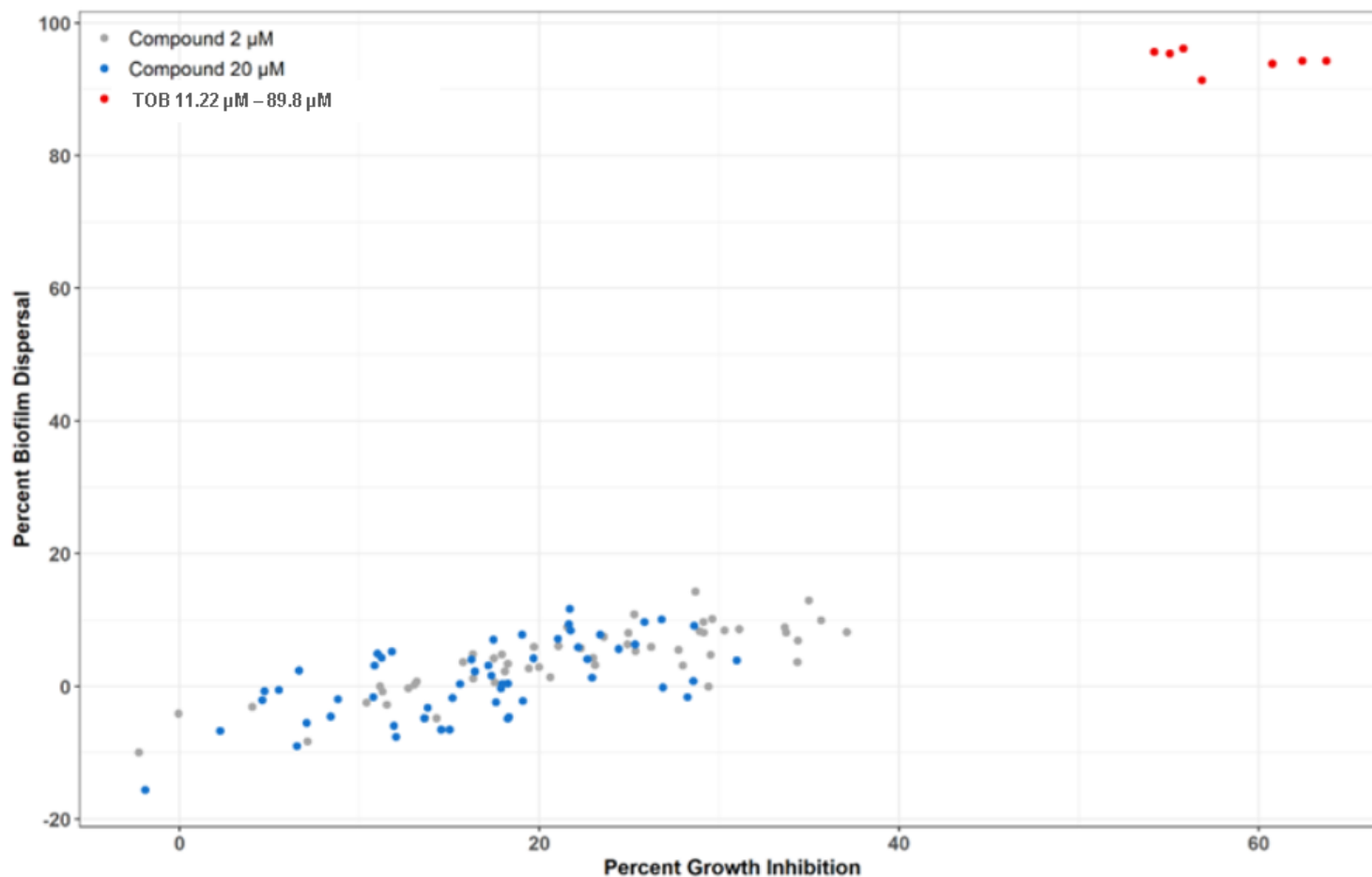


Figure 3.18 Effects of 54 NatureBank compounds on dispersing preformed biofilms of PAO1. Bacteria were treated with the compounds at two different concentrations two μM and 20 μM . TOB with concentrations ranging from 11.22 μM to 89.8 μM were positive controls. Experiment was carried out with three technical replicates.

3.5 References

1. World Health Organization., WHO priority pathogens list for R&D of new antibiotics. *World Health Organization* **2017**. Available online: <http://www.who.int/mediacentre/news/releases/2017/bacteria-antibiotics-needed/en/> (accessed on
2. Moradali, M.F.; Ghods, S.; Rehm, B.H. *Pseudomonas aeruginosa* Lifestyle: A Paradigm for Adaptation, Survival, and Persistence. *Front Cell Infect Microbiol* **2017**, *7*, 39, doi:10.3389/fcimb.2017.00039.
3. Martin, F.; Grkovic, T.; Sykes, M.L.; Shelper, T.; Avery, V.M.; Camp, D.; Quinn, R.J.; Davis, R.A. Alkaloids from the Chinese vine *Gnetum montanum*. *J Nat Prod* **2011**, *74*, 2425-2430, doi:10.1021/np200700f.
4. Zetterstrom, C.E.; Hasselgren, J.; Salin, O.; Davis, R.A.; Quinn, R.J.; Sundin, C.; Elofsson, M. The resveratrol tetramer (-)-hopeaphenol inhibits type III secretion in the gram-negative pathogens *Yersinia pseudotuberculosis* and *Pseudomonas aeruginosa*. *PLoS One* **2013**, *8*, e81969, doi:10.1371/journal.pone.0081969.
5. Crouzet, M.; Le Senechal, C.; Brözel, V.S.; Costaglioli, P.; Barthe, C.; Bonneau, M.; Garbay, B.; Vilain, S. Exploring early steps in biofilm formation: set-up of an experimental system for molecular studies. *BMC Microbiol* **2014**, *14*, 253-253, doi:10.1186/s12866-014-0253-z.
6. Chambers, J.R.; Cherny, K.E.; Sauer, K. Susceptibility of *Pseudomonas aeruginosa* Dispersed Cells to Antimicrobial Agents Is Dependent on the Dispersion Cue and Class of the Antimicrobial Agent Used. *Antimicrob Agents Chemother* **2017**, *61*, e00846-00817, doi:10.1128/AAC.00846-17.
7. Yokochi, T.; Narita, K.; Morikawa, A.; Takahashi, K.; Kato, Y.; Sugiyama, T.; Koide, N.; Kawai, M.; Fukada, M.; Yoshida, T. Morphological change in *Pseudomonas aeruginosa* following antibiotic treatment of experimental infection in mice and its relation to susceptibility to phagocytosis and to release of endotoxin. *Antimicrob Agents Chemother* **2000**, *44*, 205-206, doi:10.1128/aac.44.1.205-206.2000.

8. Grage, K.; Jahns, A.C.; Parlane, N.; Palanisamy, R.; Rasiah, I.A.; Atwood, J.A.; Rehm, B.H.A. Bacterial Polyhydroxyalkanoate Granules: Biogenesis, Structure, and Potential Use as Nano-/Micro-Beads in Biotechnological and Biomedical Applications. *Biomacromolecules* **2009**, *10*, 660-669, doi:10.1021/bm801394s.
9. Pham, T.H.; Webb, J.S.; Rehm, B.H. The role of polyhydroxyalkanoate biosynthesis by *Pseudomonas aeruginosa* in rhamnolipid and alginate production as well as stress tolerance and biofilm formation. *Microbiology* **2004**, *150*, 3405-3413, doi:10.1099/mic.0.27357-0.
10. Camp, D.; Campitelli, M.; Carroll, A.R.; Davis, R.A.; Quinn, R.J. Front-loading natural-product-screening libraries for log P: background, development, and implementation. *Chem Biodivers* **2013**, *10*, 524-537, doi:10.1002/cbdv.201200302.
11. Shi, L.; Gunther, S.; Hubschmann, T.; Wick, L.Y.; Harms, H.; Muller, S. Limits of propidium iodide as a cell viability indicator for environmental bacteria. *Cytometry A* **2007**, *71*, 592-598, doi:10.1002/cyto.a.20402.
12. Rosenberg, M.; Azevedo, N.F.; Ivask, A. Propidium iodide staining underestimates viability of adherent bacterial cells. *Sci Rep* **2019**, *9*, 6483, doi:10.1038/s41598-019-42906-3.
13. Neve, R.L.; Carrillo, B.D.; Phelan, V.V. Impact of Artificial Sputum Medium Formulation on *Pseudomonas aeruginosa* Secondary Metabolite Production. *J Bacteriol* **2021**, *203*, e0025021, doi:10.1128/JB.00250-21.
14. Das, T.; Manefield, M. Phenazine production enhances extracellular DNA release via hydrogen peroxide generation in *Pseudomonas aeruginosa*. *Commun Integr Biol* **2013**, *6*, e23570, doi:10.4161/cib.23570.
15. Lessie, T.G.; Phibbs, P.V. ALTERNATIVE PATHWAYS OF CARBOHYDRATE UTILIZATION IN PSEUDOMONADS. *Annual Review of Microbiology* **1984**, *38*, 359-388, doi:10.1146/annurev.mi.38.100184.002043.
16. Sriramulu, D.D.; Lünsdorf, H.; Lam, J.S.; Römling, U. Microcolony formation: a novel biofilm model of *Pseudomonas aeruginosa* for the cystic fibrosis lung. *Journal of Medical Microbiology* **2005**, *54*, 667-676, doi:<https://doi.org/10.1099/jmm.0.45969-0>.

CHAPTER 4: Screening of Davis Open Access library

4.1 Introduction

Pseudomonas aeruginosa is a major human pathogen causing devastating acute and chronic infections in individuals with compromised immune systems such as patients with human immunodeficiency virus (HIV) or cystic fibrosis (CF). Biofilm-associated diseases leading to chronic infections are the main reason for treatment failures as bacteria inside biofilms are highly recalcitrant to antimicrobials and protected from host immune response [1]. According to the National Institute of Health (NIH), approximately 65% of bacterial infections involve biofilms and 80% of chronic infections are biofilm-related [2]. To cope with the rapid decline of antibiotic effectiveness due to increasing drug resistance, the search for novel therapeutic strategies targeting biofilms formation and more importantly eradicating established biofilms is urgently needed. Drug repurposing is an attractive alternative approach since it lowers the associated costs, shortens the development timeline, and alleviates the risks of using new drugs with insufficient safety data. It is a shortcut to obtain safe and bioavailable molecules that can be used as drug leads or can quickly enter human clinical trials [3]. In this respect, we explored the use of 505 compounds with known biological activities including tuberculosis, cancer, malaria, bacterial infections and neurodegenerative disorders and their analogues as preformed biofilm dispersing agents.

4.2 Materials and Methods

4.2.1 Compound library

The library, David Open Access, consisting of 505 compounds was kindly provided by Associated Professor Rohan Davis (Nature Bank). These compounds at a stock concentration of 5 mM are stored in Compound Australia facility under robust environmental conditions (inert environment (liquid nitrogen) at 18°C) and supplied in an assay-ready plate format ([Compounds-Australia-Storage-Platforms.pdf](https://www.compoundaustralia.com/Compounds-Australia-Storage-Platforms.pdf) ([griffith.edu.au](https://www.griffith.edu.au))). The library possesses a wide range of biological activities against different diseases such as

tuberculosis [4], cancer [5], malaria [6], bacterial infections [7], HIV and neurodegenerative disorders including Parkinson's disease [8]. In this study, we set out to explore the use of this library for dispersing established biofilms.

4.2.2 Biofilm dispersal assay

Overnight cultures of wild-type *P. aeruginosa* PAO1 at 37°C in LB medium were washed once with sterile saline 0.9 % and adjusted to an OD₆₀₀ of 0.05, and 1% inoculum was transferred into fresh LB medium. Following the incubation at 37°C, 200 rpm for 6 h to reach the mid-log phase, the cells were washed once with sterile saline 0.9 % (w/v) and diluted to an OD₆₀₀ of 0.01. 45 µL aliquots were dispensed into 384-well plates (Greiner Bio-One, catalog no. 781091). After incubation for 14 h at 37°C in a static condition, compounds (5 µL) were added to each well at a final concentration of 50 µM. The plates were incubated for a further 24 h at 37°C. The effect of compounds on bacterial growth and viability of biofilm bacteria were determined by the OD₆₀₀ and resazurin metabolic assay, respectively. The negative controls or untreated cultures consisted of inoculum and 1% DMSO (v/v). Antibiotic tobramycin (0.45 µM and 44.9 µM) was used as positive controls. The initial OD₆₀₀ and final OD₆₀₀ were read before incubation at 37°C and after a total 38 h incubation using a Biotek synergy 2 microplate reader, respectively, followed by an assessment of biofilm viability by resazurin metabolic assay. In the resazurin assay, cultures were withdrawn from the wells, and the plates were washed twice with sterile water. Resazurin at a final concentration of 0.004% was then added to the plates followed by incubation at 37°C for 5- 6 h. Fluorescence intensities (excitation 530 nm, emission 590 nm) were read using a microplate reader (BioTek Synergy 2). The experiments were carried out with three technical replicates. Compounds that can disperse preformed biofilms will be selected for confirmatory screening to confirm their activities.

4.2.3 Data analysis

Please refer to **Chapter 2** – General materials and methods, **section 2.2.10**.

4.3 Results and discussion

There are three distinct stages of biofilm dispersal, *i.e.*, (1) detachment and liberation of biofilm cells from the microcolonies, (ii) cell migration to new colonization sites, and (iii) adherence of the cells to new surfaces [9]. As shown in the previous study, cells detached from the biofilm matrix are more susceptible to antimicrobial treatments than cells residing inside the biofilms [10]. Actively activating the biofilm dispersal process using biofilm dispersing agents is another alternative approach to treat biofilm-related infections. Matrix degrading enzyme, such as alginate lyase, has been proved to have therapeutic effects against biofilm-associated pulmonary diseases [10]. Small molecule, NO donor sodium nitroprusside, has been reported to be effective in detaching established biofilms of *P. aeruginosa* [11]. Other agents, including quorum sensing (QS) inhibitors and surfactants, also have great potential for controlling pre-existing biofilms.

Based on the data obtained in RSZ assay, the compounds displayed up to 40% of biofilm dispersal relative to DMSO control. Thus, the compounds reduced at least 34% of established biofilms with a coefficient of variation (CV) of less than 20% were chosen for subsequent experiments. Twenty-one compounds (4.2%) with the coefficient of variation of less than 20% were selected. Since the list of active compounds contains antimalarial agents, we decided to re-screen other antimalarial compounds, including **5**, **7**, **8**, **10**, **14** and **15**, that displayed dispersal activity lower than the cut-off (**Figure 4.1**). Notably, although these compounds did not adversely affect the growth of wild-type PAO1, they dispersed established biofilms up to ~ 42%.

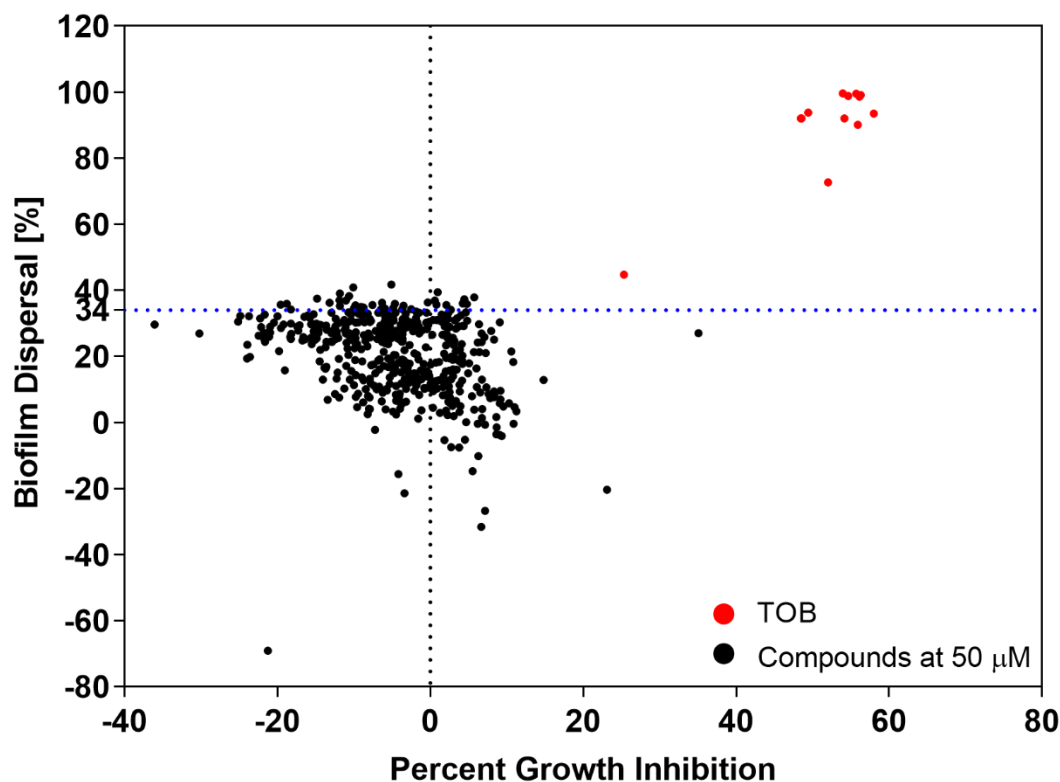


Figure 4. 1 Effect of 505 pure compounds on inhibiting growth and dispersing preformed biofilms of wild-type *P. aeruginosa* PAO1. Compounds were screened at 50 µM. A threshold of 34% for biofilm dispersal (blue line) was used to select active compounds. Twenty-seven compounds with the coefficient of variation (CV%) less than 20% were selected for the confirmatory screen. TOB (0.45 – 44.9 µM) and DMSO 1% (v/v) were used as positive and negative controls, respectively. Experiments were performed in triplicate.

Next, 27 active compounds were subjected to a secondary screen to confirm their effect on pre-existing biofilms. The growth of free-living bacteria was increased upon exposure to the compounds, while the viability of preformed biofilms was inhibited by up to 54%. It has been previously reported that dispersed populations are more susceptible to antibiotic treatments than their biofilm counterparts [12,13]. It raises the possibility of using adjunctive approaches in which biofilm dispersing agents could be applied with antibiotics to treat biofilm-associated infections. The enhanced planktonic growth observed in current experiments may be the result of the liberation of biofilm bacteria into the medium,

suggesting the potential use of these molecules in combination approaches. Out of 27 compounds, five compounds **1**, **2**, **13**, **14** and **15** did not exhibit reproducible activity against preformed biofilms. Hence, they were excluded from subsequent experiments. Compounds **26** and **27** had CV% more than 20%, therefore, they were also eliminated (**Figure 4.2**). Collectively, 15 of the initial active compounds, including five antimalarial molecules, were confirmed (55.6%) by the second screen (**Figure 4.3**). Due to insufficient supply, compounds **3**, **7** and **11** would not be tested in follow-up experiments. The chemical structures and bioactivity of 15 compounds are provided in **Figure 4.4** and **Table 4.1**, respectively.

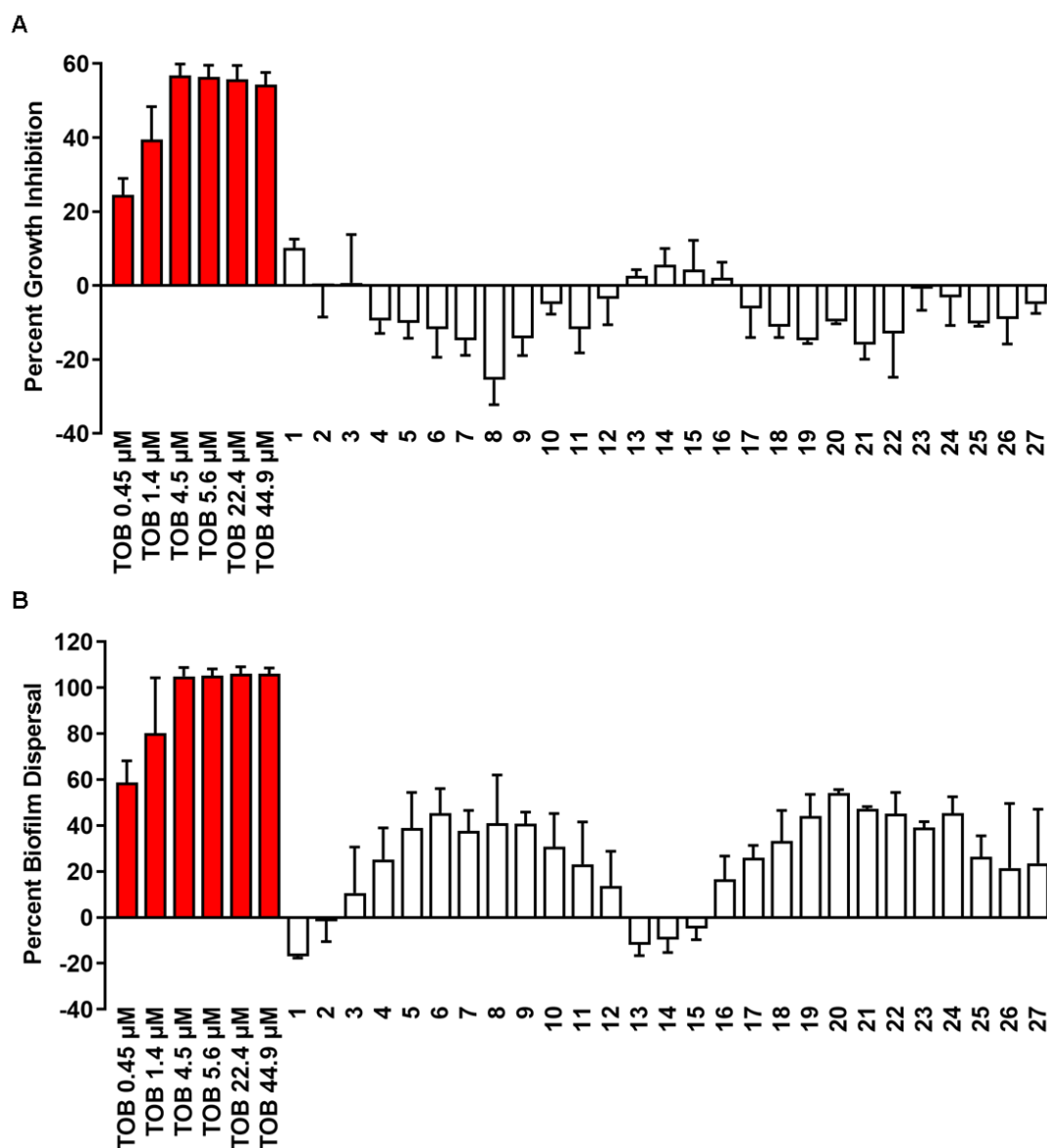


Figure 4.2 (A) Growth inhibition and **(B)** biofilm dispersal activity of 27 compounds in confirmatory screen. Compounds were re-screened at 50 μ M. TOB (0.45 – 44.9 μ M) was positive control and DMSO 1% (v/v) was the negative control. Experiments were carried out in triplicate. Data are the percentage of growth inhibition and biofilm dispersal. The error bars represent the coefficient of variation. Abbreviation: TOB, tobramycin.

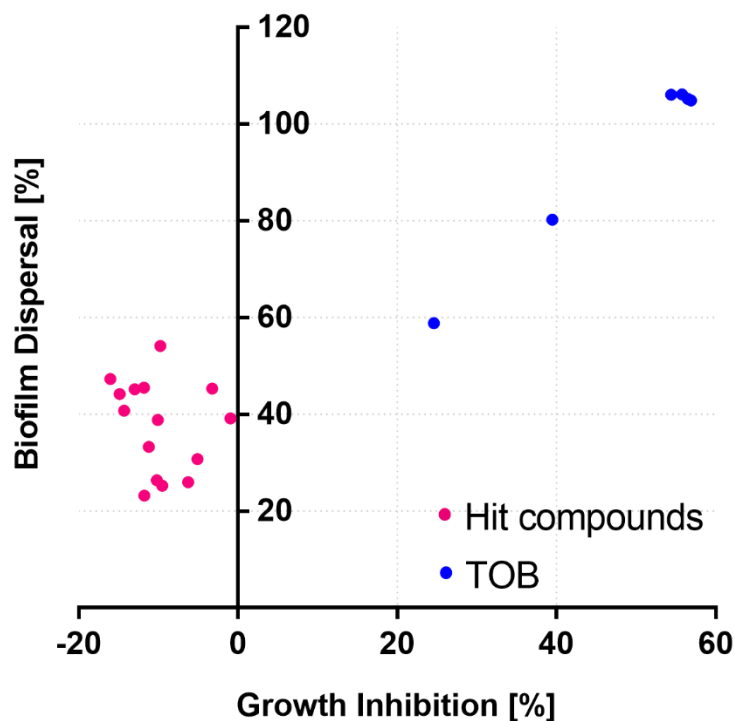


Figure 4.3 Activity of 15 confirmed compounds. A scatter plot displays the percentage of growth inhibition on the x-axis and the percentage of biofilm dispersal on the y-axis. These compounds dispersed preformed biofilms without inhibiting the growth of *P. aeruginosa* PAO1. Compounds were re-screened at 50 μ M. TOB (0.45 – 44.9 μ M) was the positive control and DMSO 1% (v/v) was the negative control. Experiments were carried out in triplicate.

The effects of 15 active compounds individually on preformed *P. aeruginosa* biofilms have not been previously determined. Among these, three molecules were reported to modulate the biofilm development of *P. aeruginosa*. Psammaphin A was found to interact with the QS system, indicating that it may be a QS inhibitor [14]. Mefloquine, a potent antimalarial drug, functioned synergistically with colistin *in vitro* and *in vivo* to reduce the viability of colistin-resistant *P. aeruginosa*, impede biofilm formation, and disperse established biofilms [15]. Essential oil, α -bisabolol, has been found to strongly hamper biofilm formation of *Staphylococcus aureus* methicillin-resistant (MRSA) and *P. aeruginosa* [16].

Table 4.1 Bioactivity of 15 confirmed compounds

Compound	Trivial Name	Bioactivity	References
1	Atropine sulfate	Anti-influenza Antibacterial	[7]
2	Piperaquine tetraphosphate tetra hydrate	Anti-malarial	[17-19]
3	Psammaphysin analogue	Antiviral, antimalaria, anti-cancer	[20-22]
4	Indole analogue	Antibacterial, antifungal, anti-inflammatory, antihypertensive, antiproliferative	[23,24]
5	Mefloquine	Antimalarial	[25]
6	Phosphonoacetic acid (PAA) analogue	Antiviral	[26]
7	EBC analogue	Anticancer	[27]
8	Bisabolol	Antibacterial, anti-inflammatory	[28]
9	EBC analogue	Anticancer	[29]
10	Proguanil HCl	Antimalarial	[30]
11	Thiaplakortone A analogue	Antimalarial	[31]
12	Thiaplakortone A analogue		
13	Thiaplakortone A analogue		
14	Thiaplakortone A analogue		
15	Papaverine HCl	Vasodilator, antidepressant, anti-tumor	[8,32,33]

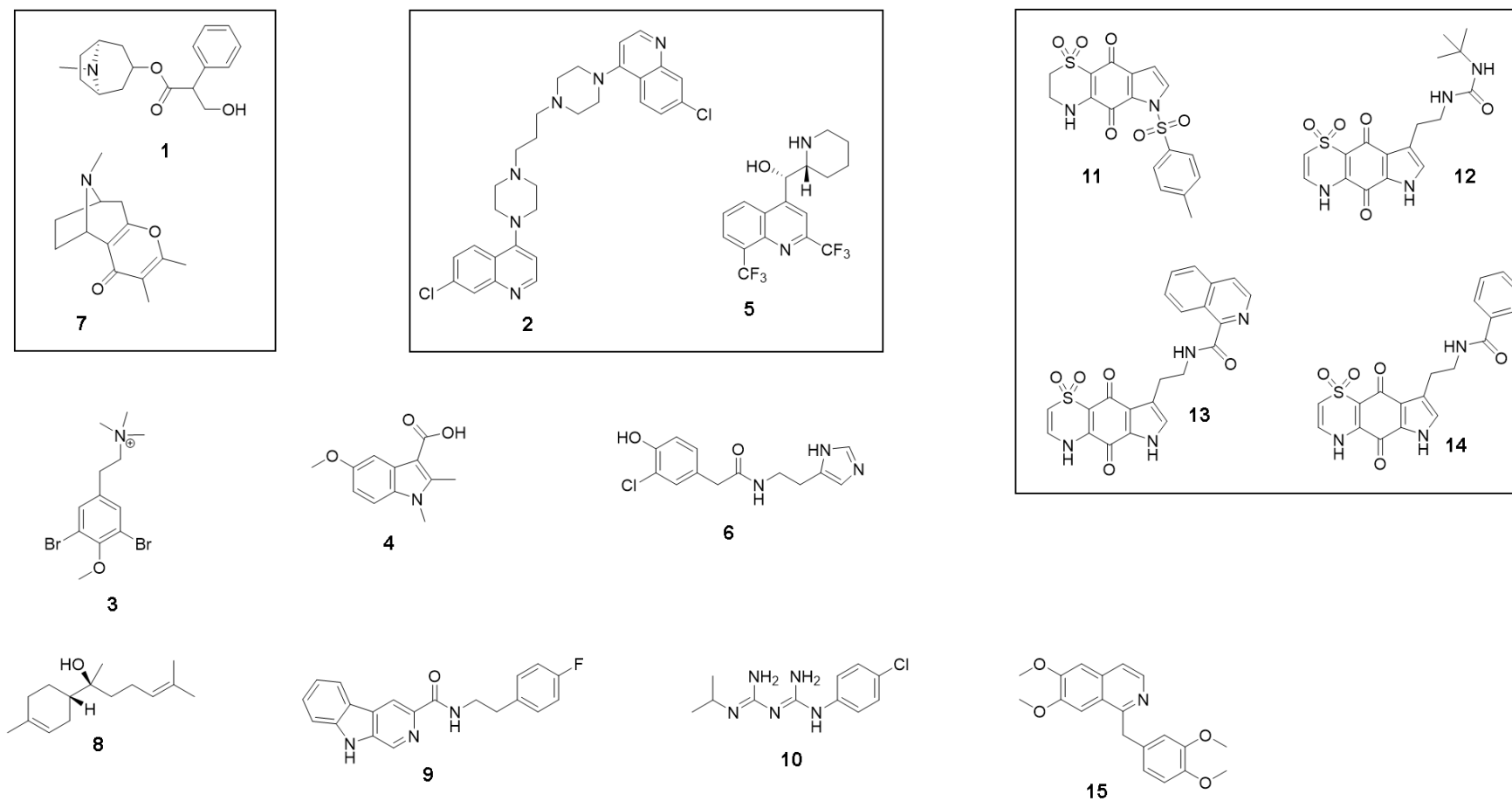


Figure 4.4 Chemical structures of 15 confirmed hit compounds. Compounds with similar structures are grouped and represented in boxes.

4.4 Conclusion

Drug repurposing offers various advantages such as lower initial investment, sufficient safety data for human uses, and reduced development timeframe. In the present work, we explored the side activities of known compounds and their analogues. We identified 15 antibiofilm compounds that can interfere with established biofilms of *P. aeruginosa* without adversely affecting the planktonic growth, indicating that they have diverse functions and interact with unintended targets. The preliminary data suggested that these compounds may be promising drug leads for the future development of anti-*P. aeruginosa* treatments.

Following the identification of the 15 hit compounds from the Davis Open Access Natural Product-based Library, chemical clustering analysis was undertaken, and three distinct clusters were identified, which included compounds **1** and **7** (tropane cluster), compounds **2** and **5** (quinoline cluster) and compounds **11-14** (thiazine-benzoquinone cluster); the remaining bioactive compounds were all singleton hits. The current data support further testing of analogs associated with any of the seven singleton hits or hit clusters in order to better delineate and understand structure-activity relationships (SAR). Preliminary data analysis of the three chemical clusters indicates the bicyclic tropane, quinoline and the thiazine-fused benzoquinone scaffolds are required for activity but with variations of these core scaffolds tolerated. It is interesting to note that three commercial antimalarial drugs (piperaquine (**2**), mefloquine (**5**) and proguanil (**10**) are all hits compounds in biofilm dispersal assay, suggesting other antiplasmodial drugs should be tested in the future with the possibility of drug repurposing feasible [24,28,33]. Furthermore, cluster 3 (compounds **11-14**) consists of semi-synthetic analogs of the marine natural product, thiaplakortone A, which was first isolated from the Great Barrier Reef marine sponge *Plakortis lita* in 2013 [34] and was shown to display in vitro IC₅₀ values of 6.6 nM and 51 nM against 3D7 and Dd2 *Plasmodium falciparum* strains, respectively [34]. These data indicate more research needs to be undertaken on the 15 hits and especially the three clusters identified to date in order to obtain more concise SAR data. These additional

studies are beyond the scope of the current thesis; however, they may be pursued by the research team in the future.

4.5 References

1. Ciofu, O.; Tolker-Nielsen, T. Tolerance and Resistance of *Pseudomonas aeruginosa* Biofilms to Antimicrobial Agents—How *P. aeruginosa* Can Escape Antibiotics. *Frontiers in Microbiology* **2019**, *10*.
2. Jamal, M.; Ahmad, W.; Andleeb, S.; Jalil, F.; Imran, M.; Nawaz, M.A.; Hussain, T.; Ali, M.; Rafiq, M.; Kamil, M.A. Bacterial biofilm and associated infections. *Journal of the Chinese Medical Association* **2018**, *81*, 7-11, doi:<https://doi.org/10.1016/j.jcma.2017.07.012>.
3. Wermuth, C.G. Selective optimization of side activities: the SOSA approach. *Drug Discovery Today* **2006**, *11*, 160-164, doi:[https://doi.org/10.1016/S1359-6446\(05\)03686-X](https://doi.org/10.1016/S1359-6446(05)03686-X).
4. Ribeiro, D.; Keller, K.M.; Soto-Blanco, B. Ptaquiloside and Pterosin B Levels in Mature Green Fronds and Sprouts of *Pteridium arachnoideum*. *Toxins (Basel)* **2020**, *12*, doi:10.3390/toxins12050288.
5. Shaala, L.A.; Youssef, D.T.A. Cytotoxic Psammaphysin Analogues from the Verongid Red Sea Sponge *Aplysinella* Species. *Biomolecules* **2019**, *9*, doi:10.3390/biom9120841.
6. Gaillard, T.; Madamet, M.; Tsombeng, F.F.; Dormoi, J.; Pradines, B. Antibiotics in malaria therapy: which antibiotics except tetracyclines and macrolides may be used against malaria? *Malaria Journal* **2016**, *15*, 556, doi:10.1186/s12936-016-1613-y.
7. Ozcelik, B.; Kartal, M.; Orhan, I. Cytotoxicity, antiviral and antimicrobial activities of alkaloids, flavonoids, and phenolic acids. *Pharm Biol* **2011**, *49*, 396-402, doi:10.3109/13880209.2010.519390.
8. Aggarwal, M.; Leser, G.P.; Lamb, R.A. Repurposing Papaverine as an Antiviral Agent against Influenza Viruses and Paramyxoviruses. *J Virol* **2020**, *94*, e01888-01819, doi:10.1128/JVI.01888-19.

9. Kaplan, J.B. Biofilm dispersal: mechanisms, clinical implications, and potential therapeutic uses. *J Dent Res* **2010**, 89, 205-218, doi:10.1177/0022034509359403.
10. Alipour, M.; Suntres, Z.E.; Omri, A. Importance of DNase and alginate lyase for enhancing free and liposome encapsulated aminoglycoside activity against *Pseudomonas aeruginosa*. *J Antimicrob Chemother* **2009**, 64, 317-325, doi:10.1093/jac/dkp165.
11. Barraud, N.; Hassett, D.J.; Hwang, S.-H.; Rice, S.A.; Kjelleberg, S.; Webb, J.S. Involvement of nitric oxide in biofilm dispersal of *Pseudomonas aeruginosa*. *J Bacteriol* **2006**, 188, 7344-7353, doi:10.1128/JB.00779-06.
12. Lewis, K. Persister cells, dormancy and infectious disease. *Nat Rev Microbiol* **2007**, 5, 48-56, doi:10.1038/nrmicro1557.
13. Lewis, K. Persister cells. *Annu Rev Microbiol* **2010**, 64, 357-372, doi:10.1146/annurev.micro.112408.134306.
14. Oluwabusola, E.T.; Katermeran, N.P.; Poh, W.H.; Goh, T.M.B.; Tan, L.T.; Diyaolu, O.; Tabudravu, J.; Ebel, R.; Rice, S.A.; Jaspars, M. Inhibition of the Quorum Sensing System, Elastase Production and Biofilm Formation in *Pseudomonas aeruginosa* by Psammaphin A and Bisaprasin. *Molecules* **2022**, 27, 1721, doi:10.3390/molecules27051721.
15. Zhang, X.; Zhao, Y.; Feng, L.; Xu, M.; Ge, Y.; Wang, L.; Zhang, Y.; Cao, J.; Sun, Y.; Wu, Q., et al. Combined With Mefloquine, Resurrect Colistin Active in Colistin-Resistant *Pseudomonas aeruginosa* in vitro and in vivo. *Frontiers in microbiology* **2021**, 12, 790220-790220, doi:10.3389/fmicb.2021.790220.
16. Farias, K.S.; Kato, N.N.; Boaretto, A.G.; Weber, J.I.; Brust, F.R.; Alves, F.M.; Tasca, T.; Macedo, A.J.; Silva, D.B.; Carollo, C.A. Nectandra as a renewable source for (+)- α -bisabolol, an antibiofilm and anti-*Trichomonas vaginalis* compound. *Fitoterapia* **2019**, 136, 104179, doi:<https://doi.org/10.1016/j.fitote.2019.104179>.
17. Sacchi, P.; Loconte, L.; Macetti, G.; Rizzato, S.; Lo Presti, L. Correlations of Crystal Structure and Solubility in Organic Salts: The Case of the Antiplasmodial Drug Piperaquine. *Crystal Growth & Design* **2019**, 19, 1399-1410, doi:10.1021/acs.cgd.8b01794.

18. Leong, F.J.; Jain, J.P.; Feng, Y.; Goswami, B.; Stein, D.S. A phase 1 evaluation of the pharmacokinetic/pharmacodynamic interaction of the anti-malarial agents KAF156 and piperaquine. *Malaria Journal* **2018**, *17*, 7, doi:10.1186/s12936-017-2162-8.
19. Davis, T.M.E.; Hung, T.-Y.; Sim, I.-K.; Karunajeewa, H.A.; Ilett, K.F. Piperaquine. *Drugs* **2005**, *65*, 75-87, doi:10.2165/00003495-200565010-00004.
20. Ramsey, D.M.; Amirul Islam, M.; Turnbull, L.; Davis, R.A.; Whitchurch, C.B.; McAlpine, S.R. Psammaphysin F: A unique inhibitor of bacterial chromosomal partitioning. *Bioorganic & Medicinal Chemistry Letters* **2013**, *23*, 4862-4866, doi:<https://doi.org/10.1016/j.bmcl.2013.06.082>.
21. Kumar, R.; Bidgood, C.L.; Levrier, C.; Gunter, J.H.; Nelson, C.C.; Sadowski, M.C.; Davis, R.A. Synthesis of a Unique Psammaphysin F Library and Functional Evaluation in Prostate Cancer Cells by Multiparametric Quantitative Single Cell Imaging. *Journal of Natural Products* **2020**, *83*, 2357-2366, doi:10.1021/acs.jnatprod.0c00121.
22. Shaala, L.A.; Youssef, D.T.A. Cytotoxic Psammaphysin Analogues from the Verongid Red Sea Sponge Aplysinella Species. *Biomolecules* **2019**, *9*, 841, doi:10.3390/biom9120841.
23. Tan, C.; Yang, S.-J.; Zhao, D.-H.; Li, J.; Yin, L.-Q. Antihypertensive activity of indole and indazole analogues: A review. *Arabian Journal of Chemistry* **2022**, *15*, 103756, doi:<https://doi.org/10.1016/j.arabjc.2022.103756>.
24. Tunbridge, G.A.; Oram, J.; Caggiano, L. Design, synthesis and antiproliferative activity of indole analogues of indanocine. *MedChemComm* **2013**, *4*, 1452-1456, doi:10.1039/C3MD00200D.
25. Croft, A.M.; Herxheimer, A. Adverse effects of the antimalaria drug, mefloquine: due to primary liver damage with secondary thyroid involvement? *BMC Public Health* **2002**, *2*, 6, doi:10.1186/1471-2458-2-6.
26. Coen, D.M.; Lawler, J.L.; Abraham, J. Chapter Four - Herpesvirus DNA polymerase: Structures, functions, and mechanisms. In *The Enzymes*, Cameron, C.E., Arnold, J.J., Kaguni, L.S., Eds. Academic Press: 2021; Vol. 50, pp. 133-178.

27. Cullen, J.K.; Boyle, G.M.; Yap, P.-Y.; Elmlinger, S.; Simmons, J.L.; Broit, N.; Johns, J.; Ferguson, B.; Maslovskaya, L.A.; Savchenko, A.I., et al. Activation of PKC supports the anticancer activity of tigilanol tiglate and related epoxytiglanes. *Scientific Reports* **2021**, *11*, 207, doi:10.1038/s41598-020-80397-9.
28. Kamatou, G.P.P.; Viljoen, A.M. A Review of the Application and Pharmacological Properties of α -Bisabolol and α -Bisabolol-Rich Oils. *Journal of the American Oil Chemists' Society* **2010**, *87*, 1-7, doi:<https://doi.org/10.1007/s11746-009-1483-3>.
29. Boyle, G.M.; D'Souza, M.M.A.; Pierce, C.J.; Adams, R.A.; Cantor, A.S.; Johns, J.P.; Maslovskaya, L.; Gordon, V.A.; Reddell, P.W.; Parsons, P.G. Intra-lesional injection of the novel PKC activator EBC-46 rapidly ablates tumors in mouse models. *PLoS One* **2014**, *9*, e108887-e108887, doi:10.1371/journal.pone.0108887.
30. Scholar, E. Proguanil. In *xPharm: The Comprehensive Pharmacology Reference*, Enna, S.J., Bylund, D.B., Eds. Elsevier: New York, 2007; <https://doi.org/10.1016/B978-008055232-3.62471-7>pp. 1-4.
31. Pouwer, R.H.; Deydier, S.M.; Le, P.V.; Schwartz, B.D.; Franken, N.C.; Davis, R.A.; Coster, M.J.; Charman, S.A.; Edstein, M.D.; Skinner-Adams, T.S., et al. Total Synthesis of Thiaplakortone A: Derivatives as Metabolically Stable Leads for the Treatment of Malaria. *ACS Medicinal Chemistry Letters* **2014**, *5*, 178-182, doi:10.1021/ml400447v.
32. Benej, M.; Hong, X.; Vibhute, S.; Scott, S.; Wu, J.; Graves, E.; Le, Q.-T.; Koong Albert, C.; Giaccia Amato, J.; Yu, B., et al. Papaverine and its derivatives radiosensitize solid tumors by inhibiting mitochondrial metabolism. *Proceedings of the National Academy of Sciences* **2018**, *115*, 10756-10761, doi:10.1073/pnas.1808945115.
33. Gaber, A.; Alsanie, W.F.; Kumar, D.N.; Refat, M.S.; Saied, E.M. Novel Papaverine Metal Complexes with Potential Anticancer Activities. *Molecules* **2020**, *25*, doi:10.3390/molecules25225447.
34. Davis, R.A.; Duffy, S.; Fletcher, S.; Avery, V.M.; Quinn, R.J. Thiaplakortones A–D: Antimalarial Thiazine Alkaloids from the Australian Marine Sponge Plakortis lita. *The Journal of Organic Chemistry* **2013**, *78*, 9608-9613, doi:10.1021/jo400988y.

CHAPTER 5: Bromotyrosine-derived metabolites from a marine sponge inhibit *Pseudomonas aeruginosa* biofilms

Statement of Contribution to Co-authored Published Paper

This chapter is an unpublished research article (currently under review). The bibliographical details are:

Tam Thi Minh Tran, Russell S. Addison, Rohan A. Davis, Bernd H.A. Rehm

Appropriate acknowledgements of those who contributed to the research but did not qualify as authors are included in each paper.

My contribution to the published paper involved:

- Conception and design
- Manuscript preparation

Signed: **Minh Tam Tran Thi**

PhD Candidate

Date: 10th April, 2022

Countersigned: **Bernd Rehm**

Principal Supervisor

Date: 10th April, 2022

5.1 Abstract

Pseudomonas aeruginosa (*P. aeruginosa*) forms stable biofilms providing a major barrier for multiple classes of antibiotics severely impairing treatments of infected patients. The biofilm matrix of this Gram-negative bacterium is primarily composed of three major exopolysaccharides: alginate, Psl and Pel. Here, we studied the antibiofilm properties of sponge-derived natural products ianthelliformisamines A–C and their combinations with clinically used antibiotics. Wild-type *P. aeruginosa* strain and its isogenic exopolysaccharide deficient mutants were employed to determine the interference of the compounds with biofilm matrix components. We identified that ianthelliformisamines A and B worked synergistically with ciprofloxacin to kill planktonic and biofilm cells. Ianthelliformisamines A and B reduced the minimum inhibitory concentration (MIC) of ciprofloxacin to 1/3 and 1/4 MICs. In contrast, ianthelliformisamine C (MIC = 53.1 µg/mL) alone exhibited bactericidal effects dose-dependently on both free-living and biofilm populations of wild-type PAO1, PAO1Δ*pslA* (Psl deficient), PDO300 (alginate overproducing and mimicking clinical isolates) and PDO300Δ*alg8* (alginate deficient). Interestingly, the biofilm of the clinically relevant mucoid variant PDO300 was more susceptible to ianthelliformisamine C than strains with impaired polysaccharide synthesis. Ianthelliformisamines exhibited low cytotoxicity towards HEK293 cells in the resazurin viability assay. Mechanism of action studies showed that ianthelliformisamine C inhibited the efflux pump of *P. aeruginosa*. Metabolic stability analyses indicated that ianthelliformisamine C is stable and ianthelliformisamines A and B are rapidly degraded. Overall, these findings suggest the ianthelliformisamine chemotype could be a promising candidate for the treatment of *P. aeruginosa* biofilms.

5.2 Introduction

P. aeruginosa is an opportunistic Gram-negative bacterium that causes various severe infections in hospitalized patients, hosts with impaired immune systems caused by human immunodeficiency virus (HIV) and cancer, and individuals with cystic fibrosis (CF). This

bacterium possesses a range of virulence factors and adaptation mechanisms such as the ability to form biofilms, which have enabled resistance to multiple classes of antibiotics leading to the treatment of infected patients being ineffective [1,2]. Indeed, bacteria in the biofilm can resist antimicrobials up to 1000 times [3]. Evidently, highly structural biofilms are often identified in people with chronic infections (e.g. lung, wound, and rhinosinusitis) [4]. Therefore, much effort has been made towards the development of antibiofilm agents targeting these components and/or combination therapies with existing antibiotics to disarm and eventually eradicate this Gram-negative bacterium.

Polysaccharides, extracellular DNA (eDNA), proteins and lipids are the typical components of the *P. aeruginosa* biofilm matrix. The three exopolysaccharides (Psl, Pel and alginate) were found to play critical roles in surface attachment, the formation and the development of biofilms [5]. Psl, a neutral pentasaccharide composed of L-rhamnose, D-glucose and D-mannose, is essential for cell attachment during the initial stage of biofilm formation [6-8]. Pel is a cationic polymer rich in N-acetyl-D-glucosamine and N-acetyl-D-galactosamine. It is necessary for surface adhesion, biofilm integrity and the formation of pellicle biofilm at the air-liquid interface [9,10]. Alginate is an anionic acetylated polysaccharide polymer made of mannuronic acid and guluronic acid residues. Unlike Psl and Pel, alginate substantially produced by the mucoid *P. aeruginosa*, typically isolated from the lung of CF patients, is a hallmark of chronic infections. This polysaccharide is involved in biofilm maturation and confers tolerance to antimicrobial treatments [11,12].

Natural products have been invaluable sources of medicinal agents for millennia. Indeed, their uses have been documented throughout history for the treatment of ailments including inflammation [13], cancer, cardiovascular [14], neurological [15], and infectious diseases [16,17]. Many molecules from plants, marine organisms and microorganisms have been shown to possess antibiofilm attributes such as organosulfur (garlic extracts) [18,19], brominated furanones and their analogs (Red alga *Delisea pulchra*) [20,21], and promysalin (*Pseudomonas putida* RW10S1) [22,23]. Previously, ianthelliformisamines A–C isolated from the marine sponge *Suberea ianthelliformis* and several synthetic analogs were shown

to have antibacterial activity against *P. aeruginosa* and enhance the efficacy of doxycycline and chloramphenicol [24,25]. The anti-biofilm properties of ianthelliformisamines have not been investigated. In the present study, we investigated the effect of these compounds against *P. aeruginosa* biofilms. The synergistic interactions between ianthelliformisamines and clinically used antibiotics were determined. Furthermore, the interference of these molecules with different components of the biofilm matrix and the mode of action was studied. We further assessed the metabolic stability and cytotoxicity of ianthelliformisamines to evaluate their utility for treatment of *P. aeruginosa* infections.

5.3 Materials and methods

5.3.1 Bacterial strains, chemicals, and media

Wild-type *P. aeruginosa* strains PAO1 (prototrophic wild-type) [26] and different isogenic mutant strains including PAO1 Δ *pslA* (*ΔpslA*, Psl deletion mutant), PAO1 Δ *pelF* (*ΔpelF*, Pel deletion mutant) [27], PDO300 (mucoid, *ΔmucA22*, alginate-overproducing mutant) [28], and PDO300 Δ *alg8* (*Δalg8*, alginate deletion mutant) [29] were used in this study. Bacterial strains were grown in Luria-Bertani (LB) medium (10 g/L tryptone, 10 g/L sodium chloride and 5 g/L yeast extract) at 37°C. Ciprofloxacin hydrochloride hydrate was purchased from Alfa Aesar. Meropenem trihydrate, resazurin, polymyxin B and *N*-phenyl-naphthylamine (NPN) were obtained from Aldrich-Sigma.

Ianthelliformisamines A–C (**1–3**) were obtained from the Davis Open Access Natural Product-based Library. The details of the marine sponge material source and the extraction and isolation processes used to purify and identify these marine natural products are described elsewhere [24]. Structures, formulas and molecular weights for compounds **1–3** are shown in **Supplementary Table 1**.

The Davis Open Access Natural Product-based Library currently consists of 512 distinct compounds, the majority (53%) of which are natural products that have been obtained from Australian natural sources (<https://www.griffith.edu.au/institute-drug->

discovery/unique-resources/naturebank), such as endophytic fungi [30], plants [31], macrofungi [32], and marine invertebrates [33]. Approximately 28% of this library contains semi-synthetic natural product analogues [34], while a smaller percentage (19%) are known commercial drugs or synthetic compounds inspired by natural products. The Davis Open Access Library is housed within Compounds Australia (www.compoundsaustralia.com) as 5 mM DMSO solutions. Library compounds were either isolated in quantities ranging from 0.2 mg to >50 mg or purchased from commercial suppliers. The natural product isolation procedures or semi-synthetic studies for the majority of compounds in this unique library have been previously published [30-33]. All compounds were >95% pure when submitted for storage within Compounds Australia.

5.3.2 Determination of minimum inhibitory concentration (MIC)

The minimum inhibitory concentration (MIC) of compounds and antibiotics were performed as previously described, with minor modification [35]. The overnight cultures of *P. aeruginosa* PAO1 at 37°C and 200 rpm in LB medium were washed once with sterile saline 0.9 % (w/v) and adjusted to an OD₆₀₀ of 0.05, and 1% inoculum was transferred into fresh LB medium. After incubation at 37°C and 200 rpm for 6 h to reach the mid-log phase, the cells were washed once with sterile saline 0.9 % (w/v) and diluted to an OD₆₀₀ of 0.0004 (v/v). Three antibiotics including tobramycin (10 mg/mL), ciprofloxacin (10 mg/mL) and meropenem (3 mg/mL) were dissolved in water and filter-sterilized. Ten microliters of two-fold serially diluted antibiotics were transferred to 96 well Costar plate (Corning) followed by the addition of 90 µL of diluted cultures. After an 18 h incubation at 37°C in the static condition, optical density OD₆₀₀ was monitored using a Synergy 2 microplate reader (BioTek). The growth control (90 µL of diluted cells and 10 µL of sterile water) and the sterility control/background value (90 µL of LB medium and 10 µL of sterile water) were included in each plate. The MIC was determined as the lowest concentrations of antibiotics that inhibit complete bacterial growth compared to growth control.

5.3.3 Checkerboard assay

The synergistic activity of compounds with antibiotics including tobramycin, ciprofloxacin and meropenem (1/4 – 1/16 MICs) was investigated by a checkerboard dilution assay [39,40]. Briefly, mid-log cultures of *P. aeruginosa* were diluted 1:1250 before adding to the plates. Next, 90 μ L aliquots of diluted cells were added to a 96 well Costar (Corning) plate containing either 10 μ L of compounds and/or 10 μ L of antibiotics. Compounds and antibiotics were tested at 11 and 7 concentrations, respectively. The first row contained antibiotics alone while the first column contained compounds alone and the remaining columns were for combinations. Since the compounds did not exhibit significant bactericidal activity apart from compound **3**, the recorded data were not analyzed using the FIC (fractional inhibitory concentration) index. The combinations were considered synergistic if the compounds decreased 3-4 fold in the MIC of antibiotics at which visible growth of bacteria was not observed.

5.3.4 Biofilm inhibition assay

The overnight cultures at 37°C in LB medium were washed once with sterile saline 0.9 % (w/v) and adjusted to an OD₆₀₀ of 0.05, and 1% inoculum was transferred into fresh LB medium. Following the incubation at 37°C, 200 rpm for 6-6.5 h to reach the mid-log phase, the cells were washed once with sterile saline 0.9 % (w/v) and diluted to an OD₆₀₀ of 0.01. 45 μ L aliquots were dispensed into 384-well plates (Greiner Bio-One, catalog no. 781091). In biofilm inhibition assays, test compounds (5 μ L) were loaded prior to the addition of bacteria. The plates were incubated for 24 h at 37°C in static conditions. The effects of compounds on bacterial growth and viability of biofilm bacteria were determined by the OD₆₀₀ and resazurin metabolic assay, respectively. The final concentrations of DMSO in the assays were 1% - 2% (v/v). The negative controls or untreated cultures consisted of inoculum and different concentrations of DMSO. Antibiotic ciprofloxacin (0.25 μ g/mL and 25 μ g/mL) was used as positive controls. The initial OD₆₀₀ and final OD₆₀₀ were read before incubation at 37°C and after 24 h incubation, respectively, followed by assessment

of biofilm viability by resazurin metabolic assay. The experiments were carried out with three technical replicates and repeated at least twice. The growth inhibition calculated as a function of the percentage of the total bacterial inhibition using equation (1) where A_B is the OD_{600} of LB medium, and A_{T0} and A_{Tf} are the OD_{600} recorded at inoculating time and at the end of the assay.

$$\% \text{ Inhibition} = 100 \times \left[1 - \frac{OD_{600} (A_{\text{sample } Tf} - A_{\text{sample } T0}) - (A_B Tf - A_B T0)}{OD_{600} (A_{\text{negative control } Tf} - A_{\text{negative control } T0}) - (A_B Tf - A_B T0)} \right] \quad (1)$$

Resazurin (RSZ) is a non-toxic and non-fluorescent blue compound that is irreversibly reduced by living cells through electron transfer reactions to highly fluorescent resorufin derivatives. RSZ has been extensively used to assess antibacterial and anti-parasite activities and as an indicator for cell viability [36,37].

Resazurin sodium salt (Sigma-Aldrich) was dissolved in Milli-Q water at 0.2 % (w/v) and filter-sterilized. The solution was stored at -20°C in the dark. The assay was performed as previously described with modification [38]. The cultures were withdrawn, and the plates were washed three times with sterile water using the plate washer (BioTek). To remove the remaining water in the wells, the plates were tapped with autoclaved paper towels. 50 μ L of diluted RSZ solution in LB medium was added into each well followed by incubation at 37°C for 5-6 h. A microplate reader (BioTek Synergy 2) was used to measure the fluorescence intensity (excitation 530 nm, emission 590 nm). Data collected was determined as a function of fluorescence percentage using equation (2) where F_B is the fluorescence of the diluted RSZ solution in LB medium in the absence of *P. aeruginosa* cells.

$$\% \text{ Inhibition} = \left[\frac{(F_{\text{negative control}} - F_B) - (F_{\text{sample}} - F_B)}{(F_{\text{negative control}} - F_B)} \right] \times 100 \quad (2)$$

5.3.5 Ethidium bromide efflux assay

To investigate the efflux pump inhibiting activity of test compounds on wild-type PAO1, an efflux assay using ethidium bromide (EtBr) as substrate was performed as previously described [41]. An overnight culture of PAO1 in LB broth was incubated in a shaker at 37°C until it reached an OD₆₀₀ of 0.5. The bacterial cells were washed with phosphate buffered saline (PBS), centrifuged and the pellet was resuspended in PBS. Test compounds, 5 µL, were added to the flat-bottomed, black 96-well-plate followed by addition of 90 µL of the bacterial suspension. EtBr at a non-toxic concentration (5 µL, 2 µg/mL) was added before the plates were read. The fluorescence reading was recorded at an excitation of 530 nm and emission of 590 nm every min for 60 min using a BioTek Synergy H1 Hybrid microplate reader. Carbonyl cyanide m-chlorophenyl hydrazone (CCCP), a chemical inhibitor of efflux pumps, was used as positive control and DMSO (1%-2%) was used as vehicle control as compounds were dissolved in DMSO. Untreated cells were used as negative control.

5.3.6 NPN uptake assay

The permeability of the outer membrane upon exposure to test compounds was assessed using a 1-*N*-phenyl-naphthylamine (NPN) uptake assay [42,43]. An overnight culture of PAO1 was grown to an OD₆₀₀ of 0.5, centrifuged, washed with HEPES buffer (5mM, pH 7.2) and re-suspended in HEPES buffer containing 100 µM CCCP. The mixture was then incubated in the dark at room temperature for 15 min to inactivate efflux pumps, followed by washing with HEPES buffer. The pellet was resuspended in assay buffer (5mM HEPES, 5mM glucose, pH 7.2) supplemented with 10 µM NPN. Ninety microliters of the cell suspension were added to the flat-bottomed, black 96-well-plate containing 10 µL of test compounds and the NPN fluorescence was immediately monitored using a BioTek Synergy H1 Hybrid microplate reader at an excitation of 350 nm and emission of 420 nm every min for 30 min. Polymyxin B at 6.4 µg/mL and 10 µg/mL was used as

positive control and DMSO (1%-2%) was used as vehicle control as compounds were dissolved in DMSO. Untreated cells were used as the negative control.

5.3.7 Cellular bioluminescent assay

The reporter strain MDM-623 was kindly provided by Dr. Timothy Opperman (Microbiotix, Inc., MA, US). The strain harbors promoter region from *PA0614* fused to *Photorhabdus luminescens* luciferase *luxCDABE* operon which was constructed to respond to DNA damage. All experiments were carried out as previously described with minor modification [44]. The bacteria were grown overnight in LB medium containing 1mM IPTG, 20 µg/mL gentamicin and 12.5 µg/mL tetracycline. Next, overnight cultures were inoculated in LB medium containing 1mM IPTG, 20 µg/mL gentamicin and 12.5 µg/mL tetracycline and grown in a shaker until they reached an OD₆₀₀ of 0.5. The bacteria were centrifuged, washed with 0.9% (w/v) saline and then 90 µL of the washed cells were transferred into 96-well-plates containing 10 µL of test compounds. Luminescence was monitored using a BioTek Synergy H1 Hybrid microplate reader for 8 h at 30 min intervals. Ciprofloxacin at different concentrations (0.0625 µg/mL, 0.083 µg/mL, 0.25 µg/mL and 25 µg/mL) was used as a positive control and DMSO was also included as the negative control.

5.3.8 Cytotoxicity assay

Cytotoxicity of the test compounds was assessed on human embryonic kidney (HEK293) cells as previously described [45]. Cells were grown and diluted in Dulbecco's Modified Eagle Medium: Nutrient Mixture F-12 (DMEM: Ham F12) medium (Gibco – Life Technologies, Australia) supplemented with 10% FBS. Test compounds (10 µL) were added into 384-well-plates prior to the transfer of 55 µL of cells at a concentration of 3.2×10^5 cells/mL. The plates were incubated for 24h at 37°C followed by the addition of 10 µL of resazurin at a final concentration of 70 µM and further incubation for 5h at 37°C. The

resazurin fluorescence was read at an excitation of 530 nm and an emission of 595 nm in the BioTek Synergy H1 Hybrid microplate reader.

5.3.9 Fluorescence microscopy

For biofilm bacteria imaging, bacteria were cultured, treated with test compounds, and washed as previously mentioned in the biofilm inhibition assay. The biofilm bacteria were stained using a LIVE/DEAD BacLight bacterial viability kit (Molecular Probes, Inc., Eugene, OR) which consists of SYTO9 (green; staining cells with intact membrane) and propidium iodide (red; staining cells with compromised membrane) [27]. Images were captured using a high-content imaging system Operetta CLS (Perkin Elmer) with a 60× water-immersion objective.

5.3.10 Stability of ianthelliformisamines A–C (1–3) in mouse and human liver microsomes

5.3.10.1 *In vitro* incubation

Microsomes were obtained commercially: (1) mouse microsomes (male CD-1, 100 donor pool; Gibco Lot # MS042-C); (2) human microsomes (mixed-sex, 50 donor pool; Gibco Lot # PL050E-C). The metabolic assays were performed based on a previously described method [46]. Briefly, each tube (12 x 75 mm glass) contained potassium phosphate buffer (0.1 M, pH 7.4, containing glucose-6-phosphate dehydrogenase (G-6-P-DH; 1 IU/mL), microsomes (0.5 mg/mL) and test compound (**1**, **2** or **3**) or positive control (verapamil [VPL]), 1.0 µM. Reactions were initiated by the addition of 25 µL of a 20x stock of an NADPH regeneration system (NRS) containing NADP, glucose-6-phosphate (G-6-P) and MgCl₂, to provide final concentrations of 1.3 mM, 3.5 mM and 3.3 mM, respectively. Total incubation volume was 0.5 mL. Metabolic stability of **1**, **2** or **3** was determined in triplicate in an oscillating waterbath (Grant) at 37°C and 100 RPM. Positive control (verapamil, 1.0 µM) and negative control (**1**, **2** or **3** without NRS) incubations were

conducted concurrently in singlicate. Stock solutions of the test compounds (5.0 or 10.0 mM) were prepared in DMSO and spiking solutions of these, as well as verapamil, were prepared in acetonitrile at 100 μ M. Final organic (ACN) concentration in the incubation tubes was 1 %. Tubes containing buffer, microsomes and test (or control) compound (5 mM) were preincubated at 37°C for 5 min prior to the reaction being initiated by the addition of NRS. The negative control was initiated by the addition of the test compound. Samples (50 μ L) were removed at $t = 0$ (immediately after reaction start), 5, 10, 20, 30 and 60 min. Samples were added to microcentrifuge tubes containing 150 μ L of ice-cold acetonitrile containing internal standard (clotrimazole; for **1** = 10.0 ng/mL + 0.5 % (v/v) formic acid; for **1** and **2** = 2.0 ng/mL + 0.5 % (v/v) formic acid; for VPL = 20.0 ng/mL + 0.1 % (v/v) formic acid). Tubes were centrifuged (13000 \times g, 5 min) and ~135 μ L of supernatant transferred to polypropylene 96-well plates for analysis

5.3.10.2 Analysis

Samples were analysed by HPLC-MS/MS (Waters 2795 solvent delivery system linked to a MicroMass Quatromicro tandem MS/MS). Chromatographic separation was achieved using a biphenyl column (Kinetix, 100 mm \times 4.6 mm \times 2.6 μ m; Phenomenex), coupled with a gradient elution with mobile phases containing acetonitrile / H₂O / 0.5 % formic acid. Analysis was conducted in positive ion multiple reaction monitoring mode (MRM) with argon as collision gas. Optimum MS/MS conditions were established prior to incubations by direct infusion of individual solutions of **1**, **2** and **3** into the LC-MS/MS. To ensure adequate sensitivity of analysis, multiple mass transitions were summed for all three test compounds. The mass transitions monitored for **1** were m/z 521.4 $>$ 447.5 + 521.4 $>$ 375.7 amu, for **2** = m/z 464.3 $>$ 375.7 + 464.3 $>$ 318.9 amu, for **3** = m/z 839.7 $>$ 447.3 + 839.7 $>$ 375.5 amu, while for VPL and CTZ, single transitions were monitored (VPL: m/z 455.3 $>$ 164.9; CTZ: m/z 277.1 $>$ 165.1 amu). Linearity of LC-MS/MS analysis of the three test compounds in buffer was confirmed over a suitable concentration range prior to incubations being undertaken.

5.3.10.3 Calculations

Peak area ratios (**1**, **2** or **3**, or VPL: clotrimazole [internal standard]) were determined for each timepoint for each tube and expressed as % remaining (normalized to t = 0 as 100 %). LN % remaining *versus* time data for each data set were fitted to an exponential decay function to determine the first-order rate constant (k) for substrate depletion. Where possible, the rate of depletion for each sample was used to calculate additional values, as shown in **Table 5.1**. For equations 5 – 7, scaling parameters used were described elsewhere [47].

Table 5. 1 Additional parameters were calculated using listed equations

Parameter	Units	Equation used
Half life	min	$t_{1/2} = \frac{\ln(2)}{k}$ (3)
$Cl_{int, in vitro}$	$\mu\text{L}/\text{min}/\text{mg}$ protein	$k \times V$ where V = incubation volume (μL) / microsomal protein (mg) (4)
Cl_{int}	$\text{mL}/\text{min}/\text{kg}$	$Cl_{int, in vitro} \times \frac{\text{liver mass (g)}}{\text{body weight (kg)}} \times \frac{\text{microsomal protein (mg)}}{\text{liver mass (g)}}$ (5)
Cl_{blood}	$\text{mL}/\text{min}/\text{kg}$	$\frac{Q \times Cl_{int}}{Q + Cl_{int}}$ where Q = hepatic blood flow ($\text{mL}/\text{min}/\text{kg}$ body weight) (6)
$E_H^{1,2}$	---	$\frac{Cl_{blood}}{Q} = \frac{Cl_{int}}{Q + Cl_{int}}$ (7)

¹ Hepatic extraction rate is based on microsomal degradation of each test compound *in vitro*, and assumes that NADPH-dependant oxidative metabolism is the dominant metabolic route. No allowance was made for other Phase 1 or Phase 2 metabolic pathways.

² Microsomal binding of **1**, **2**, or **3** was not determined. It was assumed that the fraction unbound (f_u) = 1.

5.3.10.4 Statistical analysis

All experiments were performed in triplicate. The data are the means and standard deviation of two independent experiments. In cytotoxicity assay, non-parametric one-way ANOVA followed by Dunnett's multiple comparison post-hoc test was performed to compare treatments with negative control (GraphPad Prism 8.0, GraphPad Software, Inc., San Diego, CA).

5.4 Results

5.4.1 Minimum inhibitory concentrations of ianthelliformisamines and antibiotics

Ianthelliformisamines A–C (defined as compounds **1–3**) were previously shown to exhibit anti-bacterial activity against planktonic *P. aeruginosa*. Minimum inhibitory concentrations (MICs) of clinically used antimicrobials and compounds **1–3** were assessed against planktonic *P. aeruginosa* PAO1. The results revealed that MIC of ciprofloxacin, tobramycin and meropenem against free-living PAO1 were 0.25 µg/mL, 2 µg/mL and 0.375 µg/mL, respectively. MIC of **3** was observed at 53.1 µg/mL. Compounds **1** and **2** showed no antimicrobial activity against *P. aeruginosa* PAO1 up to the highest concentrations applied in the present study.

5.4.2 Ianthelliformisamines A–C (**1–3**) synergistically interact with ciprofloxacin to inhibit biofilm formation

Initially, we investigated the antibiofilm activity of **1–3** (**Figure 5.1B**) against wild-type *P. aeruginosa* PAO1 using the biofilm inhibition assay (**Figure 5.1A**). **1** and **2** did not yield any antimicrobial activity and/or prevent biofilm formation (data not shown), whereas ianthelliformisamine C induced potent killing of free-living and biofilm bacteria (data shown in **Figure 5.1E–F**). The activity of these compounds against existing biofilms of *P. aeruginosa* was also examined. No killing and/or dispersing effects on pre-formed biofilms were detected (data not shown). Since these molecules were previously reported as

antibiotic enhancers against planktonic PAO1, we then carried out a checkerboard assay to evaluate the potency of these compounds in the presence of other antibiotics including ciprofloxacin, tobramycin and meropenem, which are used clinically either alone or in combination to treat *P. aeruginosa* infections. However, the current effectiveness of these agents is challenged by the rapid adaptation of the organism, due to an arsenal of virulence factors and biofilm architecture, resulting in an increasing prevalence of resistance in this Gram-negative bacterium. We reasoned that if the molecules could weaken the bacterial pathogenicity to some extent by attenuating virulence properties and impeding the capability of forming a biofilm, the antibiotics would be able to kill the bacteria at lower doses, thus alleviating the selection pressure-caused-tolerance. The checkerboard assay revealed **1** and **2** worked synergistically with ciprofloxacin at concentrations ranging from 5.39 µg/mL to 86.2 µg/mL for **1** and 34.55 µg/mL to 69.1 µg/mL for **2**, resulting in 4 - 16-fold MIC reduction against wild-type PAO1. Although **3**'s chemical structure is similar to compounds **1** and **2**, it exhibited limited synergy with ciprofloxacin (**Figure 5.1C**).

Chapter 5 - Bromotyrosine-derived metabolites from a marine sponge inhibit *Pseudomonas aeruginosa* biofilms

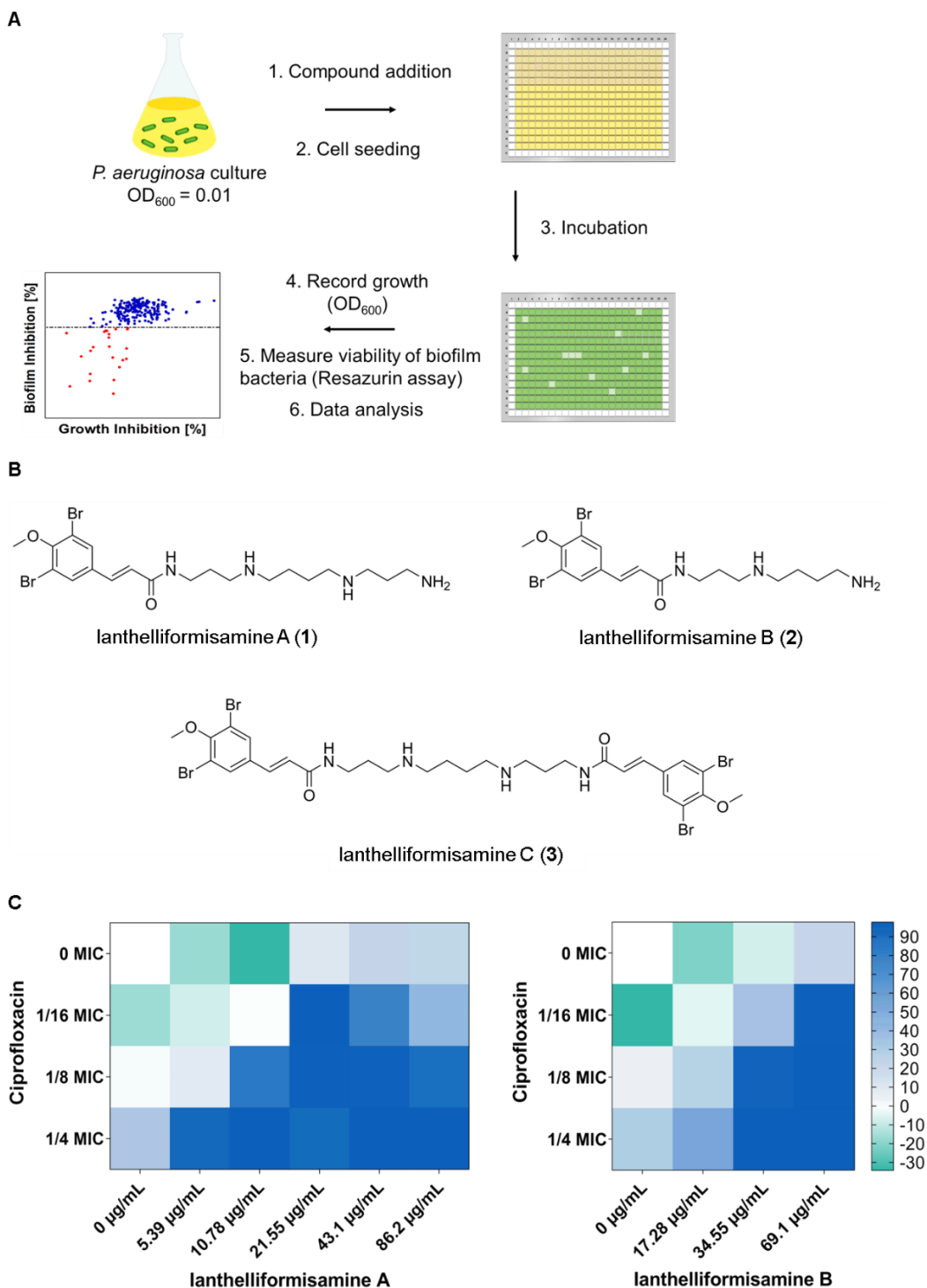


Figure 5.1 Biofilm assays to identify compounds that prevent biofilm formation. (A) Biofilm inhibition assay. *P. aeruginosa* cultures were seeded into 384-well plates after

dispensing compounds and antibiotic. The plates were incubated for 24 h at 37°C followed by recording bacterial growth (OD₆₀₀) and measuring the viability of biofilm bacteria using resazurin. (B) Chemical structures of compounds used in this study. (C) Ianthelliformisamine A and ianthelliformisamine B synergized with ciprofloxacin (CIP). Heat plots showing growth inhibition of planktonic PAO1 in the presence of compound and ciprofloxacin. Percent of growth inhibition is illustrated with different colors where green color represents growth stimulation and dark blue 100% inhibition.

In order to target *P. aeruginosa* biofilms, synergistic combinations of **1**+ ciprofloxacin and **2**+ ciprofloxacin were selected for biofilm inhibition assays against wild-type and different isogenic mutant strains of *P. aeruginosa*. Due to the intrinsic recalcitrance of biofilms to antibiotics, high concentrations of **1** and **2** in combination with 1/3 and 1/4 MIC of ciprofloxacin were selected. While these combinations showed no effects on established biofilms (data not shown), they displayed different degrees of biofilm formation inhibition. Compound **1** + ciprofloxacin at 86.2 µg/mL at 1/3 MIC (0.083 µg/mL), respectively, significantly disrupted growth and prevented biofilm formation of PAO1 and isogenic mutant strain PAO1Δ*pelF* (> 90%) as compared to ciprofloxacin or **1** alone (**Figure 5.2A**). In contrast, ciprofloxacin alone at 1/3 MIC moderately inhibited the bacterial growth and completely prevented biofilm formation of Psl-deficient strain PAO1Δ*pslA*. Therefore, the observed activity of the combination was attributed solely to the sublethal level of ciprofloxacin. Similar synergism between **1** and ciprofloxacin was observed for alginate-overproducing mutant PDO300 which was generated to mirror pathogenesis of clinical isolates from the lung of CF patients. The combination exhibited similar levels of effect on viability and biofilm of PDO300 at all tested concentrations. We expected the thick, but loosely attached biofilm of the mucoid strain PDO300 [47] would hinder the penetration of **1** and the alginate deficient biofilm of *alg8*-knockout mutant PDO300Δ*alg8* would ease the access of **1**. Unexpectedly, **1** acted alone on PDO300 growth at 43.1 µg/mL and 86.2 µg/mL (>70%) whereas only **1** at 86.2 µg/mL could reduce biofilm formation (~80%). Ciprofloxacin at 1/3 and 1/4 MICs only synergized with **1** at 43.1 µg/mL to improve their uptake into biofilms (from 20% to approximately 100%). This compound had minimal to

moderate activity against PDO300 Δ *alg8* biofilm bacteria (< 60%), albeit showing the significant killing of its planktonic counterparts, as indicated by the results of the biofilm assay (**Figure 5.2B**).

Chapter 5 - Bromotyrosine-derived metabolites from a marine sponge inhibit *Pseudomonas aeruginosa* biofilms

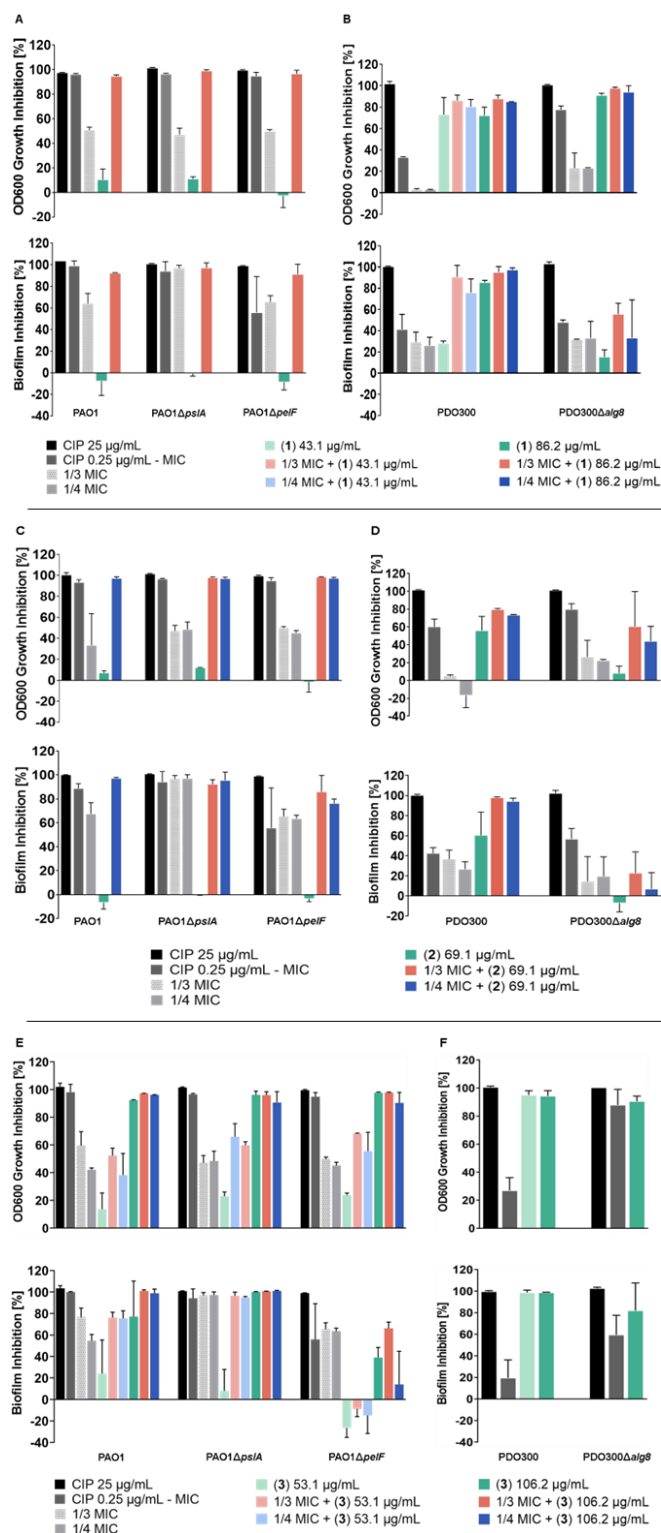


Figure 5.2 Ianthelliformisamine A–C (1–3) combined with ciprofloxacin resulted in decreased cell growth and biofilm formation. To assess interference with biofilm matrix

components, wild-type and different isogenic mutant strains of *P. aeruginosa* PAO1, PAO1 Δ *pslA*, PAO1 Δ *pelF*, PDO300 and PDO300 Δ *alg8* were treated with **1** (A–B) or **2** (C–D) or **3** (E–F), or ciprofloxacin, alone or in combination for 24 h. Cell growth (OD₆₀₀) was monitored and the resazurin assay was performed to determine the viability of biofilm bacteria. A culture with matched percentages of DMSO was used as negative (untreated) controls. The experiment was conducted in triplicate. The results are percent means and standard deviation (SD) of two independent experiments. Abbreviation: CIP, ciprofloxacin.

Compound **2** required a lower dose of ciprofloxacin to generate comparable effects with a combination of **1** and the fluoroquinolone. Compound **2** (69.1 μ g/mL) combined with 1/4 MIC (0.0625 μ g/mL) ciprofloxacin caused growth inhibition and antibiofilm activity against PAO1 and PAO1 Δ *pelF*. (Figure 5.2C). Nonetheless, the addition of 1/3 and 1/4 MIC improved the suppression of PAO1 Δ *pelF* biofilm by 20% and 13%, respectively. Again, ciprofloxacin alone at 1/3 and 1/4 MIC modestly reduced bacterial growth (> 40%), but markedly suppressed biofilm formation of PAO1 Δ *pslA* (~ 100%), while **2** alone produced marginal effects, indicating there was no synergistic interaction between both. Exposure to **2** led to a blockage of the cellular progression of PDO300 (> 50%) which appeared to be advanced in the presence of ciprofloxacin at 1/3 and 1/4 MICs (> 70%) (Figure 5.2D). Additionally, the 2/ciprofloxacin combination boosted the inhibition of PDO300 biofilms by nearly 40%. While survival of PDO300 Δ *alg8* was compromised by 40% and 60% when treated with **2** + ciprofloxacin at 1/4 and 1/3 MIC, accordingly, its biofilms were much less susceptible, suggesting the diffusion through the biofilm matrix is impaired.

Compound **3** at 53.1 μ g/mL had negligible synergistic interactions with ciprofloxacin against planktonic forms as well as biofilms of PAO1, PAO1 Δ *pslA* and PAO1 Δ *pelF* (Figure 5.2E). It, however, independently inhibited planktonic growth of the above strains at 106.2 μ g/mL demonstrating its antibacterial property. Additionally, biofilms of PAO1 and PAO1 Δ *pslA* were significantly reduced by **3** alone at 106.2 μ g/mL, up to 70% and 100%, respectively. In contrast, PAO1 Δ *pelF* biofilms exhibited a reduced response to **3**

(~40%) as opposed to ciprofloxacin alone (~60%) and the combinations (~60%). MIC of **3** against PAO1 was observed at 53.1 µg/mL, instead of 106.2 µg/mL, in the MIC assay. The possible explanation could be the differences in the initial cell seeding densities between the MIC assay and the biofilm inhibition assay. The latter had a higher seeding density. Intriguingly, **3** (106.2 µg/mL) antagonized ciprofloxacin (1/4 MIC), which is evident by the decreased effectiveness against biofilm of PAO1Δ*pelF* whilst the observed effects on planktonic cells was fully assigned to **3** in the presence of both compounds. The inability of PAO1Δ*pslA* to generate Psl may result in profound biofilm inhibition (~100%) when **3** (106.2 µg/mL) and sub-lethal doses of ciprofloxacin were applied. These concentrations of ciprofloxacin, on the other hand, partly affected survival of suspended cells (~50%). In addition, complete elimination of biofilm formation suggested that surviving cells remained in their planktonic forms after 24h ciprofloxacin exposure. Unlike sub-MIC of ciprofloxacin, **3** at 106.2 µg/mL completely killed planktonic and biofilm populations of PAO1Δ*pslA*. Notably, the molecule **3** targeted both mutant strains PDO300 and PDO300Δ*alg8* at various degrees (**Figure 5.2F**). Free-living cells of both strains were eradicated but the remaining survivors of PDO300Δ*alg8* were still able to form biofilms. Biofilm viability was severely reduced for PDO300 (~ 100%), albeit to a lesser extent for PDO300Δ*alg8* (80%).

Overall, the data suggested that ianthelliformisamines A–C (**1–3**) had the potential to function solely or to interact synergistically with the antibiotic ciprofloxacin against planktonic and biofilms of wild-type *P. aeruginosa* and an array of its isogenic mutants. **1** and **2** worked in combination with ciprofloxacin to compromise cell growth and biofilm adherence of PAO1 and PAO1Δ*pelF*. Only combinations of **2** and ciprofloxacin could effectively alter the biofilm formation of PDO300. **3** alone targeted bacterial viability of PAO1, PAO1Δ*pslA*, PAO1Δ*pelF*, PDO300 and PDO300Δ*alg8*. Biofilms of these strains, apart from PAO1Δ*pelF* biofilms, were significantly inhibited by **3**. The absence of Psl considerably impaired the ability of PAO1Δ*pslA* to form biofilms when sub-inhibitory of ciprofloxacin or **3** at 106.2 µg/mL was present. In the current experiments, PAO1Δ*pelF* biofilms were the least affected by compound **3**. Furthermore, biofilms of PDO300Δ*alg8*

were less susceptible to the compounds, ciprofloxacin and the combinations as compared to that of PDO300.

5.4.3 Influence of Ianthelliformisamines on the outer membrane integrity

The effect of ianthelliformisamines on the permeability of the outer membrane was determined using an NPN uptake assay. NPN (1-*N*-phenylnaphthylamine), a hydrophobic fluorescent probe, is excluded from the intact outer membrane of Gram-negative bacteria such as *P. aeruginosa*. It intensely fluoresces once it gains access to the phospholipid layer of membrane-compromised cells (**Figure 5.3A**) [42]. The experiments were conducted with different concentrations of ianthelliformisamines and sub-inhibitory doses of ciprofloxacin. We observed that cells treated with polymyxin B at 6.4 µg/mL and 10 µg/mL, an outer membrane-active compound, exhibited prominent fluorescence compared to DMSO solvent treated cells and untreated cells (**Figure 5.3B**). The level of fluorescence intensity in bacteria challenged with test compounds, even at highest testing concentrations, resembled that in cells treated with DMSO. The results indicated that ianthelliformisamines are not membrane permeabilizers.

Chapter 5 - Bromotyrosine-derived metabolites from a marine sponge inhibit *Pseudomonas aeruginosa* biofilms

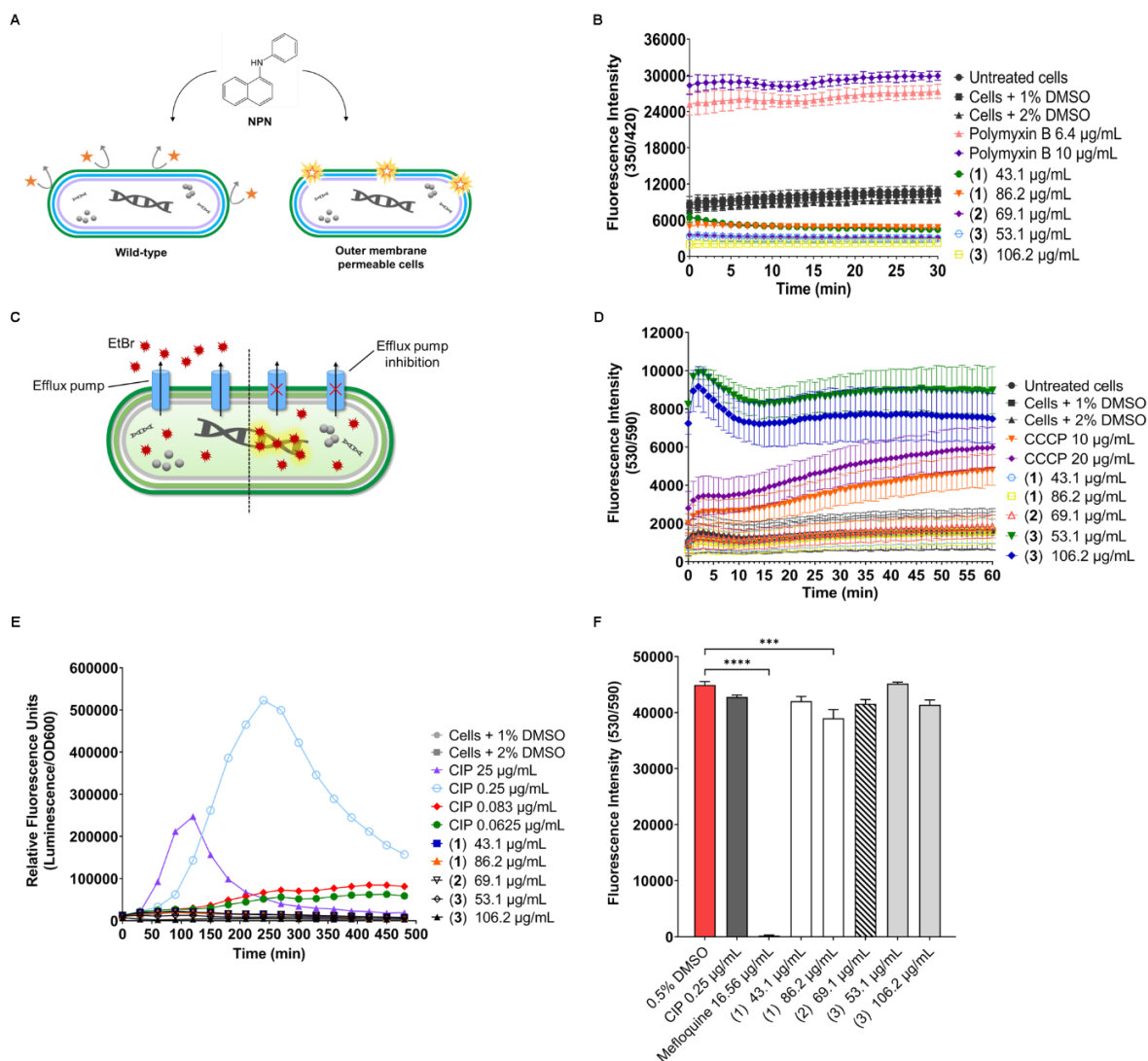


Figure 5.3 (A) The NPN dye is a lipophilic molecule that is used to determine permeability changes in bacteria. Such molecule is weakly fluorescent in an aqueous environment and impermeable to the cell with an intact outer membrane. However, once the membrane is damaged, NPN penetrates the cells and binds to the phospholipid layer, giving rise to pronounced fluorescence. (B) Wild-type PAO1 cells were treated with CCCP with 100 μ M prior to exposure to test compounds at different concentrations. The permeability changes in the outer membrane were assessed by monitoring the fluorescence of NPN for 30 min. Cells treated with DMSO solvent was included as the negative control. Polymyxin B was used as a positive control. (C) Ethidium bromide (EtBr) is a common substrate of the resistance-nodulation-cell division (RND) pump, which is used to measure

the amount of intracellular accumulation as it only fluoresces when bound to DNA. **(D)** The accumulation of EtBr in the presence of CCCP and test compounds was monitored for 60 min. Cells treated with DMSO solvent was included as the negative control. CCCP was used as a positive control. **(E)** Test compounds do not inhibit DNA synthesis. The reporter strain MDM-623 harbouring the promoter region from *PA0614* fused to *P. luminescens luxCDABE* operon, a promoter-luciferase reporter gene, constructed to respond to DNA damage in general. The optical density OD₆₀₀ and the kinetics of luminescence of the reporter strain were monitored for 8 h. Cells treated with DMSO solvent were included as the negative control while ciprofloxacin at different concentrations was used as a positive control. **(F)** HEK293 resazurin viability assay. HEK293 cells were incubated with test compounds to evaluate cytotoxicity by resazurin assay. After 24 h of incubation, resazurin was dispensed into the wells and the plate was further incubated for 5 h at 37°C. Cells treated with DMSO solvent were included as the negative control. Mefloquine was used as a positive control. Experiments were performed in triplicate. The data are the means and SD of two independent experiments. A non-parametric one-way ANOVA followed by Dunnett's multiple comparison post-hoc test was carried out to determine statistical significance between each treatment and the negative control (0.5% DMSO). *, $p < 0.05$; **, $p < 0.01$; ***, $p < 0.001$; ****, $p < 0.0001$. Abbreviation: CIP, ciprofloxacin.

5.4.4 Efflux assay

We performed the ethidium bromide (EtBr) efflux assay to assess the ability of test compounds to inhibit efflux pumps of *P. aeruginosa*. DNA-intercalating dye EtBr is a common substrate of the resistance-nodulation-cell division (RND) family. The dye only fluoresces when bound to DNA in the cytoplasm. The disruption of the efflux pump enhances the accumulation of the substrate within the cells over time until it reaches a steady-state [49]. **(Figure 5.3C)**. Cells treated with compounds **1** and **2** produced comparable EtBr accumulation with untreated bacteria and DMSO treated population. It was shown that only compound **3** at 53.1 µg/mL and 106.2 µg/mL inhibited the efflux pump. The level of intracellular EtBr accumulation by **3** was greater than that mediated by

reference compound CCCP, a chemical efflux pump inhibitor which blocks gradient of protons across the membrane [50]. The fluorescence intensity induced by **3** at 53.1 $\mu\text{g/mL}$ (MIC) remained higher than at 106.2 $\mu\text{g/mL}$ ($2 \times \text{MIC}$) over the time course, suggesting it may be dose-dependent inhibition (**Figure 5.3D**).

5.4.5 Do ianthelliformisamines share the mode of action with ciprofloxacin?

Ciprofloxacin, a fluoroquinolone antibiotic, has been extensively utilized to treat various bacterial infections. It targets bacterial DNA topoisomerase and DNA-gyrase, which produce breakage of double-stranded DNA, ultimately leading to cell death [51]. In the present study, compounds **1** and **2** did not enhance the activity of tobramycin (aminoglycoside) or meropenem (carbapenem), but exclusively worked with ciprofloxacin (**Figure 5.1C**). In the effort of identifying mechanisms of action of test compounds, we employed a DNA damage reporter strain MDM-623 which was constructed based on the promoter-luciferase reporter gene. The increased luminescence readouts are indicative of *gyrase* inhibition-induced promoter up-regulation through the *recA* pathway [44]. Luminescence signal was steadily enhanced in response to ciprofloxacin treatments (positive controls) at 1/4 MIC, 1/3 MIC, $1 \times \text{MIC}$ and $100 \times \text{MIC}$, equivalent to 0.0625, 0.083, 0.25, 25 $\mu\text{g/mL}$, as compared to DMSO treated cells (negative control). Nevertheless, there was no difference in response of MDM-623 upon exposure to test compounds and the solvent (**Figure 5.3E**). The above results may imply that test compounds are unlikely to be DNA gyrase inhibitors and that their mechanism of action is unrelated to that of ciprofloxacin.

5.4.6 Effect of test compounds on HEK293 cells

DMSO is a common solvent used to dissolve compounds [52]. As the compounds were solubilized in DMSO, the effect of DMSO on the mammalian cells should also be considered. It has been reported that DMSO induced cytotoxicity and reduced cell viability at 1% (v/v) and higher [53]. Thus, DMSO concentrations should be kept as low as possible,

between 0.1% and 0.5% [54]. Higher concentration of stock compound was required to achieve lower concentration of DMSO in the assay. However, the solubility of compounds decreased as the solution became more concentrated. Hence, 0.5% DMSO was used in cytotoxic assay.

We sought to determine the cytotoxicity of the compounds using a resazurin viability assay. The compound treatments induced low toxicity to HEK293 cells up to the highest testing concentrations (**Figure 5.3F**), indicating their potential suitability for therapeutic use.

5.4.7 Fluorescence microscopy imaging demonstrate synergism between Ianthelliformisamines A–C (1–3) and ciprofloxacin

Wild-type PAO1 and isogenic mutants were treated with ianthelliformisamines or ciprofloxacin alone and the combinations. Their biofilms were simultaneously stained with SYTO9 (green) and propidium iodide (red). Cells with intact membranes were stained green whilst cells with compromised membranes were stained red. Representative images of cells challenged with different treatments including DMSO, ianthelliformisamines, ciprofloxacin and synergistic combinations are given in **Figures 5.4–5.8**. Analysis of the images showed that ciprofloxacin treatment induced filamentous growth in dose-dependent and strain-specific manners. This observation was in accordance with the previous study [55]. At $1 \times \text{MIC}$, ciprofloxacin produced reduced viability and long, filamentous phenotypes in all tested strains apart from PAO1 $\Delta pslA$. The phenotypes were also observed at sub-lethal doses in ciprofloxacin treated PAO1 and PAO1 $\Delta pelF$. In addition, ciprofloxacin generated another small, round cell population, namely spheroplasts [56].

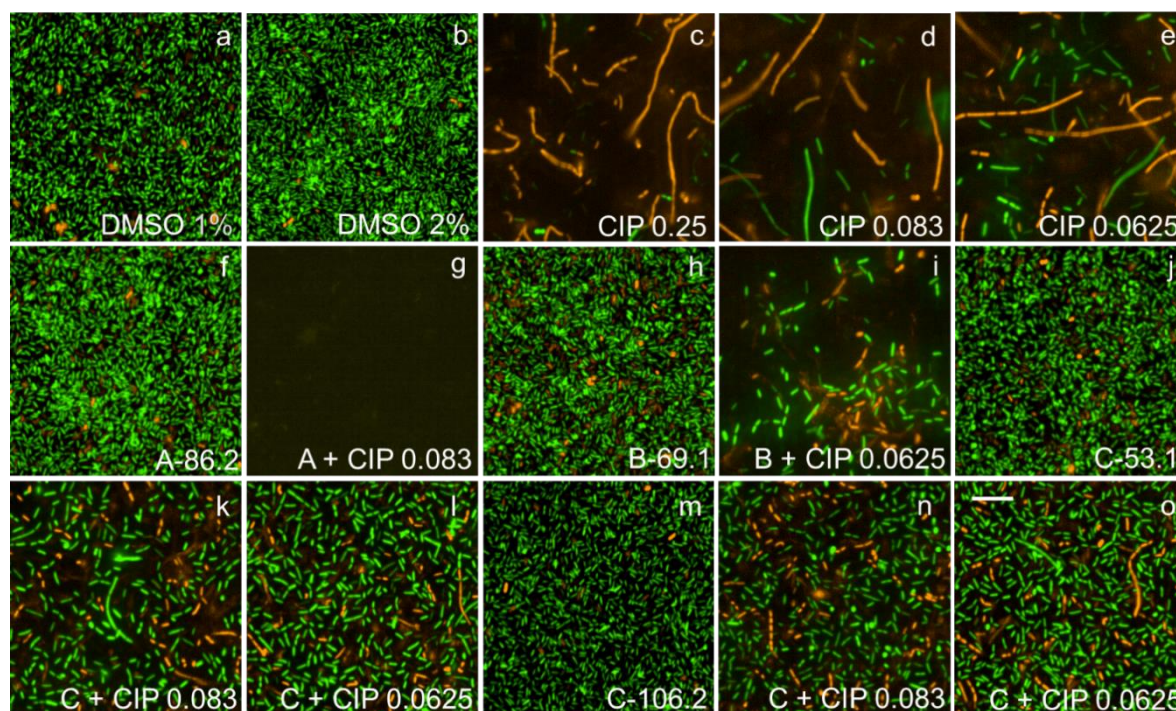


Figure 5.4 Representative fluorescence images of treated and untreated PAO1 biofilms. Cells treated with ciprofloxacin and test compounds **1–3** were stained with SYTO9 (green) and propidium iodide (red). Ciprofloxacin generated long, filamentous phenotypes as well as small, round spheroplasts. Biofilms challenged with **1** and **2** remained unaffected while that with **C** slightly reduced. Complete biofilm inhibition was observed with **1** + 1/3 MIC. Abbreviations: **1–3** (ianthelliformisamines A–C), CIP (ciprofloxacin). Cells treated with (a) DMSO 1%, (b) DMSO 2%, (c) ciprofloxacin at $1 \times \text{MIC}$, (d) ciprofloxacin at $1/3 \text{ MIC}$, (e) ciprofloxacin at $1/4 \text{ MIC}$, (f) **1** at $86.2 \mu\text{g/mL}$, (g) $86.2 \mu\text{g/mL}$ **1** + CIP $1/3 \text{ MIC}$, (h) **2** at $69.1 \mu\text{g/mL}$, (i) **2** $69.1 \mu\text{g/mL}$ + CIP $1/4 \text{ MIC}$, (j) **3** at $53.15 \mu\text{g/mL}$, (k) **3** $53.1 \mu\text{g/mL}$ + CIP $1/3 \text{ MIC}$, (l) **3** $53.1 \mu\text{g/mL}$ + CIP $1/4 \text{ MIC}$, (m) **3** at $106.2 \mu\text{g/mL}$, (n) **3** $106.2 \mu\text{g/mL}$ + CIP $1/3 \text{ MIC}$, (o) **3** $106.2 \mu\text{g/mL}$ + CIP $1/4 \text{ MIC}$. Scale bar $10 \mu\text{M}$.

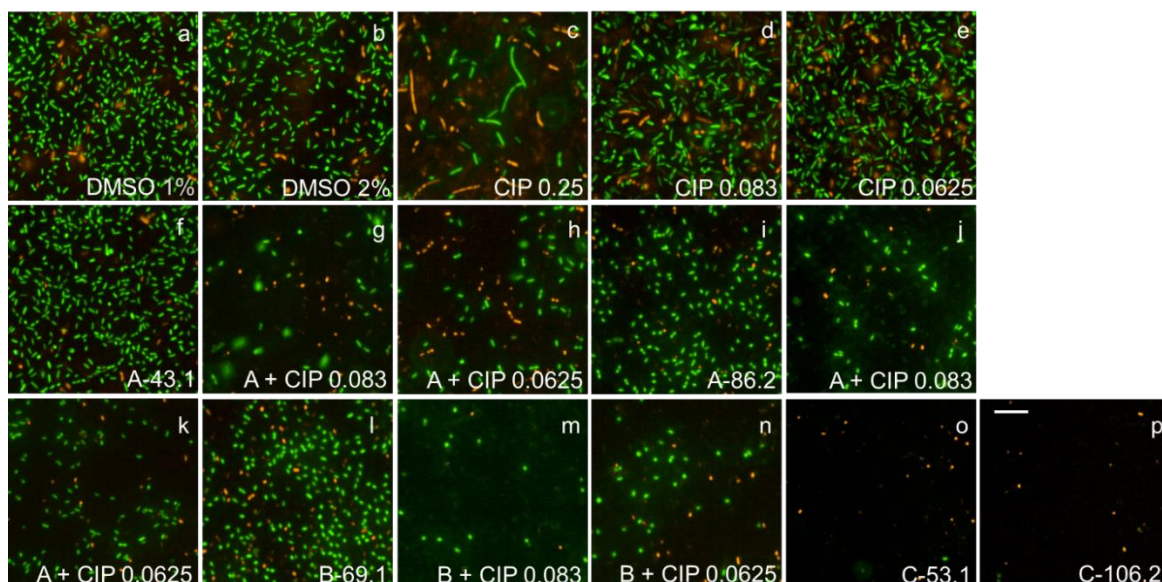


Figure 5.5 Representative fluorescence images of treated and untreated PDO300 biofilms. Cells treated with ciprofloxacin and test compounds **1–3** were stained with SYTO9 (green) and propidium iodide (red). Ciprofloxacin generated long, filamentous phenotypes as well as small, round spheroplasts. Biofilms challenged with **1** and **2** slightly reduced while that with **3** were completely eradicated. Abbreviations: **1–3** (ianthelliformisamines A–C), CIP (ciprofloxacin). Cells treated with (a) DMSO 1%, (b) DMSO 2%, (c) ciprofloxacin at $1 \times$ MIC, (d) ciprofloxacin at $1/3$ MIC, (e) ciprofloxacin at $1/4$ MIC, (f) **1** at $43.1 \mu\text{g/mL}$, (g) $43.1 \mu\text{g/mL}$ **1** + CIP $1/3$ MIC, (h) $43.1 \mu\text{g/mL}$ **1** + CIP $1/4$ MIC, (i) **1** at $86.2 \mu\text{g/mL}$, (j) $86.2 \mu\text{g/mL}$ **1** + CIP $1/3$ MIC, (k) $86.2 \mu\text{g/mL}$ **1** + CIP $1/4$ MIC, (l) **2** $69.1 \mu\text{g/mL}$, (m) $69.1 \mu\text{g/mL}$ **2** + CIP $1/3$ MIC, (n) $69.1 \mu\text{g/mL}$ **2** + CIP $1/4$ MIC, (o) **3** $53.1 \mu\text{g/mL}$, (p) **3** at $106.2 \mu\text{g/mL}$. Scale bar $10 \mu\text{M}$.

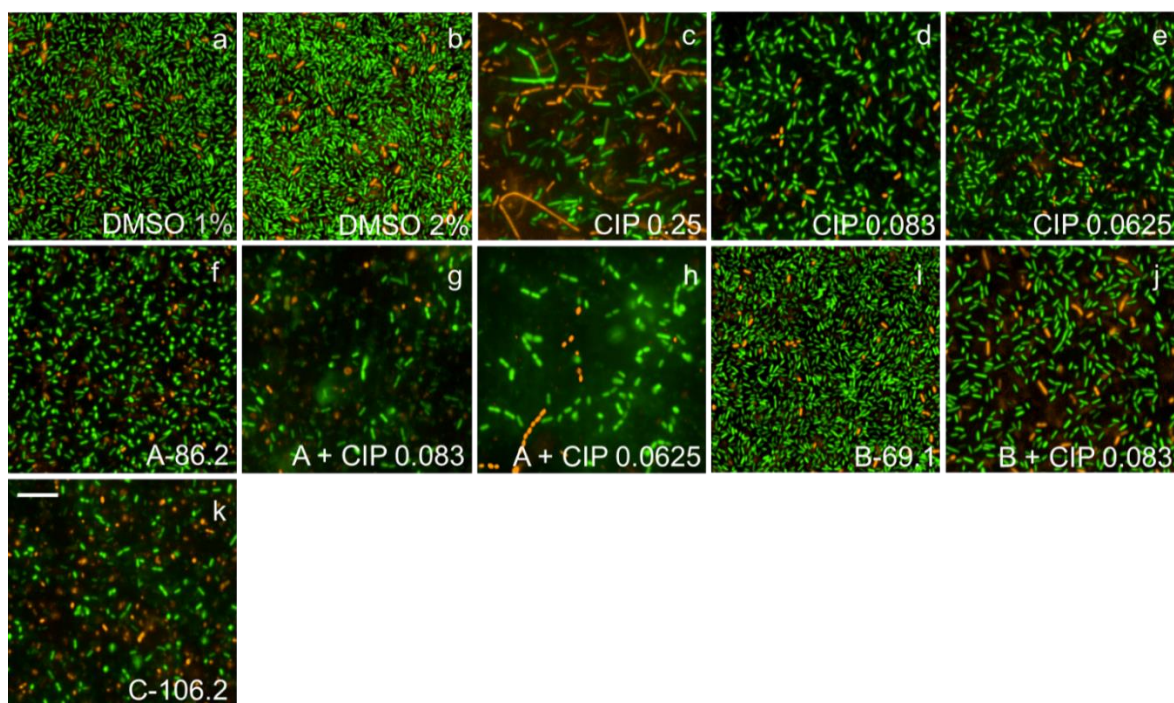


Figure 5.6 Representative fluorescence images of treated and untreated PDO300 Δ alg8 biofilms. Cells treated with ciprofloxacin and test compounds **1–3** were stained with SYTO9 (green) and propidium iodide (red). Ciprofloxacin generated long, filamentous phenotypes as well as small, round spheroplasts. Biofilms challenged with **1–3** were inhibited at different levels. Abbreviations: **1–3** (ianthelliformisamines A–C), CIP (ciprofloxacin). Cells treated with (a) DMSO 1%, (b) DMSO 2%, (c) ciprofloxacin at $1 \times$ MIC, (d) ciprofloxacin at $1/3$ MIC, (e) ciprofloxacin at $1/4$ MIC, (f) **1** at 86.2 μ g/mL, (g) 86.2 μ g/mL **1** + CIP $1/3$ MIC, (h) 86.2 μ g/mL **1** + CIP $1/4$ MIC, (i) **2** at 69.1 μ g/mL, (j) **2** 69.1 μ g/mL + CIP $1/3$ MIC, (k) **3** at 106.2 μ g/mL. Scale bar 10 μ M.

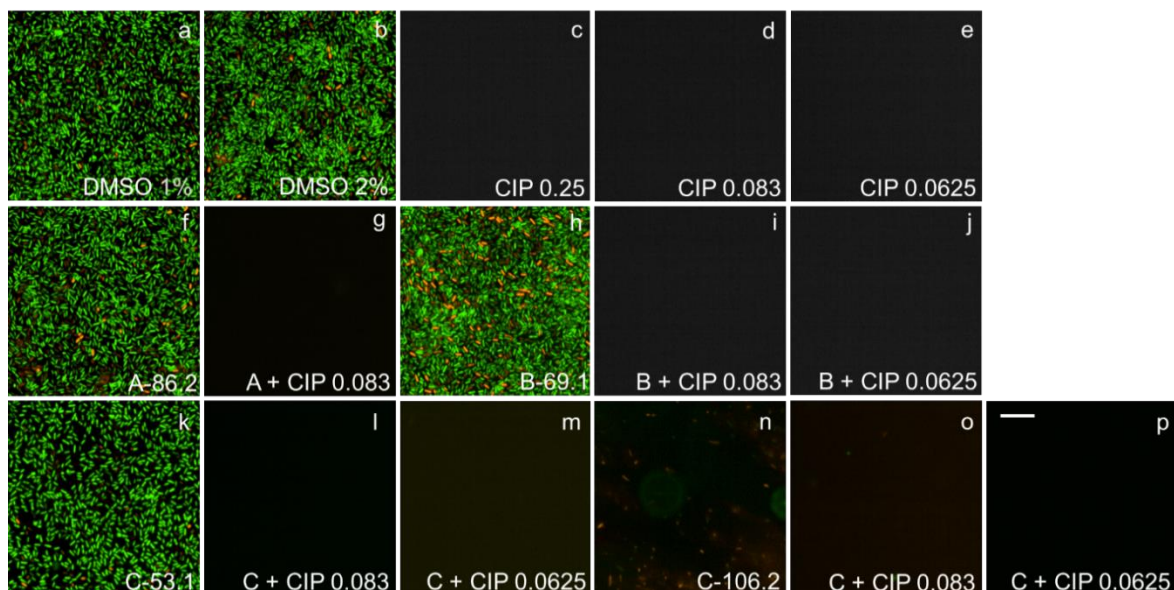


Figure 5.7 Representative fluorescence images of treated and untreated PAO1 Δ *pslA* biofilms. Cells treated with ciprofloxacin and test compounds **1–3** were stained with SYTO9 (green) and propidium iodide (red). PAO1 Δ *pslA* was unable to form biofilms in the presence of ciprofloxacin. Biofilms challenged with **1–3** remained unaffected. Abbreviations: **1–3** (ianthelliformisamines A–C), CIP (ciprofloxacin). Cells treated with (a) DMSO 1%, (b) DMSO 2%, (c) ciprofloxacin at $1 \times$ MIC, (d) ciprofloxacin at $1/3$ MIC, (e) ciprofloxacin at $1/4$ MIC, (f) **2** + CIP $1/3$ MIC, (j) 69.1 μ g/mL **2** + CIP $1/4$ MIC, (k) **3** at 53.1 μ g/, (l) **3** 53.1 μ g/mL + CIP $1/3$ MIC, (m) **3** 53.1 μ g/mL + CIP $1/4$ MIC, (n) **3** at 106.2 μ g/, (o) **3** 106.2 + CIP $1/3$ MIC μ g/mL, (p) **3** 106.2 + CIP $1/4$ MIC μ g/mL. Scale bar 10 μ M.

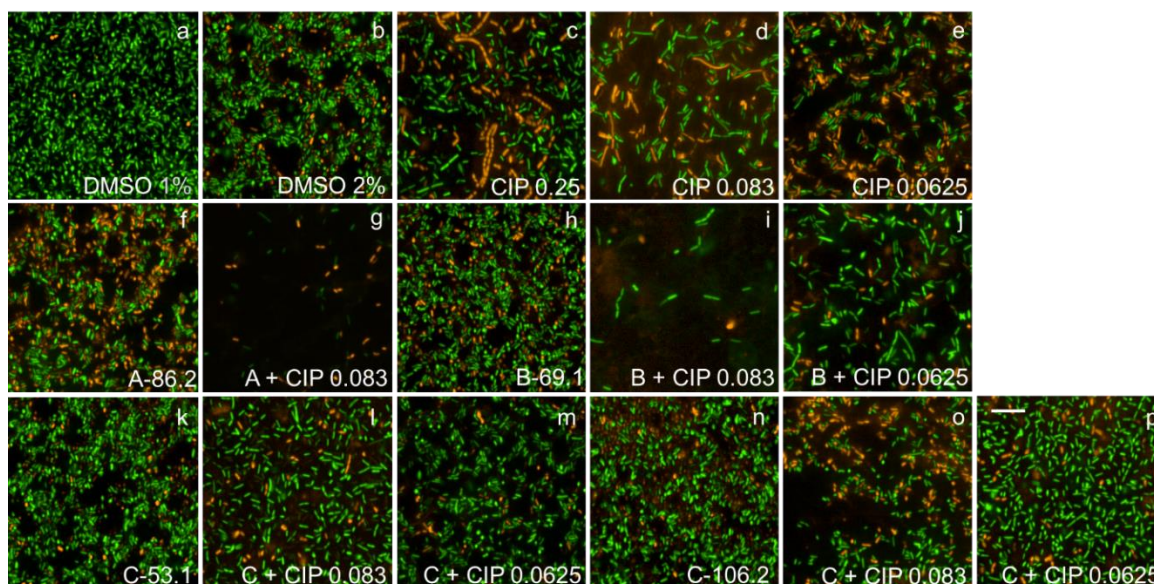


Figure 5.8 Representative fluorescence images of treated and untreated PAO1 Δ *pelA* biofilms. Cells treated with ciprofloxacin and test compounds **1–3** were stained with SYTO9 (green) and propidium iodide (red). Ciprofloxacin generated long, filamentous phenotypes as well as small, round spheroplasts. Biofilms challenged with **1–3** remained unaffected. Abbreviations: **1–3** (ianthelliformisamines A–C), CIP (ciprofloxacin). Cells treated with (a) DMSO 1%, (b) DMSO 2%, (c) ciprofloxacin at $1 \times$ MIC, (d) ciprofloxacin at $1/3$ MIC, (e) ciprofloxacin at $1/4$ MIC, (f) **1** at 86.2 μ g/mL, (g) 86.2 μ g/mL **1** + CIP $1/3$ MIC, (h) **2** at 69.1 μ g/mL, (i) 69.1 μ g/mL **2** + CIP $1/3$ MIC, (j) 69.1 μ g/mL **2** + CIP $1/4$ MIC, (k) **3** at 53.1 μ g/mL, (l) **3** 53.1 μ g/mL + CIP $1/3$ MIC, (m) **3** 53.1 μ g/mL + CIP $1/4$ MIC, (n) **3** at 106.2 μ g/mL, (o) **3** 106.2 μ g/mL + CIP $1/3$ MIC, (p) **3** 106.2 μ g/mL + CIP $1/4$ MIC. Scale bar 10 μ M.

5.4.8 *In vitro* metabolism of ianthelliformisamines A–C (1–3)

5.4.8.1 Positive controls

A single positive control sample, using verapamil as the control substance, was run concurrently with the test samples in microsomes from all species. Verapamil was rapidly metabolized using the experimental conditions used for compounds **1–3**, with half-lives of approx. 6 min (mouse) and 16 min (human). These results were consistent with published data [57] and confirmed suitable activity of the microsomes under the conditions used. Results for the positive control incubations are provided in the **Supplementary data**.

5.4.8.2 Ianthelliformisamine A (1)

The results for the degradation of **1** (as % remaining vs time) in mouse liver microsomes are provided in **Supplementary Table 2** and **Supplementary Figure 1A**, while the graphical representation for LN-transformed data is shown in **Supplementary Figure 1B**. In mouse microsomes, **1** exhibited essentially linear degradation over the 0 to 30-min-period (mean half-life of degradation = 38.2 min), with a decrease in the rate of degradation evident between the 30- and 60-min timepoints. As the clearance of any compound should be determined to reflect that resulting from initial kinetics, the LN-transformed data and clearance estimations were calculated over the 0 to 30-min-period in these microsomes.

In contrast, the negative control tube (no NRS added, therefore no CYP450 metabolism possible) displayed no degradation to **1** over the first 20 min of incubation, followed by a decrease between 20 and 60 min with a half-life of approximately 45 min. Any degradation in a negative control tube without added NRS may be due to non-NADPH-dependent enzymatic metabolism (i.e., non-CYP450 metabolism) such as carboxylesterases, or to general instability in aqueous media [58]. Given the difference between the test and negative control samples over the first 20 min, it is reasonable to conclude that oxidative metabolism was still the dominant metabolic process occurring to **1** in these microsomes,

but this non-oxidative degradation observed after the 20-min-point should still be considered in the overall stability of this compound. Results for individual tubes for incubations of **1** in mouse liver microsomes are provided in the **Supplementary data**, while calculated stability parameters based on the NADPH-dependent degradation profiles obtained, are provided in **Supplementary Table 3**. In human microsomes, **1** demonstrated substantial instability, with no meaningful half-life or clearance data being able to be obtained in these microsomes. Indeed, the response to the test compound in the LC-MS/MS decreased to minor levels over the time taken to analyze the samples from a metabolism experiment (approx. 2.5 h). All samples were kept on ice following addition to the internal standard solution, and for **1**, the samples were only moved to the LC-MS/MS in small batches immediately prior to analysis. These investigations in human microsomes were repeated on separate occasions but no meaningful data was obtained from either attempt. In contrast, the results obtained for the positive control (verapamil) conducted alongside the test compound worked well on all occasions, confirming the validity of the actual incubations conducted. In addition, the linearity of response for **1** over an appropriate concentration range, using standards prepared in phosphate buffer (but no microsomal protein), was confirmed prior to the metabolism experiments, thereby confirming that the analytical conditions used were appropriate.

Based on the experimental half-life of 38.2 min, **1** showed moderate degradation in mouse liver microsomes. This result equated to a hepatic extraction of 0.48, which corresponds to an intermediate level of hepatic extraction in this species, based on the classification system proposed by Houston 1994 [59].

5.4.8.3 Ianthelliformisamine B (2)

The results for the degradation of **2** (as % remaining vs time) in mouse and human liver microsomes are provided in **Supplementary Table 4** and **Supplementary Figure 2A**, while graphical representations for LN-transformed data are shown in **Supplementary Figure 2B** and **Supplementary Figure 2C**. For both species, the degradation of **2** was

essentially linear over the 5 to 30-min time period, and LN-transformed data from this period was used for clearance determinations due to superior linearity. The rates of degradation of **2** observed in microsomes from both species were similar (mean \pm SD = 42.8 ± 7.6 min [mouse] and 35.7 ± 2.1 min [human]), which in turn were similar to that observed for **1** in mouse liver microsomes (38.2 min).

It is noted that the results shown in **Supplementary Table 4** for the mouse microsomes, and for the $t = 5$ min sample in human microsomes, when normalized to the $t = 0$ result, were $> 100\%$. This is most likely due to an artefactually low result being obtained for the $t = 0$ samples; the cause of this is not known. Given the good linearity obtained between 5 and 30 min, the data for calculation of clearance has been normalized to the $t = 5$ min result.

In both species, the negative control tubes (no NRS added) showed a slow level of degradation over the 30-min incubation period (half-life of degradation = 90.0 min [mouse] and 103.4 min [human]). As indicated above for **1**, any degradation observed in the negative control tube may occur due to non-NADPH-dependent enzymatic metabolism (i.e., non-CYP450 metabolism) such as carboxylesterases, or to general instability in aqueous media [58], and it is again reasonable to conclude that oxidative metabolism was still the dominant metabolic process occurring to **2** in the microsomes. However, the slow non-oxidative degradations observed should still be considered in the overall stability of this compound.

Results for individual tubes for incubations of **2** in microsomes from both species are provided in the **Supplementary data**. Calculated stability parameters for **2**, based on the NADPH-dependent degradation profiles obtained, are provided in **Supplementary Table 5**.

Based on the mean experimental half-lives of 42.8 and 35.7 min, **2** showed moderate degradation in both mouse and human liver microsomes. These results equated to hepatic

extractions of 0.42 and 0.61 in mouse and human liver microsomes respectively, which correspond to intermediate levels of hepatic extraction, based on the classification system proposed by Houston 1994 [59].

5.4.8.4 Ianthelliformisamine C (3)

Compound **3** was metabolically stable in incubations with both mouse and human microsomes under the conditions employed. No decrease in concentration was observed over the 0 – 60 min incubation period in human microsomes or for the 0 – 30 min period in mouse microsomes, with only a slight decrease in mean concentration in mouse liver microsomes between 30 and 60 min (mainly caused by a lower result for one of the triplicate tubes – see Supplementary data). Consequently, no calculations for half-life or hepatic extraction were possible for **3** in either species.

The results for **3** (as % remaining vs time) in mouse and human liver microsomes are provided in **Supplementary Table 6** and **Supplementary Figure 3A**, while graphical representations for LN-transformed data are shown in **Supplementary Figures 3B and 3C**.

Generally, in the presence of human liver microsomes, **1** demonstrated substantial instability, with no meaningful half-life or clearance data being able to be obtained in these microsomes despite repeated attempts. For **2**, the mean (n = 3) degradation half-lives in mouse and human liver microsomes were 42.8 min and 35.7 min, respectively, over the 0 to 30-min incubation period. These equated to calculated in vivo hepatic extractions of 0.42 and 0.61, respectively. In contrast, **3** was metabolically stable in incubations using both mouse and human microsomes under the conditions employed. No decrease in concentration was observed over the 0 – 60 min incubation period, therefore no calculation of half-life or hepatic extraction was possible.

5.5 Discussion

The rapidly increasing antibiotic resistance among bacterial pathogens has posed global health threats. Therefore, there is an urgent need of new antimicrobial compounds, especially for Gram-negative bacteria, as emphasized by the World Health Organization. One of the key defense mechanisms of bacteria is the formation of biofilms which confer protection to embedded cells from antibiotic treatments and an escape from the host immune system, eventually leading to chronic infections. Several strategies such as combination therapies that combine two or more therapeutic agents have been proven to be efficient in addressing this increasingly widespread multi-drug resistance (MDR) and their biofilm-associated infections by targeting various molecular pathways in a synergistically or additive manner [60].

Previously, compounds **1–3** and their derivatives have been reported as promising and broad-spectrum antimicrobials as well as antibiotic enhancers against *Enterobacter aerogenes*, *P. aeruginosa* and *Klebsiella pneumoniae* MDR strains [24,25]. To our knowledge, the efficacy of **1–3** and their combinations with antibiotics against biofilms of *P. aeruginosa* has not been investigated. In the present study, we sought to determine the antibiofilm activities of these molecules individually and in combinations with common antibiotics used in clinical settings.

In current experimental conditions, **1** and **2** alone exerted insignificant effects on free-living cells and biofilm formation of all the studied strains up to the highest tested concentrations. The results were in accordance with previous work which reported MICs were 172.4 µg/mL for **1** and >138.2 µg/mL for **2**, which were 2-fold the currently studied doses [25]. MIC of **3** was previously determined at ~ 26.55 µg/mL [25], whereas it was ~ 53.1 µg/mL in the current study. The variation could be due to the differences in experimental conditions such as culture medium and initial inoculum.

Interestingly, **3** at 106.2 µg/mL displayed potent activity on planktonic forms of all the strains, despite its high molecular weight (833.96 g/mol) as opposed to its analogues, suggesting its bactericidal properties. It raised the possibility that the outer membrane was permeabilized to allow the intake of such a large molecule. The cell envelope of Gram-negative bacteria is a complex structure consisting of an outer membrane, a peptidoglycan cell wall and an inner membrane. The outer membrane contains channel-forming proteins, porins, which serve as a selective barrier allowing the influx of essential nutrients into the cells, extruding waste and defending against toxic chemicals. Generally, these porins allow passive diffusion of hydrophilic solutes with sizes up to 600 Daltons. *P. aeruginosa* possesses a low number of porins with a slow penetration rate, thus reducing the permeability of the outer membrane, further aiding resistance to antibiotics [61,62]. Nonetheless, the data of the NPN uptake assay indicated that none of the test compounds were membrane-active.

Furthermore, compound **3** impeded the biofilm formation of PAO1Δ*pslA*, PDO300 and PDO300Δ*alg8* (~ 100%) but to a less extent to that of wild-type PAO1 (> 70%). It was shown that deletion of *pslA* resulted in impairment of initial surface attachment due to decreased level of signaling molecule c-di-GMP (bis-(3'-5')-cyclic dimeric guanosine monophosphate) [63] and increased production of Pel in static biofilms, the latter was incapable of compensating for this deficiency, as corroborated by a reduction in biofilm volume [27]. It is worth mentioning that Pel-rich biofilms enhanced the tolerance to DNase digestion and charged antibiotics such as tobramycin [64]. Hence, the elevated level of Pel in the biofilms of PAO1Δ*pslA* did not confer any protection from the neutral antibiotic ciprofloxacin. Psl plays an essential role in initial adherence and functions as protective layer for biofilm bacteria against antibiotics such as tobramycin and ciprofloxacin [65], and host immune responses like phagocytosis [66]. Moreover, it is commonly found in many cystic fibrosis (CF) isolates and its combination with alginate triggered severe damages to surrounding host tissues via substantial production of extracellular reactive oxygen species (ROS) [66]. Collectively, these perhaps explain the susceptibility of PAO1Δ*pslA* biofilms to compound **3** and sublethal ciprofloxacin. It also suggested that Psl may be a promising

target to improve biofilm eradication treatments [67]. Biofilms of PAO1 $\Delta pelF$ were the least affected by **3** and its combinations compared to that of other studied strains. The only difference in biofilms of PAO1 $\Delta pelF$ is the deficiency of Pel. It is unclear why the absence of Pel generated the tolerance to treatments. A conversion from nonmucoid to mucoid phenotype appears to be a crucial adaptative mechanism for chronic infections of CF lung [68]. The mutant PDO300 was constructed to mimic the adaptation in CF patient lung infected with *P. aeruginosa* [44]. It is interesting that molecule **3** effectively reduced the viability of suspended cells and biofilm formation of the mucoid variant PDO300, whose biofilms have been shown to have a high level of tolerance to tobramycin (up to 1000 times) than biofilms formed by nonmucoid PAO1 [69]. The overproduction of alginate in PDO300 due to defective *mucA22* allele hindered solid surface attachment [48] and retarded the growth rate (data not shown). The presence of **3** may further impact the viability and impede its ability to form biofilms. Previous work reported that although PDO300 $\Delta alg8$ formed flat biofilms, its biofilms were found to be more compact and contained more dead cells and extracellular DNA than other biofilms. Additionally, a lack of alginate led to increased production of Pel polysaccharide which subsequently enhanced cell-to-cell interaction as well as the biofilm compactness [27], thus possibly making it less accessible to compound **3**. This might be the reason why the effect of **3** on PDO300 $\Delta alg8$ biofilms was weaker than PDO300. Of note, Pel-deficient biofilms (PAO1 $\Delta pelF$) were more resistant to **3** treatment (106.2 $\mu\text{g/mL}$) than alginate-deficient biofilms (PDO300 $\Delta alg8$) and mucoid biofilm (PDO300), in spite of similar planktonic killing.

To improve the activities of **1–3**, we carried out synergy assays. In our experiment, these compounds exclusively synergized with fluoroquinolone ciprofloxacin, a DNA synthesis inhibitor. Improvement of planktonic killing and antibiofilm activity in a strain-specific manner, though at different levels, following the treatment with combinations of **1** or **2** or **3** and ciprofloxacin were observed. This is in line with a recent study suggesting ianthelliformisamines and its derivatives were antibiotic potentiators [25]. In addition to reduced outer membrane permeability, *P. aeruginosa* possesses an efficient efflux system, contributing to antibiotic resistance worldwide. Our next attempt was to explore the modes

of action of these molecules. In efflux assays, only compound **3** was able to advance the intracellular EtBr accumulation. The fact that the fluorescence intensity was higher in cells treated with **3** as opposed to that in cells treated with CCCP, a known efflux pump inhibitor, indicated that **3** is an efflux pump inhibitor. Additionally, the interactions between ianthelliformisamines and ciprofloxacin were also studied. Synergy interactions occur when two molecules work on distinct signaling pathways which could be activated by the same signal. Additivity, on the other hand, happens when two molecules share the same mechanism of action [70]. Since ciprofloxacin induces cell filamentation and inhibits DNA synthesis, we used DNA damaging reporter strain MDM-623 to assess the interaction between Ianthelliformisamines and ciprofloxacin. The data illustrated that ianthelliformisamines did not target DNA gyrase, implying that ciprofloxacin and Ianthelliformisamines do not share the same signaling pathway. Thus, their interaction may potentially be synergism rather than additivity.

The biofilm inhibition assay here employed LB to grow *in vitro* biofilms which possibly share some of the properties of clinical isolates, however, biofilms grown in mucin-rich medium mimicking CF lung sputum would further validate the potency and the efficacy of these combinations. Additionally, the compounds and/or their combinations were not tested on clinical isolates which are clearly more clinically relevant. The biofilm inhibition assay here employed LB to grow *in vitro* biofilms which possibly share some of the properties of clinical isolates, however, biofilms grown in mucin-rich medium mimicking CF lung sputum would further validate the potency and the efficacy of these combinations. Additionally, the compounds and/or their combinations were not tested on clinical isolates which are clearly more clinically relevant. Bacterial isolates recovered from infections sites *in vivo*, i.e., hypermutator strains derived from patients with bronchiectasis display distinct phenotypes (mucoid phenotype and motility impairment) and have higher tolerance to antimicrobials [71]. Hence, testing the compounds and/or their combinations against clinical isolates would provide valuable insights for the efficacy of compounds individually and in combination with ciprofloxacin *in vivo*. We focused on exploring the mechanisms of action of the compounds individually but did not take into account that of

the combinations, as the action of one compound could be altered in the presence of another molecule. Though the test compounds showed low toxicity on HEK293 cells, their combination with ciprofloxacin could exert serious undesired effects on human cells. As with all antibiotic treatments, the bactericidal activity of **3** may induce mutagenesis that eventually confers rampant drug resistance. Hence, mutation frequency should be studied to address the concern.

We focused on exploring the mechanisms of action of the compounds individually but did not take into account that of the combinations, as the action of one compound could be altered in the presence of another molecule. Though the test compounds showed low toxicity on HEK293 cells, their combination with ciprofloxacin could exert serious undesired effects on human cells. As with all antibiotic treatments, the bactericidal activity of **3** may induce mutagenesis that eventually confers rampant drug resistance. Hence, mutation frequency should be studied to address the concern.

Under the *in vitro* conditions used in this study, **1** underwent moderate degradation in mouse liver microsomes but displayed significant instability in the presence of human microsomes, while **2** was moderately degraded in microsomes from both species. In contrast, **3** was metabolically stable, with virtually no degradation observed in incubations with liver microsomes from either species. This information may serve as guidance for additional structure optimization to improve potency and avoid metabolic liabilities.

5.6 Conclusion

In summary, we demonstrated that ianthelliformisamines A–C (**1–3**) had potential bactericidal activity and prevented *P. aeruginosa* biofilm formation with low cytotoxicity. Compounds **1** and **2** synergistically interacted with ciprofloxacin to influence bacterial growth and mitigate biofilm formation while **3** solely targeted both growth modes which were also dependent on the ability to produce various exopolymers. These findings further emphasize the crucial roles of exopolysaccharides constituting the biofilm

matrix in antibiotic recalcitrance and it might shed light on the development of novel targets to counteract this superbug. Although the detailed mechanisms of action of these compounds and their combinations remain to be determined, compound **3** mode of action studies showed that it is an effective efflux pump inhibitor. Of the three compounds, **3** showed greatest metabolic stability in the presence of mouse and human liver microsomes. Collectively, we suggest ianthelliformisamines as promising drug leads for future investigations into development treatments for *P. aeruginosa* infections.

5.7 References

1. Moradali, M.F.; Ghods, S.; Rehm, B.H. *Pseudomonas aeruginosa* Lifestyle: A Paradigm for Adaptation, Survival, and Persistence. *Front Cell Infect Microbiol* **2017**, *7*, 39, doi:10.3389/fcimb.2017.00039.
2. Moradali, M.F.; Rehm, B.H.A. Bacterial biopolymers: from pathogenesis to advanced materials. *Nature Reviews Microbiology* **2020**, *18*, 195-210, doi:10.1038/s41579-019-0313-3.
3. Lewis, K. Riddle of biofilm resistance. *Antimicrob Agents Chemother* **2001**, *45*, 999-1007, doi:10.1128/AAC.45.4.999-1007.2001.
4. Romling, U.; Balsalobre, C. Biofilm infections, their resilience to therapy and innovative treatment strategies. *J Intern Med* **2012**, *272*, 541-561, doi:10.1111/joim.12004.
5. Ryder, C.; Byrd, M.; Wozniak, D.J. Role of polysaccharides in *Pseudomonas aeruginosa* biofilm development. *Curr Opin Microbiol* **2007**, *10*, 644-648, doi:10.1016/j.mib.2007.09.010.
6. Byrd, M.S.; Sadovskaya, I.; Vinogradov, E.; Lu, H.; Sprinkle, A.B.; Richardson, S.H.; Ma, L.; Ralston, B.; Parsek, M.R.; Anderson, E.M., et al. Genetic and biochemical analyses of the *Pseudomonas aeruginosa* Psl exopolysaccharide reveal overlapping roles for polysaccharide synthesis enzymes in Psl and LPS production. *Mol Microbiol* **2009**, *73*, 622-638, doi:10.1111/j.1365-2958.2009.06795.x.
7. Jones, C.J.; Wozniak, D.J. Psl Produced by Mucoid *Pseudomonas aeruginosa* Contributes to the Establishment of Biofilms and Immune Evasion. *mBio* **2017**, *8*, doi:10.1128/mBio.00864-17.
8. Ma, L.; Wang, S.; Wang, D.; Parsek, M.R.; Wozniak, D.J. The roles of biofilm matrix polysaccharide Psl in mucoid *Pseudomonas aeruginosa* biofilms. *FEMS Immunol Med Microbiol* **2012**, *65*, 377-380, doi:10.1111/j.1574-695X.2012.00934.x.

9. Friedman, L.; Kolter, R. Genes involved in matrix formation in *Pseudomonas aeruginosa* PA14 biofilms. *Molecular Microbiology* **2004**, *51*, 675-690, doi:<https://doi.org/10.1046/j.1365-2958.2003.03877.x>.
10. Jennings Laura, K.; Storek Kelly, M.; Ledvina Hannah, E.; Coulon, C.; Marmont Lindsey, S.; Sadovskaya, I.; Secor Patrick, R.; Tseng Boo, S.; Scian, M.; Filloux, A., et al. Pel is a cationic exopolysaccharide that cross-links extracellular DNA in the *Pseudomonas aeruginosa* biofilm matrix. *Proceedings of the National Academy of Sciences* **2015**, *112*, 11353-11358, doi:10.1073/pnas.1503058112.
11. Ciofu, O.; Tolker-Nielsen, T.; Jensen, P.O.; Wang, H.; Hoiby, N. Antimicrobial resistance, respiratory tract infections and role of biofilms in lung infections in cystic fibrosis patients. *Adv Drug Deliv Rev* **2015**, *85*, 7-23, doi:10.1016/j.addr.2014.11.017.
12. Tseng, B.S.; Zhang, W.; Harrison, J.J.; Quach, T.P.; Song, J.L.; Penterman, J.; Singh, P.K.; Chopp, D.L.; Packman, A.I.; Parsek, M.R. The extracellular matrix protects *Pseudomonas aeruginosa* biofilms by limiting the penetration of tobramycin. *Environ Microbiol* **2013**, *15*, 2865-2878, doi:10.1111/1462-2920.12155.
13. Cragg, G.M.; Newman, D.J. Natural products: a continuing source of novel drug leads. *Biochim Biophys Acta* **2013**, *1830*, 3670-3695, doi:10.1016/j.bbagen.2013.02.008.
14. Zjawiony, J.K. Biologically active compounds from Aphyllophorales (polypore) fungi. *J Nat Prod* **2004**, *67*, 300-310, doi:10.1021/np030372w.
15. Heinrich, M.; Lee Teoh, H. Galanthamine from snowdrop—the development of a modern drug against Alzheimer’s disease from local Caucasian knowledge. *Journal of Ethnopharmacology* **2004**, *92*, 147-162, doi:<https://doi.org/10.1016/j.jep.2004.02.012>.
16. Ojima, I. Modern natural products chemistry and drug discovery. *J Med Chem* **2008**, *51*, 2587-2588, doi:10.1021/jm701291u.

17. Butler, M.S.; Robertson, A.A.; Cooper, M.A. Natural product and natural product derived drugs in clinical trials. *Nat Prod Rep* **2014**, *31*, 1612-1661, doi:10.1039/c4np00064a.
18. Bjarnsholt, T.; Jensen, P.O.; Rasmussen, T.B.; Christophersen, L.; Calum, H.; Hentzer, M.; Hougen, H.P.; Rygaard, J.; Moser, C.; Eberl, L., et al. Garlic blocks quorum sensing and promotes rapid clearing of pulmonary *Pseudomonas aeruginosa* infections. *Microbiology (Reading)* **2005**, *151*, 3873-3880, doi:10.1099/mic.0.27955-0.
19. Nakamoto, M.; Kunimura, K.; Suzuki, J.I.; Kodera, Y. Antimicrobial properties of hydrophobic compounds in garlic: Allicin, vinylthiin, ajoene and diallyl polysulfides. *Exp Ther Med* **2020**, *19*, 1550-1553, doi:10.3892/etm.2019.8388.
20. Hentzer, M.; Wu, H.; Andersen, J.B.; Riedel, K.; Rasmussen, T.B.; Bagge, N.; Kumar, N.; Schembri, M.A.; Song, Z.; Kristoffersen, P., et al. Attenuation of *Pseudomonas aeruginosa* virulence by quorum sensing inhibitors. *EMBO J* **2003**, *22*, 3803-3815, doi:10.1093/emboj/cdg366.
21. Wu, H.; Song, Z.; Hentzer, M.; Andersen, J.B.; Molin, S.; Givskov, M.; Hoiby, N. Synthetic furanones inhibit quorum-sensing and enhance bacterial clearance in *Pseudomonas aeruginosa* lung infection in mice. *J Antimicrob Chemother* **2004**, *53*, 1054-1061, doi:10.1093/jac/dkh223.
22. Steele, A.D.; Knouse, K.W.; Keohane, C.E.; Wuest, W.M. Total synthesis and biological investigation of (-)-promysalin. *J Am Chem Soc* **2015**, *137*, 7314-7317, doi:10.1021/jacs.5b04767.
23. Steele, A.D.; Keohane, C.E.; Knouse, K.W.; Rossiter, S.E.; Williams, S.J.; Wuest, W.M. Diverted Total Synthesis of Promysalin Analogs Demonstrates That an Iron-Binding Motif Is Responsible for Its Narrow-Spectrum Antibacterial Activity. *Journal of the American Chemical Society* **2016**, *138*, 5833-5836, doi:10.1021/jacs.6b03373.
24. Xu, M.; Davis, R.A.; Feng, Y.; Sykes, M.L.; Shelper, T.; Avery, V.M.; Camp, D.; Quinn, R.J. Ianthelliformisamines A-C, antibacterial bromotyrosine-derived

- metabolites from the marine sponge *Suberea ianthelliformis*. *J Nat Prod* **2012**, 75, 1001-1005, doi:10.1021/np300147d.
25. Pieri, C.; Borselli, D.; Di Giorgio, C.; De Meo, M.; Bolla, J.M.; Vidal, N.; Combes, S.; Brunel, J.M. New Ianthelliformisamine derivatives as antibiotic enhancers against resistant Gram-negative bacteria. *J Med Chem* **2014**, 57, 4263-4272, doi:10.1021/jm500194e.
 26. Holloway, B.W.; Matsumoto, H.; Phibbs, P.V., Jr. The chromosome map of *Pseudomonas aeruginosa* PAO. *Acta Microbiol Pol* **1986**, 35, 161-164.
 27. Ghafoor, A.; Hay, I.D.; Rehm, B.H. Role of exopolysaccharides in *Pseudomonas aeruginosa* biofilm formation and architecture. *Appl Environ Microbiol* **2011**, 77, 5238-5246, doi:10.1128/AEM.00637-11.
 28. Mathee, K.; Ciofu, O.; Sternberg, C.; Lindum, P.W.; Campbell, J.I.A.; Jensen, P.; Johnsen, A.H.; Givskov, M.; Ohman, D.E.; Soren, M., et al. Mucoid conversion of *Pseudomonas aeruginosa* by hydrogen peroxide: a mechanism for virulence activation in the cystic fibrosis lung. *Microbiology (Reading)* **1999**, 145 (Pt 6), 1349-1357, doi:10.1099/13500872-145-6-1349.
 29. Remminghorst, U.; Rehm, B.H. In vitro alginate polymerization and the functional role of Alg8 in alginate production by *Pseudomonas aeruginosa*. *Appl Environ Microbiol* **2006**, 72, 298-305, doi:10.1128/AEM.72.1.298-305.2006.
 30. Davis, R.A. Isolation and structure elucidation of the new fungal metabolite (-)-xylariamide A. *J Nat Prod* **2005**, 68, 769-772, doi:10.1021/np050025h.
 31. Levrier, C.; Balastrier, M.; Beattie, K.D.; Carroll, A.R.; Martin, F.; Choomuenwai, V.; Davis, R.A. Pyridocoumarin, aristolactam and aporphine alkaloids from the Australian rainforest plant *Goniothalamus australis*. *Phytochemistry* **2013**, 86, 121-126, doi:10.1016/j.phytochem.2012.09.019.
 32. Choomuenwai, V.; Andrews, K.T.; Davis, R.A. Synthesis and antimalarial evaluation of a screening library based on a tetrahydroanthraquinone natural product scaffold. *Bioorg Med Chem* **2012**, 20, 7167-7174, doi:10.1016/j.bmc.2012.09.052.
 33. Barnes, E.C.; Said, N.A.B.M.; Williams, E.D.; Hooper, J.N.A.; Davis, R.A. Ecionines A and B, two new cytotoxic pyridoacridine alkaloids from the Australian

- marine sponge, *Ecionemia geodides*. *Tetrahedron* **2010**, 66, 283-287, doi:<https://doi.org/10.1016/j.tet.2009.10.109>.
34. Barnes, E.C.; Kumar, R.; Davis, R.A. The use of isolated natural products as scaffolds for the generation of chemically diverse screening libraries for drug discovery. *Natural Product Reports* **2016**, 33, 372-381, doi:<https://doi.org/10.1039/c5np00121h>.
35. Andrews, J.M. Determination of minimum inhibitory concentrations. *Journal of Antimicrobial Chemotherapy* **2001**, 48, 5-16, doi:10.1093/jac/48.suppl_1.5.
36. O'Brien, J.; Wilson, I.; Orton, T.; Pognan, F. Investigation of the Alamar Blue (resazurin) fluorescent dye for the assessment of mammalian cell cytotoxicity. *Eur J Biochem* **2000**, 267, 5421-5426, doi:10.1046/j.1432-1327.2000.01606.x.
37. Bowling, T.; Mercer, L.; Don, R.; Jacobs, R.; Nare, B. Application of a resazurin-based high-throughput screening assay for the identification and progression of new treatments for human African trypanosomiasis. *Int J Parasitol Drugs Drug Resist* **2012**, 2, 262-270, doi:10.1016/j.ijpddr.2012.02.002.
38. Paytubi, S.; de La Cruz, M.; Tormo, J.R.; Martin, J.; Gonzalez, I.; Gonzalez-Menendez, V.; Genilloud, O.; Reyes, F.; Vicente, F.; Madrid, C., et al. A High-Throughput Screening Platform of Microbial Natural Products for the Discovery of Molecules with Antibiofilm Properties against Salmonella. *Front Microbiol* **2017**, 8, 326, doi:10.3389/fmicb.2017.00326.
39. Mangiaterra, G.; Laudadio, E.; Cometti, M.; Mobbili, G.; Minnelli, C.; Massaccesi, L.; Citterio, B.; Biavasco, F.; Galeazzi, R. Inhibitors of multidrug efflux pumps of *Pseudomonas aeruginosa* from natural sources: An in silico high-throughput virtual screening and in vitro validation. *Medicinal Chemistry Research* **2016**, 26, 414-430, doi:10.1007/s00044-016-1761-1.
40. Laudadio, E.; Cedraro, N.; Mangiaterra, G.; Citterio, B.; Mobbili, G.; Minnelli, C.; Bizzaro, D.; Biavasco, F.; Galeazzi, R. Natural Alkaloid Berberine Activity against *Pseudomonas aeruginosa* MexXY-Mediated Aminoglycoside Resistance: In Silico and in Vitro Studies. *J Nat Prod* **2019**, 82, 1935-1944, doi:10.1021/acs.jnatprod.9b00317.

41. Szemerédi, N.; Kincses, A.; Rehorová, K.; Hoang, L.; Salardon-Jimenez, N.; Sevilla-Hernandez, C.; Viktorova, J.; Dominguez-Alvarez, E.; Spengler, G. Ketone- and Cyano-Selenoesters to Overcome Efflux Pump, Quorum-Sensing, and Biofilm-Mediated Resistance. *Antibiotics (Basel)* **2020**, *9*, doi:10.3390/antibiotics9120896.
42. Helander, I.M.; Mattila-Sandholm, T. Fluorometric assessment of Gram-negative bacterial permeabilization. *Journal of Applied Microbiology* **2000**, *88*, 213-219, doi:<https://doi.org/10.1046/j.1365-2672.2000.00971.x>.
43. Johnson, L.; Mulcahy, H.; Kanevets, U.; Shi, Y.; Lewenza, S. Surface-localized spermidine protects the *Pseudomonas aeruginosa* outer membrane from antibiotic treatment and oxidative stress. *J Bacteriol* **2012**, *194*, 813-826, doi:10.1128/JB.05230-11.
44. Moir, D.T.; Ming, D.; Opperman, T.; Schweizer, H.P.; Bowlin, T.L. A high-throughput, homogeneous, bioluminescent assay for *Pseudomonas aeruginosa* gyrase inhibitors and other DNA-damaging agents. *J Biomol Screen* **2007**, *12*, 855-864, doi:10.1177/1087057107304729.
45. Sykes, M.L.; Avery, V.M. Development and application of a sensitive, phenotypic, high-throughput image-based assay to identify compound activity against *Trypanosoma cruzi* amastigotes. *Int J Parasitol Drugs Drug Resist* **2015**, *5*, 215-228, doi:10.1016/j.ijpddr.2015.10.001.
46. Charman, S.A.; Andreu, A.; Barker, H.; Blundell, S.; Campbell, A.; Campbell, M.; Chen, G.; Chiu, F.C.K.; Crighton, E.; Katneni, K., et al. An in vitro toolbox to accelerate anti-malarial drug discovery and development. *Malar J* **2020**, *19*, 1, doi:10.1186/s12936-019-3075-5.
47. Ring, B.J.; Chien, J.Y.; Adkison, K.K.; Jones, H.M.; Rowland, M.; Jones, R.D.; Yates, J.W.; Ku, M.S.; Gibson, C.R.; He, H., et al. PhRMA CPCDC initiative on predictive models of human pharmacokinetics, part 3: comparative assessment of prediction methods of human clearance. *J Pharm Sci* **2011**, *100*, 4090-4110, doi:10.1002/jps.22552.
48. Hay, I.D.; Gatland, K.; Campisano, A.; Jordens, J.Z.; Rehm, B.H. Impact of alginate overproduction on attachment and biofilm architecture of a supermucoid

- Pseudomonas aeruginosa* strain. *Appl Environ Microbiol* **2009**, 75, 6022-6025, doi:10.1128/AEM.01078-09.
49. Blair, J.M.; Piddock, L.J. How to Measure Export via Bacterial Multidrug Resistance Efflux Pumps. *mBio* **2016**, 7, doi:10.1128/mBio.00840-16.
 50. Bhattacharyya, T.; Sharma, A.; Akhter, J.; Pathania, R. The small molecule IITR08027 restores the antibacterial activity of fluoroquinolones against multidrug-resistant *Acinetobacter baumannii* by efflux inhibition. *Int J Antimicrob Agents* **2017**, 50, 219-226, doi:10.1016/j.ijantimicag.2017.03.005.
 51. Hooper, D.C. Mechanisms of action of antimicrobials: focus on fluoroquinolones. *Clin Infect Dis* **2001**, 32 Suppl 1, S9-S15, doi:10.1086/319370.
 52. de Abreu Costa, L.; Henrique Fernandes Ottoni, M.; Dos Santos, M.G.; Meireles, A.B.; Gomes de Almeida, V.; de Fatima Pereira, W.; Alves de Avelar-Freitas, B.; Eustaquio Alvim Brito-Melo, G. Dimethyl Sulfoxide (DMSO) Decreases Cell Proliferation and TNF-alpha, IFN-gamma, and IL-2 Cytokines Production in Cultures of Peripheral Blood Lymphocytes. *Molecules* **2017**, 22, doi:10.3390/molecules22111789.
 53. Pal, R.; Mamidi, M.K.; Das, A.K.; Bhonde, R. Diverse effects of dimethyl sulfoxide (DMSO) on the differentiation potential of human embryonic stem cells. *Archives of Toxicology* **2012**, 86, 651-661, doi:10.1007/s00204-011-0782-2.
 54. Chen, X.; Thibeault, S. Effect of DMSO concentration, cell density and needle gauge on the viability of cryopreserved cells in three dimensional hyaluronan hydrogel. *Annu Int Conf IEEE Eng Med Biol Soc* **2013**, 2013, 6228-6231, doi:10.1109/EMBC.2013.6610976.
 55. Chamberlin, J.; Story, S.; Ranjan, N.; Chessier, G.; Arya, D.P. Gram-negative synergy and mechanism of action of alkynyl bisbenzimidazoles. *Sci Rep* **2019**, 9, 14171, doi:10.1038/s41598-019-48898-4.
 56. Diver, J.M.; Wise, R. Morphological and biochemical changes in *Escherichia coli* after exposure to ciprofloxacin. *J Antimicrob Chemother* **1986**, 18 Suppl D, 31-41, doi:10.1093/jac/18.supplement_d.31.

57. Siddiqui-Jain, A.; Hoj, J.P.; Cescon, D.W.; Hansen, M.D. Pharmacology and in vivo efficacy of pyridine-pyrimidine amides that inhibit microtubule polymerization. *Bioorganic & Medicinal Chemistry Letters* **2018**, *28*, 934-941, doi:<https://doi.org/10.1016/j.bmcl.2018.01.053>.
58. Knights, K.M.; Stresser, D.M.; Miners, J.O.; Crespi, C.L. In Vitro Drug Metabolism Using Liver Microsomes. *Current Protocols in Pharmacology* **2016**, *74*, 7.8.1-7.8.24, doi:<https://doi.org/10.1002/cpph.9>.
59. Houston, J.B. Utility of in vitro drug metabolism data in predicting in vivo metabolic clearance. *Biochem Pharmacol* **1994**, *47*, 1469-1479, doi:10.1016/0006-2952(94)90520-7.
60. Marimani, M. Chapter 2 - Combination therapy against multidrug resistance. In *Combination Therapy Against Multidrug Resistance*, Wani, M.Y., Ahmad, A., Eds. Academic Press: 2020; <https://doi.org/10.1016/B978-0-12-820576-1.00002-3pp>. 39-64.
61. Delcour, A.H. Outer membrane permeability and antibiotic resistance. *Biochim Biophys Acta* **2009**, *1794*, 808-816, doi:10.1016/j.bbapap.2008.11.005.
62. Silhavy, T.J.; Kahne, D.; Walker, S. The bacterial cell envelope. *Cold Spring Harb Perspect Biol* **2010**, *2*, a000414-a000414, doi:10.1101/cshperspect.a000414.
63. Irie, Y.; Borlee Bradley, R.; O'Connor Jennifer, R.; Hill Preston, J.; Harwood Caroline, S.; Wozniak Daniel, J.; Parsek Matthew, R. Self-produced exopolysaccharide is a signal that stimulates biofilm formation in *Pseudomonas aeruginosa*. *Proceedings of the National Academy of Sciences* **2012**, *109*, 20632-20636, doi:10.1073/pnas.1217993109.
64. Jennings, L.K.; Dreifus, J.E.; Reichhardt, C.; Storek, K.M.; Secor, P.R.; Wozniak, D.J.; Hisert, K.B.; Parsek, M.R. *Pseudomonas aeruginosa* aggregates in cystic fibrosis sputum produce exopolysaccharides that likely impede current therapies. *Cell Rep* **2021**, *34*, 108782, doi:10.1016/j.celrep.2021.108782.
65. Billings, N.; Millan, M.; Caldara, M.; Rusconi, R.; Tarasova, Y.; Stocker, R.; Ribbeck, K. The extracellular matrix Component Psl provides fast-acting antibiotic

- defense in *Pseudomonas aeruginosa* biofilms. *PLoS Pathog* **2013**, 9, e1003526, doi:10.1371/journal.ppat.1003526.
66. Rybtke, M.; Jensen, P.Ø.; Nielsen, C.H.; Tolker-Nielsen, T. The Extracellular Polysaccharide Matrix of *Pseudomonas aeruginosa* Biofilms Is a Determinant of Polymorphonuclear Leukocyte Responses. *Infect Immun* **2020**, 89, e00631-00620, doi:10.1128/IAI.00631-20.
67. Ray, V.A.; Hill, P.J.; Stover, C.K.; Roy, S.; Sen, C.K.; Yu, L.; Wozniak, D.J.; DiGiandomenico, A. Anti-Psl Targeting of *Pseudomonas aeruginosa* Biofilms for Neutrophil-Mediated Disruption. *Scientific Reports* **2017**, 7, 16065, doi:10.1038/s41598-017-16215-6.
68. Rao, J.; Damron, F.H.; Basler, M.; DiGiandomenico, A.; Sherman, N.E.; Fox, J.W.; Mekalanos, J.J.; Goldberg, J.B. Comparisons of Two Proteomic Analyses of Non-Mucoid and Mucoid *Pseudomonas aeruginosa* Clinical Isolates from a Cystic Fibrosis Patient. *Front Microbiol* **2011**, 2, 162, doi:10.3389/fmicb.2011.00162.
69. Ciofu, O.; Mandsberg, L.F.; Wang, H.; Hoiby, N. Phenotypes selected during chronic lung infection in cystic fibrosis patients: implications for the treatment of *Pseudomonas aeruginosa* biofilm infections. *FEMS Immunol Med Microbiol* **2012**, 65, 215-225, doi:10.1111/j.1574-695X.2012.00983.x.
70. Rogliani, P.; Ritondo, B.L.; Zerillo, B.; Matera, M.G.; Calzetta, L. Drug interaction and chronic obstructive respiratory disorders. *Current Research in Pharmacology and Drug Discovery* **2021**, 2, 100009, doi:<https://doi.org/10.1016/j.crphar.2020.100009>.
71. Folkesson, A.; Jelsbak, L.; Yang, L.; Johansen, H.K.; Ciofu, O.; Høiby, N.; Molin, S. Adaptation of *Pseudomonas aeruginosa* to the cystic fibrosis airway: an evolutionary perspective. *Nature Reviews Microbiology* **2012**, 10, 841-851, doi:10.1038/nrmicro2907.

5.8 Acknowledgements

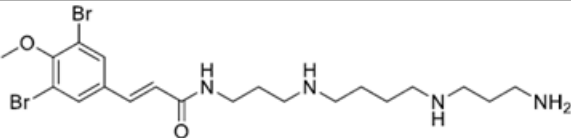
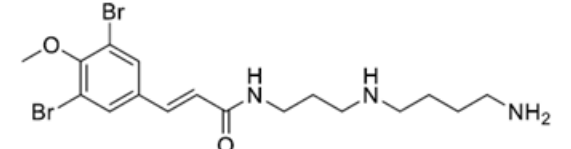
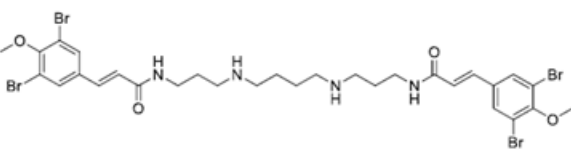
The authors acknowledge the NatureBank biota repository (<https://www.griffith.edu.au/institute-drug-discovery/unique-resources/naturebank>) from which ianthelliformisamines A–C were obtained. Sasha Hayes is acknowledged for the large-scale extraction and isolation studies on the NatureBank marine sponge that supplied larger quantities of ianthelliformisamines A–C. We are grateful to Compounds Australia (www.compoundsaustralia.com) for curating the Davis Open Access Natural Product-based Library. We acknowledge the Australian Research Council (ARC) for support towards NMR and MS equipment (grants LE0668477, LE140100119, and LE0237908). We thank Dr. Timothy Opperman (Microbiotix, Inc., MA, US) for providing the reporter strain MDM-623. The support of the GRIDD strategic initiative for preclinical ADME studies is gratefully acknowledged.

5.9 Supplementary Information

- **Supplementary tables**
- **Supplementary figures**
- **Supplementary data**

Supplementary Tables

Supplementary Table 5.1 Structures, formulas and molecular weight of ianthelliformisamines A–C (1–3).

Compound	Structure	Formula	Molecular weight
1		$C_{20}H_{32}Br_2N_4O_2$	520.30
2		$C_{17}H_{25}Br_2N_3O_2$	463.21
3		$C_{30}H_{38}Br_4N_4O_4$	838.26

Supplementary Table 5.2 The results for the degradation of 1 normalized to t = 0) in mouse liver microsomes.

Time (min)	% Remaining	
	Mouse	
	Mean	SD
0	100.00	0.00
5	93.32	14.29
10	96.74	27.23
20	66.26	19.36
30	57.28	20.01
60	53.42	17.07

Supplementary Table 5.3 Metabolic stability parameters for 1 based on NADPH-dependent degradation profiles in mouse liver microsomes.

Parameter	Units	Result
k^1	min ⁻¹	0.0218 ± 0.0125
Half life ¹	min	38.2 ± 17.2
Cl _{int, in vitro}	μL/min/mg protein	43.6
Cl _{int}	mL/min/kg	112.5
Cl _{blood}	mL/min/kg	58.1
Hepatic Extraction (E _H) ²	---	0.48

¹ mean ± SD, n = 3

² based on mean data for k

**Chapter 5 - Bromotyrosine-derived metabolites from a marine sponge inhibit
Pseudomonas aeruginosa biofilms**

Supplementary Table 5. 4 The results for degradation of 2 (normalized to t = 0) in mouse and human liver microsomes.

Time (min)	% Remaining			
	Mouse		Human	
	Mean	SD	Mean	SD
0	100.00	0	100.00	0
5	153.98	14.66	112.15	16.61
10	160.70	65.50	98.42	9.88
20	138.91	39.12	80.61	3.04
30	119.60	41.51	68.41	7.28
60	122.66	35.50	76.42	16.88

Supplementary Table 5.5 Metabolic stability parameters for 2 based on NADPH-dependent degradation profiles in mouse and human liver microsomes.

Parameter	Units	Mouse	Human
k^1	min ⁻¹	0.0165 ± 0.0030	0.0195 ± 0.0011
Half life ¹	min	42.8 ± 7.6	35.7 ± 2.1
$Cl_{int, in vitro}$	μL/min/mg protein	33.0	39.0
Cl_{int}	mL/min/kg	85.1	32.1
Cl_{blood}	mL/min/kg	49.8	12.6
Hepatic Extraction (E _H) ²	---	0.42	0.61

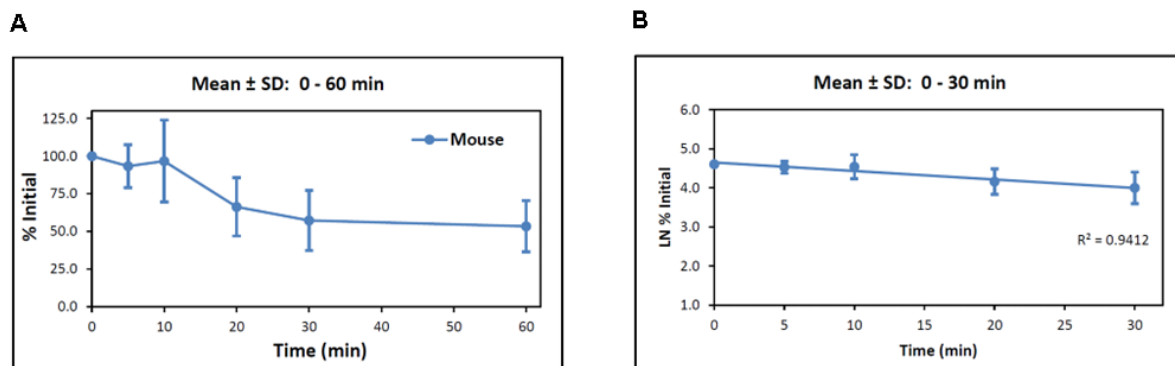
¹ mean ± SD, n = 3

² based on mean data for k

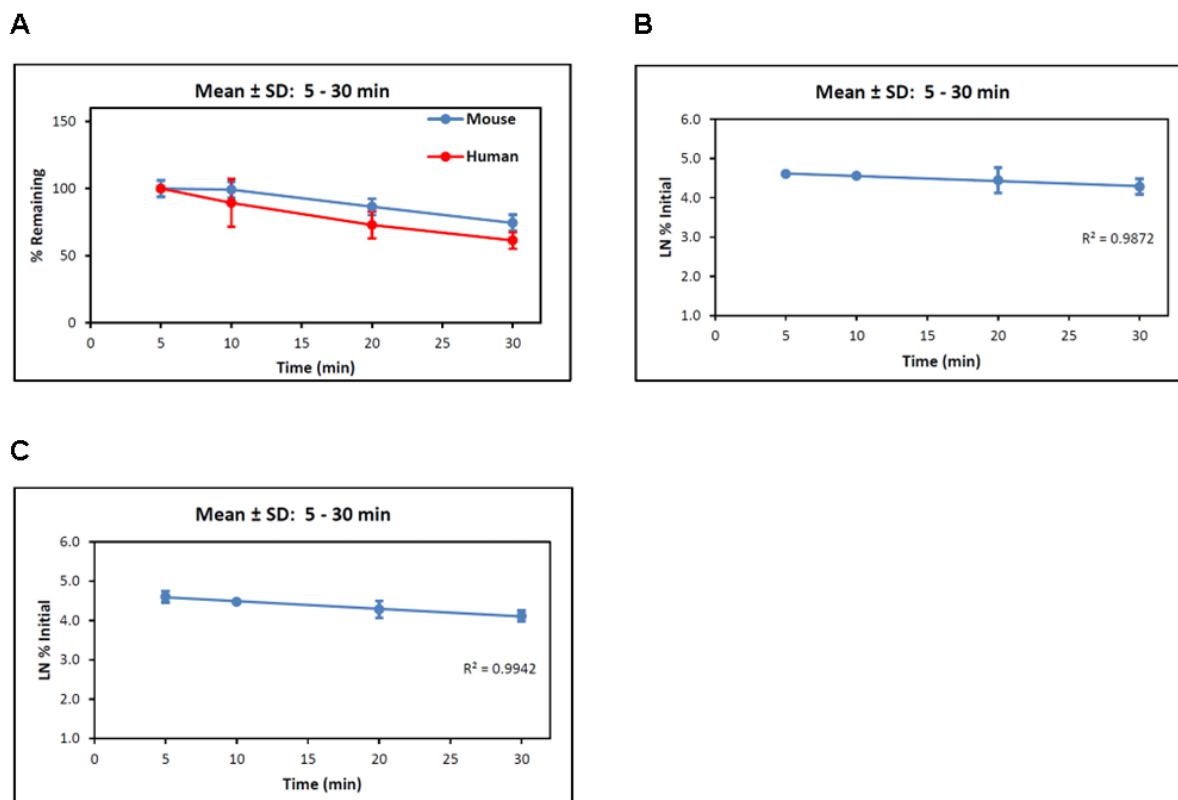
Supplementary Table 5.6 The results for degradation of 3 (normalized to t = 0) in mouse and human liver microsomes.

Time (min)	% Remaining			
	Mouse		Human	
	Mean	SD	Mean	SD
0	100.00	0	100.00	0
5	102.69	7.394	105.22	7.357
10	107.54	14.67	102.09	11.38
20	106.48	7.882	104.88	18.772
30	107.42	7.931	101.07	10.566
60	95.80	13.574	99.19	3.752

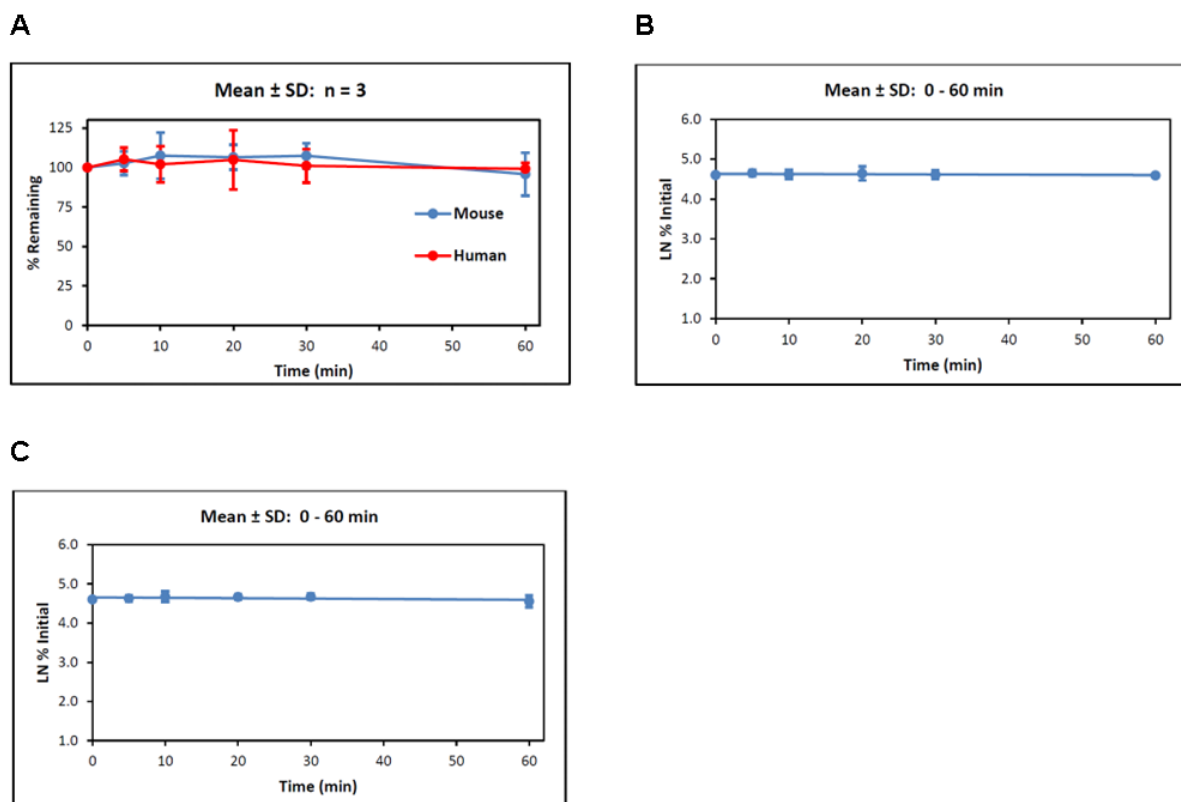
Supplementary Figures



Supplementary Figure 5.1 (A) Metabolic stability parameters for 1 based on NADPH-dependent degradation profiles in mouse liver microsomes. (B) Metabolic stability of 1 (mean \pm SD; $n = 3$; 0 – 30 min) in mouse liver microsomes: LN-transformed data.



Supplementary Figure 5.2 (A) Metabolic stability of **2** (mean \pm SD; n = 3) in mouse and human liver microsomes. (B) Metabolic stability of **2** (mean \pm SD; n = 3) in mouse liver microsomes: LN-transformed data (normalized to t = 5 min). (C) Metabolic stability of **2** (mean \pm SD; n = 3) in human liver microsomes: LN-transformed data (normalized to t = 5 min).



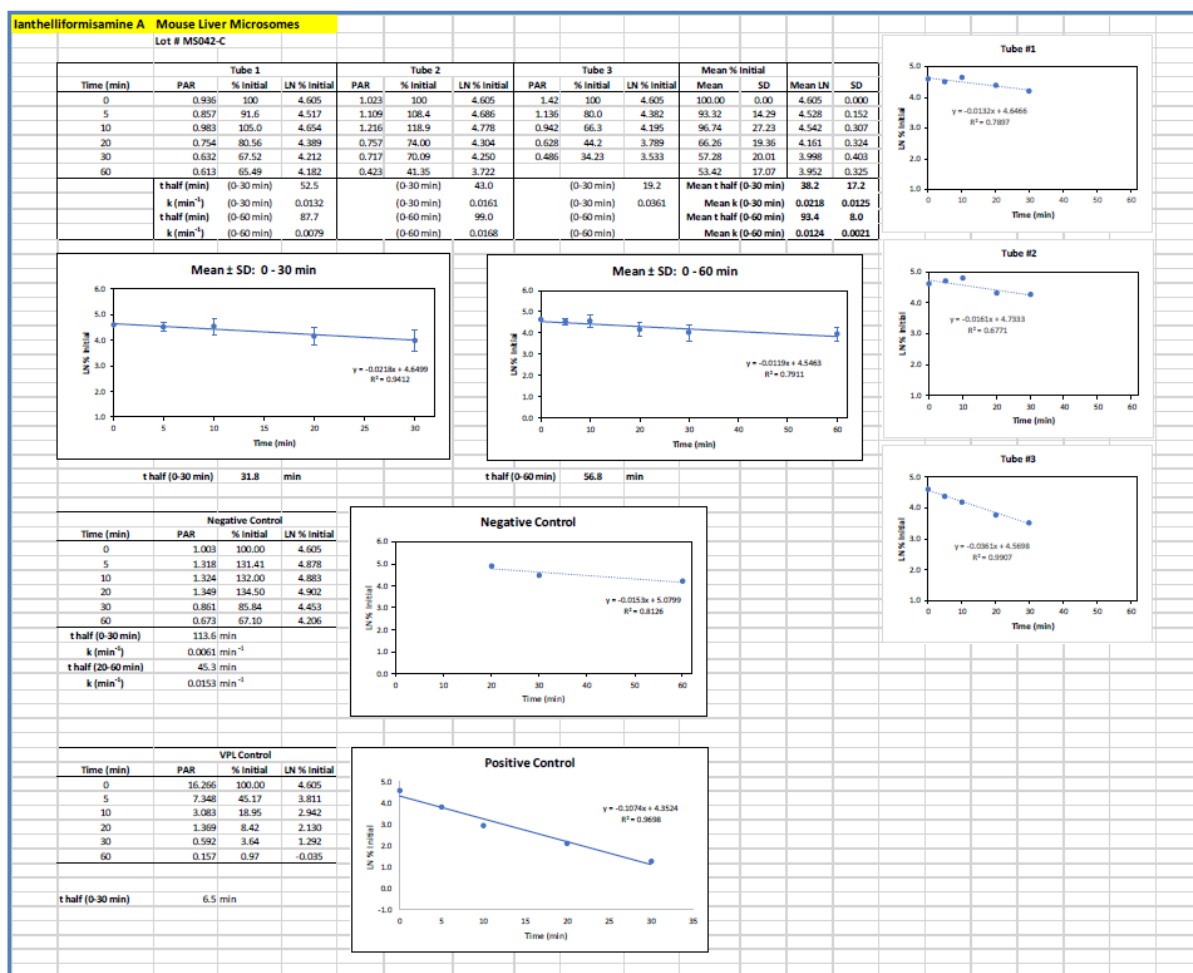
Supplementary Figure 5.3 (A) Metabolic stability of **3** (mean \pm SD; n = 3) in mouse and human liver microsomes. (B) Metabolic stability of **3** (mean \pm SD; n = 3) in human liver microsomes: LN-transformed data. (C) Metabolic stability of **3** (mean \pm SD; n = 3) in mouse liver microsomes: LN-transformed data.

Chapter 5 - Bromotyrosine-derived metabolites from a marine sponge inhibit *Pseudomonas aeruginosa* biofilms

Supplementary Data

Ianthelliformisamine A

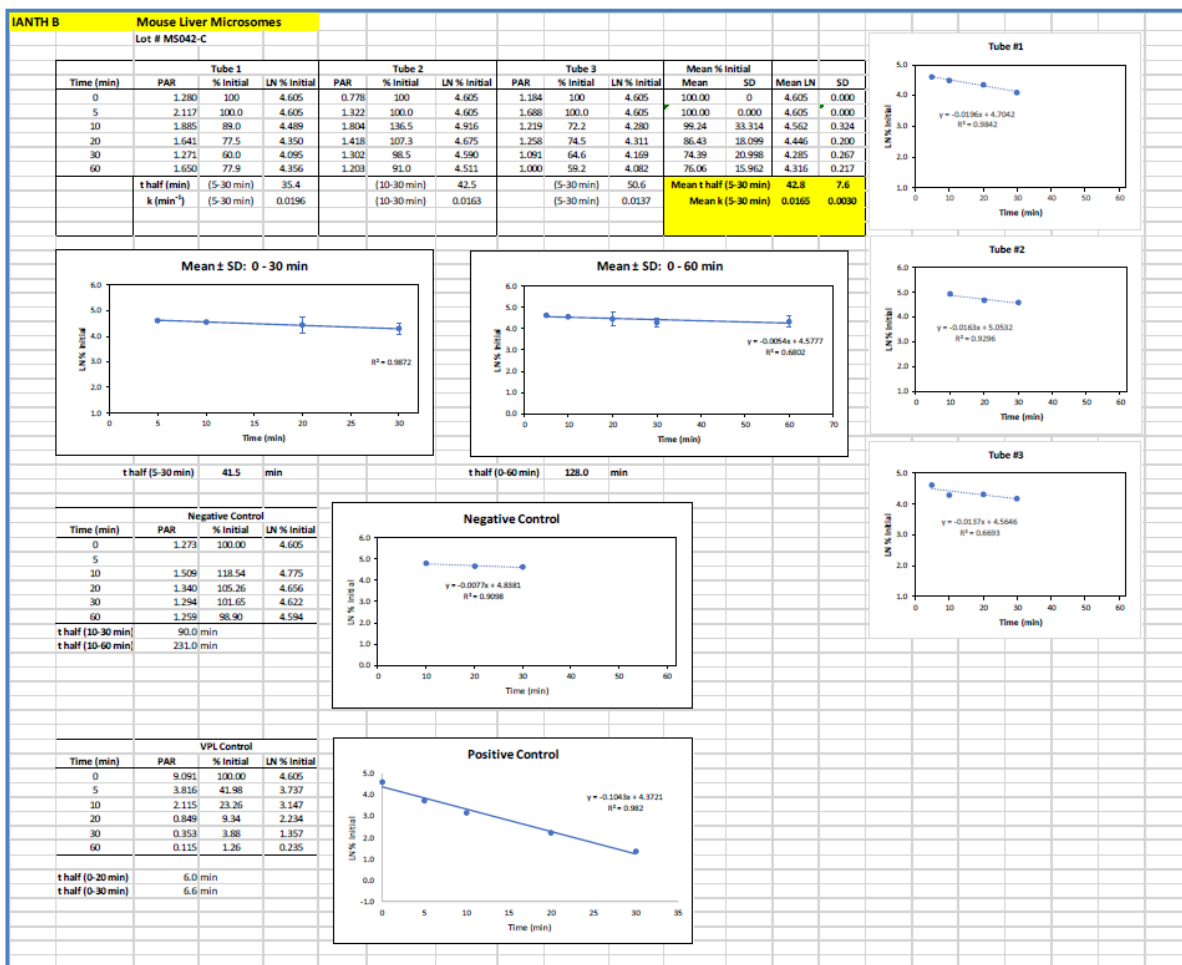
- Mouse liver microsomes



Chapter 5 - Bromotyrosine-derived metabolites from a marine sponge inhibit *Pseudomonas aeruginosa* biofilms

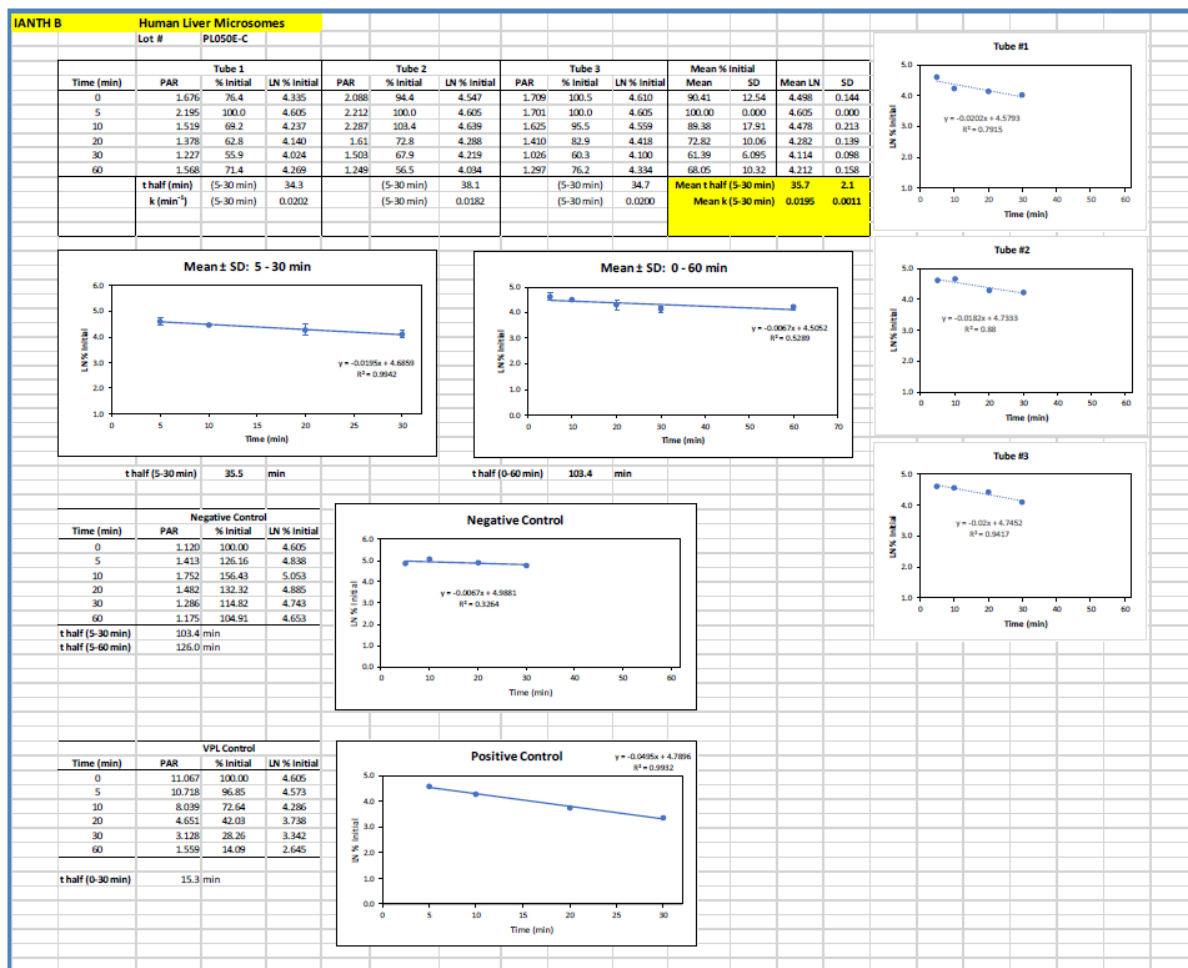
Ianthelliformisamine B

- Mouse liver microsomes



Chapter 5 - Bromotyrosine-derived metabolites from a marine sponge inhibit *Pseudomonas aeruginosa* biofilms

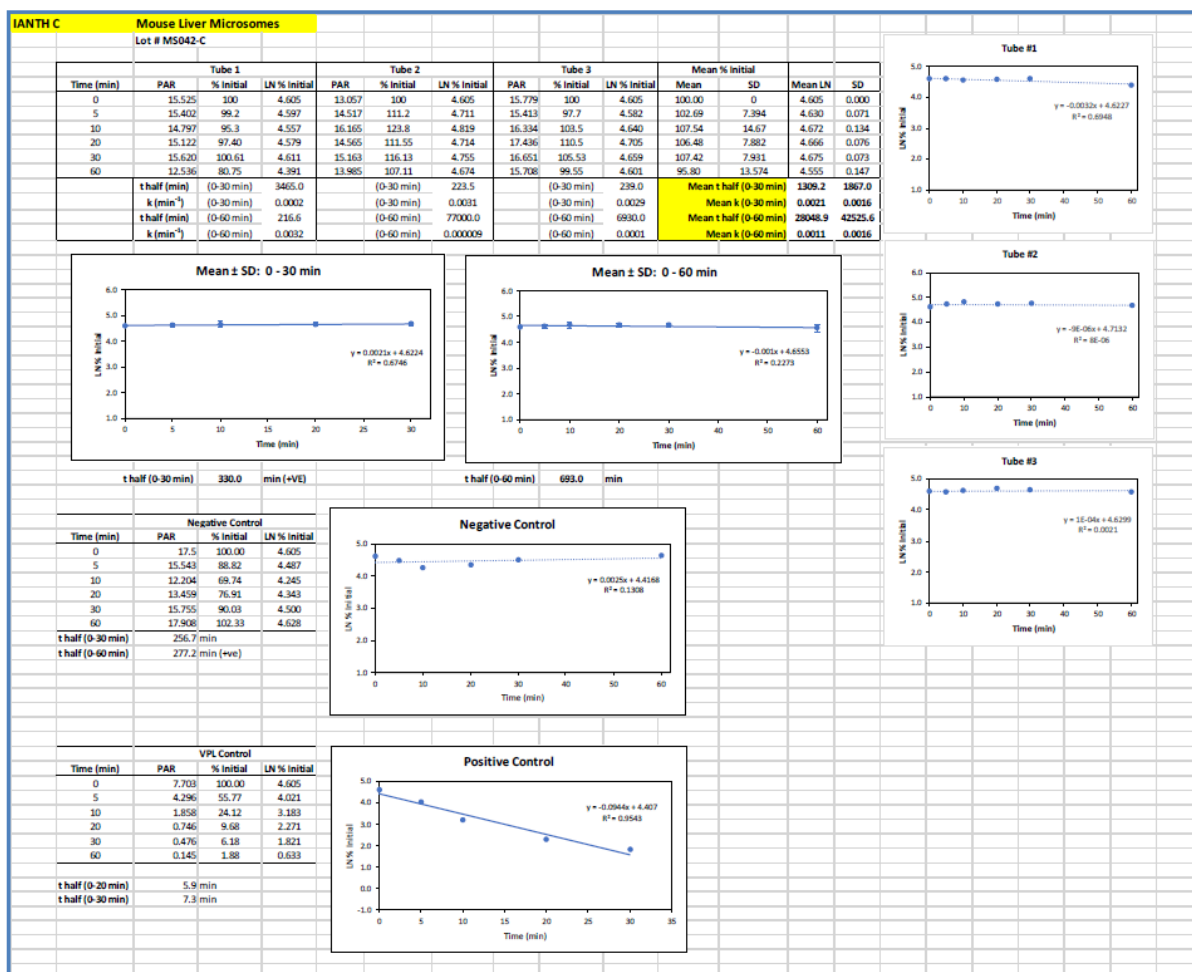
- Human liver microsomes



Chapter 5 - Bromotyrosine-derived metabolites from a marine sponge inhibit *Pseudomonas aeruginosa* biofilms

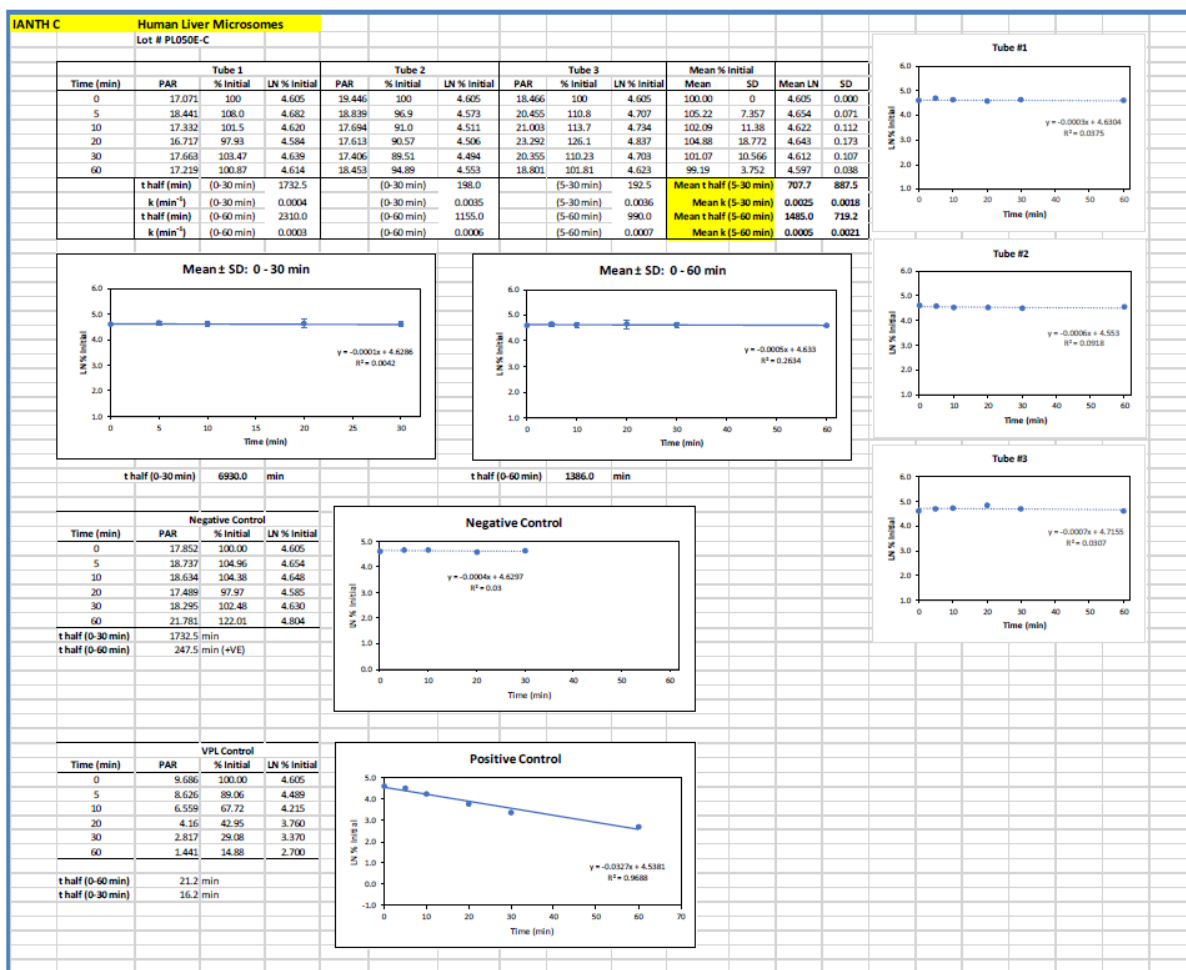
Ianthelliformisamine C

- Mouse liver microsomes



Chapter 5 - Bromotyrosine-derived metabolites from a marine sponge inhibit *Pseudomonas aeruginosa* biofilms

- Human liver microsomes



CHAPTER 6: General discussion and conclusion

P. aeruginosa is recognized as one of the leading causes of persistent infections in patients with cystic fibrosis (CF), which have been enabled by a range of virulence factors and adaptation mechanisms such as the ability to form biofilms. Bacterial biofilms are substantially recalcitrant to antimicrobial therapies posing significant challenges in healthcare settings. The majority of available antibiotic treatments are designed to target the planktonic mode of life. Therefore, they show limited effect against biofilm bacteria. Several strategies have been developed to tackle *P. aeruginosa* biofilms including biofilm inhibitors to prevent biofilm formation at the early stages of infections and biofilm dispersers to disrupt the established biofilm community [1]. Other options to dampen this pathogen are combination therapies of biofilm matrix modulators such as biofilm degrading enzymes with antibiotics which can improve drug penetration and thus maximizing efficacy against established biofilms [2,3]. However, very few novel molecules or approaches could be translated into the clinic. As a result, it is essential to keep searching for novel antibiofilm agents to treat and counteract biofilm-associated infections.

In this study, we developed and optimized a biofilm dispersal assay in 384-well format. The assay involved the use of artificial sputum medium (ASM) to mimic the adaptation in the lungs of CF patients, and several laboratory-generated biofilm impaired mutants (individual knockouts of the three secreted exopolysaccharides that are alginate, Psl and Pel) to assess whether the biofilm matrix components interfering with the compound efficacy. In addition, the alginate overproducing strain, PDO300, was included to replicate the persistence in *in vivo*-formed biofilms.

Chapter 3. The biofilm dispersal assay using ASM was utilized to profile the antibiofilm activity of two libraries, the fraction library and the NatureBank library. The former has been reported to possess cidal effects on planktonic growth of *P. aeruginosa*, but their activity against biofilm has not been examined. The latter is a new compound collection provided by NatureBank, and there has been no screening performed on these compounds. In the first library, 14 active fractions belonging to 12 different biotas were

identified as potential biofilm dispersers. Their activity was confirmed in the secondary screen where refractionated fractions were used instead of initial fractions (small-scale refractionation, 5 fractions per biota). Two active fractions with reproducible effects on preformed biofilms of wild-type PAO1 were chosen for further separation to identify active compounds (large-scale refractionation, 60 fractions per biota). Unexpectedly, these fractions produced non-reproducible biofilm dispersing activity, decreasing from more than 30% to less than 20%. We reasoned that if there was a synergy between compounds within fractions, further separation would dismiss the activity, and the fractions acquired from small-scale refractionation would retain their effects against established biofilms. Hence, an attempt has been made to re-screened fractions from large-scale refractionation (fractions 18 - 48) and fractions obtained from small-scale refractionation. However, the screen did not yield any fractions with comparable antibiofilm effects. Of note, there was a change in mucin suppliers due to a supply shortage. The primary and secondary screens were conducted using Sigma mucin, while all subsequent screens were performed with Lee Biosolution mucin. A recent study has demonstrated that a high level of iron in commercial mucins impacted the production of secondary metabolites, including increased levels of phenazines (1-hydroxyphenazine, pyocyanin, and phenazine-1-carboxylic acid) and decreased production of rhamnolipid and siderophore. Furthermore, concentrations of individual components of commercial mucins fluctuate between suppliers [4]. Enhanced production of phenazines, especially pyocyanin - a vital virulence factor, has been linked to the formation and development of thick biofilms. The co-presence of pyocyanin and eDNA in the sputum of CF patients promoted biofilm formation and exacerbated the host immune system [5]. The variations in metabolite levels produced in ASM containing mucins attained from different vendors would likely affect the outcomes between experiments.

Chapter 4. Drug repurposing is an attractive approach that offers several advantages, such as lower initial investment costs, reduced development timeline and considerable information regarding safety issues [6]. This is a shortcut to obtaining safe and bioactive molecules, which can be useful starting points for drug optimization programs. The library was chosen because it is comprised of natural products and their synthetic analogs, thereby providing source of diversity. The natural products have previously shown activities against

a range of diseases such as tuberculosis [7], cancer [8], malaria [9], bacterial infections [10], HIV and neurodegenerative disorders including Parkinson's disease [11]. However, they had not been tested against pre-formed biofilms of *P. aeruginosa*. In this project, 15 active compounds were identified and confirmed as potential biofilm dispersers which did not influence the viability of suspended cells. These compounds have been previously shown to have biological activities selected for various diseases, *i.e.*, bacterial infections, viral infections, cancer, and malaria. Among these, five compounds also possess antimalarial activity.

Chapter 5. Ianthelliformisamines A-C, previously reported as antibiotic adjuvants, were identified to be active against *P. aeruginosa* biofilms. Ianthelliformisamines A and B exclusively synergized with ciprofloxacin to inhibit planktonic growth and biofilm formation of wild-type PAO1 and its isogenic mutants PAO1 Δ *pslA*, PAO1 Δ *pelF*, PDO300, and PDO300 Δ *alg8*, at various degrees in a dose-dependent manner. Indeed, the required concentrations of ciprofloxacin were 1/3 and 1/4 MIC. In contrast, Ianthelliformisamine C alone planktonic and biofilm populations of the studied strains. Perhaps, the lack of Psl in the biofilm matrix induced the sensitivity of PAO1 Δ *pslA* to sub-lethal concentrations of ciprofloxacin and Ianthelliformisamine C. An interesting but unexpected finding was the high susceptibility of mucoid variant PDO300 to this molecule at both tested concentrations 53.1 μ g/mL and 106.2 μ g/mL. It remains unclear why the biofilm of PAO1 Δ *pelF* was more resistant to Ianthelliformisamine C treatment than PDO300 and PDO300 Δ *alg8*. A cytotoxicity study revealed that these natural products are not toxic to the HEK-293 cell line. The data suggested the compounds do not share the mechanism of action with ciprofloxacin, a DNA synthesis inhibitor. Additionally, Ianthelliformisamine C may be a potential efflux pump inhibitor. The physicochemical properties of these molecules have been investigated. Ianthelliformisamine A showed moderate degradation in mouse liver microsomes, whereas, demonstrated substantial instability in human microsomes. Ianthelliformisamine B displayed average degradation in both mouse and human microsomes. Ianthelliformisamine C, on the other hand, was metabolically stable in both mouse and human microsomes.

6.1 Future directions

Global interest in *P. aeruginosa* biofilm research, *i.e.*, mechanism of biofilm formation, the development of new agents to treat infection and biofilm related infections, and *in vitro* and *in vivo* studies of these molecules, has rapidly risen [12]. *P. aeruginosa* biofilm research begun in 1994 and since then substantial research activity in the field has been carried out, with significant increase in publication output worldwide over the past 20 years. It has become particular importance since WHO announced high priority need for new antibiotics to treat *P. aeruginosa* resisting to carbapenems which are considered as “antibiotics of last resort” [13,14]. In the coming years, *P. aeruginosa* biofilms are likely to be prominent topics of intense research due to longstanding clinical concern of biofilm associated diseases, especially those caused by multi-drug resistant strains [12].

One of the biggest challenges facing the biofilm research is to recreate *in vivo* like environment for bacteria to grow, form biofilms and express specific virulence factors. In this aspect, different synthetic media including ASM were established, which mimics lung physiology of CF patients [4]. In this work, biofilms were allowed to form in microtiter plates containing ASM before addition of fractions and/or compounds. One of the main ingredients of ASM is mucin. The variation in metabolite levels in commercial mucins, especially iron concentration [4], may influence the outcomes of the primary and confirmatory screenings. Further research is required to confirm the observation. Source of mucin should be considered. Additional screenings need to be performed to re-evaluate the activity of the fractions in dispersing pre-existing biofilms.

Although it was demonstrated that alginate overproduction and PHA biosynthesis are competitive and associated with stress tolerance and biofilm formation [15], formation of PHA inclusions in response to meropenem treatments has not been reported previously. Here, for the first time PHA inclusions were observed in biofilms of PAO1, PDO300 and PDO300 Δ alg8, although at different levels, upon exposure to meropenem at 2 μ g/mL. The underlying mechanisms of the association between PHA accumulation, stress tolerance and

antibiotic recalcitrance are beyond the scope of the present study, whereas it will be pursued in the future.

The identification of the biofilm dispersers from Davis Open Access Library containing compounds with known biological activities highlights the great utility of the drug-repurposing strategy. As the molecules were initially screened at a single dose against preformed biofilms of wild-type PAO1, the dose-response study is required to assess their efficacy and potency against biofilms. A biofilm inhibition assay would be useful to determine if these compounds could inhibit biofilm formation. Further screening of these compounds against different biofilm impaired mutants to better understand interactions between biofilm matrix components and the compounds. As they did not produce any adverse effects on bacterial growth, there might be scope for synergism between compounds and antibiotics which may be promising adjunctive therapies for biofilm treatments.

These results describe for the first time that ianthelliformisamines A–C individually and/or in combination with ciprofloxacin possess antibiofilm activities. Future work should be conducted to fully understand mechanisms of action of the compounds. The development of new analogues would be necessary to improve compound efficacy and potency. In addition, the promising *in vitro* antibiofilm activity, low cytotoxicity and metabolic stability warrant further research for ianthelliformisamine C.

6.2 References

1. Verderosa, A.D.; Totsika, M.; Fairfull-Smith, K.E. Bacterial Biofilm Eradication Agents: A Current Review. *Frontiers in Chemistry* **2019**, *7*.
2. Liu, Y.; Kamesh, A.C.; Xiao, Y.; Sun, V.; Hayes, M.; Daniell, H.; Koo, H. Topical delivery of low-cost protein drug candidates made in chloroplasts for biofilm disruption and uptake by oral epithelial cells. *Biomaterials* **2016**, *105*, 156-166, doi:10.1016/j.biomaterials.2016.07.042.
3. Baelo, A.; Levato, R.; Julian, E.; Crespo, A.; Astola, J.; Gavalda, J.; Engel, E.; Mateos-Timoneda, M.A.; Torrents, E. Disassembling bacterial extracellular matrix with DNase-coated nanoparticles to enhance antibiotic delivery in biofilm infections. *J Control Release* **2015**, *209*, 150-158, doi:10.1016/j.jconrel.2015.04.028.
4. Neve, R.L.; Carrillo, B.D.; Phelan, V.V. Impact of Artificial Sputum Medium Formulation on *Pseudomonas aeruginosa* Secondary Metabolite Production. *J Bacteriol* **2021**, *203*, e0025021, doi:10.1128/JB.00250-21.
5. Das, T.; Kutty, S.K.; Kumar, N.; Manefield, M. Pyocyanin facilitates extracellular DNA binding to *Pseudomonas aeruginosa* influencing cell surface properties and aggregation. *PLoS One* **2013**, *8*, e58299-e58299, doi:10.1371/journal.pone.0058299.
6. Pushpakom, S.; Iorio, F.; Eyers, P.A.; Escott, K.J.; Hopper, S.; Wells, A.; Doig, A.; Williams, T.; Latimer, J.; McNamee, C., et al. Drug repurposing: progress, challenges and recommendations. *Nat Rev Drug Discov* **2019**, *18*, 41-58, doi:10.1038/nrd.2018.168.
7. Ribeiro, D.; Keller, K.M.; Soto-Blanco, B. Ptaquiloside and Pterosin B Levels in Mature Green Fronds and Sprouts of *Pteridium arachnoideum*. *Toxins (Basel)* **2020**, *12*, doi:10.3390/toxins12050288.
8. Shaala, L.A.; Youssef, D.T.A. Cytotoxic Psammaphysin Analogues from the Verongid Red Sea Sponge *Aplysinella* Species. *Biomolecules* **2019**, *9*, doi:10.3390/biom9120841.

9. Gaillard, T.; Madamet, M.; Tsombeng, F.F.; Dormoi, J.; Pradines, B. Antibiotics in malaria therapy: which antibiotics except tetracyclines and macrolides may be used against malaria? *Malaria Journal* **2016**, *15*, 556, doi:10.1186/s12936-016-1613-y.
10. Ozcelik, B.; Kartal, M.; Orhan, I. Cytotoxicity, antiviral and antimicrobial activities of alkaloids, flavonoids, and phenolic acids. *Pharm Biol* **2011**, *49*, 396-402, doi:10.3109/13880209.2010.519390.
11. Aggarwal, M.; Leser, G.P.; Lamb, R.A. Repurposing Papaverine as an Antiviral Agent against Influenza Viruses and Paramyxoviruses. *J Virol* **2020**, *94*, e01888-01819, doi:10.1128/JVI.01888-19.
12. Zhu, Y.; Li, J.J.; Reng, J.; Wang, S.; Zhang, R.; Wang, B. Global trends of *Pseudomonas aeruginosa* biofilm research in the past two decades: A bibliometric study. *Microbiologyopen* **2020**, *9*, 1102-1112, doi:10.1002/mbo3.1021.
13. Tacconelli, E.; Carrara, E.; Savoldi, A.; Harbarth, S.; Mendelson, M.; Monnet, D.L.; Pulcini, C.; Kahlmeter, G.; Kluytmans, J.; Carmeli, Y., et al. Discovery, research, and development of new antibiotics: the WHO priority list of antibiotic-resistant bacteria and tuberculosis. *The Lancet Infectious Diseases* **2018**, *18*, 318-327, doi:10.1016/S1473-3099(17)30753-3.
14. Papp-Wallace, K.M.; Endimiani, A.; Taracila, M.A.; Bonomo, R.A. Carbapenems: past, present, and future. *Antimicrob Agents Chemother* **2011**, *55*, 4943-4960, doi:10.1128/AAC.00296-11.
15. Pham, T.H.; Webb, J.S.; Rehm, B.H. The role of polyhydroxyalkanoate biosynthesis by *Pseudomonas aeruginosa* in rhamnolipid and alginate production as well as stress tolerance and biofilm formation. *Microbiology* **2004**, *150*, 3405-3413, doi:10.1099/mic.0.27357-0.